ZooKeys 1118: 1–19 (2022)
doi: 10.3897/zookeys.1118.89593
https://zookeys.pensoft.net

RESEARCH ARTICLE

A peer-reviewed open-access journal
ZooKeys
Launched to accelerate biodiversity research

Review of the millipede genus *Malayorthomorpha* Mršić, 1996 (Diplopoda, Polydesmida, Paradoxosomatidae), with descriptions of two new species from Thailand and a key to its species

Natdanai Likhitrakarn[1,2], Sergei I. Golovatch[3], Wisut Sittichaya[4]

1 *Program of Agriculture, Faculty of Agricultural Production, Maejo University, Chiang Mai, 50290, Thailand* **2** *Biodiversity and Utilization Research Center of Maejo University, Maejo University, Chiang Mai, 50290, Thailand* **3** *Institute for Problems of Ecology and Evolution, Russian Academy of Sciences, Leninsky pr.33, Moscow 119071, Russia* **4** *Agricultural Innovation and Management Division, Faculty of Natural Resources, Prince of Songkla University, Hat Yai, Songkhla, 90112, Thailand*

Corresponding author: Wisut Sittichaya (wisut.s@psu.ac.th)

Academic editor: Dragan Antić | Received 28 June 2022 | Accepted 1 August 2022 | Published 16 August 2022

https://zoobank.org/B1B42B9E-1CCA-4E85-A22E-39710CFA755E

Citation: Likhitrakarn N, Golovatch SI, Sittichaya W (2022) Review of the millipede genus *Malayorthomorpha* Mršić, 1996 (Diplopoda, Polydesmida, Paradoxosomatidae), with descriptions of two new species from Thailand and a key to its species. ZooKeys 1118: 1–19. https://doi.org/10.3897/zookeys.1118.89593

Abstract

The millipede genus *Malayorthomorpha* Mršić, 1996, so far monospecific and previously known only from Park Belum, Perak State, northern Malaysia, is recorded from a mountain in Betong District, Yala Province, southern Thailand for the first time, being represented there by two new species: *M. halabala* **sp. nov.** and *M. hulutbeeda* **sp. nov.** Both new species are found to occur syntopically and can be assumed as narrowly endemic to the Titiwangsa Mountain Range which begins in southern Thailand, crosses the Malaysian border, and extends into east and west coast regions of the Malay Peninsula. In addition, the generic diagnosis is slightly updated, and a key to all three species is provided.

Keywords

Malaysia, *Malayorthomorpha halabala* sp. nov., *Malayorthomorpha hulutbeeda* sp. nov., Orthomorphini, taxonomy

Introduction

The millipede genus *Malayorthomorpha* Mršić, 1996 was established for a single, and type species, *Malayorthomorpha siveci* Mršić, 1996, based on two males from northern Malaysia (Mršić 1996). This genus was immediately assigned, and still belongs, to the tribe Orthomorphini Brölemann, 1916, all 25 genera of which are basically confined to the Oriental Region (Nguyen and Sierwald 2013; Srisonchai et al. 2018a, b, c, d). The tribe is characterized by the gonopod that shows an elongate (not shortened) femorite and both solenophore (= tibiotarsus) and solenomere of medium size, the former's both mesal and lateral lobes (a lamina medialis and a lamina lateralis, respectively) sheathing, supporting and protecting a flagelliform solenomere (Jeekel 1968). The latest key to the genera of the tribe belongs to Golovatch (1997), but presently it is considerably out of date.

Thailand is located in the central part of mainland Southeast Asia within two significant biodiversity hotspots, Indo-Burma and Sundaland (Myers et al. 2000), both outstanding in supporting an especially rich and diverse diplopod fauna (Likhitrakarn et al. 2011, 2020; Pimvichai et al. 2018, 2020). To date, the Thai millipede list comprises 256 species in 52 genera, 17 families and nine orders, largely reported based on explorations during 2007–2022 throughout Thailand (e.g., Pimvichai et al. 2018, 2020; Srisonchai et al. 2018a, b, c, d, 2021; Likhitrakarn et al. 2020, 2021a, b, 2022; Rosenmejer et al. 2021; Bhansali and Wesener 2022).

However, there are still some areas that have never been explored and prospected sufficiently well for millipedes, such as three southern border provinces within the Malay Peninsula: Pattani, Narathiwat and Yala. Some Diplopoda have only been documented from the Yala and Narathiwat provinces, while the Pattani Province has remained devoid of any millipede records (Enghoff 2005). Only ten species have been reported from the Yala Province (Table 1), nine of which share a single locality, the Bang Lang National Park (5°30'7"N, 101°26'21"E). Four species are only known from one locality, and three from two localities with a range of less than 50 km^2. These seven species are presumably endemic to the country or restricted to a small area in the Malay Peninsula. However, only relatively small areas have been prospected, with just five sampling locations in the three provinces that have provided reports of millipede species.

Luckily, we have recently been privileged to survey an evergreen forest in the Betong District, Yala Province near the Thai-Malaysia border during the rainy season. Based on morphological examinations of the new specimens, we are able to herewith describe and illustrate two new species of the genus *Malayorthomorpha* which is formally reported from Thailand for the first time.

Materials and methods

New material was collected in a montane forest at a rather high elevation near the Thai-Malaysian border. The specimens collected were euthanized by a two-step method following the AVMA Guidelines for the Euthanasia of Animals (AVMA 2013). Material was then preserved in 75% ethanol for morphological observations and brought

to the laboratory. The specimens were examined, measured and photographed under a Nikon SMZ 745T trinocular stereo microscope equipped with a Canon EOS 5DS R digital SLR camera. Digital images obtained were processed and edited with Adobe Photoshop CS5. Line drawings were based on photographs and examined under the stereo microscope equipped with a digital SLR camera. For scanning electron microscopy (SEM), the gonopods were coated with 8 nm gold layer using a CCU-010 high vacuum sputter and a carbon coater (Safematic), then imaged with a TESCAN VEGA3 scanning electron microscope operated at 5 keV of acceleration voltage and returned to alcohol after SEM examination. The holotypes and paratype are housed in the Museum of Zoology, Chulalongkorn University (**CUMZ**), Bangkok, Thailand.

In the synonymy sections, **D** stands for the original description and/or subsequent descriptive notes, **K** for the appearance in a key, **L** for the appearance in a species list, while **M** for a mere mention.

Table 1. Localities of millipede species recorded from the Yala and Narathiwat provinces, Thailand.

No.	Species	Locality	Remark
Order Sphaerotheriida			
1	*Sphaerobelum meridionalis* Bhansali & Wesener, 2022	Yala Province, Than To District, Bang Lang National Park (Than To Waterfall), 150 m a.s.l., 6°11'47.5"N, 101°09'50.9"E (Bhansali and Wesener 2022).	
Order Spirostreptida			
2	*Anurostreptus barthelemyae* Demange, 1961	Yala Province, Bang Lang National Park, 6°04'N, 101°11'E; Narathiwat Province, Khao Mala (Enghoff 2005).	Originally described from Peninsular Malaysia (Demange 1961) and also reported from the Satun and the Songkhla Province, Thailand (Enghoff 2005).
3	*Thyropygus aterrimus* (Pocock, 1889)	Yala Province, Bang Lang National Park, 6°11'47.5"N, 101°09'50.9"E; Naratiwat Province, Waeng District, Hala-Bala WS Research Station, 5°47'44.8"N, 101°50'4.2"E (Enghoff 2005).	Also known from Myanmar (Pocock 1889) and Malaysia (Sinclair 1901; Wang and Tang 1965).
4	*Thyropygus floweri* (Demange, 1961)	Bukit Jalor (=Yala) (Demange, 1961); Yala Province, Bang Lang National Park, 6°04'12"N, 101°11'18"E (Pimvichai et al. 2009).	
Order Polydesmida			
5	*Eutrichodesmus cavernicola* (Sinclair, 1901)	Yala Province, Mueang Yala District, Wat Khuhapimuk (adjust the precise position of Sinclair (1901) based on Huber et al. (2015) by Srisonchai et al. (2020)).	
6	*Anoplodesmus malayanus* (Golovatch, 1993) (E)	Records from Thailand: Yala Province, Bang Lang National Park, 6°04'N, 101°11'E, <400m (Golovatch 1993).	
7	*Desmoxytes delfae* (Jeekel, 1964)	Yala Province, Bang Lang National Park, lowland rainforest, 6°4'N, 101°11'E (Srisonchai et al. 2018a).	The species was found in abundance in the provinces of Surat Thani, Krabi, Nakhon Si Thammarat, Phatthalung, Trang, Satun, and Songkhla, which cover the majority of southern Thailand (Srisonchai et al. 2018a).
8	*Haplogonomorpha gogalai* Mršić, 1996	Yala Province, Bang Lang National Park, 6°04'N, 101°11'E, <400m (Golovatch 1998).	This monotypic species was originally described from Peninsular Malaysia (Mršić 1996).
9	*Orthomorpha banglangensis* Golovatch 1998	Yala Province, Bang Lang National Park, 6°04'N, 101°11'E (Golovatch 1998).	
10	*Substrongylosoma moniliforme* Golovatch, 1993	Yala Province, 20 km south of Tham To, 5°50'N, 101°10'E, 200 m; Yala Province, Bang Lang National Park, 6°04'N, 101°11'E, 400 m a.s.l. (Golovatch 1993).	

The terminology concerning gonopodal and somatic structures mostly follows Mršić (1996), Golovatch and Enghoff (1993), Golovatch (1997), and Srisonchai et al. (2018b, 2018c). Abbreviations of certain gonopodal structures are as follows:

g groove, a distinct groove line running parallel to the solenomere, clearly seen in mesal view
ll lamina lateralis, a flat lobe in the distal part of the gonopod
lm lamina medialis, a large part located distally on the gonopod, tapered apically and unciform
sl solenomere, usually a long and flagelliform structure originating at the base of the solenophore
sph solenophore (= tibiotarsus), the apical part of the telopodite, consisting of a lamina lateralis and a lamina medialis

The Animal Care and Use Protocol Review No. 1723018 was applied.

Coordinates and elevations were recorded by Garmin GPSMAP 60 CSx and Garmin eTrex 30 using the WGS84 datum and subsequently double-checked with Google Earth ver. 7.3.4

Taxonomy

Family Paradoxosomatidae Daday, 1889
Subfamily Paradoxosomatinae Daday, 1889
Tribe Orthomorphini Brölemann, 1916

Genus *Malayorthomorpha* Mršić, 1996

Malayorthomorpha Mršić, 1996: 139 (D).
Malayorthomorpha – Golovatch 1997: 134 (M, K); Shelley et al. 2000: 111 (L).

Amended diagnosis. Body medium-sized to large (ca. 24–41 mm long, ca. 1.2–2.7 mm wide), with 20 segments. Paraterga from poorly to rather well developed, without lateral incisions. Transverse metatergal sulcus distinct. Leg relatively long and slender, without modifications. ♂ tarsal brushes absent. Sternal lobe between ♂ coxae 4 present, other sternites unmodified.

Gonopods rather simple to relatively complex; coxites elongate, subcylindrical, sparsely setose distoventrally, without tubercles; prefemoral (= setose) part of telopodite moderate to relatively large, 1/3–1/2 as long as acropodite; femorite moderately long and stout, slightly curved, devoid of a distinct distolateral sulcus demarcating a postfemoral part; a well-developed lamina medialis and a hypertrophied lamina lateralis of solenophore; the latter subterminally with a long, distally pointed and curved

lobe broadened at base and protecting the tip of a curved solenomere. Apex of solenophore subquadrate. Solenomere flagelliform, starting about level to demarcation cingulum between femorite and solenophore, seminal groove running entirely or mostly mesally along an excavate femorite.

Type species. *Malayorthomorpha siveci* Mršić, 1996, by original designation.

Affinities. As noted earlier (Golovatch 1997, 1998), the gonopodal conformation of *Malayorthomorpha* seems to especially similar to that of *Cleptomorpha* Golovatch, 1997, a monospecific genus of Orthomorphini from Sumatra, Indonesia. Yet both genera compared differ clearly in the gonopod femorite showing an indistinct, oblique, mesal fold, a relatively slender solenophore and an apically terminating solenomere in *Cleptomorpha* compared to the gonopod femorite that is clearly excavated mesally, has a considerably stouter solenophore, and the solenomere termnating mesally about the solenophore midway in *Malayorthomorpha* (Golovatch 1997).

Key to species of *Malayorthomorpha*, chiefly based on ♂ characters

1 Sternal lobe between ♂ coxae 4 linguiform with a rounded tip (Figs 6H, I, 7E). Gonopod lamina lateralis (**ll**) triangular in shape, bifid at tip, and protruded laterally (Figs 7B–D, 8A, C–F) ..... ***Malayorthomorpha hulutbeeda* sp. nov.**

– Sternal lobe between ♂ coxae 4 deeply notched medially (Figs 1D, 3H, I, 4E). Gonopod lamina lateralis (**ll**) elevated and expanded apically (Figs 1E–G, 4A–D, 5) **2**

2 Pleurosternal carinae present until segment 11. Sternal lobe between ♂ coxae 4 with a pair of small cones near base (Figs 3H, I, 4E). Gonopod tip with a denticulate margin (Figs 4A, B, 5C, D) ..... ***Malayorthomorpha halabala* sp. nov.**

– Pleurosternal carinae present until segment 5. Sternal lobe between ♂ coxae 4 without cones near base (Fig. 1D). Gonopod tip with a smooth margin (Fig. 1E–G) ..... ***Malayorthomorpha siveci***

***Malayorthomorpha siveci* Mršić, 1996**

Fig. 1

Malayorthomorpha siveci Mršić, 1996: 139 (D).
Malayorthomorpha siveci – Shelley et al. 2000: 111 (L).

Remark. This species was described from Park Belum, 5°30'7"N, 101°26'21"E, ca. 320–350 m a.s.l., Hulu (Sungani), Perak, Malaysia (Mršić 1996). Only two male specimens have been obtained, and both have been discovered in a small area. This species is considered endemic to northern Malaysia.

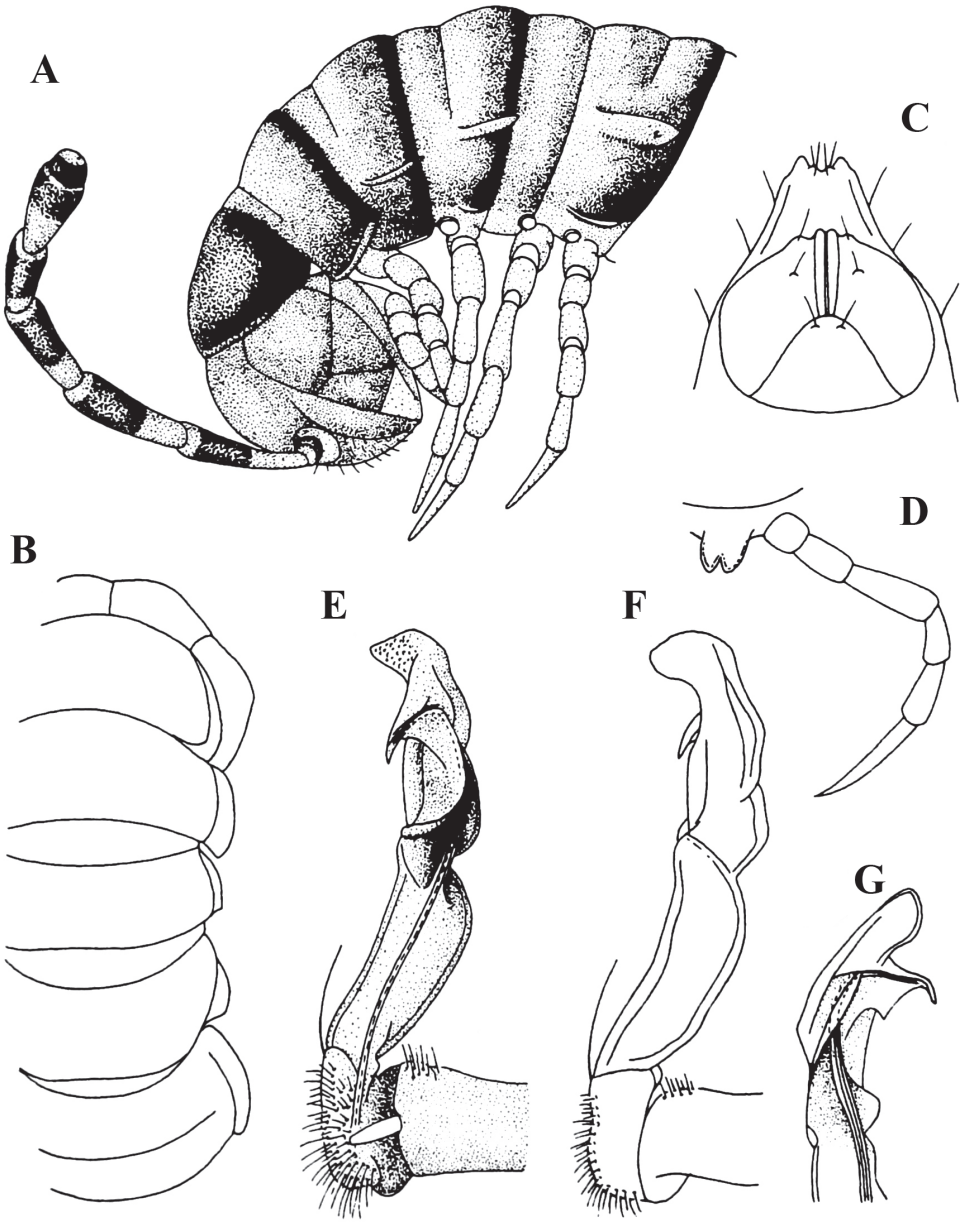

Figure 1. *Malayorthomorpha siveci* Mršić, 1996, ♂ holotype **A, B** anterior part of body, lateral and dorsal views, respectively **C** anal segment, ventral view **D** sternal process and left anterior leg of body segment 5, suboral view **E–G** right gonopod, mesal, lateral and suboral views, respectively. Photos not to scale (after Mršić 1996).

***Malayorthomorpha halabala* sp. nov.**
https://zoobank.org/3FB913EC-E071-4A1A-A306-9657A857AFDB
Figs 2A, 3–5

Material examined. ***Holotype*:** Thailand – Yala Province • ♂; Betong District, hill in evergreen forest, on forest floor; 1440 m a.s.l.; 5°55'N, 101°26'E; 22 May 2021; Wisut Sittichaya leg.; CUMZ. ***Paratype*:** Thailand – Yala Province • ♀; same District, elfin montane forest (Malaya Phytochorion province); 1430 m a.s.l.; 25 May 2022; Wisut Sittichaya leg.; CUMZ.

Diagnosis. This new species seems to be particularly similar to *M. siveci* Mršić, 1996, with which it shares most of the gonopodal characters. It differs from *M. siveci* by the wider body, 2.7–3.2 mm (vs smaller, 1.2 mm), the colour pattern which is uniformly red brown with lighter red brown paraterga (Fig. 3A–F) (vs a light brown body with the collum and caudal edges of metazonae margined darker brown; Fig. 1A), as well as the pleurosternal carinae present until segment 11 (vs until segment 5), the sternal lobe between ♂ coxae 4 with a pair of small cones laterally near base (Fig. 3E, H, I) (vs absent, Fig. 1D), and the tip of the gonopod with a denticulate margin (Figs 4A, B, 5C, D) (vs smooth and rounded; Fig. 1E–G).

Description. Length 29.3 (♂) or 36.2 mm (♀), width of midbody pro- and metazonae 2.1 and 2.7 mm (♂) or 2.7 and 3.2 mm (♀), respectively.

Colouration of live animal rusty red (Fig. 2A), edges of paraterga light red brown; antennae dark brownish, legs and venter contrasting light yellow (Fig. 2A); colouration in alcohol, after one week of preservation, red brown (Fig. 3A–F); edges of paraterga light red brown, head and antennae brown, legs, venter and a few basal antennomeres contrasting light yellow (Fig. 3A–G).

Clypeolabral region sparsely setose; epicranial suture distinct. Antennae long, extending caudally past metaterga 5 (♂) or metaterga 3 (♀) when stretched dorsally. In width, segment 3 < 4 = collum < segment 2 = head < segment 5 < 6–17, body gently and gradually tapering thereafter.

Collum with three transverse rows of setae: 4+4 in anterior, 2+2 in intermediate, and 3+3 in posterior row, all mostly abraded, but still traceable as insertion points; lateral incisions absent; caudal corner of paraterga very broadly rounded, declined ventrad, produced slightly past rear tergal margin (Fig. 3A, B).

Tegument generally smooth and shining, prozonae finely shagreened, metaterga finely leathery and faintly rugulose (Fig. 3A, C, F), surface below paraterga leathery and rugose (Fig. 3B, D, E). Postcollum metaterga with two transverse rows of setae traceable at least as insertion points when setae broken off: 2+2 in anterior (presulcus) and 3+3 in posterior (post-sulcus) row. Tergal setae simple, slender, ca. 1/3 as long as metaterga. Axial line barely traceable both on pro- and metazonae.

Paraterga rather well developed (Fig. 3A, C, F), lying rather high (at upper 1/3 of body), slightly upturned, but lying below dorsum; anterior edge broadly rounded and narrowly bordered, fused to callus; lateral edge without incisions; caudal corner

very narrowly rounded, not produced past rear tergal margin except in rings 2 and 3 (Fig. 3A, B); posterior edge nearly straight. Paraterga 2 broad, anterior edge angular and rounded, lateral edge without incisions (Fig. 3A).

Calluses on paraterga rather narrow, delimited by a sulcus fully on dorsal side and in about posterior 2/3 on ventral side; on poreless rings more narrow than on pore-bearing ones in dorsal view (Fig. 3B, D, E). Ozopores evident, lateral, lying in an ovoid groove at about 1/3 in front of posterior edge of metaterga.

Transverse sulcus usually distinct (Fig. 3A, C, F), complete on metaterga 5–17, narrow, line-shaped, rather deep, not reaching the bases of paraterga, very faintly ribbed at bottom, incomplete and nearly wanting on segment 18. Stricture between pro- and metazona wide, deep, ribbed at bottom down to base of paraterga starting with segment 5 (Fig. 3A–E, F). Pleurosternal carinae complete crests with a sharp caudal tooth on rings 2–4, increasingly reduced and retaining a sharp caudal tooth on rings 5 and 6 thereafter, further retained as a small caudal tooth and increasingly reduced until segment 11, absent from segment 12 on (♂, ♀) (Fig. 3B, D, E).

Epiproct (Fig. 3E–G) conical, flattened dorsoventrally, with two evident, but small, rounded, apical papillae; tip subtruncate; pre-apical papillae small, but evident, lying close to tip. Paraprocts regularly convex, each with premarginal sulci medially

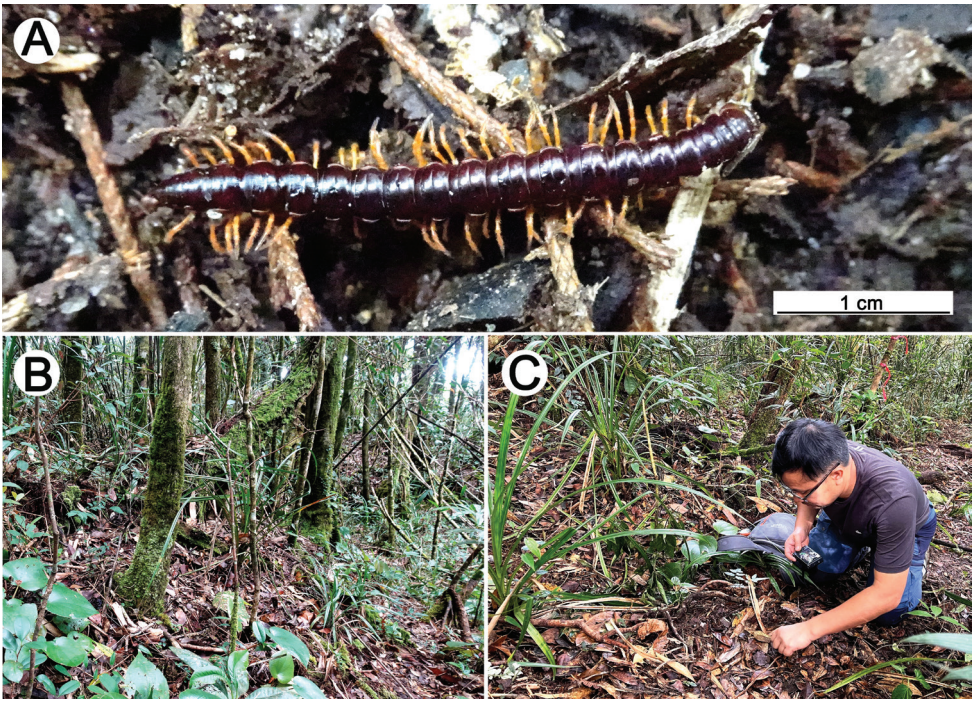

Figure 2. Habitat at the type locality of *Malayorthomorpha halabala* sp. nov., ♀ **A** live colouration **B, C** elfin montane forest floor and collecting the specimens **B, C** pictures taken not to scale.

and two pairs of setigerous knobs at medial margin (Fig. 3G). Hypoproct roundly subtrapeziform, setigerous knobs at caudal edge very small and well-separated (Fig. 3G).

Sterna sparsely setose, shining, cross-impressions shallow, without modifications; a single, linguiform, medially rather deeply notched sternal lobe between ♂ coxae 4, with a pair of small cones laterally near base (Fig. 3E, H, I). A conspicuous and high ridge present in front of gonopod aperture. Legs long and slender (Fig. 3B), midbody ones ca. 1.4–1.6 (♂) or 1.2–1.3 (♀) times as long as body height, without modifications, ♂ tarsal brushes absent.

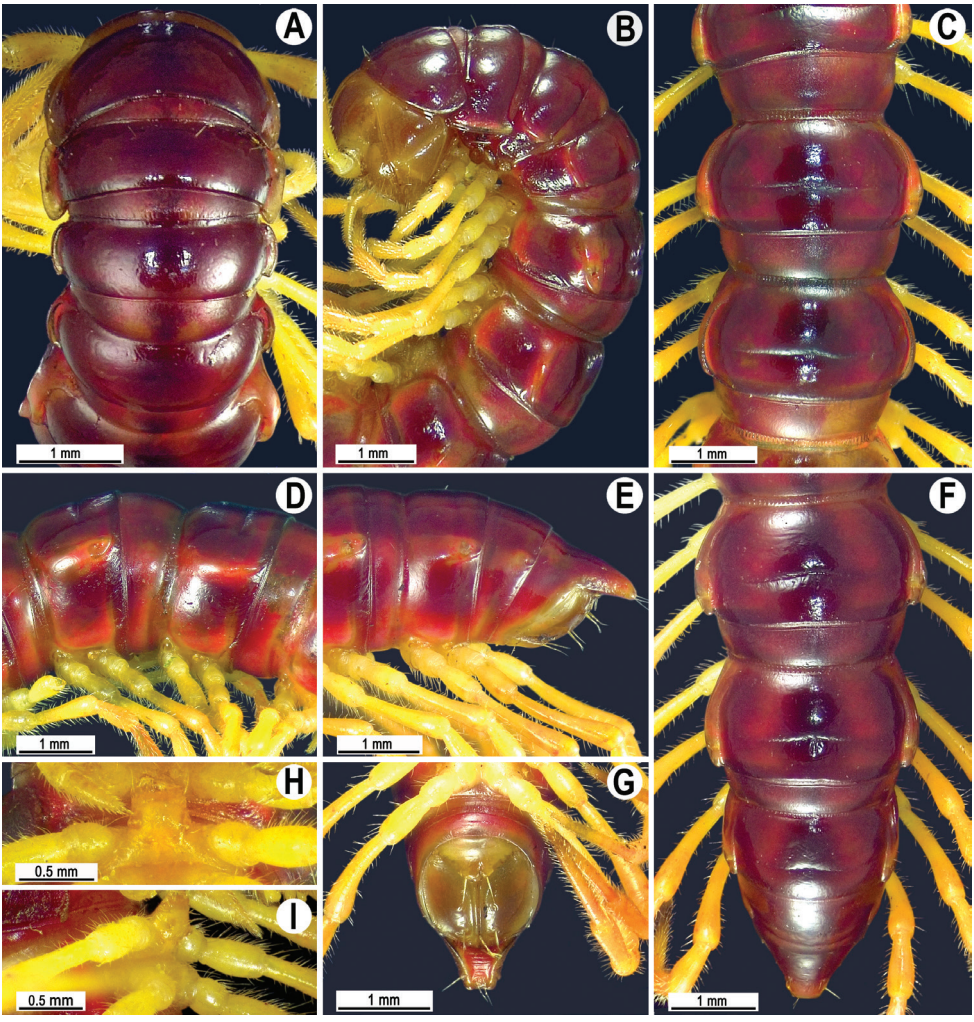

Figure 3. *Malayorthomorpha halabala* sp. nov., ♂ holotype **A, B** anterior part of body, dorsal and lateral views, respectively **C, D** segments 10 and 11, dorsal and lateral views, respectively **E–G** posterior part of body, lateral, dorsal and subventral views, respectively **H, I** sternal cones between coxae 4, subcaudal and sublateral views, respectively.

Gonopods (Figs 4A–D, 5) simple; coxa a little curved caudad, densely setose distoventrally. Prefemur as usual, densely setose, about 1/3 as long as femorite + postfemoral part. Femorite rather stout, wider than prefemur or postfemur, slightly expanded distad, suberect, showing a distinct mesal groove/hollow (**g**), with a sulcus demarcating a postfemoral part; seminal groove running entirely mesally along fermorite, solenomere (**sl**) flagelliform, almost fully sheathed by solenophore (**sph**). Lamina medialis (**lm**) well developed, short and unciform, terminal lobe sheathing the tip of solenomerite. Lamina lateralis (**ll**) elevated, prominent, stout, expanded apically, denticulate at caudal edge (Figs 3A, B, 4C, D).

Etymology. To emphasize Hala-Bala Wildlife Sanctuary, the type locality. Noun in apposition.

Remarks. A comparison of these two species shows only a few differences, but they are sufficient to distinguish both. The type locality of *M. siveci*, Park Belum, is located quite far away (ca. 50 km) from this new place. In addition, because the elevations between the two localities are greater than 1000 meters above sea-level, it seems

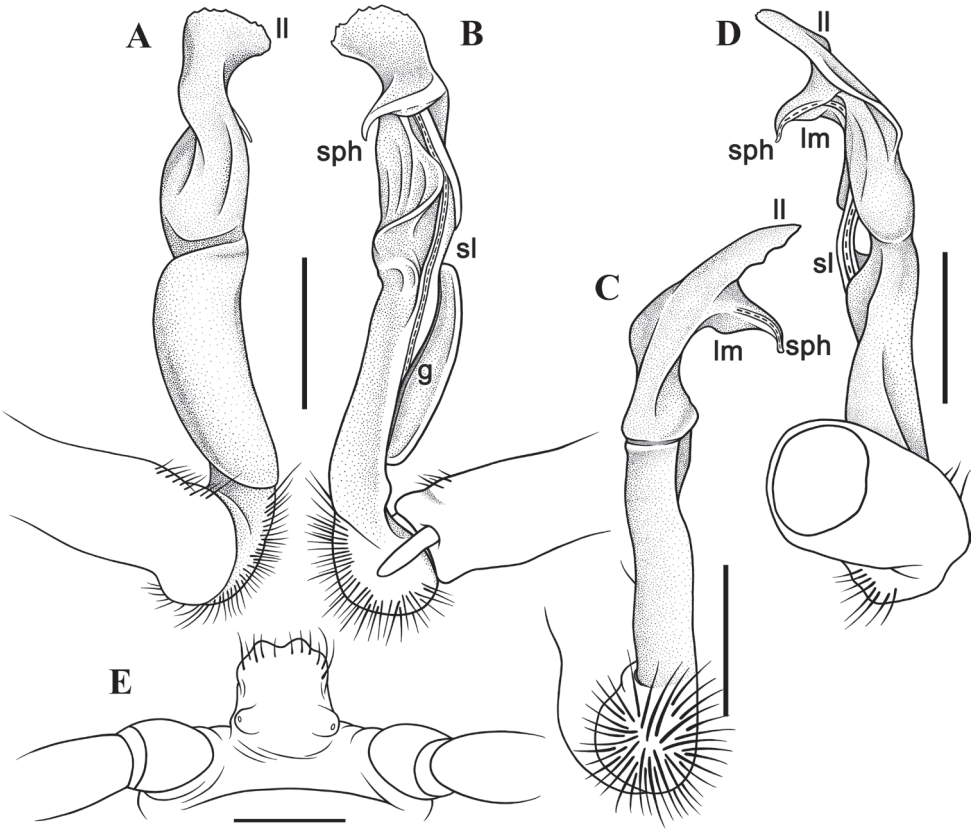

Figure 4. *Malayorthomorpha halabala* sp. nov., ♂ holotype, right gonopod **A–D** lateral, mesal, suboral and subcaudal views, respectively **E** sternal cones between coxae 4, subcaudal view. Abbreviations: **ll** lamina lateralis, **lm** lamina medialis, **sl** solenomere, **sph** = solenophore. Scale bars: 0.5 mm.

improbable that the species is one and the same. Consequently, we conclude that the two are obviously distinct species.

The specimens were collected in a primary sub-elfin montane forest with no significant disturbance due to human activity, in a high mountainous area of southernmost Thailand (Fig. 2B, C). The area is dominated by a single plant species, *Dacrydium elatum*. The canopy of *Dacrydium elatum* is low (ca. 10–15 m above ground), flat and continuously covering the area. The understorey is dense and covered with dwarf branches of small hardwood trees and teeming with bryophytes, lichens, orchids and ferns. The forest floor is with abundant orchids, ferns, liverworts, and thick slowly degraded bio-litters. The female specimen was easy to spot on the substrate and observed crawling on the leaf litter surface (Fig. 1A).

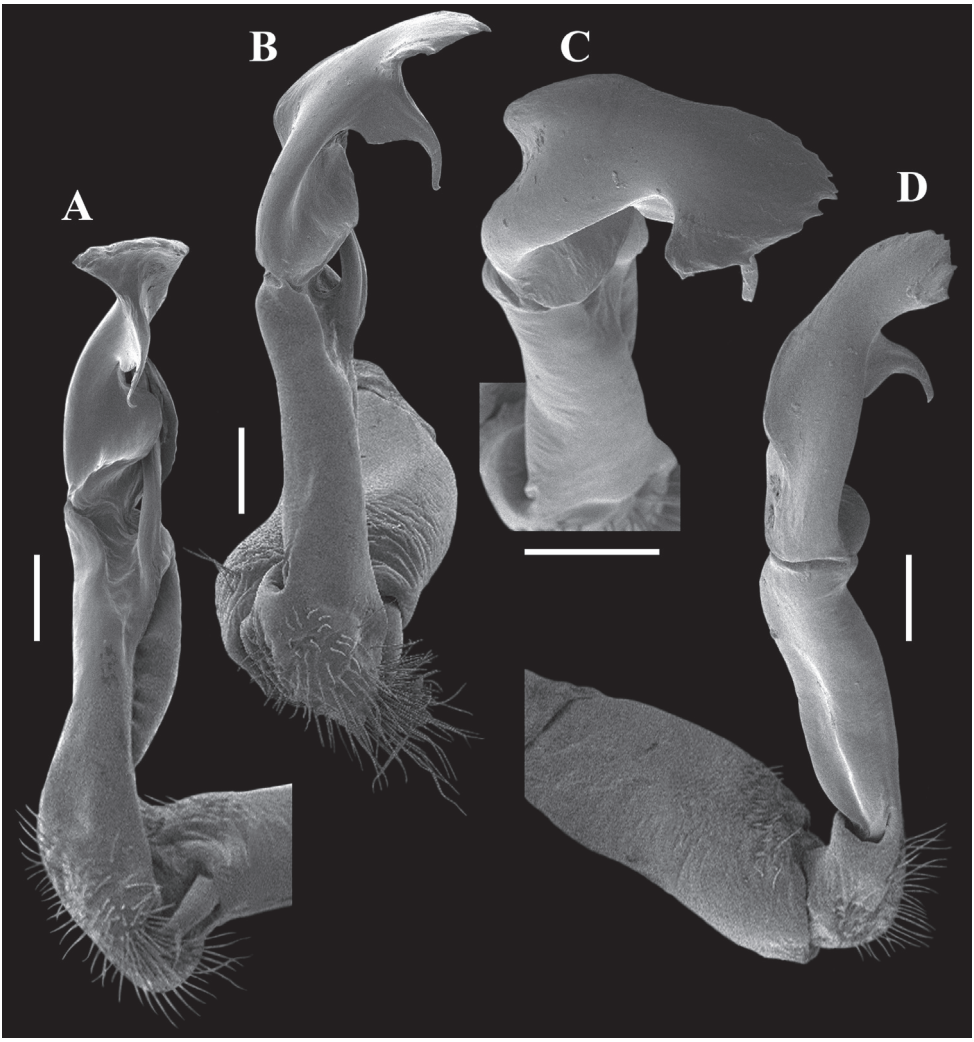

Figure 5. *Malayorthomorpha halabala* sp. nov., ♂ holotype, right gonopod **A–D** submesal, oral, subsuperior and sublateral views, respectively. Scale bars: 0.2 mm.

***Malayorthomorpha hulutbeeda* sp. nov.**
https://zoobank.org/49D76123-EB7C-4682-BD8F-48881036EDDC
Figs 6–8

Material examined. ***Holotype*:** Thailand – Yala Province • ♂; Betong District, elfin montane forest (Malaya Phytochorion province); 1430 m a.s.l.; 25 May 2022; Wisut Sittichaya leg.; CUMZ.

Diagnosis. This new species is distinguished from its two congeners in sternal process between male coxae 4 linguiform with a rounded tip, and lamina lateralis of gonopodal solenophore triangular, apically bifid and protruded laterally.

Description. Length of holotype 31.5 mm, width of midbody pro- and metazonae 2.7 and 3.0 mm, respectively.

Colouration of alcohol material after one week of preservation dark red brown (Fig. 6A–F); paraterga paler, head and antennae light brown to brown (Fig. 6A, B), legs and venter contrasting light yellow to brown (Fig. 6), antennae and legs increasingly darker brown distally (Fig. 6B, E, G).

All characters as in *M. halabala* sp. nov., except as follows.

Antennae rather long, extending caudally past metaterga 4 when stretched dorsally. Collum with three transverse rows of setae: 4+4 in anterior, 2+2 in intermediate, and 3+3 in posterior row; with a small lateral setigerous incision near midway (Fig. 6A, B).

Paraterga 2 broad, anterior edge angular and rounded, lateral edge with a small notch at about 1/4 in front of caudal corner (Fig. 6A). Calluses on paraterga rather narrow, delimited by a sulcus fully on dorsal side and in posterior half on ventral side; on poreless rings narrower than on pore-bearing ones in dorsal view (Fig. 6B, D, E).

Transverse sulcus distinct (Fig. 6A, C, F), complete on metaterga 5–17, narrow, line-shaped, rather deep, not reaching the bases of paraterga, smooth at bottom, incomplete and nearly wanting on ring 18. Stricture between pro- and metazona wide, deep, beaded at bottom down to base of paraterga starting with segment 5 (Fig. 6A–F). Pleurosternal carinae complete crests with a sharp caudal tooth on rings 2–4, increasingly reduced and retaining a sharp caudal tooth on rings 5 and 6 thereafter, retaining a small caudal tooth on ring 7, missing further on (Fig. 6B, D, E).

Hypoproct roundly subtriangular, setigerous knobs at caudal edge very small and well-separated (Fig. 6G).

Sterna moderately setose, shining, cross-impressions shallow, without modifications; an entire, large, linguiform, sternal lobe between ♂ coxae 4, with a pair of small denticles laterally near base (Figs 6H, I, 7E). An inconspicuous and low ridge present in front of gonopod aperture. Legs long and slender, midbody ones ca. 1.6–1.9 times as long as body height, without modifications, ♂ tarsal brushes absent.

Gonopods (Figs 7A–D, 8) rather simple; coxa almost straight caudad, densely setose distoventrally. Prefemur as usual, densely setose, about 1/3 as long as femorite + postfemoral part. Femorite stout, suberect, showing a distinct mesal groove/hollow (**g**), with a sulcus demarcating a postfemoral part; seminal groove running entirely mesally

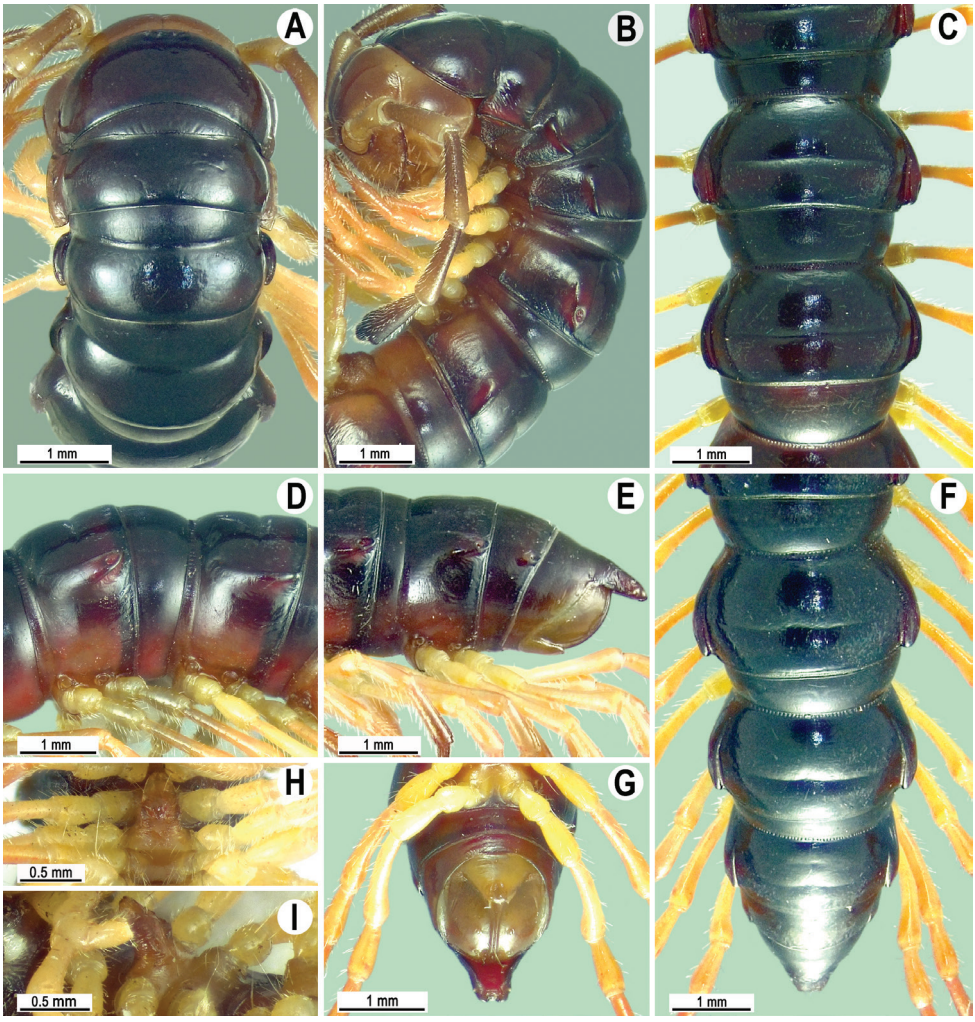

Figure 6. *Malayorthomorpha hulutbeeda* sp. nov., ♂ holotype **A, B** anterior part of body, dorsal and lateral views, respectively **C, D** segments 10 and 11, dorsal and lateral views, respectively **E–G** posterior part of body, lateral, dorsal and subventral views, respectively **H, I** sternal cones between coxae 4, subcaudal and sublateral views, respectively

along fermorite, solenomere (**sl**) flagelliform, almost fully sheathed by solenophore (**sph**). Lamina medialis (**lm**) well developed, thick and large, unciform, terminal lobe sheathing the tip of solenomere. Lamina lateralis (**ll**) triangular in shape, protruding laterally, tapered apically, bifid at tip (Figs 7C, D, 8A, 8C–D).

Etymology. To emphasize "*hulutbeeda*" which means "flat-back millipede" in Malay dialect, a noun in apposition. A Malay dialect language is mainly used in three provinces of southern Thailand where the holotype was obtained.

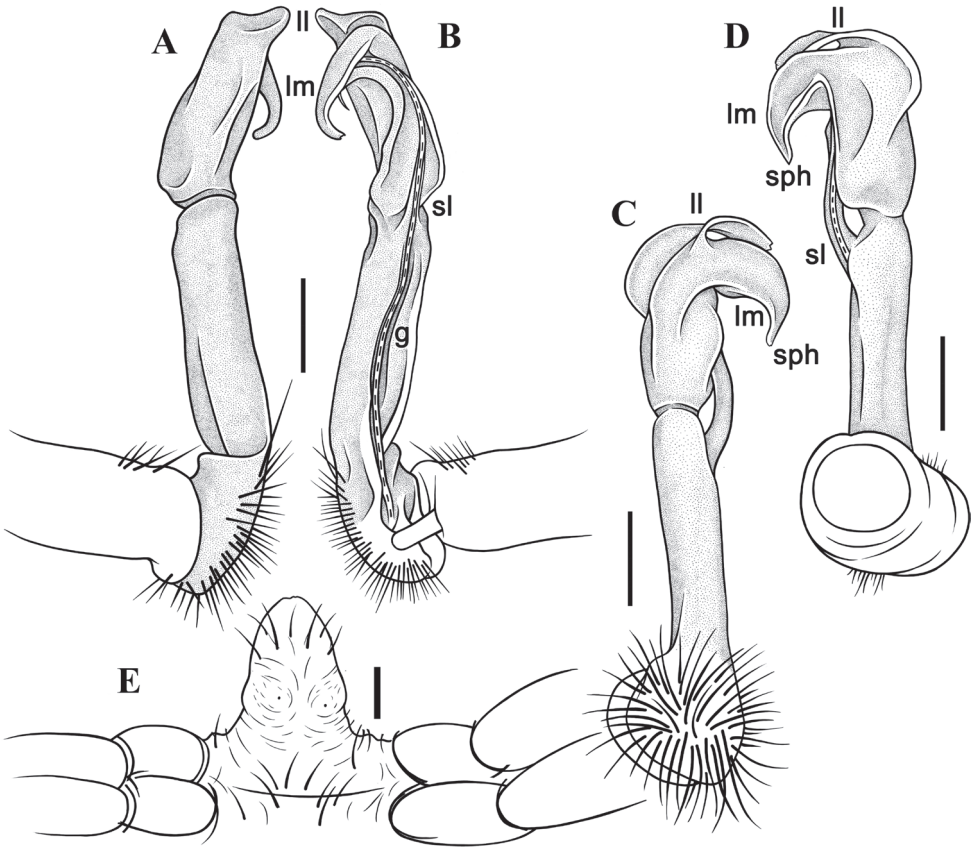

Figure 7. *Malayorthomorpha hulutbeeda* sp. nov., ♂ holotype, right gonopod **A–D** lateral, mesal, oral and caudal views, respectively **E** sternal cones between coxae 4, subcaudal view. Abbreviations: **ll** lamina lateralis, **lm** lamina medialis, **sl** solenomere, **sph** solenophore. Scale bars: 0.2 mm.

Remark. This species was found living together with *M. halabala* sp. nov. Moreover, according to our observations, they may even occur syntopically, sharing the same habitat: leaf litter surface, branches of trees and tree trunks.

Discussion and conclusion

In accordance with the previous observations of related genera such as *Orthomorpha* Bollman, 1893, *Desmoxytes* Chamberlin, 1923 and *Tylopus* Jeekel, 1968, the coexistence of congeners is quite common to come across in Paradoxosomatidae generally and Orthomorphini in particular. So the syntopy of *Malayorthomorpha halabala* sp. nov. and *M. hulutbeeda* sp. nov. is not unusual. For example, *Desmoxytes planata* (Pocock, 1895) was discovered beside *D. octoconigera* Srisonchai, Enghoff & Panha, 2018, *D. golovatchi* Srisonchai, Enghoff & Panha, 2018 and *D. purpurosea* Enghoff, Sutcharit

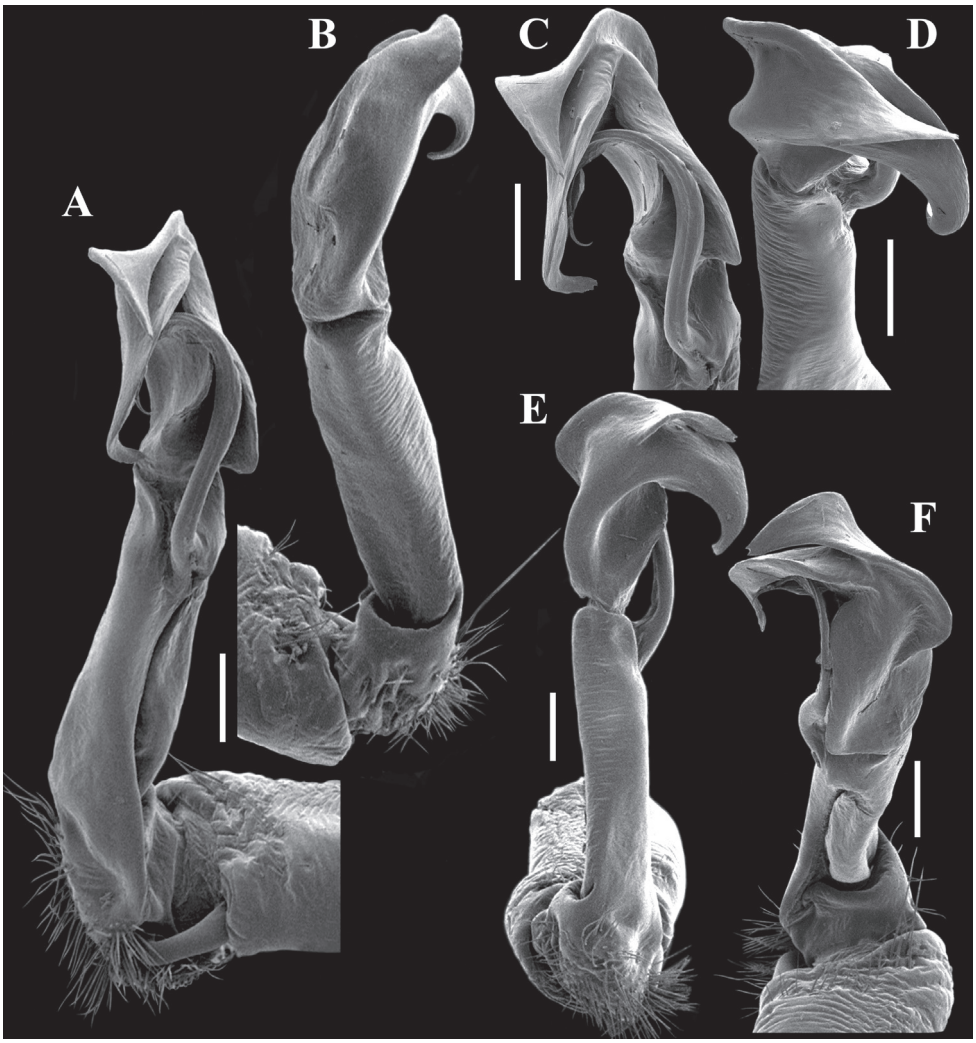

Figure 8. *Malayorthomorpha hulutbeeda* sp. nov., ♂ holotype, right gonopod **A, B** mesal and lateral views, respectively **C–F** submesal, subsuperior, oral and subcaudal views, respectively. Scale bars: 0.2 mm

& Panha, 2007 in several places (Srisonchai et al. 2018a). *Nagaxytes erecta* Srisonchai, Enghoff & Panha, 2018 and *N. gracilis* Srisonchai, Enghoff & Panha, 2018 were found jointly at Daowadueng Cave and Wat Sunantha Wanaram in Kanchanaburi Province, Thailand. Both latter species also show a very similar pattern of gonopodal structure (Srisonchai et al. 2018b). In the genus *Tylopus*, numerous species have been reported co-occurring in larger mountainous regions, such as Doi Inthanon (10 species) and Doi Suthep (10 species) in Thailand. However, some of them, at least in adult stages, appear to reflect separate phenofaunas that are restricted to relatively limited time periods and therefore do not overlap with others (Likhitrakarn et al. 2010, 2014, 2016).

Therefore, it is far from surprising that both new species have been found to coexist at the same place. Although they share the same habitat, they may have distinct microhabitats, although this remains speculation at this stage.

Malayorthomorpha species are presently endemic to southern Thailand and northern Peninsular Malaysia, both of which are located within the Titiwangsa Mountain Range, which is known as Peninsular Malaysia's backbone and longest mountain ridge. It begins in the north of southern Thailand, crosses the Malaysian border, enters the Negeri Sembilan valley, and terminates in the south near Jelebu, Negeri Sembilan (Chan et al. 2019). Mount Korbun is the highest peak in the Titiwangsa Range, reaching 2183 m above sea-level, and the second highest mountain in Peninsular Malaysia. In terms of biodiversity, the Mount Korbun area alone supports at least 18 amphibian, 134 bird, 42 mammal, and 18 reptile species, in addition to around 460 kinds of flowering plants and approximately 100 species of ferns and fern allies (Chan et al. 2019; Musthafa and Abdullah 2019). Due to the high biodiversity this mountain range supports, there are still many undiscovered species of flora and fauna. Thus, there are numerous unexplored millipede habitats in southern Thailand, particularly in the Pattani and Narathiwat provinces. Without doubt, new and exciting species will be discovered, and new localities reported, in this and surrounding regions in the future.

Acknowledgements

This research was encouraged and supported by Professor Dr Somsak Panha, Animal Systematics Research Unit, Department of Biology, Faculty of Science, Chulalongkorn University. One of us (SIG) was partly supported by the Presidium of the Russian Academy of Sciences, Program No. 41 "Biodiversity of Natural Systems and Biological Resources of Russia". We are most grateful to Mr Sunate Karapan and all members of Hala-Bala Wildlife Research Station for facilitating us in the collection of material. Special thanks go to Assistant Professor Dr Surasak Kuimalee, Science and Technology Service center, Faculty of Science, Maejo University, for skillfully taking SEM micrographs.

References

AVMA (2013) AVMA guidelines for the euthanasia of animals. https://www.avma.org/KB/Policies/Documents/euthanasia.pdf [Accessed on: 2022-2-2]

Bhansali S, Wesener T (2022) New Thai Giant Pill-Millipede species, with genetic barcoding data for Thai species (Diplopoda, Sphaerotheriida, Zephroniidae). Zootaxa 5105(3): 357–380. https://doi.org/10.11646/zootaxa.5105.3.2

Chan KO, Muin MA, Anuar S, Andam J, Razak N, Aziz MA (2019) First checklist on the amphibians and reptiles of Mount Korbu, the second highest peak in Peninsular Malaysia. Check List 15(6): 1055–1069. https://doi.org/10.15560/15.6.1055

Demange JM (1961) Matériaux pour servir à une révision des Harpagophoridae. Mémoires du Muséum national d`Histoire naturelle, Sér. A (Zool.) 24: 1–274.

Enghoff H (2005) The millipedes of Thailand (Diplopoda). Steenstrupia 29(1): 87–103.

Golovatch SI (1993) On several new or poorly-known Oriental Paradoxosomatidae (Diplopoda Polydesmida). Arthropoda Selecta 2(1): 3–14. https://doi.org/10.15298/arthsel.30.1.01

Golovatch SI (1997) On several new or poorly-known Oriental Paradoxosomatidae (Diplopoda Polydesmida), V. Arthropoda Selecta 5(3/4): 131–141. [for 1996]

Golovatch SI (1998) On several new or poorly-known Oriental Paradoxosomatidae (Diplopoda Polydesmida), VI. Arthropoda Selecta 6(3/4): 35–46.

Golovatch SI, Enghoff H (1993) Review of the millipede genus *Tylopus*, with descriptions of new species from Thailand (Diplopoda, Polydesmida, Paradoxosomatidae). Steenstrupia 19(3): 85–125.

Huber BA, Petcharad B, Bumrungsri S (2015) Revision of the enigmatic Southeast Asian spider genus *Savarna* (Araneae, Pholcidae). European Journal of Taxonomy 160(160): 1–23. https://doi.org/10.5852/ejt.2015.160

Jeekel CAM (1968) On the classification and geographical distribution of the family Paradxosomatidae (Diplopoda, Polydesmida). Academisch Proefschrift, Rotterdam, 162 pp.

Likhitrakarn N, Golovatch SI, Prateepasen R, Panha S (2010) Review of the genus *Tylopus* Jeekel, 1968, with descriptions of five new species from Thailand (Diplopoda, Polydesmida, Paradoxosomatidae). ZooKeys 72: 23–68. https://doi.org/10.3897/zookeys.72.744

Likhitrakarn N, Golovatch SI, Panha S (2011) Revision of the Southeast Asian millipede genus *Orthomorpha* Bollman, 1893, with the proposal of a new genus (Diplopoda, Polydesmida, Paradoxosomatidae). ZooKeys 131: 1–161. https://doi.org/10.3897/zookeys.131.1921

Likhitrakarn N, Golovatch SI, Panha S (2014) Three new species of the millipede genus *Tylopus* Jeekel, 1968 from Thailand, with additional notes on species described by Attems (Diplopoda, Polydesmida, Paradoxosomatidae). ZooKeys 435: 63–91. https://doi.org/10.3897/zookeys.435.8086

Likhitrakarn N, Golovatch SI, Panha S (2016) The millipede genus *Tylopus* Jeekel, 1968 (Diplopoda, Polydesmida, Paradoxosomatidae), with a key and descriptions of eight new species from Indochina. European Journal of Taxonomy 195(195): 1–47. https://doi.org/10.5852/ejt.2016.195

Likhitrakarn N, Golovatch SI, Jeratthitikul E, Srisonchai R, Sutcharit C, Panha S (2020) A remarkable new species of the millipede genus *Trachyjulus* Peters, 1864 (Diplopoda, Spirostreptida, Cambalopsidae) from Thailand, based both on morphological and molecular evidence. ZooKeys 925: 55–72. https://doi.org/10.3897/zookeys.925.49953

Likhitrakarn N, Golovatch SI, Jantarit S (2021a) Two new species of the millipede genus *Glyphiulus* Gervais, 1847 (Diplopoda, Spirostreptida, Cambalopsidae) from caves in northern Thailand. ZooKeys 1056: 173–189. https://doi.org/10.3897/zookeys.1056.71395

Likhitrakarn N, Golovatch SI, Srisonchai R, Sutcharit C (2021b) Two New Species of the Giant Pill-Millipede Genus *Zephronia* Gray, 1832 from Thailand (Diplopoda: Sphaerotheriida: Zephroniidae). Tropical Natural History 21(1): 12–26.

Likhitrakarn N, Golovatch SI, Panha S (2022) The Oriental millipede genus *Nepalella* Shear, 1979, with the description of a new species from Thailand and an updated key (Diplopoda,

Chordeumatida, Megalotylidae). ZooKeys 1084: 183–199. https://doi.org/10.3897/zookeys.1084.78744

Mršić N (1996) On three new Paradoxosomatidae from Malaysia (Diplopoda Polydesmida). Arthropoda Selecta 5(1/2): 139–144.

Musthafa MM, Abdullah F (2019) Coleoptera of Genting Highland, Malaysia: Species richness and diversity changes along the elevations. Museu de Ciències Naturals de Barcelona. Miscel·lània. Zoològica 17: 123–144. https://doi.org/10.15470/i0uuis

Myers N, Mittermeier RA, Mittermeier CG, Da Fonseca G, Kent J (2000) Biodiversity hotspots for conservation priorities. Nature 403(6772): 853–858. https://doi.org/10.1038/35002501

Nguyen AD, Sierwald P (2013) A worldwide catalog of the family Paradoxosomatidae Daday, 1889 (Diplopoda: Polydesmida). Check List 9(6): 1132–1353. https://doi.org/10.15560/9.6.1132

Pimvichai P, Enghoff H, Panha S (2009) A revision of the *Thyropygus allevatus* group. Part 1: the *T. opinatus* subgroup (Diplopoda: Spirostreptida: Harpagophoridae). Zootaxa 2016(1): 17–50. https://doi.org/10.11646/zootaxa.2016.1.2

Pimvichai P, Enghoff H, Panha S, Backeljau T (2018) Morphological and mitochondrial DNA data reshuffle the taxonomy of the genera *Atopochetus* Attems, *Litostrophus* Chamberlin and *Tonkinbolus* Verhoeff (Diplopoda: Spirobolida: Pachybolidae), with descriptions of nine new species. Invertebrate Systematics 32(1): 159–195. https://doi.org/10.1071/IS17052

Pimvichai P, Enghoff H, Panha S, Backeljau T (2020) Integrative taxonomy of the new millipede genus *Coxobolellus*, gen. nov. (Diplopoda: Spirobolida: Pseudospirobolellidae), with descriptions of ten new species. Invertebrate Systematics 34: 591–617. https://doi.org/10.1071/IS20031

Pocock RI (1889) Contributions to the fauna of Mergui and its archipelago, Volume 1: Myriopoda. Report on the Myriopoda of the Mergui Archipelago, collected for the Trustees of the Indian Museum, Calcutta, by Dr. John Anderson, F.R.S., Superintendant of the Museum. Zoological Journal of the Linnean Society 21: 287–330. https://doi.org/10.1111/j.1096-3642.1889.tb00980.x

Rosenmejer T, Enghoff H, Moritz L, Wesener T (2021) Integrative description of new giant pill-millipedes from southern Thailand (Diplopoda, Sphaerotheriida, Zephroniidae). European Journal of Taxonomy 762: 108–132. https://doi.org/10.5852/ejt.2021.762.1457

Shelley RM, Sierwald P, Kiser SB, Golovatch SI (2000) Nomenclator generum et familiarum Diplopodorum II. A List of the Genus and Family-Group Names in the Class Diplopoda from 1958 through 1999. Pensoft, Sofia, 167 pp.

Sinclair FG (1901) On the myriapods collected during the "Skeat Expedition" to the Malay Peninsula, 1899–1900. Proceedings of the Zoological Society of London 71(2): 505–533. https://doi.org/10.1111/j.1469-7998.1902.tb08186.x

Srisonchai R, Enghoff H, Likhitrakarn N, Panha S (2018a) A revision of dragon millipedes I: Genus *Desmoxytes* Chamberlin, 1923, with the description of eight new species (Diplopoda, Polydesmida, Paradoxosomatidae). ZooKeys 761: 1–177. https://doi.org/10.3897/zookeys.761.24214

Srisonchai R, Enghoff H, Likhitrakarn N, Panha S (2018b) A revision of dragon millipedes II: The new genus *Nagaxytes* gen. nov., with the description of three new species (Diplopoda, Polydesmida, Paradoxosomatidae). European Journal of Taxonomy 462(462): 1–44. https://doi.org/10.5852/ejt.2018.462

Srisonchai R, Enghoff H, Likhitrakarn N, Panha S (2018c) A revision of dragon millipedes III: The new genus *Gigaxytes* gen. nov., with the description of three new species (Diplopoda, Polydesmida, Paradoxosomatidae). European Journal of Taxonomy 463(463): 1–43. https://doi.org/10.5852/ejt.2018.463

Srisonchai R, Enghoff H, Likhitrakarn N, Panha S (2018d) A revision of dragon millipedes IV: The new genus *Spinaxytes*, with the description of nine new species (Diplopoda, Polydesmida, Paradoxosomatidae). ZooKeys 797: 19–69. https://doi.org/10.3897/zookeys.797.29510

Srisonchai R, Likhitrakarn N, Sutcharit C, Jeratthitikul E, Siriwut W, Thrach P, Chhuoy S, Ngor PB, Panha S (2020) A new micropolydesmoid millipede of the genus *Eutrichodesmus* Silvestri, 1910 from Cambodia, with a key to species in mainland Southeast Asia (Diplopoda, Polydesmida, Haplodesmidae). ZooKeys 996: 59–91. https://doi.org/10.3897/zookeys.996.57411

Srisonchai R, Sutcharit C, Likhitrakarn N (2021) The giant pill-millipede genus *Zephronia* Gray, 1832 from Thailand, with a redescription of *Z. siamensis* Hirst, 1907 and descriptions of three new species (Diplopoda, Sphaerotheriida, Zephroniidae). ZooKeys 1067: 19–56. https://doi.org/10.3897/zookeys.1067.72369

Wang YM, Tang MC (1965) Seria 1R: The millipedes of Malay Archipelago and South Sea Islands: Singapore, Sarawak and Sumatra. Quarterly Journal of the Taiwan Museum 18: 399–441.

ZooKeys 1118: 21–38 (2022)
doi: 10.3897/zookeys.1118.85810
https://zookeys.pensoft.net

RESEARCH ARTICLE

A peer-reviewed open-access journal
ZooKeys
Launched to accelerate biodiversity research

An updated list of butterflies (Lepidoptera, Papilionoidea) of two Guatemalan seasonally dry forests

Jiichiro Yoshimoto[1], José Luis Salinas-Gutiérrez[2], Mercedes Barrios[3], Andrew D. Warren[4]

1 *Laboratorio de Entomología Sistemática, Centro de Estudios Ambientales y Biodiversidad, Universidad del Valle de Guatemala, Apartado Postal 82, 01901, Guatemala City, Guatemala* **2** *Departamento de Biología Evolutiva, Facultad de Ciencias, Universidad Nacional Autónoma de México, Apartado Postal 70–399, México 04510 DF, Mexico* **3** *Centro de Estudios Conservacionistas (CECON), Universidad de San Carlos de Guatemala, Avenida La Reforma 0-53, Zona 10, Guatemala City, Guatemala* **4** *McGuire Center for Lepidoptera and Biodiversity, Florida Museum of Natural History, University of Florida, 3215 Hull Rd., UF Cultural Plaza, Gainesville, Florida 32611-2710, USA*

Corresponding author: Jiichiro Yoshimoto (jyoshimoto@uvg.edu.gt)

Academic editor: Martin Wiemers | Received 25 April 2022 | Accepted 26 July 2022 | Published 17 August 2022

https://zoobank.org/65FEBFBE-4565-4D86-8DFA-8D79F03C2533

Citation: Yoshimoto J, Salinas-Gutiérrez JL, Barrios M, Warren AD (2022) An updated list of butterflies (Lepidoptera, Papilionoidea) of two Guatemalan seasonally dry forests. ZooKeys 1118: 21–38. https://doi.org/10.3897/zookeys.1118.85810

Abstract

Guatemala has a great diversity of butterflies, although there have been few intensive surveys on Lepidoptera in the country so far. We present an updated list of 218 species in 149 genera, 19 subfamilies, and six families of butterflies sampled at two seasonally dry forests in the Salamá and Motagua valleys in central and eastern Guatemala, by integrating new data from field surveys conducted in 2014–2021 into our previously published data (Yoshimoto et al. 2018, 2019), with *Amblyscirtes elissa elissa* Godman, 1900, *Repens florus* (Godman, 1900), and *Niconiades nikko* Hayward, 1948 (Hesperiidae: Hesperiinae) as new country records. We collected a hairstreak species, *Chalybs hassan* (Stoll, 1790) (Lycaenidae: Theclinae), at the Motagua Valley site, representing the second record for Guatemala since the early 20th century, after we rediscovered it at the Salamá Valley site in 2011 and 2012 (Yoshimoto and Salinas-Gutiérrez 2015). Nymphalidae and Hesperiidae had larger numbers of species than the other four families at both sites. In Pieridae and Nymphalidae, species composition was similar between the sites, whereas in Lycaenidae, Riodinidae, and Papilionidae it differed more greatly between the sites. These results confirm the relatively high lepidopteran diversity of Guatemalan dry forests, noteworthy for the small areas that comprise the study sites, and represent marked similarities and differences in butterfly fauna and phenology within these forests.

Keywords
Annotated list, dissimilarity, Hesperiidae, inventory, Mesoamerica, Neotropics, seasonality

Introduction

Neotropical seasonally dry forests are rich in flora and fauna (Pennington et al. 2006; Dirzo et al. 2011), although their ecosystems have been deteriorating because of various anthropogenic disturbances, such as deforestation due to agricultural expansion (e.g., Chazdon et al. 2011). Dry forests in Guatemala also harbor high lepidopteran diversity as well; our previous studies documented more than 150 and 100 butterfly species at the two small forest reserves in central and eastern Guatemala, respectively (Yoshimoto et al. 2018, 2019). These species lists, however, are still incomplete, and obviously, more species remain to be sampled at these sites. Moreover, we detected marked seasonal patterns in butterfly species richness and several conspicuous differences in the lepidopteran fauna between the two sites (Yoshimoto et al. 2019). Thus, it was apparent that additional field surveys were needed to make quantitative between-site comparisons of species composition, in order to enhance our understanding of butterfly fauna and phenology of these forests.

In Guatemala, approximately 400 species of Hesperiidae and nearly 700 species of the remaining families of Papilionoidea have been reported (Austin et al. 1998; Barrios et al. 2006; Salinas-Gutiérrez et al. 2009, 2012; Salinas-Gutiérrez 2013). Despite such high lepidopteran diversity, Guatemala's butterfly fauna has been studied less intensively compared to neighboring countries; for example, in Mexico, exhaustive species lists for the whole country and for several states have been published (de la Maza et al. 1989, 1991; Luis-Martínez et al. 2011, 2016; Llorente-Bousquets et al. 2014), whereas Guatemala has had little research on Lepidoptera and few published inventories since the 20th century (but see Austin et al. 1996 and Yoshimoto et al. 2021). Continued field surveys in various parts of Guatemala are thus important to fill a gap in our knowledge of the Neotropical butterfly fauna, which will in turn contribute to biodiversity conservation in the country.

Here, we present an updated and integrated list of papilionoid species (including Hesperiidae; van Nieukerken et al. 2011) for the same dry forest sites where we conducted our previous studies (Yoshimoto et al. 2018, 2019), by adding the new data from subsequent field surveys performed in 2014–2021, correcting identification errors, and modifying some of the species names based on taxonomic changes. Additionally, we examine between-site differences in butterfly fauna by comparing species composition at the family level, and identify seasonal patterns at the species level.

Materials and methods

This study was conducted at the Los Cerritos Municipal Park (hereafter, Los Cerritos; Fig. 1a) in the Salamá Valley (a subwatershed of the Chixoy region) of Baja Verapaz

Department in central Guatemala (15°05'N, 90°18'W, 960–1160 m a.s.l., 69 ha), and at the Heloderma Natural Reserve (hereafter, Heloderma Reserve; Fig. 1b) in the Motagua Valley of Zacapa Department in eastern Guatemala (14°53'N, 89°47'W, 510–790 m a.s.l., 58 ha). The rainfall patterns are similar between the two areas, in which the rainy season usually begins in late May and ends in October; these six months were accordingly defined as the rainy season and the remaining months (November-April) as the dry season. This climatic trait fits the definition of seasonally dry tropical forests (4–6 months with rainfall being < 100 mm; Dirzo et al. 2011); see fig. 1 in Yoshimoto et al. (2018) and fig. 3 in Yoshimoto et al. (2019) for detailed precipitation information of each area.

The vegetation of both regions is characterized by an abundance of various aculeate plants such as cacti (Cactaceae). The most dominant species is a columnar cactus *Stenocereus pruinosus* (Otto) Buxb., with *Pilosocereus leucocephalus* (Poselg.) Byles & G. D. Rowley and *Pereskia lychnidiflora* DC., also being abundant at both sites. On the other hand, there exist some marked differences in flora and in forest landscape. Heloderma Reserve has a dense forest with many arboreal species such as *Bucida macrostachya* Standl. (Combretaceae), *Lysiloma divaricatum* (Jacq.) J. F. Macbr., *Leucaena collinsii* Britton & Rose (both Mimosaceae), and *Bursera excelsa* (Kunth) Engl. (Burseraceae), all of which can grow taller than the columnar cactus (Ariano-Sánchez and Salazar 2015; D. Ariano-Sánchez, pers. comm.; Fig. 1b). By contrast, none of these species have been reported from Los Cerritos (M. R. Álvarez, pers. comm.), where there are fewer high arboreal species and abundant shrubs and herbaceous plants (thus commonly called a spiny bush or scrub), thereby the columnar cactus being prominent in its forest landscape (Fig. 1a).

Field surveys were conducted on 21 days from July 2014 to August 2021 at Los Cerritos, and on 19 days from October 2017 to November 2021 at Heloderma Reserve. We collected adult butterflies with an insect net or photographed them in the daytime (09:00–17:00) at each site and in neighboring areas (a small garden at the foot of Los Cerritos and on a farm road adjacent to Heloderma Reserve). The individuals collected were mounted as voucher specimens and were deposited at the Colección de Artrópodos, Laboratorio de Entomología Sistemática, Universidad del Valle de Guatemala. All the individuals collected or photographed were identified to species or subspecies according to Warren et al. (2017). We did not include data for specimens that were not identified to species, except for *Calephelis* spp. (Riodinidae) and *Bolla* sp. (Hesperiidae: Pyrginae); see the footnotes of the Appendix 1 for the rationales for the inclusion of these data. We added all these data to our previous data (Yoshimoto et al. 2018, 2019), corrected identification errors, and modified scientific names of some of the species based on taxonomic changes, in order to compile an updated and integrated species list of the two sites. Note that the sampling methods were partially different in the previous surveys; only netting was done at Los Cerritos from January 2011 to November 2012, whereas at Heloderma Reserve between February 2016 and March 2017, data were obtained through netting, photographing, and observation; see Yoshimoto et al. (2018, 2019) for detailed information on the sampling methods for each site.

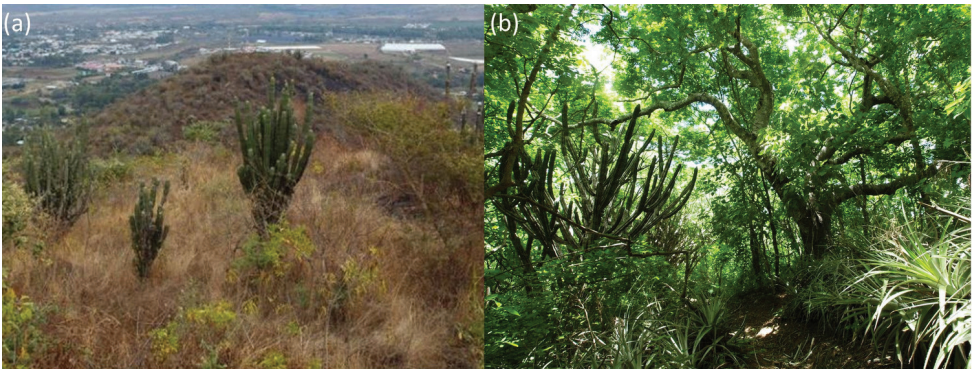

Figure 1. a Forest landscape of Los Cerritos Municipal Park and **b** Heloderma Natural Reserve.

The site-level estimated species richness was calculated by using the Chao II index (Chao et al. 2005; Gotelli and Colwell 2011), after pooling the data across observation dates for each month for each site. The total estimated species richness was similarly obtained after pooling these data across both sites. The Jaccard dissimilarity index was used to quantify the between-site similarity in species composition; this index was calculated for all data and for each of the six families (Papilionidae, Pieridae, Lycaenidae, Riodinidae, Nymphalidae, and Hesperiidae). All the analyses were performed using R 4.1.2. (R Development Core Team 2021) with the package Vegan (Oksanen et al. 2020).

Results

By integrating our previous data (Yoshimoto et al. 2018, 2019), a total of 218 species (including one unidentified taxon and 107 subspecies) in 149 genera from 19 subfamilies of six families were recorded at the two sites (Appendix 1). Hesperiidae was the richest family (71 species), followed by Nymphalidae, Lycaenidae, Pieridae, Riodinidae, and Papilionidae (66, 36, 20, 16, and 9 species, respectively). Los Cerritos had 166 species in 117 genera, and Heloderma Reserve had 139 species in 107 genera (Appendix 1), 16 and 41 species of which had been newly recorded in the subsequent surveys, respectively (Fig. 2). The estimated species richness (mean±SE) of each site based on the Chao II index is 216.27±16.35 and 187.35±17.74, respectively, indicating that approximately 76.8% and 74.2% of the species inhabiting each site were sampled. The total estimated species richness for both sites is 272.80±17.85 (79.9%).

We detected identification errors for 20 individuals (identified as 11 species in our previous studies) and determined them to represent 13 species in this study; ten individuals from Los Cerritos and ten from Heloderma Reserve have been determined to number eight and six different species, respectively, with one species, *Cissia themis*, shared between sites (Table 1). Additionally, Yoshimoto et al. (2019) incorrectly listed *Piruna* (Hesperiidae: Heteropterinae) in the subfamily Hesperiinae.

The following three skipper species (Hesperiidae: Hesperiinae) were recorded for the first time in Guatemala:

- ***Amblyscirtes elissa elissa*** **Godman, 1900.** Reserva Heloderma, Cabañas, Zacapa, GUATEMALA. Three specimens: 30-08-2016, J442; 26-09-2016, J478; 01-06-2018, J769. Collected by Jiichiro Yoshimoto. Identified by Andrew D. Warren. Note that the two individuals (J442 and J478) were misidentified as *Piruna* sp.1 in Yoshimoto et al. (2019), as shown in Table 1. The specimens were deposited in the Colección de Artrópodos, Laboratorio de Entomología Sistemática, Universidad del Valle de Guatemala, and are being cataloged (Fig. 3c). Distribution: Southwestern Mexico (Warren et al. 2017).
- ***Repens florus*** **(Godman, 1900).** Reserva Heloderma, Cabañas, Zacapa, GUATEMALA. One specimen: 23-10-2018, J800. Collected by Jiichiro Yoshimoto. Identified by Andrew D. Warren. The specimen was deposited as above and is being cataloged (Fig. 3d). Distribution: Eastern and Western Mexico, Belize, and Nicaragua (Warren et al. 2017).
- ***Niconiades nikko*** **Hayward, 1948.** Los Cerritos, Salamá, Baja Verapaz, GUATEMALA. One specimen: 16-11-2020, J1024. Collected and identified by Jiichiro Yoshimoto. The specimen was deposited as above and is being cataloged (Fig. 3e). Distribution: Eastern Mexico to Ecuador, Southern Brazil, and Paraguay (Warren et al. 2017).

Eighty-six species were shared between Los Cerritos and Heloderma Reserve (Table 2), which amounts to 51.8% and 61.9% of the species sampled at each site (the Jaccard dissimilarity index is 0.606). At both sites, species richness of Nymphalidae

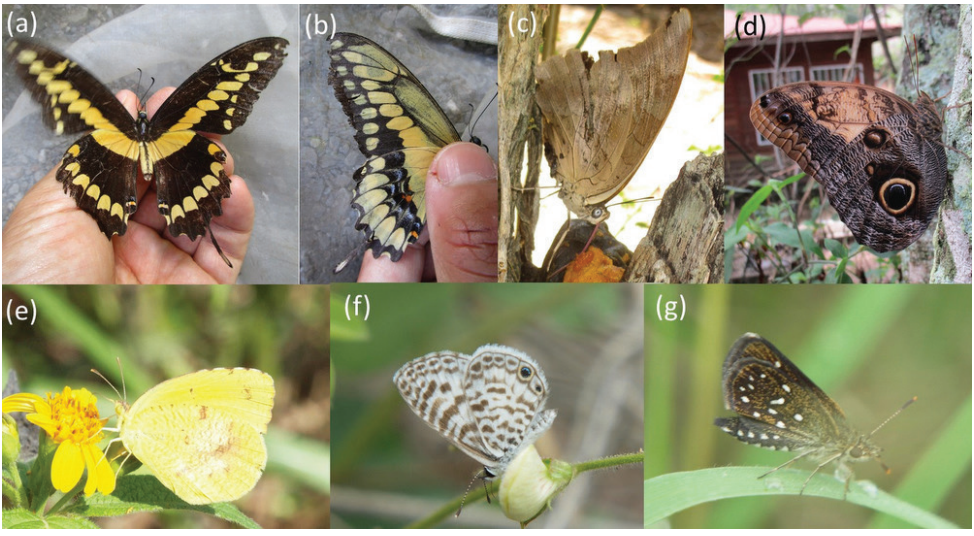

Figure 2. Six of the species that were newly recorded in the present study at Los Cerritos or Heloderma Reserve **a, b** *Heraclides rumiko* Shiraiwa & Grishin, 2014 (Papilionidae) **c** *Archaeoprepona demophon centralis* (Fruhstorfer, 1905) **d** *Caligo telamonius memnon* (C. Felder & R. Felder, 1867) (both Nymphalidae) **e** *Abaeis nicippe* (Cramer, 1779) (Pieridae) **f** *Leptotes cassius cassidula* (Boisduval, 1870) (Lycaenidae) **g** *Piruna aea* (Dyar, 1912) (Hesperiidae) **a–d, g** Heloderma Reserve **e, f** Los Cerritos. Note that *P. aea* had already been collected and identified to genus (*Piruna* sp.1) by Yoshimoto et al. (2019).

Table 1. Butterfly species that were sampled at Los Cerritos and Heloderma Reserve (abbreviated as LC and HR, respectively) and were misidentified in Yoshimoto et al. (2018, 2019). Corrected species names are shown in bold.

Family	Species		Sampling month, year, and site
	Correct identification	Previous identification	
Papilionidae	***Heraclides rumiko* Shiraiwa & Grishin, 2014**	*Heraclides cresphontes* (Cramer, 1777) [A]	Oct 2016 HR*
Pieridae	***Abaeis nicippe* (Cramer, 1779)**	*Pyrisitia proterpia* (Fabricius, 1775) [A]	Jul 2016 HR
Lycaenidae	***Strymon megarus* (Godart, [1824])**	*Strymon melinus franki* W. D. Field, 1938 [A]	Oct 2016 HR
Nymphalidae	***Anthanassa tulcis* (H. Bates, 1864)**	*Anthanassa dracaena phlegias* (Godman, 1901) [B]	May 2011 LC
Nymphalidae	***Chlosyne erodyle erodyle* (H. Bates, 1864)**	*Chlosyne lacinia lacinia* (Geyer, 1837) [B]	Oct 2011 LC, Jul 2012 LC
Nymphalidae	***Chlosyne rosita rosita* A. Hall, 1924**	*Chlosyne lacinia lacinia* (Geyer, 1837) [B]	Sep 2011 LC
Nymphalidae	***Cissia similis* (A. Butler, 1867)**	*Cissia pompilia* (C. Felder & R. Felder, 1867) [B]	May 2012 LC, Jun 2012 LC
Nymphalidae	***Cissia themis* (A. Butler, 1867)**	*Cissia pompilia* (C. Felder & R. Felder, 1867) [A, B]	Aug 2011 LC, Aug 2016 HR**, Oct 2016 HR
Hesperiidae	***Urbanus viterboana* (Ehrmann, 1907)**	*Urbanus proteus proteus* (Linnaeus, 1758) [B]	Nov 2011 LC
Hesperiidae	***Heliopetes macaira macaira* (Reakirt, [1867])**	*Heliopyrgus domicella domicella* (Erichson, [1849]) [B]	Jul 2012 LC
Hesperiidae	***Amblyscirtes elissa elissa* Godman, 1900**	*Piruna* sp.1 [A]	Aug 2016 HR, Sep 2016 HR
Hesperiidae	***Copaeodes aurantiaca* (Hewitson, 1868)**	*Ancyloxypha arene* (W. H. Edwads, 1871) [B]	Mar 2011 LC
Hesperiidae	***Cymaenes trebius* (Mabille, 1891)**	*Cymaenes tripunctus theogenis* (Capronnier, 1874) [A]	Sep 2016 HR**

[A] Listed in Yoshimoto et al. (2019).

[B] Listed in Yoshimoto et al. (2018).

*Specimen not collected (recorded only by photographing; see Fig. 2a, b for its images).

**Two individuals collected.

and Hesperiidae was greater than that of the other four families, although family-level species richness differed greatly between the sites (Table 2; Fig. 4). In particular, the proportion of Lycaenidae was much higher at Los Cerritos (18.7%) than at Heloderma Reserve (8.6%), which was mainly due to differences in the subfamily Theclinae (26 and 7 species, respectively: Appendix 1).

Family-level species composition also differed between the sites, and the magnitude of this difference varied among the six families (Table 2). The dissimilarity indices for Riodinidae, Lycaenidae, and Papilionidae were considerably larger, indicating that species composition differed more greatly between the sites in these families. Pieridae and Nymphalidae, by contrast, had smaller indices with many shared species, demonstrating that their species composition was relatively similar between the sites.

Ninety-three species (42.7%) occurred in both dry and rainy seasons, whereas 103 (47.2%) appeared only in the rainy season and 22 species (10.1%) only in the

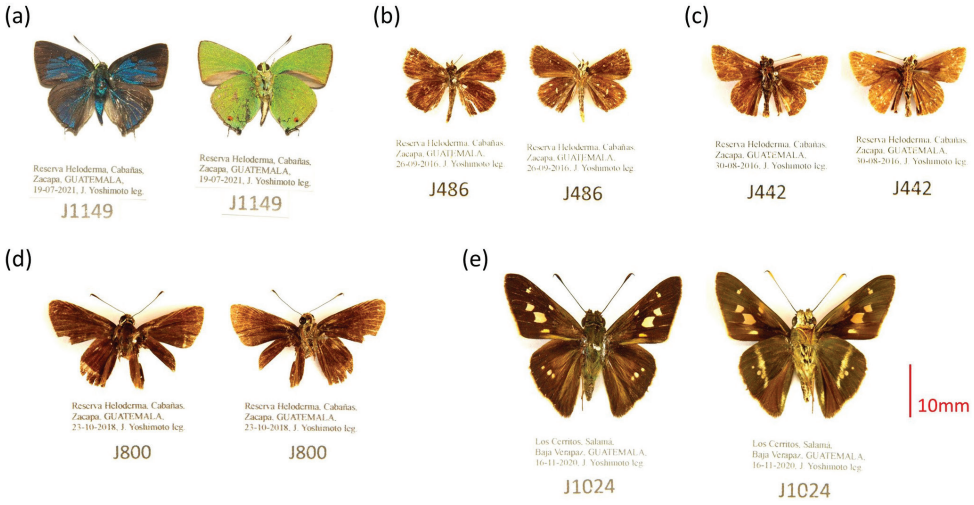

Figure 3. One species of hairstreak (Lycaenidae: Theclinae) **a** *Chalybs hassan* (Stoll, 1790), one species of skipperling (Hesperiidae: Heteropterinae) **b** *Piruna aea* (Dyar, 1912), and three species of grass-skippers (Hesperiidae: Hesperiinae) **c** *Amblyscirtes elissa elissa* Godman, 1900 **d** *Repens florus* (Godman, 1900), and **e** *Niconiades nikko* Hayward, 1948. The three grass-skipper species were newly recorded for Guatemala. Dorsal and ventral views, respectively, are shown at the left and right in each photograph.

Table 2. Species richness for six families at Los Cerritos and Heloderma Reserve, and comparisons of species composition at the family level between the sites, based on the number of shared species and the Jaccard dissimilarity index.

Family	Total No. species		No. shared species	Jaccard index
	Los Cerritos	Heloderma Reserve		
Papilionidae	7	4	2	0.778
Pieridae	16	17	13	0.350
Lycaenidae	31	12	7	0.806
Riodinidae	10	9	3	0.813
Nymphalidae	57	46	37	0.439
Hesperiidae	45	51*	24	0.662*

*The data for *Bolla* sp. were included in the species count but excluded from the Jaccard index analysis (see the footnote 7 of the Appendix 1 for its rationale).

dry season. The most frequently recorded species was *Eurema daira eugenia* (Wallengren, 1860) (Pieridae: Coliadinae), which was collected or observed throughout the year (Appendix 1). The second most frequently recorded species (in 11 months) were *Kricogonia lyside* (Godart, 1819) (Coliadinae) and *Hamadryas glauconome glauconome* (H. Bates, 1864) (Nymphalidae: Biblidinae), followed by *Pyrisitia proterpia* (Fabricius, 1775) (Coliadinae: in ten months), *Phoebis sennae marcellina* (Cramer, 1777) (Coliadinae), *Mestra amymone* (Ménétriés, 1857) (Biblidinae), and *Urbanus dorantes dorantes* (Stoll, 1790) (Hesperiidae: Eudaminae: all in nine months).

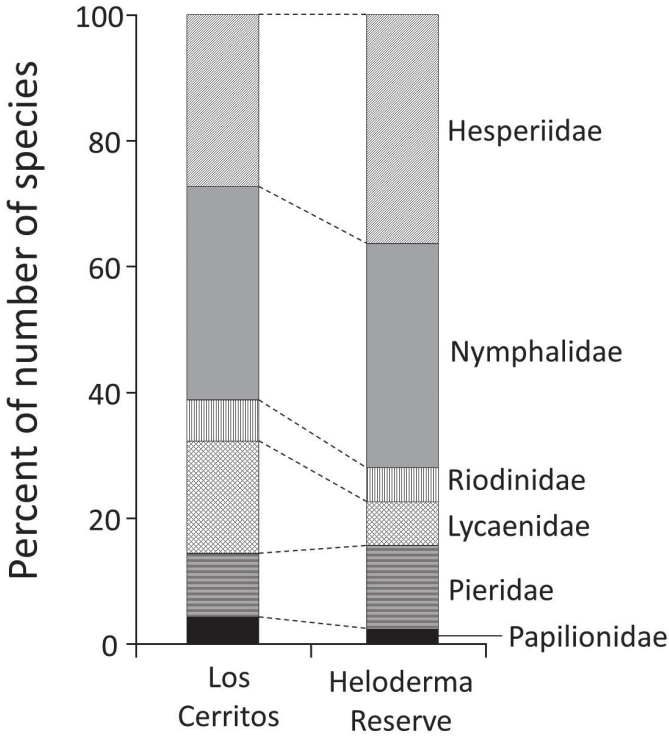

Figure 4. Proportion of species richness at the family level at Los Cerritos and Heloderma Reserve.

Discussion

A total of 218 species were recorded at the two dry forest sites during our 10-year field surveys, which confirms the relatively high lepidopteran diversity of Guatemalan seasonally dry forests for the small areas that comprise the study sites (<70 ha each). The estimated species richness suggests that nearly a quarter of the species inhabiting each site have yet to been recorded. The number of the additional species yielded in the subsequent surveys was more than twice greater at Heloderma Reserve than at Los Cerritos. The proportion of newly recorded species was much higher in Lycaenidae and Riodinidae; seven lycaenid species were added to the list for Los Cerritos, and seven lycaenid and four riodinid species were added to that of Heloderma Reserve, which nearly doubled the species richness of each family at this site (six lycaenid and five riodinid species in Yoshimoto et al. 2019). Among these species, the record of *Chalybs hassan* (Stoll, 1790) at Heloderma Reserve is highly important (Fig. 3a), as this species had not been reported for more than 100 years in Guatemala before we collected four individuals at Los Cerritos in 2011 and 2012 (Yoshimoto and Salinas-Gutiérrez 2015). These results highlight the importance of continuing butterfly surveys at both sites to create more exhaustive inventories, especially on small and taxonomically difficult taxa such as Lycaenidae and Riodinidae. Moreover, it is important to conduct research in other dry regions (e.g., the Nentón Valley in

northwestern Guatemala) and to make quantitative among-site comparisons of species richness and composition as well. All these studies will contribute to a comprehensive understanding of Neotropical butterfly fauna and distribution, and would serve as a scientific baseline for biodiversity conservation in Guatemalan dry regions.

More than half of the species sampled at each site were shared between the sites, suggesting that species composition is partially and moderately similar between Los Cerritos and Heloderma Reserve. Importantly, between-site similarity greatly differed among the six families. Higher similarity in Pieridae (especially in Coliadinae) would likely be associated with the distribution and abundance of their host plants, considering that coliadine larvae mostly feed on fabaceous plants such as *Senna* (e.g., DeVries 1987) and that these plants appear to be abundant at both sites.

In Lycaenidae and Riodinidae, species composition largely differed between the sites; in particular, Theclinae had considerable differences in species richness and composition (Appendix 1). In addition, most of these thecline species tended to be highly seasonal, as 25 out of 30 species were sampled only in the rainy season. In contrast to their marked seasonal pattern, *Strymon megarus* (Godart, [1824]) and *S. rufofusca* (Hewitson, 1877) occurred frequently also in the dry period at Heloderma Reserve; three and five individuals of each species were collected in both December and January at this site (Appendix 1). It should also be mentioned that *Hechtia guatemalensis* Mez (Bromeliaceae), one of the dominant bromeliad species at Heloderma Reserve (Fig. 1b), may be a possible foodplant for *S. megarus* at this site, as the larvae of this species are known to feed on bromeliads (Robbins 2010). Examination of abundance and distribution of host- and nectar-plants, as well as of larval and adult feeding behavior in relation to their phenology, would be an initial step to elucidate the bionomics of these species. Such surveys may also identify factors underlying the regional similarity and dissimilarity in the butterfly fauna.

We recorded *Amblyscirtes elissa elissa* Godman, 1900, *Repens florus* (Godman, 1900), and *Niconiades nikko* Hayward, 1948 (Hesperiidae: Hesperiinae) for the first time in Guatemala (Fig. 3c, d, e). Austin et al. (1998) listed *A. e. elissa* and *N. nikko* as species with a potential distribution in Guatemala. *Repens florus* could have been included in this category as well, as it is known to be distributed in the adjacent countries (Mexico, Belize, and Nicaragua; Warren et al. 2017). These results indicate that there still exists a gap in our knowledge of geographic distribution of Neotropical skipper species, again emphasizing the importance of more intensive research in Guatemala to bridge this gap.

Four individuals of *Piruna aea* (Dyar, 1912) (two in the previous survey and two in the subsequent one: Figs 2g, 3b) were collected at Heloderma Reserve. This is an interesting result, since most species in this genus are distributed in humid areas at higher elevation (1000–2700 m; Warren and González-Cota 1998). As Yoshimoto et al. (2019) pointed out, the wing pattern of these individuals is somewhat different from Mexican *P. a. aea* (Dyar, 1912), implying that *Piruna cingo sombra* Evans, 1955, described from Guatemala and currently considered a synonym of *P. a. aea*, may be a valid subspecies-level taxon. At present, this is difficult to determine, as very few specimens of this species have been sampled in Guatemala (Barrios et al. 2006).

Acknowledgements

We are grateful to Robert K. Robbins and Arturo Arellano Covarrubias for verifying some of our identifications of Theclinae and Riodinidae, respectively. We also thank Daniel Ariano Sánchez and María Renée Álvarez for providing us useful information on the fauna, flora, and geography of Guatemalan dry forests, Asociación Zootropic for permitting us to use the scientific station of Heloderma Reserve during our field surveys, Gilberto Salazar and Erick López for their logistic assistance at Heloderma Reserve, Edwin Reyes for helping us with butterfly sampling at Heloderma Reserve, and Fundación de Defensa del Medio Ambiente de Baja Verapaz (FUNDEMABV) for allowing us to conduct entomological surveys continuously at Los Cerritos. The authors have no support to report.

References

Ariano-Sánchez D, Salazar G (2015) Spatial ecology of the endangered Guatemalan Beaded Lizard *Heloderma charlesbogerti* (Sauria: Helodermatidae), in a tropical dry forest of the Motagua Valley, Guatemala. Mesoamerican Herpetology 2(1): 64–74. https://library.iucn-isg.org/documents/2015/Ariano-Sanchez_2015_Mesoamerican_Herpetology.pdf

Austin GT, Haddad NM, Méndez C, Sisk TD, Murphy DD, Launer AE, Ehrlich PR (1996) Annotated checklist of the butterflies of the Tikal National Park area of Guatemala. Tropical Lepidoptera 7(1): 21–37. https://journals.flvc.org/troplep/article/view/90056

Austin GT, Méndez C, Launer AE (1998) A preliminary checklist of Guatemala butterflies: Hesperiidae (Lepidoptera: Hesperioidea). Tropical Lepidoptera 9(Supplement 2): 8–19. https://journals.flvc.org/troplep/article/view/90138

Barrios MV, Méndez CA, Austin GT (2006). Las Hesperiidae (Lepidoptera: Hesperioidea) de Guatemala. In: Cano EB (Ed.) Biodiversidad de Guatemala Vol. I. Universidad del Valle de Guatemala, Guatemala, 431–439.

Brower AVZ (2006) Problems with DNA barcodes for species delimitation: 'ten species' of *Astraptes fulgerator* reassessed (Lepidoptera: Hesperiidae). Systematics and Biodiversity 4(2): 127–132. https://doi.org/10.1017/S147720000500191X

Brower AVZ (2010) Alleviating the taxonomic impediment of DNA barcoding and setting a bad precedent: names for ten species of '*Astraptes fulgerator*' (Lepidoptera: Hesperiidae: Eudaminae) with DNA-based diagnoses. Systematics and Biodiversity 8(4): 485–491. https://doi.org/10.1080/14772000.2010.534512

Chao A, Chazdon RL, Colwell RK, Shen TJ (2005) A new statistical approach for assessing similarity of species composition with incidence and abundance data. Ecology Letters 8(2): 148–159. https://doi.org/10.1111/j.1461-0248.2004.00707.x

Chazdon RL, Harvey CA, Martínez-Ramos M, Balvanera P, Stoner KE, Schondube JE, Avila Cabadilla LD, Flores-Hidalgo AM (2011) Seasonally dry tropical forest biodiversity and conservation value in agricultural landscapes of Mesoamerica. In: Dirzo R, Young HS, Mooney HA, Ceballos G (Eds) Seasonally dry tropical forests: ecology and conservation. Island Press, Washington DC, 195–219.

Cong Q, Grishin NV (2014) A new *Hermeuptychia* (Lepidoptera, Nymphalidae, Satyrinae) is sympatric and synchronic with *H. sosybius* in southeast US coastal plains, while another new *Hermeuptychi*a species not *hermes* inhabits south Texas and northeast Mexico. ZooKeys 379: 43–91. https://doi.org/10.3897/zookeys.379.6394

de la Maza RG, de la Maza J, White-López A (1989) La fauna de mariposas de México. Parte I. Papilionoidea (Lepidoptera: Rhopalocera). Revista de la Sociedad Mexicana de Lepidopterología 12: 39–98.

de la Maza J, White-López A, de la Maza RG (1991) La fauna de mariposas de México. Parte II. Hesperioidea (Lepidoptera: Rhopalocera). Revista de la Sociedad Mexicana de Lepidopterología 14: 3–44.

DeVries PJ (1987) The Butterflies of Costa Rica and their Natural History. Papilionidae, Pieridae and Nymphalidae. Princeton University Press, Princeton, 327 pp.

Dirzo R, Young HS, Mooney HA, Ceballos G (2011) Seasonally dry tropical forests: ecology and conservation. Island Press, Washington DC, 392 pp. https://doi.org/10.5822/978-1-61091-021-7

Gotelli NJ, Colwell RK (2011) Estimating species richness. In: Magurran AE, McGill BJ (Eds) Biological diversity: frontiers in measurement and assessment. Oxford University Press, Oxford, 39–54.

Hebert PDN, Penton EH, Burns JM, Janzen DH, Hallwachs W (2004) Ten species in one: DNA barcoding reveals cryptic species in the neotropical skipper butterfly *Astraptes fulgerator*. Proceedings of the National Academy of Sciences of the United States of America 101(41): 14812–14817. https://doi.org/10.1073/pnas.0406166101

Llorente-Bousquets J, Vargas-Fernández I, Luis-Martínez A, Trujano-Ortega M, Hernández-Mejía BC, Warren AD (2014) Biodiversidad de Lepidoptera en México. Revista Mexicana de Biodiversidad 85(Supplement 1): 353–371. https://doi.org/10.7550/rmb.31830

Luis-Martínez MA, Salinas-Gutiérrez JL, Llorente-Bousquets J (2011) Papilionoidea y Hesperioidea (Lepidoptera: Rhopalocera). In: Álvarez F (Ed.) Chiapas: estudios sobre su diversidad biológica. Instituto de Biología, UNAM, México D.F., 363–391.

Luis-Martínez A, Hernández-Mejía B, Trujano-Ortega M, Warren A, Salinas-Gutiérrez J, Ávalos-Hernández O, Vargas-Fernández I, Llorente-Bousquets J (2016) Avances faunísticos en los Papilionoidea sensu lato (Insecta: Lepidoptera) de Oaxaca, México. Southwestern Entomologist 41(1): 171–224. https://doi.org/10.3958/059.041.0119

Oksanen J, Blanchet FG, Friendly M, Kindt R, Legendre P, Minchin PR, O'Hara RB, Solymos P, MH Stevens H, Szoecs E, Wagner H, Barbour M, Bedward M, Bolker B, Borcard D, Carvalho G, Chirico M, De Caceres M, Durand S, Evangelista HBA, FitzJohn R, Friendly M, Furneaux B, Hannigan G, Hill MO, Lahti L, McGlinn D, Ouellette M-H, Cunha ER, Smith T, Stier A, Ter Braak CJF, Weedon J (2020) Vegan: Community Ecology Package. R package version 2.5-7. https://CRAN.R-project.org/package=vegan

Pennington T, Lewis G, Ratter J (2006) Neotropical savannas and seasonally dry forests: plant diversity, biogeography, and conservation. CRC Press, Boca Raton, Florida, 484 pp. https://doi.org/10.1201/9781420004496

R Development Core Team (2021) R: a language and environment for statistical computing. R Foundation for Statistical Computing, Vienna.

Robbins RK (2010) The "upside down" systematics of hairstreak butterflies (Lycaenidae) that eat pineapple and other Bromeliaceae. Studies on Neotropical Fauna and Environment 45(1): 21–37. https://doi.org/10.1080/01650521003751712

Salinas-Gutiérrez JL (2013) Registros nuevos y aclaratorios de ninfálidos (Papilionoidea: Nymphalidae) para Guatemala. Acta Zoológica Mexicana 29(2): 431–436. http://www.scielo.org.mx/scielo.php?script=sci_arttext&pid=S0065-7372013000200015

Salinas-Gutiérrez JL, Méndez C, Barrios M, Pozo C, Llorente-Bousquets J (2009) Hacia una síntesis de los Papilionoidea (Insecta: Lepidoptera) de Guatemala con una breve reseña histórica. Caldasia 31: 407–440. http://www.scielo.org.co/scielo.php?script=sci_arttext&pid=S0366-52322009000200013

Salinas-Gutiérrez JL, Llorente-Bousquets J, Méndez C, Barrios M, Pozo C (2012) Introducción a los Papilionoidea (Papilionidae, Pieridae, Lycaenidae, Riodinidae y Nymphalidae) de Guatemala. In: Cano EB, Schuster JC (Eds) Biodiversidad de Guatemala. Vol. II. Universidad del Valle de Guatemala, Guatemala, 155–173.

Trujano-Ortega M, Callaghan CJ, Arellano-Covarrubias A, Luis-Martínez A, Avalos-Hernández O, Llorente-Bousquets J (2021) Geographical distribution of *Emesis* Fabricius (Lepidoptera: Riodinidae) in Mexico: Updated checklist and temporal patterns. Zootaxa 4964(3): 401–442. https://doi.org/10.11646/zootaxa.4964.3.1

van Nieukerken EJ, Kaila L, Kitching IJ, Kristensen NP, Lees DC, Minet J, Mitter C, et al. (2011) Order Lepidoptera Linnaeus, 1758. In: Zhang ZQ (Ed.) Animal biodiversity: an outline of higher-level classification and survey of taxonomic richness. Zootaxa 3148: 212–221. https://doi.org/10.11646/zootaxa.3148.1.41

Warren AD, González-Cota L (1998) Notes on the genus *Piruna* in western Mexico, with description of a new species (Lepidoptera: Hesperiidae). Tropical Lepidoptera 9(Supplement 2): 1–7. https://journals.flvc.org/troplep/article/view/90137

Warren AD, Davis KJ, Stangeland EM, Pelham JP, Willmott KR, Grishin NV (2017) Illustrated Lists of American Butterflies (North and South America). [21–XI–2017] http://www.butterfliesofamerica.com/

Yoshimoto J, Salinas-Gutiérrez JL (2015) First record of *Atlides gaumeri* and notes on *Chalybs hassan* in Guatemala. Southwestern Entomologist 40(3): 497–502. https://doi.org/10.3958/059.040.0307

Yoshimoto J, Salinas-Gutiérrez JL, Barrios M (2018) Annotated list of butterflies (Lepidoptera: Papilionoidea) of a Guatemalan dry forest, with two first records for Guatemala. Tropical Lepidoptera Research 28(1): 1–8. https://doi.org/10.5281/zenodo.1248159

Yoshimoto J, Salinas-Gutiérrez JL, Barrios M (2019) Butterfly fauna and phenology in a dry forest of the Motagua Valley, Guatemala. Journal of the Lepidopterists Society 73(3): 191–202. https://doi.org/10.18473/lepi.73i3.a8

Yoshimoto J, Barrios M, Salinas-Gutiérrez JL, Warren AD (2021) Fauna y fenología de mariposas diurnas (Lepidoptera: Papilionoidea) de un bosque secundario en el área urbana de Guatemala. Revista Mexicana de Biodiversidad 92(0): e923469. https://doi.org/10.22201/ib.20078706e.2021.92.3469

Zhang J, Shen J, Cong Q, Grishin NV (2019) Genomic analysis of the tribe Emesidini (Lepidoptera: Riodinidae). Zootaxa 4668(4): zootaxa.4668.4.2. https://doi.org/10.11646/zootaxa.4668.4.2

Appendix 1

Table A1. Butterfly species observed in 2011–2021 at two dry forests in Guatemala: Los Cerritos Municipal Park and Heloderma Natural Reserve, based on our previous studies (Yoshimoto et al. 2018, 2019) and on subsequent field surveys (July 2014 to August 2021 at Los Cerritos and October 2017 to November 2021 at Heloderma Reserve). Species and months in bold indicate the data newly obtained in the subsequent surveys. Year information is also shown with sampling months, when necessary. Nomenclature follows Warren et al. (2017).

	Family / Subfamily / Species and subspecies	Months when observed: Los Cerritos	Months when observed: Heloderma Reserve
	Papilionidae		
	Papilioninae		
1	*Neographium epidaus epidaus* (E. Doubleday, 1846) [PH, A]	Apr, May, **Jun**, **Jul**, **Aug**, **Nov**	–
2	*Neographium philolaus philolaus* (Boisduval, 1836) [PH, A]	Jun, Sep	Mar, Apr, May, Jun
3	*Battus polydamas polydamas* (Linnaeus, 1758) [PH, A]	Mar, Jul, **Aug**, Sep, **Dec**	–
4	***Parides photinus* (E. Doubleday, 1844)**	**–**	**Sep**
5	*Heraclides erostratus erostratus* (Westwood, 1847) [A, Y]	May, Oct	–
6	*Heraclides thoas autocles* (Rothschild & Jordan, 1906) [PH, A]	Feb, **Mar**, Apr, **Jun**, **Aug**, **Nov**	–
7	*Heraclides ornythion ornythion* (Boisduval, 1836) [PH]	**–**	May, Jun
8	***Heraclides rumiko* Shiraiwa & Grishin, 2014** [MI, PH]	**Jul**	Oct'16[MI], **Dec**
9	*Papilio polyxenes asterius* Stoll, 1782 [PH]	Mar, Apr, May, **Nov**	–
	Pieridae		
	Coliadinae		
10	*Kricogonia lyside* (Godart, 1819) [PH, A]	Mar	Jan, Feb, Mar, Apr, May, Jun, Jul, Aug, Sep, Nov, Dec
11	*Eurema daira eugenia* (Wallengren, 1860) [PH, A, Y]	Jan, Feb, Aug, Nov	Jan, Mar, Apr, May, Jun, Jul, Aug, Sep, Oct, Dec
12	*Eurema boisduvaliana* (C. Felder & R. Felder, 1865) [PH, A]	Feb, Oct, Nov	Jun, Jul, Aug, Sep, Oct, Nov
13	***Abaeis nicippe* (Cramer, 1779)** [MI, PH]	**Nov**	Jul'16[MI]
14	*Pyrisitia proterpia* (Fabricius, 1775) [PH, A]	May, Jun, Jul, Oct, **Dec**	Feb, Apr May, Jun, Jul, Aug, Sep, Oct, Nov
15	*Pyrisitia dina westwoodi* (Boisduval, 1836) [PH, A]	**–**	Jan, Feb, Jun, Oct, Nov, Dec
16	*Pyrisitia nise nelphe* (R. Felder, 1869) [PH, A, Y]	**Jun, Jul**, **Aug**, **Nov**	Jun, Jul, Aug, Sep, Oct, **Nov**, Dec
17	*Zerene cesonia cesonia* (Stoll, 1790) [PH, Y]	Jun, Aug	Jun, **Jul**
18	*Anteos maerula* (Fabricius, 1775) [PH, A]	Jun, **Sep**, Nov	**May**, Jun, Jul, Aug, Sep, Oct
19	*Anteos clorinde* (Godart, [1824]) [PH, A]	Apr, Jun	Jun, Aug
20	*Phoebis sennae marcellina* (Cramer, 1777) [PH, A]	Feb, **Mar**, Apr, Jun, Jul, Nov	Mar, May, **Jun**, Jul, Aug, Sep
21	*Phoebis philea philea* (Linnaeus, 1763) [A, Y]	May	Jul
22	*Phoebis argante* ssp. [A]	May	Jul
23	*Aphrissa statira statira* (Cramer, 1777) [A]	Oct	–
	Pierinae		
24	*Hesperocharis crocea crocea* H. Bates, 1866	Mar, **Aug**	–
25	*Ascia monuste monuste* (Linnaeus, 1764) [PH, A, Y]	Feb, Jun	Jun

	Family / Subfamily / Species and subspecies	Months when observed: Los Cerritos	Months when observed: Heloderma Reserve
26	*Ganyra josephina josepha* (Salvin & Godman, 1868) [PH, A]	–	Jan, Oct
27	*Leptophobia aripa elodia* (Boisduval, 1836) [Y]	Jan	–
28	*Itaballia demophile centralis* Joicey & Talbot, 1928	–	Jan
29	*Glutophrissa drusilla tenuis* (Lamas, 1981) [A]	–	Jun, Aug
Lycaenidae			
Theclinae			
30	*Evenus regalis* (Cramer, 1775) [A]	Sep	–
31	*Atlides gaumeri* (Godman 1901)	Aug	–
32	*Atlides carpasia* (Hewitson, 1868) [A]	Aug	–
33	***Rekoa zebina* (Hewitson, 1869)**	**Jun, Sep**	–
34	*Rekoa stagira* (Hewitson, 1867) [A]	Aug	–
35	*Arawacus sito* (Boisduval, 1836) [A, Y]	Aug	–
36	*Arawacus jada* (Hewitson, 1867) [A]	Jul	–
37	*Kolana lyde* (Godman & Salvin, 1887) [A]	Sep	–
38	***Chlorostrymon simaethis sarita* (Skinner, 1895)** [A]	**Nov**	–
39	*Cyanophrys herodotus* (Fabricius, 1793) [A]	Aug	–
40	*Cyanophrys miserabilis* (Clench, 1946)	**–**	Oct
41	***Electrostrymon hugon* (Godart, [1824])**	**–**	**Jul**
42	***Kisutam syllis* (Godman & Salvin, 1887)** [A]	**–**	**Oct**
43	***Calycopis clarina* (Hewitson, 1874)**	**Jun**	–
44	*Calycopis isobeon* (A. Butler & H. Druce, 1872)	Aug, Sep	–
45	*Strymon melinus franki* W. D. Field, 1938	Aug, Sep	–
46	*Strymon rufofusca* (Hewitson, 1877) [PH]	**Jul**, Nov	**Jan**, Aug, Oct, Nov, **Dec**
47	*Strymon bebrycia* (Hewitson, 1868) [PH]	**Jun**, Aug	–
48	***Strymon yojoa* (Reakirt, [1867])** [A]	**Jul**	–
49	*Strymon cestri* (Reakirt, [1867]) [A]	Aug	–
50	*Strymon bazochii bazochii* (Godart, [1824]) [A]	Jul	–
51	*Strymon istapa istapa* (Reakirt, [1867])	Aug, **Nov**	–
52	***Strymon megarus* (Godart, [1824])** [MI, PH]	–	**Jan**, **Jul**, Oct'16[MI], **Dec**
53	*Strymon ziba* (Hewitson, 1868)	Jul	–
54	***Ministrymon azia* (Hewitson, 1873)** [A]	**Jun**	**Jul**
55	***Ostrinotes keila* (Hewitson, 1869)** [A, Y]	**Aug**	–
56	*Panthiades bitias* (Cramer, 1777) [A]	Jun	–
57	*Michaelus hecate* (Godman & Salvin, 1887)	Sep	–
58	*Erora gabina* (Godman & Salvin, 1887)	May, Jun, Aug, Oct	–
59	*Chalybs hassan* (Stoll, 1790)	Aug, Sep, Nov	**Jul**
Polyommatinae			
60	*Celastrina echo gozora* (Boisduval, 1870) [Y]	Nov	–
61	***Leptotes cassius cassidula* (Boisduval, 1870)** [PH, A, Y]	**Jun**, **Dec**	**Sep**, **Oct**
62	*Cupido comyntas texana* (F. Chermock, 1945) [PH, A, Y]	**Sep**, Nov	**Oct**, Nov, **Dec**
63	*Hemiargus ceraunus astenidas* (Lucas, 1857) [A]	Mar, **Jul**, **Nov**	Feb, Jun, **Dec**
64	*Hemiargus hanno hanno* (Stoll, 1790) [PH, A]	**–**	Jul, Aug, Sep, Oct
65	*Echinargus isola* (Reakirt, [1867])	Feb, **Dec**	**Jun**, **Dec**
Riodinidae			
Riodininae			
66	*Rhetus arcius castigatus* Stichel, 1909 [A]	Sep	–
67	*Calephelis* spp. [PH, 1]	Jan, May, Jul, Aug, Oct, **Nov**, **Dec**	Jan, Jul, Aug, Sep, Oct, Nov, Dec
68	*Lasaia sula sula* Staudinger, 1888 [PH]	**–**	Jun, **Oct**
69	***Lasaia maria maria* Clench, 1972**	**–**	**Jun**, **Jul**, **Oct**
70	*Melanis pixe pixe* (Boisduval, 1836) [A]	Feb, Sep, Nov, Dec	–

	Family / Subfamily / Species and subspecies	Months when observed: Los Cerritos	Months when observed: Heloderma Reserve
71	*Anteros carausius carausius* Westwood, 1851 [A]	Aug, Nov	**Sep, Nov**
72	*Calydna sturnula* (Geyer, 1837) [PH]	Aug, **Sep**, Oct	–
73	*Emesis mandana* furor A. Butler & H. Druce, 1872 [A]	Aug	–
74	*Emesis tenedia* C. Felder & R. Felder, 1861 [A, Y, 2]	Jul	–
75	*Emesis lupina lupina* Godman & Salvin, 1886 [2]	Oct	–
76	*Curvie emesia* (Hewitson, 1867) [PH, A, 3]	**–**	Jun, Oct
77	*Thisbe lycorias* (Hewitson, [1853]) [A]	Jun, Jul, Oct, Nov	–
78	***Juditha caucana* (Stichel, 1911)**	–	**Oct**
79	*Synargis mycone* (Hewitson, 1865) [A]	Mar, Jun, Jul	Jul
80	***Hypophylla zeurippa* Boisduval, 1836**	–	**Jan**
81	*Theope virgilius* (Fabricius, 1793) [A]	–	Feb, Nov
	Nymphalidae		
	Libytheinae		
82	*Libytheana carinenta mexicana* Michener, 1943 [PH, A, Y]	Jul	Jun, Aug, Sep
	Danainae		
83	*Lycorea halia atergatis* E. Doubleday [1847] * [PH, A, Y]	–	**May**, Sep
84	*Danaus eresimus montezuma* Talbot, 1943 [PH, A]	Aug, **Nov**, **Dec**	Jun, Aug, **Sep**
85	*Danaus gilippus thersippus* (H. Bates, 1863) [A]	**–**	Mar
86	*Mechanitis lysimnia utemaia* Reakirt, 1866 [PH, A, Y]	**–**	**May**, Aug, **Oct**
87	*Mechanitis polymnia lycidice* H. Bates, 1864 [PH, A, Y]	Sep	Sep, **Oct**
88	*Dircenna klugii klugii* (Geyer, 1837) [Y]	Sep, Oct, Nov	–
	Heliconiinae		
89	*Agraulis vanillae incarnata* (N. Riley, 1926) [PH, A]	Jun, Jul, **Nov**	Aug
90	*Dione moneta poeyii* A. Butler, 1873 [Y]	Jun, Nov	–
91	*Dione juno huascuma* (Reakirt, 1866) [PH, A]	Feb, Mar, **Dec**	Jul
92	*Dryas iulia moderata* (N. Riley, 1926) [PH, A, Y]	Aug	Aug, Sep, Oct
93	*Eueides isabella eva* (Fabricius, 1793) [A]	Nov	–
94	*Heliconius charithonia vazquezae* W. Comstock & F. Brown, 1950 [A, Y]	Jul	Jul, Oct
95	*Euptoieta hegesia meridiania* Stichel, 1938 [PH, A, Y]	Jun, Jul, Sep	Jun, Jul
	Limenitidinae		
96	*Adelpha paroeca paroeca* (H. Bates, 1864) [Y]	Oct, Nov	–
97	*Adelpha iphicleola iphicleola* (H. Bates, 1864) [PH]	Aug	Jun, Jul, Sep, Oct
98	*Adelpha melanthe* (H. Bates, 1864) [A]	Aug, Sep	–
	Biblidinae		
99	*Biblis hyperia aganisa* Boisduval, 1836 [PH, A]	Jul, **Dec**	Sep
100	*Mestra amymone* (Ménétriés, 1857) [A]	May, Jun, Jul	Mar, Jul, Aug, Sep, Oct, Nov, Dec
101	*Catonephele mexicana* Jenkins & R.G. Maza, 1985 [A]	Sep, Oct, Nov	–
102	*Eunica monima* (Stoll, 1782) [PH]	Jun, **Aug**	Mar, Jun, Jul, Aug, Oct, Dec
103	*Eunica tatila tatila* (Herrich-Schäffer, [1855]) [A]	Jun	–
104	*Hamadryas atlantis atlantis* (H. Bates, 1864) [PH]	Sep	Jun, Jul, Nov
105	*Hamadryas februa ferentina* (Godart, [1824]) [PH, A]	Apr, May, **Jun**, **Jul**, **Nov**, **Dec**	Feb, **Jul**, Oct
106	*Hamadryas glauconome glauconome* (H. Bates, 1864) [PH]	Jan, **Jul**, Oct, **Nov**, Dec	Jan, Feb, Mar, **May**, Jun, Jul, Aug, **Sep**, **Oct**
107	*Hamadryas guatemalena guatemalena* (H. Bates, 1864) [PH, A]	May, Jun, Jul	**Jul**
108	*Bolboneura sylphis sylphis* (H. Bates, 1864) [PH]	Jul, Aug, Sep	Mar, Jun, Jul, Sep, Oct
109	*Epiphile adrasta adrasta* Hewitson, 1861 [Y]	Aug, Oct	–

	Family / Subfamily / Species and subspecies	Months when observed: Los Cerritos	Months when observed: Heloderma Reserve
110	*Temenis laothoe hondurensis* Fruhstorfer, 1907 [A]	–	Oct
111	*Dynamine dyonis* Geyer, 1837 [A]	Jul, Aug, Oct, Nov, **Dec**	–
112	*Dynamine postverta mexicana* R.F. d'Almeida, 1952 [PH, A]	Jun, Jul, Oct, **Nov**	Sep, Oct
113	*Dynamine theseus* (C. Felder & R. Felder, 1861) [A]	**Aug**, Sep, Oct	–
114	*Diaethria astala astala* (Guérin-Méneville, [1844]) [A, Y]	May, Jul, Oct, Nov	**Oct**
	Cyrestinae		
115	*Marpesia petreus* ssp. [A, Y]	Jul, Sep	Jun
	Nymphalinae		
116	*Historis odius dious* Lamas, 1995 [PH, A]	**Jun**, **Jul**, Aug, Sep	Jul
117	*Smyrna blomfildia datis* Fruhstorfer, 1908 [PH, A, Y]	Jul	**May**, Nov
118	*Anartia fatima fatima* (Fabricius, 1793) [PH, A, Y]	May	**Jun**, Sep, Oct
119	*Siproeta epaphus epaphus* (Latreille, [1813]) [A, Y]	Sep	Sep
120	*Siproeta stelenes biplagiata* (Fruhstorfer, 1907) [PH, A, Y]	Jul, Sep	**Jun**, Aug, Sep, Oct
121	*Junonia evarete* (Cramer, 1779) [PH, A]	Jun, Jul, Aug	**Jan**, **Jul**, **Oct**
122	*Chlosyne janais janais* (Drury, 1782) [A]	Jun, **Aug**	–
123	***Chlosyne erodyle erodyle* (H. Bates, 1864)** [MI]	Jul'12[MI], **Jul'19**, Oct'11[MI], **Oct'17**	–
124	***Chlosyne rosita rosita* A. Hall, 1924** [MI]	Sep'11[MI]	**Jun**, **Jul**, **Sep**
125	*Chlosyne theona theona* (Ménétriés, 1855) [PH]	Apr, Jun, Sep	Jun, Jul, Aug, Sep
126	*Chlosyne lacinia lacinia* (Geyer, 1837) [PH, A, Y]	Mar, **Jun**, **Jul**, Aug, Nov	Jun, Jul, Aug
127	*Chlosyne melanarge* (H. Bates, 1864) [PH]	–	Aug, **Sep**, Oct
128	*Microtia elva horni* Rebel, 1906 [PH]	Jun, Jul, Aug, Nov	Jun, Jul, Aug, Sep, Oct, Nov
129	***Anthanassa tulcis* (H. Bates, 1864)** [MI, A]	May'11[MI]	**Jun**, **Sep, Dec**
130	*Anthanassa ptolyca ptolyca* (H. Bates, 1864) [Y]	Aug	**Dec**
131	*Tegosa guatemalena* (H. Bates, 1864) [A]	Feb, Nov	–
	Charaxinae		
132	*Zaretis ellops* (Ménétriés, 1855) [A]	Jul, Sep, Nov	–
133	*Anaea aidea* (Guérin-Méneville, [1844]) [PH, A]	May, Nov	Jun, Aug, Oct, Nov
134	*Fountainea glycerium glycerium* (E. Doubleday, [1849]) [PH]	Aug, Sep, Oct, **Nov**	–
135	***Archaeoprepona demophon centralis* (Fruhstorfer, 1905)** * [PH, A]	–	**Jul**
	Satyrinae		
136	*Morpho helenor* ssp.* [A]	–	Sep
137	***Caligo telamonius memnon* (C. Felder & R. Felder, 1867)** * [PH, A]	–	**Oct**
138	***Manataria hercyna maculata* (Hopffer, 1874)** [A, Y]	–	**Jun**
139	*Cissia similis* (A. Butler, 1867) [MI, PH, A]	May'12[MI], Jun'12[MI], Oct, Nov	Jan, Feb, Apr, May, Jun, Oct, Nov, Dec
140	*Cissia themis* (A. Butler, 1867) [MI, PH]	Jul, Aug'11[MI]	Feb, **Jun**, Jul, Aug'16[MI], Oct'16[MI], Dec
141	*Cyllopsis gemma freemani* (D. Stallings & J. Turner, 1947)	Sep, Nov	–
142	*Cyllopsis hedemanni hedemanni* R. Felder, 1869 [Y]	Feb	–
143	*Cyllopsis hilaria* (Godman, 1901)	Sep, Nov	–
144	*Cyllopsis pephredo* (Godman, 1901) [Y]	**Jun**, Nov	–
145	*Euptychia fetna* A. Butler, 1870	Aug, Sep	–
146	*Hermeuptychia hermes* (Fabricius, 1775) [A, Y, 4]	Jul	**Jan**, Feb, Sep, Oct
147	*Taygetis thamyra* (Cramer, 1779) [PH]	Nov	**Jun**, **Oct**

	Family	Months when observed	
	Subfamily	Los Cerritos	Heloderma Reserve
	Species and subspecies		
	Hesperiidae		
	Eudaminae		
148	***Phocides polybius lilea* (Reakirt, [1867])** [A]	**Nov**	–
149	*Phocides urania urania* (Westwood, 1852)	Aug	–
150	*Proteides mercurius mercurius* (Fabricius, 1787) [PH, A]	Jun	**Jun**, Sep
151	*Epargyreus exadeus cruza* Evans, 1952 [A, Y]	Feb, Mar, Apr, Jun, **Jul**	Aug
152	*Polygonus leo arizonensis* (Skinner, 1911)	Jul	Jun, Jul, Aug, Sep, Oct
153	*Chioides albofasciatus* (Hewitson, 1867) [A]	Jun	–
154	*Chioides zilpa* (A. Butler, 1872) [A]	Jan, Mar	–
155	*Typhedanus undulatus* (Hewitson, 1867) [A]	Feb, Mar, May	–
156	*Typhedanus ampyx* (Godman & Salvin, 1893) [A]	–	Oct
157	*Polythrix asine* (Hewitson, 1867) [PH, A, 5]	–	**Jan**, **Dec**
158	***Polythrix octomaculata* (Sepp, [1844])** [A]	–	**May**
159	*Cephise aelius* (Plötz, 1880)	–	Oct
160	*Codatractus alcaeus alcaeus* (Hewitson, 1867)	Mar, May	–
161	***Codatractus melon* (Godman & Salvin, 1893)**	–	**Jun**, **Jul**
162	*Urbanus viterboana* (Ehrmann, 1907) [MI, A, Y]	Sep, Nov'11 [MI]	Sep, Oct
163	*Urbanus esmeraldus* (A. Butler, 1877) [A, Y]	Aug, Sep	**Jun**
164	*Urbanus dorantes dorantes* (Stoll, 1790) [PH, A]	May, **Jul**, **Aug**, **Dec**	Apr, Jun, Jul, Aug, Sep, Oct, Nov
165	*Urbanus procne* (Plötz, 1881) [PH, A, Y]	May, Jul, **Nov**	–
166	*Urbanus doryssus doryssus* (Swainson, 1831) [A]	Jul	–
167	*Astraptes fulgerator azul* (Reakirt, [1867]) [A, Y, 6]	Oct, Nov	–
168	*Astraptes alector hopfferi* (Plötz, 1881) [A]	Sep	**Jan**
169	*Astraptes anaphus annetta* Evans, 1952 [PH, A, Y]	Jun, Oct	Jul
170	*Achalarus toxeus* (Plötz, 1882) [A]	–	Mar, **Apr**, Oct
171	*Achalarus albociliatus albociliatus* (Mabille, 1877) [A]	Feb, Mar	Oct, Nov
172	*Cabares potrillo potrillo* (Lucas, 1857) [A, Y]	–	Jun, **Jul**, Aug, **Oct**, Nov
173	*Cogia cajeta eluina* Godman & Salvin, 1894	May, **Jun**	–
	Pyrginae		
174	***Mysoria affinis* (Herrich-Schäffer, 1869)**	–	**Oct**
175	*Celaenorrhinus fritzgaertneri* (Bailey, 1880) [PH]	Feb, Aug	Mar, **Jun**
176	*Noctuana stator* (Godman, 1899) [PH, A, Y]	Feb, Mar, May, **Jul**, Sep	–
177	*Bolla evippe* (Godman & Salvin, 1896)	Mar	–
(177)	*Bolla* sp. [7]	–	**Oct** [7]
178	*Staphylus ascalaphus* (Staudinger, 1876) [Y]	May	Jan, Sep
179	*Staphylus azteca* (Scudder, 1872)	–	Feb, Aug, Nov
180	*Gorgythion vox* Evans, 1953 [A, Y]	–	Jun, Jul, Aug, Sep, Oct
181	***Mylon salvia* Evans, 1953**	**Nov**	–
182	***Mylon pelopidas* (Fabricius, 1793)** [A]	–	**May**, **Jun**
183	*Grais stigmaticus stigmaticus* (Mabille, 1883) [PH]	–	**Jan**, Jun, Jul
184	*Timochares trifasciata trifasciata* (Hewitson, 1868) [A]	–	Jan
185	*Chiomara georgina georgina* (Reakirt, 1868)	Jan, **Jul**, Sep, **Nov**	Aug
186	***Erynnis funeralis* (Scudder & Burgess, 1870)**	**Aug**	**Jun**
187	*Eantis tamenund* (W. H. Edwards, 1871) [PH]	Feb, Jul, Aug, **Nov**, Dec	–
188	*Atarnes sallei* (C. Felder & R. Felder, 1867) [A]	Jul	–
189	***Carrhenes fuscescens fuscescens* (Mabille, 1891)**	–	**Jun**
190	*Antigonus erosus* (Hübner, [1812]) [PH, A]	**Mar**, Oct	Feb, Mar, **Jun**, Aug, Oct
191	*Antigonus corrosus* Mabille, 1878 [A, Y]	–	Sep

	Family / Subfamily / Species and subspecies	Months when observed: Los Cerritos	Months when observed: Heloderma Reserve
192	*Zopyrion sandace* Godman & Salvin, 1896	**Mar**, Aug	**Jan**, Apr, **May**, **Jun**, Sep, Dec
193	*Pyrgus oileus* (Linnaeus, 1767) [PH, A, Y]	Apr	Jul, Aug, Sep, Oct, Dec
194	***Pyrgus orcus* (Stoll, 1780)**	–	**Jun**
195	*Heliopyrgus domicella domicella* (Erichson, [1849])	Sep	Sep, **Oct, Nov**
196	*Heliopetes laviana laviana* (Hewitson, 1868) [A]	–	Feb
197	*Heliopetes macaira macaira* (Reakirt, [1867]) [MI, A]	Jul'12[MI], **Nov**	Oct
198	*Heliopetes alana* (Reakirt, 1868) [A, Y]	Jul	–
Heteropterinae			
199	***Piruna aea* (Dyar, 1912)** [PH]	–	Jun [8], **Jul**, Sep [8], **Oct**
Hesperiinae			
200	*Perichares adela* (Hewitson, 1867) [A]	Aug, Sep	Oct
201	*Copaeodes aurantiaca* (Hewitson, 1868) [MI]	Mar'11[MI]	–
202	***Panoquina lucas* (Fabricius, 1793)** [A]		**Jan**
203	*Zenis jebus hemizona* (Dyar, 1918)	Jan	–
204	*Synapte shiva* Evans, 1955	Aug	Jun, Dec
205	*Synapte syraces* (Godman, 1901)	–	Sep
206	***Callimormus saturnus* (Herrich-Schäffer, 1869)** [A]	–	**Oct**
207	***Amblyscirtes elissa elissa* Godman, 1900** [NR, MI]	–	**Jun**, Aug'16[MI], Sep'16[MI]
208	*Amblyscirtes tolteca tolteca* Scudder, 1872 [A]	**Jun**, Jul	**May**
209	*Methionopsis ina* (Plötz, 1882) [A]	–	**Jan**, Oct, Nov
210	***Repens florus* (Godman, 1900)** [NR]	–	**Oct**
211	*Cymaenes trebius* (Mabille, 1891) [MI, A]	Aug	Sep'16[MI]
212	*Lerema liris* Evans, 1955	–	Jul, Sep
213	***Niconiades nikko* Hayward, 1948** [NR]	**Nov**	–
214	*Vettius fantasos* (Cramer, 1780) [A, Y]	Aug, Sep, Oct	**Jan**, Oct
215	*Hylephila phyleus phyleus* (Drury, 1773) [A]	Aug	–
216	*Polites vibex praeceps* (Scudder, 1872) [A]	Mar, Apr	–
217	***Pompeius pompeius* (Latreille, [1824])** [A, Y]	–	**Jun**
218	*Atrytonopsis ovinia* (Hewitson, 1866) [PH]	Jan, Feb, Mar, Apr, **Oct**	Oct, Dec

[PH] Species photographed.

[A] Species reported at Tikal in northern Guatemala by Austin et al. (1996).

[Y] Species reported at Parque Cayalá in Guatemala City by Yoshimoto et al. (2021).

* Specimens not collected (recorded only by direct observation or photographs).

[MI] Species misidentified in Yoshimoto et al. (2018 or 2019); their previous identification results are shown in Table 1.

[1] Listed at the genus level because of the difficulty of species-level identification derived from the confused taxonomic state of this genus.

[2] These two species, together with *Emesis tegula* and *E. toltec*, can be treated as a species complex. These taxa require further study, according to Trujano-Ortega et al. (2021).

[3] The genus name, treated as *Emesis* in Yoshimoto et al. (2019), was modified according to Zhang et al. (2019).

[4] The name "*hermes*" is correctly applied to a South American species, according to Cong and Grishin (2014). Thus, the individuals collected might include multiple species, none of which are true *hermes*.

[5] One sample which was photographed at Heloderma Reserve in October 2016 and was identified as this species in Yoshimoto et al. (2019) was excluded, as we found that it might have been of another species of this genus, which is unable to de determined because of the lack of a specimen.

[6] This is a species complex, which includes several species in Costa Rica (Hebert et al. 2004; Brower, 2006, 2010). Thus, the individuals collected might also be of multiple species.

[7] These data were included in the species count and Chao II analyses for Heloderma Reserve, since at this site none of the identified species of this genus had been recorded. In contrast, these data have been excluded from the Chao II analysis for all data (pooled across the sites) and from the Jaccard index analyses, as this individual might be of *Bolla evippe* (Godman & Salvin, 1896), which is unable to be examined because of the heavily damaged specimen of *Bolla* sp.

[8] Identified to genus (*Piruna* sp.1) and incorrectly listed as Hesperiinae in Yoshimoto et al. (2019).

[NR] New record for Guatemala.

ZooKeys 1118: 39–72 (2022)
doi: 10.3897/zookeys.1118.89337
https://zookeys.pensoft.net

RESEARCH ARTICLE

A peer-reviewed open-access journal
ZooKeys
Launched to accelerate biodiversity research

A new genus and nine species of jumping spiders from Hainan Island, China (Araneae, Salticidae)

Cheng Wang[1,2], Shuqiang Li[3]

1 *Guizhou Provincial Key Laboratory for Biodiversity Conservation and Utilization in the Fanjing Mountain Region, Tongren University, Tongren, Guizhou 554300, China* **2** *Ministry of Education Key Laboratory for Ecology of Tropical Islands, College of Life Sciences, Hainan Normal University, Haikou 571158, China* **3** *Institute of Zoology, Chinese Academy of Sciences, Beijing 100101, China*

Corresponding author: Shuqiang Li (lisq@ioz.ac.cn)

Academic editor: Zhiyuan Yao | Received 21 June 2022 | Accepted 1 August 2022 | Published 18 August 2022

https://zoobank.org/D21C9E91-A428-419E-AC6E-D5C82CEF6295

Citation: Wang C, Li S (2022) A new genus and nine species of jumping spiders from Hainan Island, China (Araneae, Salticidae). ZooKeys 1118: 39–72. https://doi.org/10.3897/zookeys.1118.89337

Abstract

A new genus and eight new species of jumping spiders from Hainan Island, China are reported. *Pengmarengo* **gen. nov.** is erected to accommodate the type species *P. yangi* **sp. nov.** (♂♀). Further *Pengmarengo* **gen. nov.** species including *P. chelifer* (Simon, 1990), **comb. nov.** (transferred from *Philates* Simon, 1900), *P. elongata* (Peng & Li, 2002), **comb. nov.** (transferred from *Tauala* Wanless, 1988), and two species transferred from *Indomarengo* Benjamin, 2004: *P. yui* (Wang & Li, 2020), **comb. nov.**, and *P. wengnan* (Wang & Li, 2022), **comb. nov.** Another seven new jumping spider species are described from Hainan: *Irura liae* **sp. nov.** (♂), *I. mii* **sp. nov.** (♂♀), *Marengo ganae* **sp. nov.** (♂♀), *M. zhengi* **sp. nov.** (♂♀), *Nungia tangi* **sp. nov.** (♂♀), *Philates zhoui* **sp. nov.** (♂♀), and *Toxeus hainan* **sp. nov.** (♂♀). The unknown female of the endemic species, *Irura pengi* Guo, Zhang & Zhu, 2011 is also described for the first time.

Keywords

Morphology, new combination, new taxa, rainforest, salticid, taxonomy

Introduction

Hainan, the second-largest island in China, possesses a large number of tropical rainforests. The island has high species diversity as well as high ratio of endemism (Li 2020; Wang et al 2020; Li et al 2021; Yao et al 2021; Hong et al 2022; Zhu et al 2022). A series of research on jumping spiders from this island has reported 37 endemic species and increased the species number to 118 (Peng and Kim 1997; Peng and Li 2006; Guo et al. 2011; Zhou and Li 2013). However, nearly half (17) of endemic species are known only from a single-sex, and part of them are lacking distinct diagnostic drawings indicating the jumping spider of this island remains poorly studied (WSC 2022). In our recent study of salticid samples from Hainan Island, eight species belonging to six genera (including a new genus) are recognized as new to science, and the unknown female of *Irura pengi* Guo, Zhang & Zhu, 2011 has been found.

Materials and methods

Specimens were collected by beating shrubs or hand collecting in the tropical rainforest of Hainan Island, China. They were preserved in 75% ethanol for morphological study and in absolute ethanol for molecular study. Specimens are deposited in the Institute of Zoology, Chinese Academy of Sciences in Beijing (**IZCAS**), China, and Tongren University (**TRU**) in Tongren, China. Methods follow those of Wang and Li (2021).

All measurements are given in millimeters. Leg measurements are given as: total length (femur, patella, tibia, metatarsus, tarsus). References to figures in the cited papers are listed in lowercase type (fig. or figs), and figures in this paper are noted with an initial capital (Fig. or Figs). Abbreviations used in the text and figures are as follows:

AERW anterior eye row width;
AME anterior median eye;
ALE anterior lateral eye;
AG accessory gland;
AR atrial ridge;
AS anterior chamber of spermatheca;
At atrium;
BP basal epigynal plate;
CA cymbial apophysis;
CD copulatory duct;
CO copulatory opening;
DCP dorsal cymbial process;
DTA dorsal tibial apophysis;
E embolus;
EC embolic coil;
EFL eye field length;
FD fertilization duct;
JS junction duct of spermathecae;
H epigynal hood;
MS median septum;
MiS median chamber of spermatheca;
PERW posterior eye row width;
PED process of embolic disc;
PLE posterior lateral eye;
PS posterior chamber of spermatheca;
PTA prolateral tibial apophysis;
RTA retrolateral tibial apophysis;
S spermatheca;
SD sperm duct;
St stiffener;
TF tibial flange.

Taxonomy

Family Salticidae Blackwall, 1841

Genus *Irura* Peckham & Peckham, 1901

Type species. *Irura pulchra* Peckham & Peckham, 1901 from Sri Lanka by original designation.

Comments. The genus *Irura* Peckham & Peckham, 1901 is placed in the subtribe Simaethina Simon, 1903 together with other 12 genera and is represented by 18 species mainly distributed from East and Southeast Asia (Maddison 2015; WSC 2022). It is rather poorly understood because the generotype is known from single-sex and lacks key diagnostic drawings. According to the morphological character, the genus is similar to *Stertinius* Simon, 1890 in having the PME closer to AME than to PLE, three pairs of conspicuous muscle depressions on the dorsum of abdomen (Logunov 2022), but it differs by the sub-oval carapace and the well-developed (extending exceed the cymbial base) cymbial apophysis mostly possesses a pointed terminus, whereas almost square carapace, less-developed (not extending exceed the cymbial base) cymbial apophysis without pointed terminus in *Stertinius* (see Metzner 2022).

***Irura liae* sp. nov.**
https://zoobank.org/CCC36061-F7D4-4FB4-BDA0-1D67CF4DA655
Fig. 1

Type material. ***Holotype*** ♂ (TRU-JS 0622), China: Hainan: Lingshui County, Diaoluoshan National Nature Reserve, 01–05.v.2021, F.E. Li leg.

Etymology. The specific name is a patronym of Ms Feng'E Li, the collector of the type specimen; noun (name) in genitive case.

Diagnosis. *Irura liae* sp. nov. closely resembles *I. bidenticulata* Guo, Zhang & Zhu, 2011 known from Hainan, and Hongkong of China in having a short embolus and a weakly sclerotized RTA, but it can be easily distinguished by the following characters: (1) the RTA is almost disciform in ventral view (Fig. 1A), whereas it is elongated in *I. bidenticulata* (Guo et al. 2011: fig. 8); (2) the embolus is ~ 3/5 of the bulb length (Fig. 1A), whereas it is ca. as long as the bulb in *I. bidenticulata* (Guo et al. 2011: fig. 8).

Description. Male (Fig. 1). Total length 3.89. Carapace 2.05 long, 2.17 wide. Abdomen 2.06 long, 1.96 wide. Eye sizes and inter-distances: AME 0.44, ALE 0.22, PLE 0.21, AERW 1.67, PERW 2.03, EFL 0.92. Leg measurements: I 7.56 (2.38, 1.60, 1.70, 1.13, 0.75), II 3.51 (1.25, 0.48, 0.75, 0.63, 0.40), III 3.02 (1.01, 0.48, 0.50, 0.63, 0.40), IV 3.71 (1.25, 0.63, 0.68, 0.75, 0.40). Carapace almost oval, red-brown to dark brown, covered with dense, pale setae, with dark double-humped patch medially in eye field. Chelicerae red-brown, with two promarginal teeth and one retromarginal fissidental tooth with two cusps. Endites longer than wide, with dense, dark setae on inner margins.

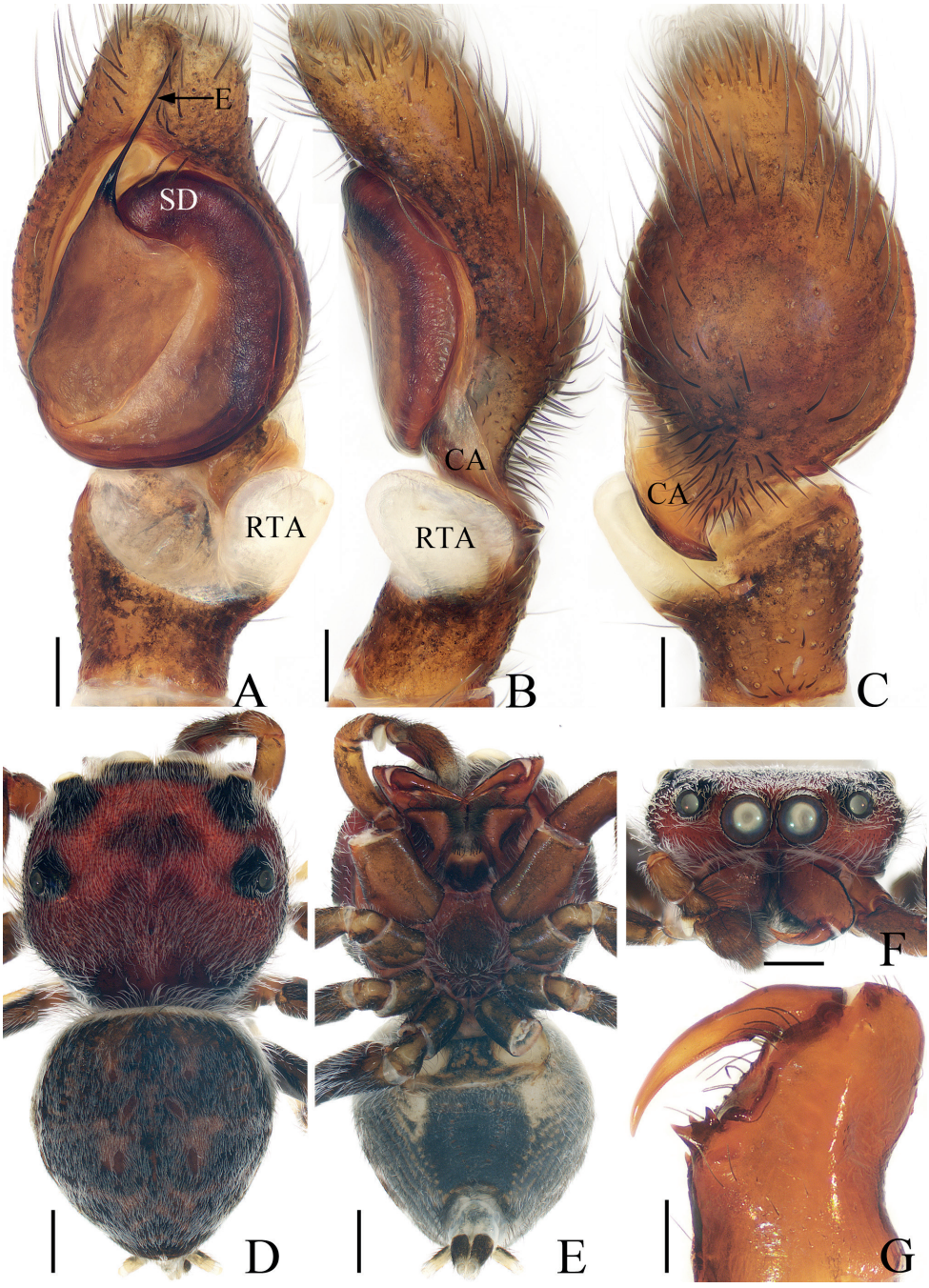

Figure 1. *Irura liae* sp. nov., male holotype **A** palp, ventral **B** ditto, retrolateral **C** ditto, dorsal **D** habitus, dorsal **E** ditto, ventral **F** carapace, frontal **G** chelicera, posterior. Scale bars: 0.1 mm (**A–C, G**); 0.5 mm (**D–F**). Abbreviations: CA – cymbial apophysis; E – embolus; RTA – retrolateral tibial apophysis; SD – sperm duct.

Labium almost linguiform, paler distally, bearing dark setae at anterior edge. Sternum red-brown to dark brown, bearing pale setae of varying lengths. Legs I robust, with two pairs of macrosetae ventrally on tibiae and metatarsi, respectively; other legs pale to brown. Abdomen oval, dorsum dark brown, covered with pale, thin setae, with three pairs of muscle depressions medially, and transverse, undulate, earthy yellow streaks posteriorly, covered entirely by a large scutum; venter dark brown medially, with anterolateral pale areas. Palp (Fig. 1A–C): tibia longer than wide, with weakly sclerotized, disciform RTA; cymbium acutely narrowed distally, with baso-retrolateral apophysis slightly curved medially and slightly pointed at distal end; bulb flat, almost round, with tapered sperm duct extending along margin; embolus filiform, strongly sclerotized, straight, originates at ~ 10:30 o'clock position on bulb, ~ 3/5 the bulb length.

Female. Unknown.

Distribution. Only known from the type locality on Hainan Island, China.

***Irura mii* sp. nov.**

https://zoobank.org/F52D4E03-401D-4E2B-8BA5-45FD166FB7BD

Figs 2, 3

Type material. ***Holotype*** ♂ (IZCAS-Ar43164), China: Hainan: Wuzhishan City, Wuzhi Mountain National Nature Reserve, hillside (18°53.83'N, 109°41.88'E, ca. 1590 m), 08.iv.2009, G. Tang leg. ***Paratypes*** 3♂9♀ (IZCAS-Ar43165–43176), same data as holotype; 2♂ (IZCAS-Ar43177–43178), hillside (18°53.84'N, 109°41.51'E, ca. 1210 m), same date and collector as holotype; 4♀ (IZCAS-Ar43179–43182), hillside (18°53.85'N, 109°41.89'E, ca. 1430 m), 09.iv.2009, G. Tang leg.; 1♂1♀ (TRUJS 0623–0624), Ledong County, Jianfengling National Nature Reserve, Peak Mountain (18°43.11'N, 108°52.32'E, ca. 1400 m), 16.iv.2019, C. Wang & Y.F. Yang leg.

Etymology. The specific name is a patronym of Dr. Xiaoqi Mi, who greatly helped us with this research; noun (name) in genitive case.

Diagnosis. The male of *Irura mii* sp. nov. can be easily distinguished from other congeners by the presence of PTA, and the distally semi-circled, filiform embolus, whereas absent, and not circled, flagelliform in others (see Metzner 2022). The female of this new species resembles *I. hamatapophysis* (Peng & Yin, 1991) known from Hunan of China in having the copulatory openings located at the posterior margin and the elongated junction ducts of spermathecae, but it can be easily distinguished by the copulatory ducts, which are longer and connected to the middle of the junction ducts of the spermathecae, and by the oval posterior chamber of the spermathecae (Fig. 3B), whereas the copulatory ducts are shorter, connected to the distal portions of the junction ducts of the spermathecae, and the posterior chamber of the spermathecae are eggplant-shaped in *I. hamatapophysis* (Peng and Yin 1991: fig. 1H, I).

Description. Male (Figs 2, 3C, D, F, G). Total length 3.67. Carapace 1.83 long, 1.98 wide. Abdomen 1.89 long, 1.75 wide. Eye sizes and inter-distances:

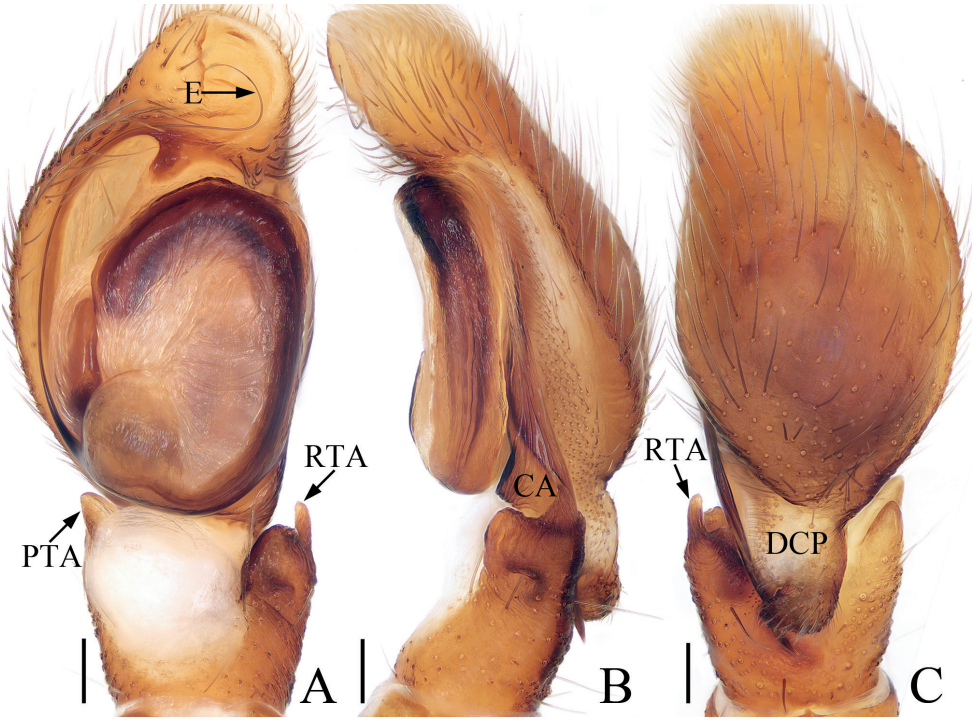

Figure 2. Male palp of *Irura mii* sp. nov., holotype **A** ventral **B** retrolateral **C** dorsal. Scale bars: 0.1 mm. Abbreviations: CA – cymbial apophysis; DCP – dorsal cymbial process; E – embolus; PTA – prolateral tibial apophysis; RTA – retrolateral tibial apophysis.

AME 0.45, ALE 0.26, PLE 0.21, AERW 1.61, PERW 1.86, EFL 0.92. Leg measurements: I 6.02 (1.83, 1.30, 1.38, 0.88, 0.63), II 3.22 (1.08, 0.58, 0.65, 0.58, 0.33), III 2.79 (0.93, 0.45, 0.53, 0.55, 0.33), IV 3.31 (1.10, 0.55, 0.70, 0.63, 0.33). Carapace almost oval, red-brown, setose, with pair of round, dark spots medially in eye field. Fovea indistinct. Chelicerae red-yellow, with two promarginal teeth and one retromarginal fissidental tooth. Endites longer than wide, bearing dense setae on distal portions of inner margins. Labium colored as endites. Sternum almost oval, with straight anterior margin. Legs I robust, with two pairs of macrosetae ventrally on tibiae and metatarsi, respectively; other legs pale to brown. Abdomen oval, dorsum covered entirely by large scutum, with white setae and three pairs of muscle depressions; venter dark brown medially, with brown, thin setae. Palp (Fig. 2A–C): tibia slightly wider than long in ventral view, with subtriangular prolateral apophysis and stout, broad RTA acutely narrowed to triangle shape distally in retrolateral view; cymbium longer than wide, with broad, irregular baso-dorsal process and spine-shaped retrolateral apophysis extending exceed dorsal process distally; bulb oval, flat, with sperm duct extending along margin; embolus slender, filiform, originating at ~ 7: 30 o'clock position of bulb, coiled into a semicircle distally.

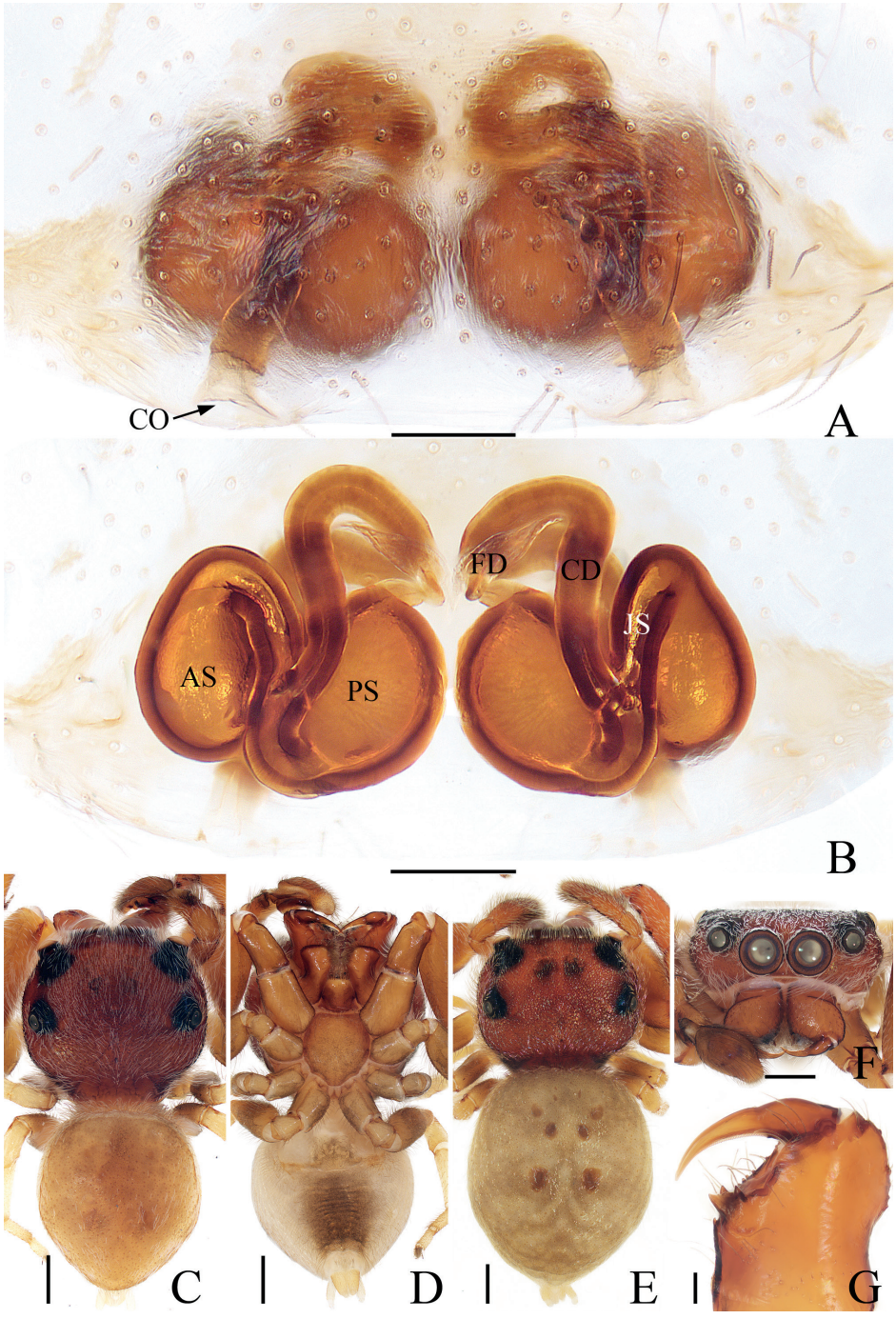

Figure 3. *Irura mii* sp. nov., male holotype and female paratype **A** epigyne, ventral **B** vulva, dorsal **C** holotype habitus, dorsal **D** ditto, ventral **E** female paratype habitus, dorsal **F** holotype carapace, frontal **G** holotype chelicera, posterior. Scale bars: 0.1 mm (**A, B, G**); 0.5 mm (**C–F**). Abbreviations: AS – anterior chamber of spermatheca; CD – copulatory duct; CO – copulatory opening; FD – fertilization duct; JS – junction duct of spermathecae; PS – posterior chamber of spermatheca.

Female (Fig. 3A, B, E). Total length 3.68. Carapace 1.49 long, 1.76 wide. Abdomen 2.30 long, 2.03 wide. Eye sizes and inter-distances: AME 0.41, ALE 0.20, PLE 0.17, AERW 1.39, PERW 1.69, EFL 0.81. Leg measurements: I 4.70 (1.63, 1.03, 1.03, 0.68, 0.33), II 3.10 (1.03, 0.58, 0.63, 0.53, 0.33), III 2.70 (0.90, 0.45, 0.50, 0.55, 0.30), IV 3.32 (1.13, 0.53, 0.68, 0.65, 0.33). Habitus (Fig. 3E) similar to that of male except with several herringbone-shaped stripes posteriorly and lacks a scutum on the dorsum of abdomen. Epigyne (Fig. 3A, B): wider than long; copulatory openings located at posterior margin, almost round, separated from each other by > 2 × the width of posterior chamber of spermathecae; copulatory ducts long, twisted, connected to the middle of junction ducts of spermathecae; spermathecae divided into two oval chambers; fertilization ducts lamellar, originate from anterior parts of posterior chamber of spermathecae.

Distribution. Only known from the type locality on Hainan Island, China.

Irura pengi Guo, Zhang & Zhu, 2011

Figs 4, 5

Irura pengi Guo, Zhang & Zhu, 2011: 91, figs 11–16 (♂, holotype, not examined).

Material examined. 2♂3♀ (TRU-JS 0625–0629), China: Hainan: Ledong County, Jianfengling National Nature Reserve, Tianchi (18°44.45'N, 108°57.49'E, ca. 860 m), 11.iv.2019, C. Wang & Y.F. Yang leg.

Diagnosis. The male of *Irura pengi* Guo, Zhang & Zhu, 2011 resembles *I. trigonapophysis* (Peng & Yin, 1991) known from Fujian, and Guangdong of China in having a flagelliform embolus originating at ~ 10 o'clock position on the bulb, but it can be distinguished by the straight RTA and terminally curved retrolateral cymbial apophysis in retrolateral view (Fig. 4B), whereas the RTA is slightly curved dorsally and the retrolateral cymbial apophysis is straight in *I. trigonapophysis* (Peng 2020: fig. 127b–d). The species also resembles that of *I. uniprocessa* Mi & Wang, 2016 known from Yunnan of China by the similar copulatory organs, but it can be distinguished by the following characters: (1) the presence of RTA (Fig. 4A–C), which is absent in *I. uniprocessa* (Mi and Wang 2016: figs 1C–E, 2a, b); (2) the absence of epigynal hoods and the distance between the anterior chambers of spermathecae is more than their width (Fig. 5B), whereas present and the distance between the anterior chambers of spermathecae is < 1/2 their width in *I uniprocessa* (Mi and Wang 2016: figs 1F, G, 2d, e).

Description. Male (Figs 4, 5C, D, F, G). Total length 4.52. Carapace 2.06 long, 2.35 wide. Abdomen 2.50 long, 2.26 wide. Eye sizes and inter-distances: AME 0.50, ALE 0.29, PLE 0.24, AERW 1.91, PERW 2.21, EFL 1.12. Leg measurements: I 7.02 (2.13, 1.63, 1.58, 1.03, 0.65), II 3.98 (1.28, 0.75, 0.85, 0.70, 0.40), III 3.32 (1.08, 0.58, 0.63, 0.63, 0.40), IV 3.87 (1.33, 0.63, 0.81, 0.70, 0.40). Carapace sub-square, red-brown, covered with dense, iridescent scales, with an irregular dark patch medially in eye field. Chelicerae red-brown, with two promarginal teeth and one large

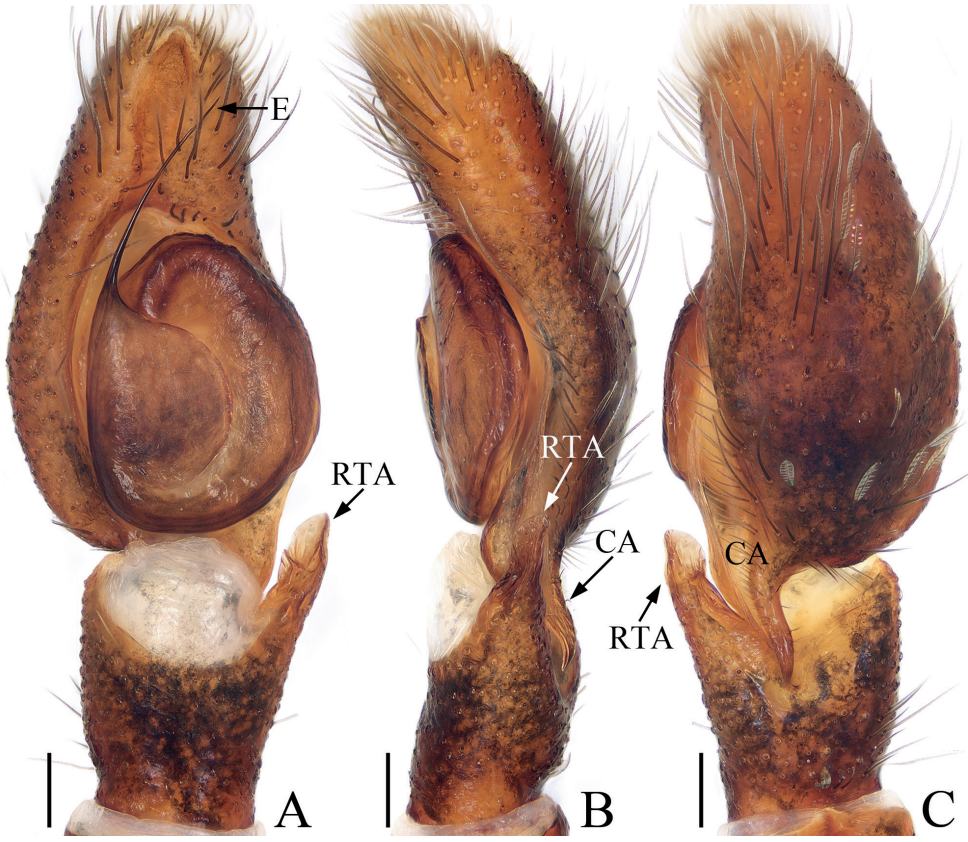

Figure 4. Male palp of *Irura pengi* Guo, Zhang & Zhu, 2011 **A** ventral **B** retrolateral **C** dorsal. Scale bars: 0.1 mm. Abbreviations: CA – cymbial apophysis; E – embolus; RTA – retrolateral tibial apophysis.

retromarginal tooth. Endites longer than wide, with dense, dark brown setae at inner-distal margins. Labium colored as endites, bearing dense, dark setae at anterior edges. Sternum sub-oval, covered with thin setae. Legs I robust, with a single and two pairs of macrosetae ventrally on tibiae and metatarsi, respectively; other legs yellow to dark. Abdomen oval, dorsum orange-red to dark brown, with longitudinal orange band anteromedially, three pairs of muscle depressions and several pairs of irregular orange patches medially and laterally, and several herringbone-shaped streaks posteriorly, covered entirely by a big scutum; venter brown to dark brown. Palp (Fig. 4A–C): tibia longer than wide, with straight RTA ~ 1/2 the tibia length, and blunt apically in retrolateral view; cymbium elongated, setose, with tapered, baso-retrolateral apophysis curved distally to a pointed tip, reaches anterior 1/3 of tibia in retrolateral view; bulb flat, almost round; embolus flagelliform, tapered, originates at ~ 10 o'clock position on bulb, slightly shorter than bulb length.

Female (Fig. 5A, B, E). Total length 4.26. Carapace 1.58 long, 2.06 wide. Abdomen 2.74 long, 2.29 wide. Eye sizes and inter-distances: AME 0.48, ALE 0.26, PLE 0.21,

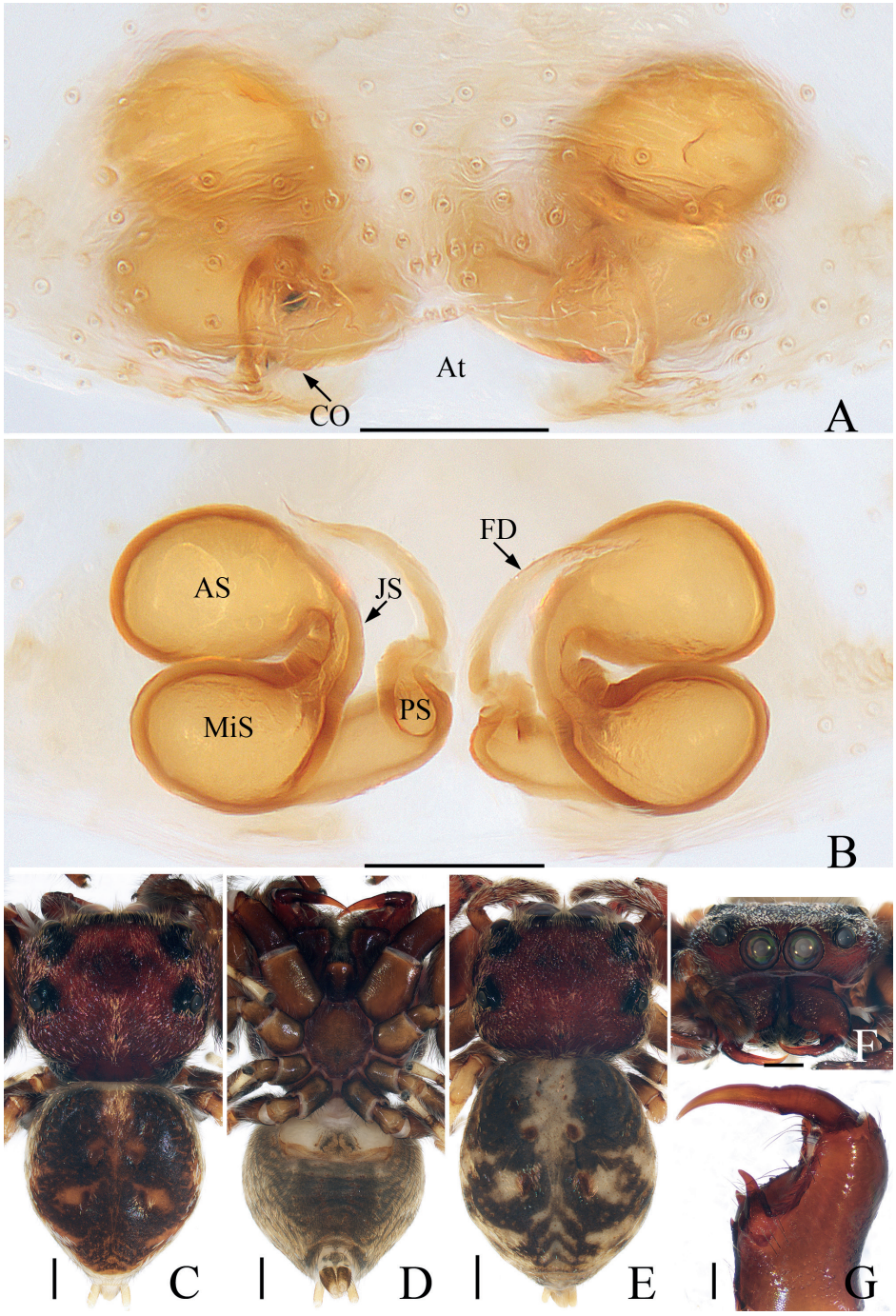

Figure 5. *Irura pengi* Guo, Zhang & Zhu, 2011 **A** epigyne, ventral **B** vulva, dorsal **C** male habitus, dorsal **D** ditto, ventral **E** female habitus, dorsal **F** male carapace, frontal **G** male chelicera, posterior. Scale bars: 0.1 mm (**A, B, G**); 0.5 mm (**C–F**). Abbreviations: AS – anterior chamber of spermatheca; At – atrium; CO – copulatory opening; FD – fertilization duct; MiS – median chamber of spermatheca; JS – junction duct of spermathecae; PS – posterior chamber of spermatheca.

AERW 1.74, PERW 2.03, EFL 0.97. Leg measurements: I 4.33 (1.40, 1.00, 0.85, 0.60, 0.48), II 3.11 (1.00, 0.53, 0.70, 0.50, 0.38), III 2.70 (0.88, 0.48, 0.48, 0.48, 0.38), IV 3.27 (1.13, 0.55, 0.63, 0.58, 0.38). Habitus (Fig. 5E) similar to that of male except pale and with less-developed retromarginal cheliceral tooth. Epigyne (Fig. 5A, B): wider than long, with broad, posteriorly-located atrium; copulatory openings beneath the antero-bilateral edge of atrium; copulatory ducts short, tapered, connected to the junction ducts of anterior and middle chambers of spermathecae; spermathecae divided into three oval chambers; fertilization ducts elongated, originate from anterior edges of the smallest posterior chamber of spermathecae.

Distribution. Only known from Hainan Island, China.

Genus *Marengo* Peckham & Peckham, 1892

Type species. *Marengo crassipes* Peckham & Peckham, 1892 from Sri Lanka by original designation.

Comments. *Marengo*, a tribe Baviini genus, contains ten species distributed in India, Sri Lanka, Thailand, and China (Maddison 2015; WSC 2022). A recent redefined of the genus was provided by Benjamin (2004), who diagnosed the genus by the presence of ventral, leaf-like scales on tibiae I and the accessory gland of copulatory ducts. However, even within a genus, the copulatory organs in the Ballini look alike and are very often useless for supraspecific diagnoses (Azarkina and Haddad 2020). And so, the above definition could not be accurate. Herein, the definition of the genus is not discussed, and we assigned the following two new species to *Marengo* because they are closely similar to some species of the genus.

Marengo ganae sp. nov.

https://zoobank.org/3F140AF9-B89C-476A-8CF0-B8E0B0BD5053
Figs 6, 7

Type material. ***Holotype*** ♂ (TRU-JS 0630), China: Hainan: Ledong County, Jianfeng Village, Jianfengling National Nature Reserve, Tianchi (18°44.90'N, 108°52.01'E, ca. 790 m), 12.viii.2020, X.Q. Mi et al. leg. ***Paratypes*** 1♂2♀ (TRU-JS 0631–0633), same data as holotype; 1♀ (IZCAS-Ar43183), Lingshui County, Diaoluoshan National Nature Reserve (18°43.44'N, 109°52.60'E, ca. 490 m), 10.viii.2010, G. Zheng leg.; 1♂1♀ (IZCAS-Ar43184–43185), Diaoluoshan National Nature Reserve, Luchang (18°43.39'N, 109°51.07'E, ca. 940 m), 10.viii.2010, G. Tang leg.

Etymology. The specific name is a patronym of Mrs. Jiahui Gan, one of the collectors of the type specimens; noun (name) in genitive case.

Diagnosis. *Marengo ganae* sp. nov. resembles *M. tangi* Wang & Li, 2021 known from Yunnan of China in having a similar habitus and copulatory organs but it can be easily distinguished by the following characters: (1) the process of the embolic disc is lamellar (Fig. 6B, D), whereas it is almost hook-shaped in *M. tangi* (Wang and Li

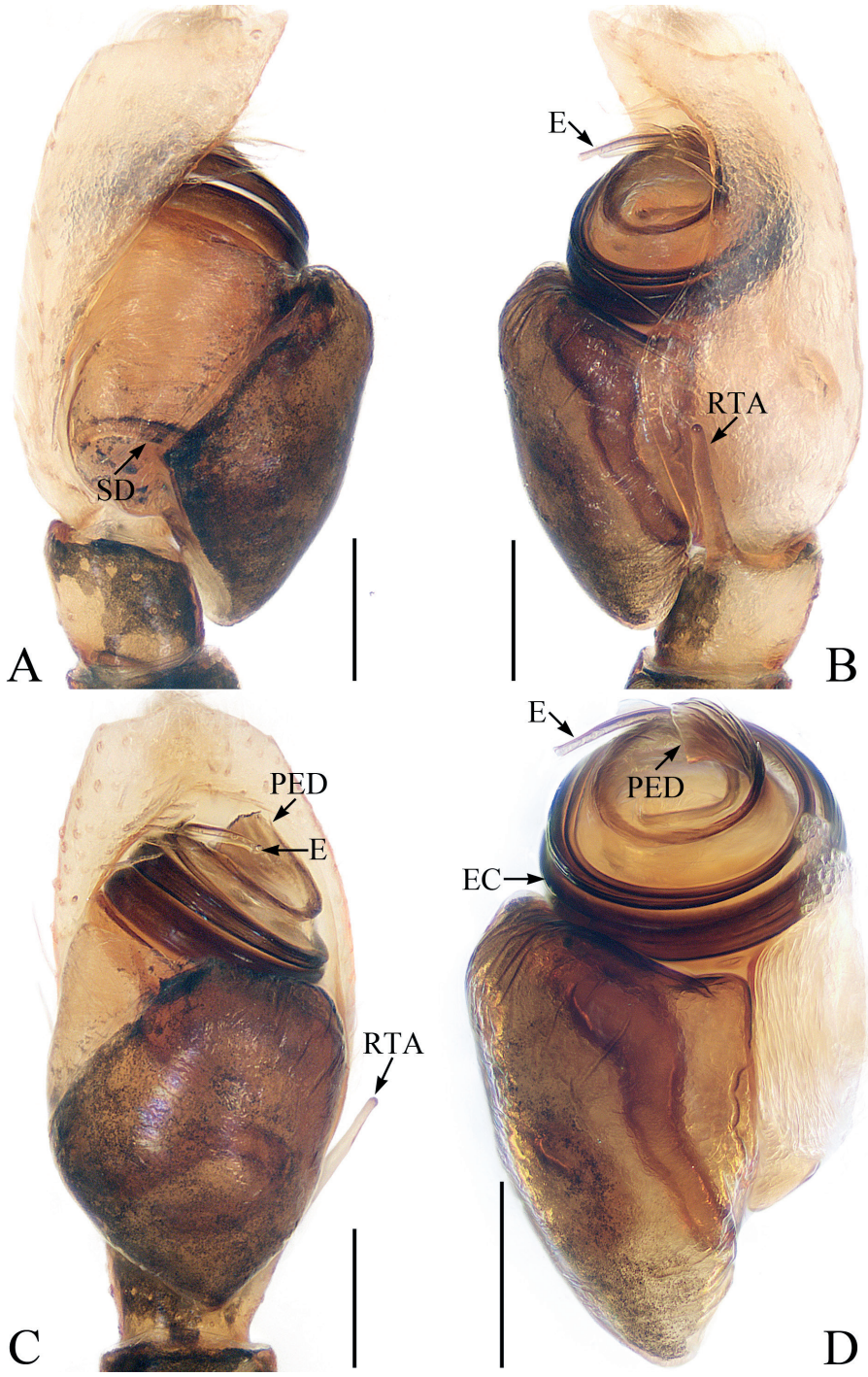

Figure 6. Male palp of *Marengo ganae* sp. nov., holotype **A** prolateral **B** retrolateral, **C** ventral **D** bulb, retrolateral. Scale bars: 0.1 mm. Abbreviations: E – embolus; EC – embolic coil; PED – process of embolic disc; RTA – retrolateral tibial apophysis; SD – sperm duct.

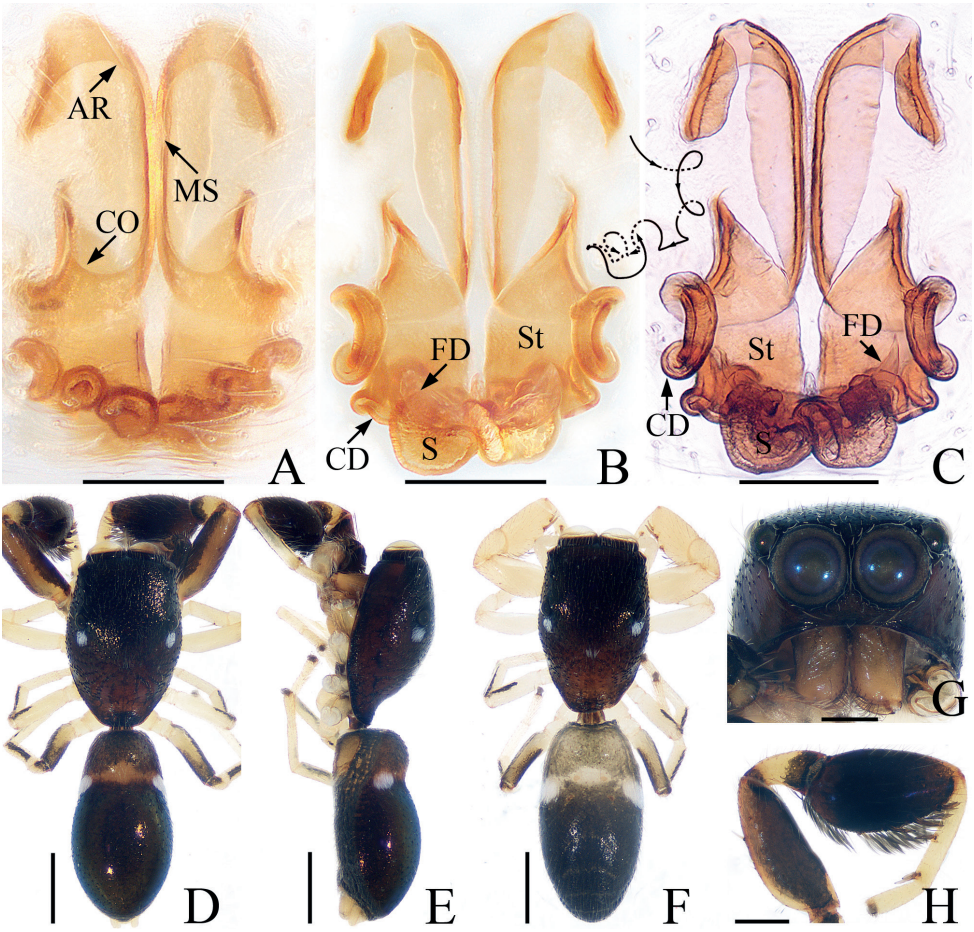

Figure 7. *Marengo ganae* sp. nov., male holotype and female paratype **A** epigyne, ventral **B, C** vulva, dorsal **D** holotype habitus, dorsal **E** ditto, lateral **F** female paratype habitus, dorsal **G** holotype carapace, frontal **H** holotype leg I, prolateral. Scale bars: 0.1 mm (**A–C**); 0.2 mm (**G, H**); 0.5 mm (**D–F**). Abbreviations: AR – atrial ridge; CD – copulatory duct; CO – copulatory opening; FD – fertilization duct; MS – median septum; S – spermatheca; St – stiffener.

2021: fig. 6B, D); (2) the RTA is slightly longer than the tibia (Fig. 6B), whereas it is ~ 1/2 the tibial length in *M. tangi* (Wang and Li 2021: fig. 6B); (3) the epigynal stiffener is ~ 4 × wider than the copulatory duct (Fig. 7B, C), whereas it is ~ 2 × wider than copulatory duct in *M. tangi* (Wang and Li 2021: fig. 7B). The species is also similar to that of *M. striatipes* Simon, 1900 known from Sri Lanka, but it can be easily distinguished by elongated atria having U-shaped posterior margins (Fig. 7A), whereas oval atria with C-shaped posterior margins in *M. striatipes* (Benjamin 2004: fig. 67B).

Description. Male (Figs 6, 7D, E, G, H). Total length 2.57. Carapace 1.19 long, 0.82 wide. Abdomen 1.35 long, 0.72 wide. Eye sizes and inter-distances: AME 0.28, ALE 0.10, PLE 0.12, AERW 0.71, PERW 0.74, EFL 0.53. Leg

measurements: I 2.92 (0.83, 0.43, 0.78, 0.60, 0.28), II 1.85 (0.55, 0.28, 0.43, 0.35, 0.24), III 1.63 (0.48, 0.23, 0.33, 0.35, 0.24), IV 2.16 (0.65, 0.30, 0.53, 0.43, 0.25). Carapace red-brown to dark brown, with pair of white spots of scales behind PLEs, covered with small papillae and brown setae. Chelicerae dark yellow, with two promarginal and three retromarginal teeth. Endites longer than wide. Labium colored as endites. Sternum almost oval. Legs I with enlarged tibiae with dense, ventral, leaf-like scales, and three pairs of ventral macrosetae; other legs pale to brown, with prolateral stripes on femora, patella, and tibiae III, IV. Abdomen elongate-oval, slightly constricted at anterior 1/4, dorsum red-brown to dark brown, anteriorly with a transverse yellow band bearing pair of white spots of scales at lateral margins, covered entirely by large scutum; venter paler than dorsum. Palp (Fig. 6A–D): tibia wider than long; RTA straight, slender, almost 1.5 × longer than tibia, blunt apically; bulb swollen, divided by cleft; embolus coiled almost twice; process of embolic disc lamellar, wrinkled.

Female (Fig. 7A–C, F). Total length 2.65. Carapace 1.17 long, 0.79 wide. Abdomen 1.40 long, 0.75 wide. Eye sizes and inter-distances: AME 0.28, ALE 0.10, PLE 0.11, AERW 0.70, PERW 0.73, EFL 0.53. Leg measurements: I 2.17 (0.63, 0.33, 0.55, 0.43, 0.23), II 1.58 (0.48, 0.25, 0.33, 0.30, 0.22), III 1.48 (0.45, 0.23, 0.30, 0.28, 0.22), IV 2.12 (0.66, 0.28, 0.50, 0.43, 0.25). Habitus (Fig. 7F) similar to that of male except paler and with unmodified tibiae I lacking ventral, leaf-like scales. Epigyne (Fig. 7A–C): with pair of anterior hood-shaped structures, and pair of stiffeners touching copulatory ducts; atria elongate-oval, separated by narrow median septum; copulatory openings beneath the posterior margins of atria; copulatory ducts curved, twisted into tortuous coils; spermathecae slightly broadened and curved medially; fertilization ducts lamellar, broad, extending anterolaterally.

Distribution. Only known from the type locality on Hainan Island, China.

***Marengo zhengi* sp. nov.**

https://zoobank.org/5690ACA3-CD79-48CB-86F9-D89B9D95415A

Figs 8, 9

Type material. ***Holotype*** ♂ (IZCAS-Ar43186), China: Hainan: Lingshui County, Diaoluoshan National Nature Reserve, mountain near the river (18°43.39'N, 109°51.27'E, ca. 930 m), 10.viii.2010, G. Zheng leg. ***Paratypes*** 3♂2♀ (IZCAS-Ar43187–43191), same data as holotype; 2♂ (IZCAS-Ar43192–43193), around the Plank Road (18°43.56'N, 109°51.99'E, ca. 950 m), 08.viii.2010, G. Zheng leg.; 1♂ (IZCAS-Ar43194), around the Plank Road (18°43.67'N, 109°51.83'E, ca. 990 m), 09.viii.2010, G. Zheng leg.; 1♀ (IZCAS-Ar43195), around the Plank road near the waterfall (18°43.44'N, 109°52.60'E, ca. 500 m), 10.viii.2010, G. Zheng leg.

Etymology. The specific name is a patronym of Prof. Guo Zheng, the collector of the new species; noun (name) in genitive case.

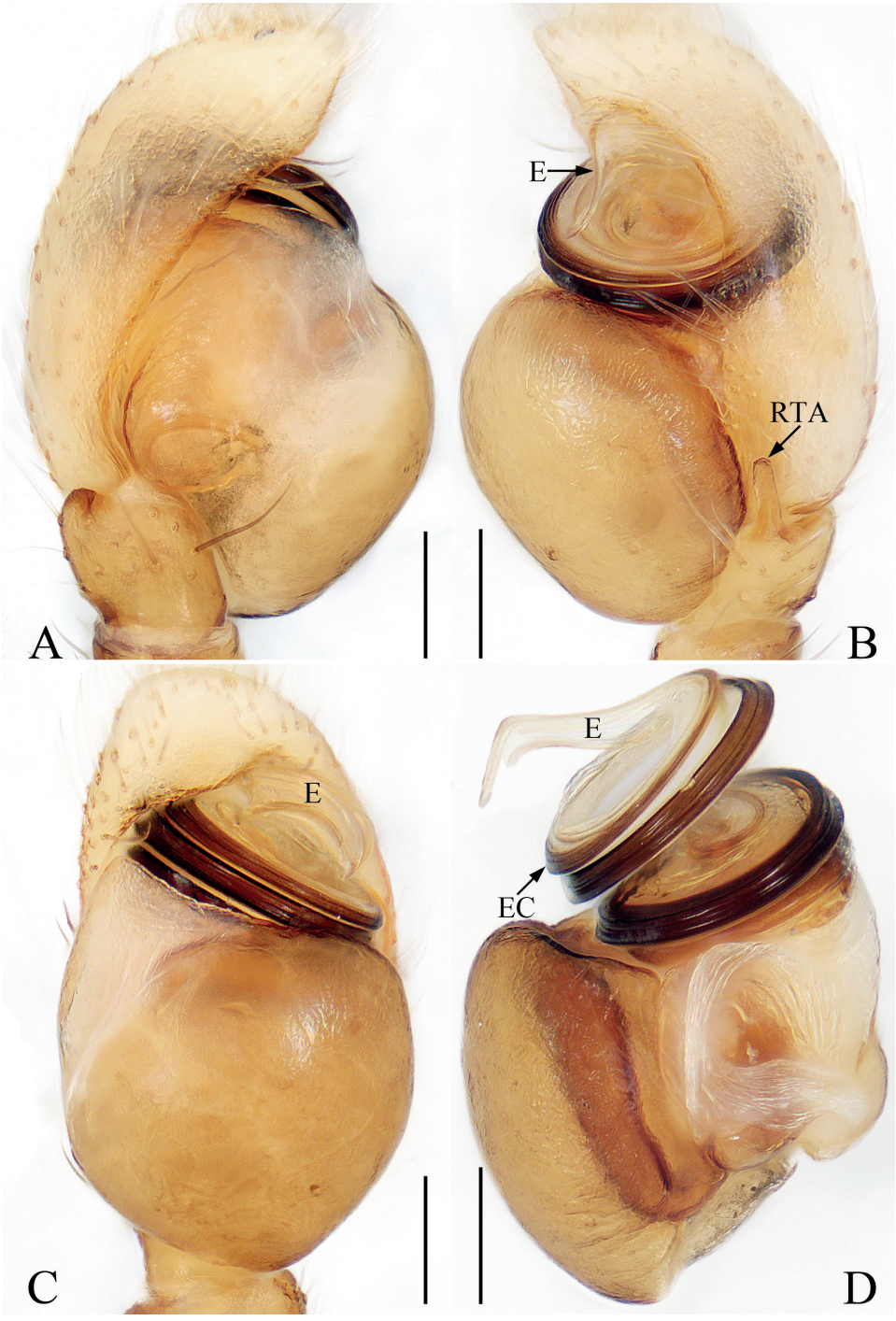

Figure 8. Male palp of *Marengo zhengi* sp. nov., holotype and paratype **A** holotype palp, prolateral **B** ditto, retrolateral **C** ditto, ventral **D** paratype bulb, retrolateral. Scale bars: 0.1 mm. Abbreviations: E – embolus; EC – embolic coil; RTA – retrolateral tibial apophysis.

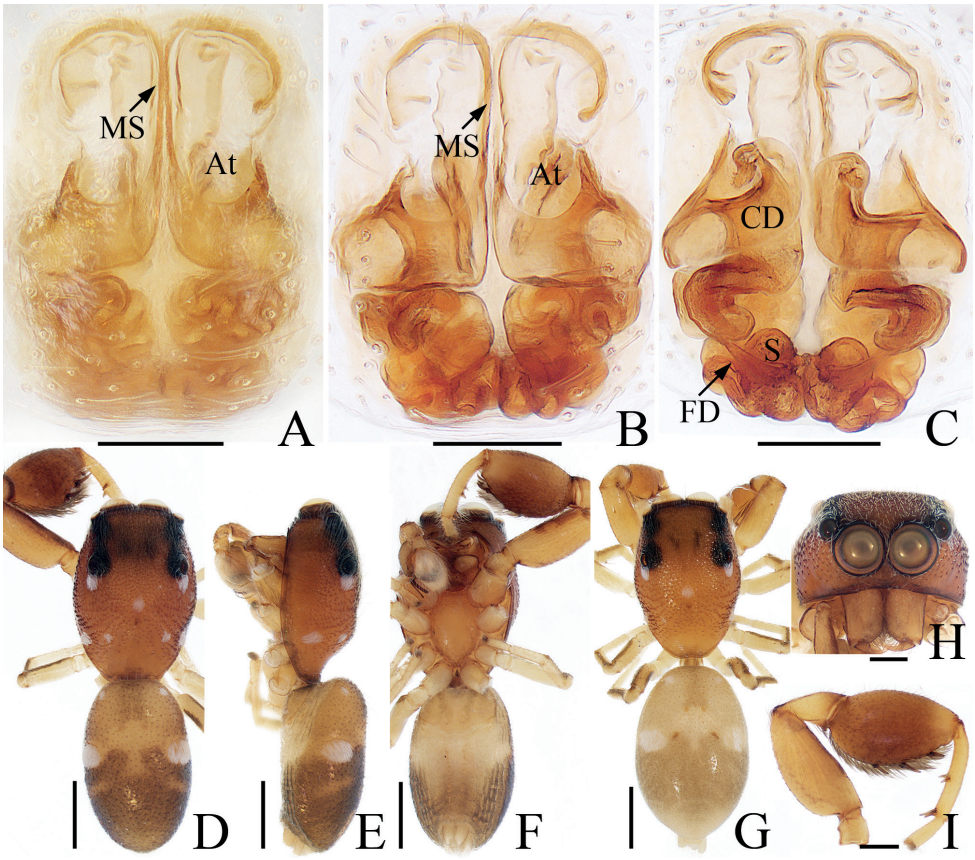

Figure 9. *Marengo zhengi* sp. nov., male holotype and female paratype **A, B** epigyne, ventral **C** vulva, dorsal **D** holotype habitus, dorsal **E** ditto, lateral **F** ditto, ventral **G** female paratype habitus, dorsal **H** holotype carapace, frontal **I** holotype leg I, retrolateral. Scale bars: 0.1 mm (**A–C**); 0.2 mm (**H, I**); 0.5 mm (**D–G**). Abbreviations: At – atrium; CD – copulatory duct; FD – fertilization duct; MS – median septum; S – spermatheca.

Diagnosis. *Marengo zhengi* sp. nov. closely resembles *M. deelemanae* Benjamin, 2004 known from Prachuap Khiri Khan of Thailand in having a similar habitus and copulatory organs, but it differs in the following characters: (1) the embolus is lamellar distally (Fig. 8B, C, D), whereas it is bar-shaped in *M. deelemanae* (Benjamin 2004: fig. 68E, F); (2) the RTA is almost uniform in width (Fig. 8B), whereas it is acutely narrowed medially in *M. deelemanae* (Benjamin 2004: fig. 68E); (3) the copulatory ducts are extending exceed the copulatory openings proximally (Fig. 9C), whereas not exceed the copulatory openings in *M. deelemanae* (Benjamin 2004: fig. 68D).

Description. Male (Figs 8, 9D–F, H, I). Total length 2.60. Carapace 1.34 long, 0.96 wide. Abdomen 1.32 long, 0.84 wide. Eye sizes and inter-distances: AME 0.28, ALE 0.10, PLE 0.12, AERW 0.71, PERW 0.75, EFL 0.48. Leg measurements: I 3.14 (0.88, 0.50, 0.83, 0.68, 0.25), II 1.81 (0.58, 0.30, 0.40, 0.33, 0.20), III 1.71 (0.53, 0.25, 0.35, 0.38, 0.20), IV 2.11 (0.68, 0.33, 0.50, 0.40, 0.20). Carapace elongate-oval,

red-yellow, with a pair of dark dots on eye field and seven clusters of white patches of scales on thorax, covered with small papillae and thin setae. Chelicerae dark yellow, with two promarginal and four retromarginal teeth. Endites colored as chelicerae, with dense, dark setae anteriorly. Labium darker than endites, almost linguiform. Sternum almost oval. Legs yellow to red-yellow; leg I robust, with enlarged tibia with dense, leaf-like scales, and three pairs of macrosetae ventrally; other legs pale to brown. Abdomen elongate-oval, dorsum yellow to dark brown, with pair of small, round, white spots of scales at anterolateral margin, a broad, longitudinal, brown band followed by irregular yellow patch, and pair of round, white patches mediolaterally, entirely covered by large scutum; venter pale to brown. Palp (Fig. 8A–D): tibia short, with straight RTA of nearly uniform width, slightly shorter than its length, and blunt apically in retrolateral view; bulb bugling; embolus coiled ~3 ×, tapered, lamellar distally.

Female (Fig. 9A–C, G). Total length 2.73. Carapace 1.23 long, 0.87 wide. Abdomen 1.40 long, 0.92 wide. Eye sizes and inter-distances: AME 0.29, ALE 0.10, PLE 0.12, AERW 0.70, PERW 0.77, EFL 0.48. Leg measurements: I 2.14 (0.65, 0.33, 0.53, 0.40, 0.23), II 1.61 (0.50, 0.25, 0.33, 0.30, 0.23), III 1.59 (0.45, 0.23, 0.30, 0.38, 0.23), IV 1.96 (0.63, 0.25, 0.45, 0.40, 0.23). Habitus (Fig. 9G) similar to that of male except pale, with unmodified tibia I lacking leaf-like scales and replaced with several long setae ventrally. Epigyne (Fig. 9A–C): atria paired, anteriorly located, ~ 1.5 × longer than wide, separated by narrow septum; copulatory openings beneath posterior edges of atria; copulatory ducts long, widened proximally, forming complicated coils; spermathecae sub-oval; fertilization ducts elongated, lamellar.

Distribution. Only known from the type locality on Hainan Island, China.

Genus *Nungia* Żabka, 1985

Type species. *Nungia epigynalis* Żabka, 1985 from Vietnam by original designation.

Comments. *Nungia* contains five species distributed mainly in Southeast Asia (WSC 2022). The original definition of the genus is just based on the butterfly-shaped vulva (Żabka 1985). Moreover, Maddison et al. (2020) transferred four species into the genus based on molecular evidence and the transferred species are inconsistent in copulatory organs. Based on that, it is hard to define the genus according to its morphological character at present.

Nungia tangi sp. nov.

https://zoobank.org/85DDE8DF-DE75-4859-9E95-8335506E73AA
Figs 10, 11

Type material. ***Holotype*** ♂ (TRU-JS 0634), China: Hainan: Ledong County, Jianfeng Village, Jianfengling National Nature Reserve, Yulingu (18°44.96'N, 108°55.32'E, ca. 650 m), 13.iv.2020, C. Wang & Y.F. Yang leg. ***Paratype*:** 1♀ (TRU-JS 0635), same data as holotype.

Etymology. The specific name is a patronym of Dr. Guo Tang, who conducted important research on the taxonomy of the crab spiders of Hainan Island; noun (name) in genitive case.

Diagnosis. *Nungia tangi* sp. nov. resembles *N. epigynalis* Żabka, 1985 known from China, Vietnam, and Japan in the general shape of copulatory organs, but it can be easily distinguished by the following characters: (1) the presence of DTA (Fig. 10B, D), whereas absent in *N. epigynalis* (Peng 2020: fig. 184f); (2) the RTA is directed upward in retrolateral view (Fig. 10B), whereas it is curved retrolaterally in *N. epigynalis* (Peng 2020: fig. 184f); (3) the spermathecae are eggplant-shaped (Fig. 11B), whereas they are oval in *N. epigynalis* (Peng 2020: fig. 184 i, j).

Description. Male (Figs 10, 11C–E, G–I). Total length 4.63. Carapace 1.83 long, 1.33 wide. Abdomen 2.63 long, 1.04 wide. Eye sizes and inter-distances: AME 0.41, ALE 0.20, PLE 0.20, AERW 1.21, PERW 1.29, EFL 0.83. Leg measurements: I 3.92 (1.13, 0.78, 0.88, 0.63, 0.50), II 2.58 (0.78, 0.50, 0.60, 0.40, 0.30), III 2.43 (0.75, 0.40, 0.45, 0.53, 0.30), IV 3.25 (1.05, 0.50, 0.75, 0.65, 0.30). Carapace red-brown, with an irregular dark patch in eye field and narrow, orange central stripe posteromedially, covered with sparse, white setae. Fovea punctiform. Chelicerae dark yellow, with two promarginal teeth and one retromarginal tooth. Endites colored as chelicerae, longer than wide, slightly widened distally, with dense setae on inner margins. Labium sub-linguiform, paler terminally. Sternum elongate-oval, > 1.5 × longer than wide. Legs I robust, with slightly enlarged femora and tibiae, and bearing dense, leaf-like scales ventrally on patellae and tibiae; other legs yellow to brown. Abdomen elongated, dorsum brown to dark brown, with the transverse, undulate streak at posterior 1/3, partly covered by a scutum anteromedially; venter pale to brown, with lateral, dotted lines. Palp (Fig. 10A–D): tibia short, with tapered RTA strongly sclerotized at distal 1/3, and blunt apically, and sub-triangular DTA; bulb swollen; embolus straight, strongly sclerotized, originates from antero-prolateral edge of bulb, extending antero-retrolaterally, with blunt apex.

Female (Fig. 11A, B, F). Total length 5.75. Carapace 2.04 long, 1.51 wide. Abdomen 3.23 long, 1.45 wide. Eye sizes and inter-distances: AME 0.43, ALE 0.22, PLE 0.22, AERW 1.30, PERW 1.43, EFL 0.89. Leg measurements: I 3.02 (0.78, 0.65, 0.78, 0.43, 0.38), II missing, III 2.65 (0.75, 0.45, 0.50, 0.65, 0.30), IV 3.66 (1.13, 0.63, 0.90, 0.70, 0.30). Habitus (Fig. 11F) similar to that of male except without dorsal abdominal scutum. Epigyne (Fig. 11A, B): almost as long as wide, with arc-shaped basal plate; copulatory openings almost round, anteriorly located, separated from each other by ~ 1/2 width of basal plate; copulatory ducts very short, with lamellar accessory glands; spermathecae eggplant-shaped, separated from each other by 1/3 their width; fertilization ducts lamellar, broad, extending anterolaterally.

Distribution. Only known from the type locality, Hainan Island, China.

Comments. The species is placed into *Nungia* due to its general resemblance to the *N. epigynalis* Żabka, 1985. However, it also possesses some characters, such as the presence of long, dense, leaf-like scales ventrally on the patellae and tibiae I in both sexes, having two tibia apophyses of male palp and elongated spermathecae which are different from the latter. And so, its generic position may need further confirmation.

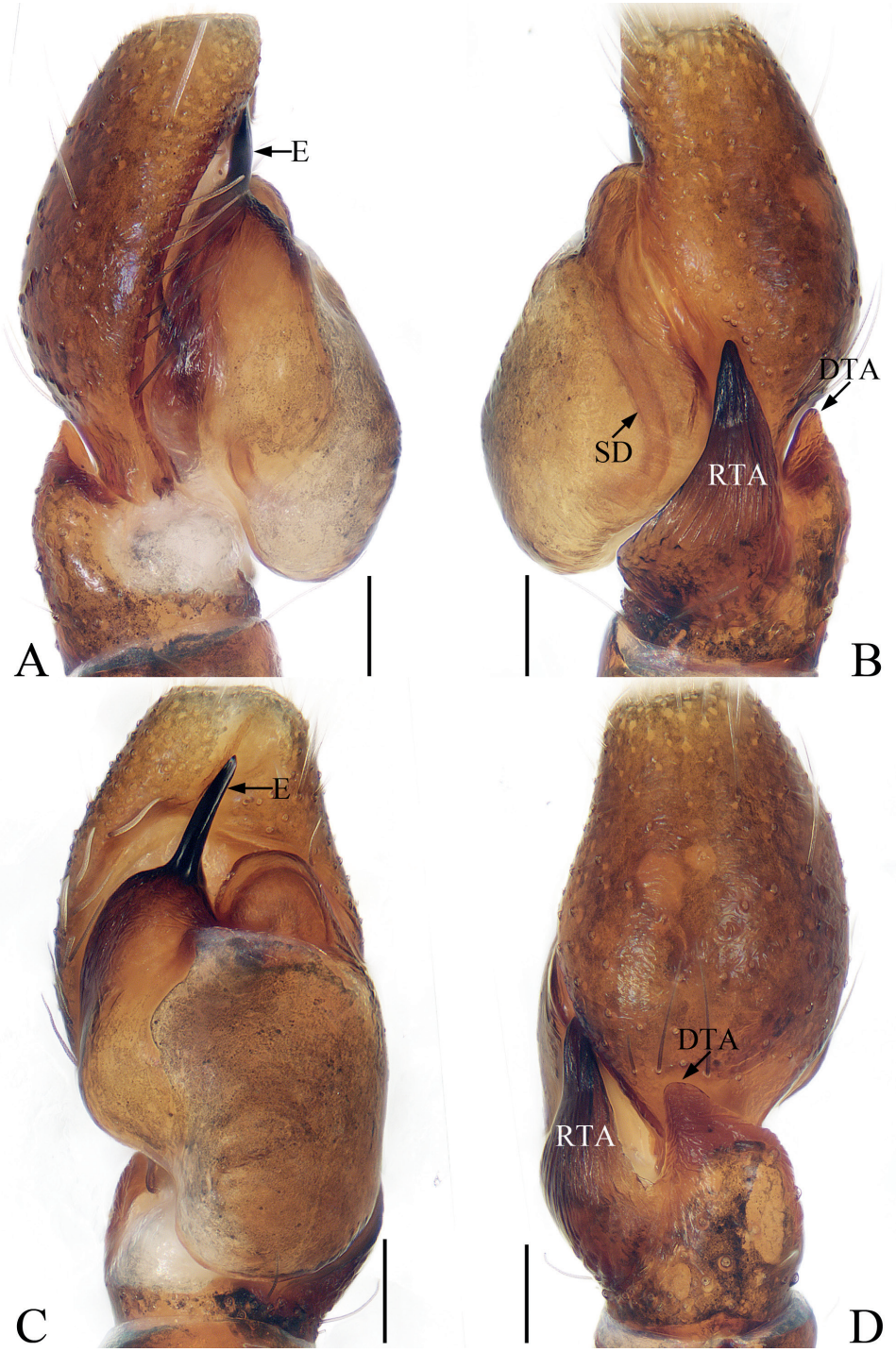

Figure 10. Male palp of *Nungia tangi* sp. nov., holotype **A** prolateral **B** retrolateral **C** ventral **D** dorsal. Scale bars: 0.1 mm. Abbreviations: DTA – dorsal tibial apophysis; E – embolus; RTA – retrolateral tibial apophysis; SD – sperm duct.

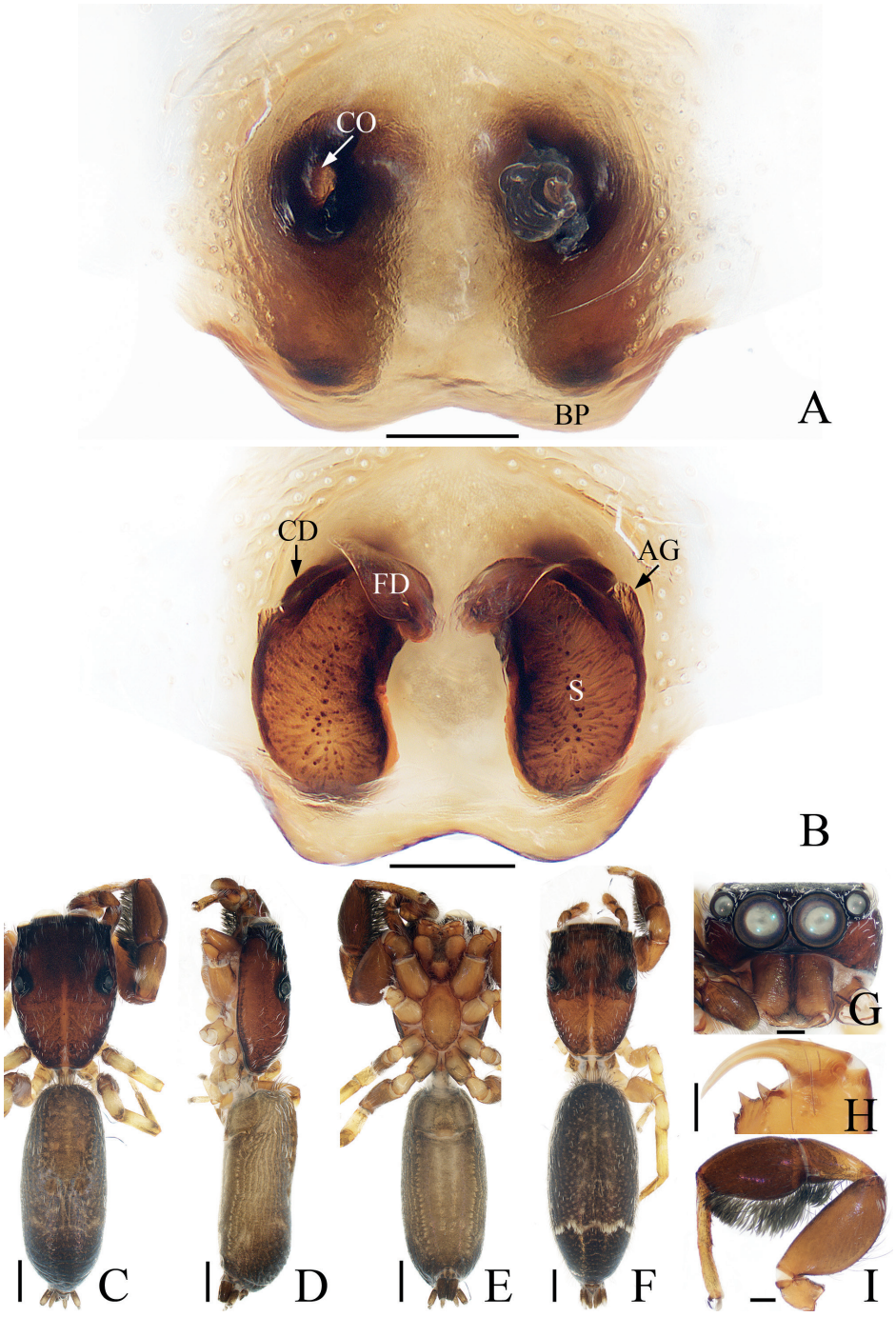

Figure 11. *Nungia tangi* sp. nov., male holotype and female paratype **A** epigyne, ventral **B** vulva, dorsal **C** holotype habitus, dorsal **D** ditto, lateral **E** ditto, ventral **F** female paratype habitus, dorsal **G** holotype carapace, frontal **H** holotype chelicera, posterior **I** holotype leg I, prolateral. Scale bars: 0.1 mm (**A, B, H**); 0.2 mm (**G, I**); 0.5 mm (**C–F**). Abbreviations: AG – accessory gland; BP – basal epigynal plate; CD – copulatory duct; CO – copulatory opening; FD – fertilization duct; S – spermatheca.

Genus *Pengmarengo* gen. nov.
https://zoobank.org/BA4E5B47-123C-4918-889C-F0C39EC9FF26

Type species. *Pengmarengo yangi* sp. nov. from China.

Etymology. The generic name is a combination of the first name of Prof. Xianjin Peng, a renowned jumping spider expert, and the related genus *Marengo*. The gender is feminine.

Diagnosis. *Pengmarengo* gen. nov. can be easily distinguished from Ballini genera except for *Afromarengo*, *Indomarengo*, *Leikung*, and *Marengo* by the presence of ventral, leaf-like scales on tibiae I (Benjamin 2004; Azarkina and Haddad 2020). It can be easily distinguished from *Leikung* by the not raised PME and only five macrosetae on tibiae I, whereas PME is raised and there are eight macrosetae on tibiae I in *Leikung* (Benjamin 2004: fig. 49D). It differs from the other three genera by the: (1) unmodified femora I, whereas enlarged in *Afromarengo*, and *Marengo* (Azarkina and Haddad 2020: figs 90, 91, 97–99, 105, 106, 112, 113; Wanless 1978: figs 1C, 3E, 10E); (2) very flat carapace, which is > 3 × longer than wide in lateral view, with the facial length almost equal to the AME diameter, and without a distinct clypeus, whereas carapace is < 3 × longer than wide in lateral view, with facial length greater than the AME diameter and with a distinct clypeus in the three genera (Wanless 1978: figs 1D, 3D; Benjamin 2004: figs 38C, 39A; Azarkina and Haddad 2020: figs 88, 89, 94, 96, 103, 104, 110, 111, 121, 122, 142, 143); (3) the presence of pair of white patches on the dorsum of abdomen, whereas absent in *Afromarengo*, and *Indomarengo* (Benjamin 2004: figs 38A, 41C, 42E; Azarkina and Haddad 2020: figs 87, 92 100, 108, 119, 142); (4) specific form of the copulatory ducts which extend posterolaterally before reversing direction completely or partly, causing the copulatory ducts to overlap anteromedially, and the prominent spermathecae, whereas copulatory ducts do not overlap and spermathecae are not prominent in the three genera (Wanless 1978: figs 1J, 3C; Benjamin 2004: fig. 39C; Azarkina and Haddad 2020: figs 83, 138).

Description. Small to medium spiders, both sexes with similar habitus. Carapace flat, > 3 × longer than wide in lateral view, covered with small papillae and larger piliferous papillae, usually with four clusters of white scales, of which two posterolateral to AMEs and other two posterolaterally located on thorax. Fovea and clypeus indistinct. Chelicerae yellow to red-brown, with two promarginal and three retromarginal teeth. Endites longer than wide, with pale ental sides bearing dark setae. Labium usual shape. Sternum elongated, sub-fusiform. Legs I robust, with enlarged tibia with a cluster of ventral, leaf-like scales and five ventral macrosetae in both sexes, other legs pale to yellow, mostly with dark brown stripes laterally on femora and tibiae. Abdomen elongated, > 2.5 × longer than wide, slightly constricted at anterior 1/3 in males, dorsum with pair of white patches of setae laterally behind constriction, entirely covered by scutum in males, and with sub-trapeziform scutum near anterior margin in females.

Palp: tibia wider than long, with bar-shaped RTA of varying lengths; bulb bulging, divided by a cleft; embolus short, coiled < 2 ×, associated with disc process or not. Epigyne: longer than wide; atria paired, oval, with arc-shaped anterior ridge;

copulatory ducts long, extending posterolaterally before reversing direction completely or partly, causing ducts to overlap anteromedially; spermathecae prominent, L- or U-shaped, with or without hemispherical processes at anterior margins; fertilization ducts originating from the median or anterior portions of longitudinal parts of spermathecae.

Distribution. China (Hainan, Yunnan, Taiwan), Indonesia.

Composition. *Pengmarengo* is a tribe Ballini genus, and currently includes five species: *P. chelifer* (Simon, 1900), comb. nov. (transferred from *Philates*), *P. elongata* (Peng & Li, 2002), comb. nov. (transferred from *Tauala*), *P. wengnan* (Wang & Li, 2022), comb. nov. (transferred from *Indomarengo*, see Wang and Li 2022), *P. yangi* sp. nov., and *P. yui* (Wang & Li, 2020), comb. nov. (transferred from *Indomarengo*).

Comments. *P. yui* and *P. wengnan* are transferred because they are sharing similar habitus and copulatory organs with generotype, especially in having the partly overlapped copulatory ducts and prominent, L-shaped spermathecae. *P. chelifer* possesses a series of characters, such as the presence of ventral scales of tibial I (rather than ventral setae in *Philates*), with sub-trapeziform scutum on the dorsum of abdomen in female, the flat carapace, pair of white patches of setae laterally on the dorsum of abdomen, and anteromedially overlapped copulatory ducts (Benjamin 2004: figs 25D, 26B, C, 27A–C), which are consistent with the generotype, and so, it also being transferred. According to the diagnostic drawings (Peng 2020: fig. 344), *P. elongata* is a Ballini species. Moreover, it has very flat carapace and anteromedially overlapped copulatory ducts. Based on that, we also transferred it into the new genus.

***Pengmarengo yangi* sp. nov.**

https://zoobank.org/1878BD48-9161-444B-8DA8-8FF3520528BB

Figs 12–14

Type material. ***Holotype*** ♂ (TRU-JS 0636), China: Hainan: Ledong County, Jianfeng Township, Jianfengling National Nature Reserve, Main Peak (18°43.11'N, 108°52.32'E, ca. 1400 m), 16.v.2019, C. Wang & Y.F. Yang leg. ***Paratypes*** 2♂3♀ (TRU-JS 0637–0641), same data as holotype.

Etymology. The specific name is a patronym of Mr. Yuanfa Yang, one of the collectors of the type specimens; noun (name) in genitive case.

Diagnosis. The male of *Pengmarengo yangi* sp. nov. resembles *P. yui* (Wang & Li, 2020) comb. nov. known from Yunnan of China by the habitus, but it can be easily distinguished by the lamellar process of the embolic disc and the flat embolus has spine-shaped distal processes (Figs 12B–D, 14B), whereas lacks the process of embolic disc and with bar-shaped embolus lacks process in *P. yui* (Wang and Li 2020: figs 5B–D, 6A, B). The female can be easily distinguished from other congeners by the prominent, L-shaped spermathecae, whereas in *P. chelifer* and *P. elongata* they are U-shaped or elongated (Benjamin 2004: fig. 26C; Peng 2020: fig. 344c).

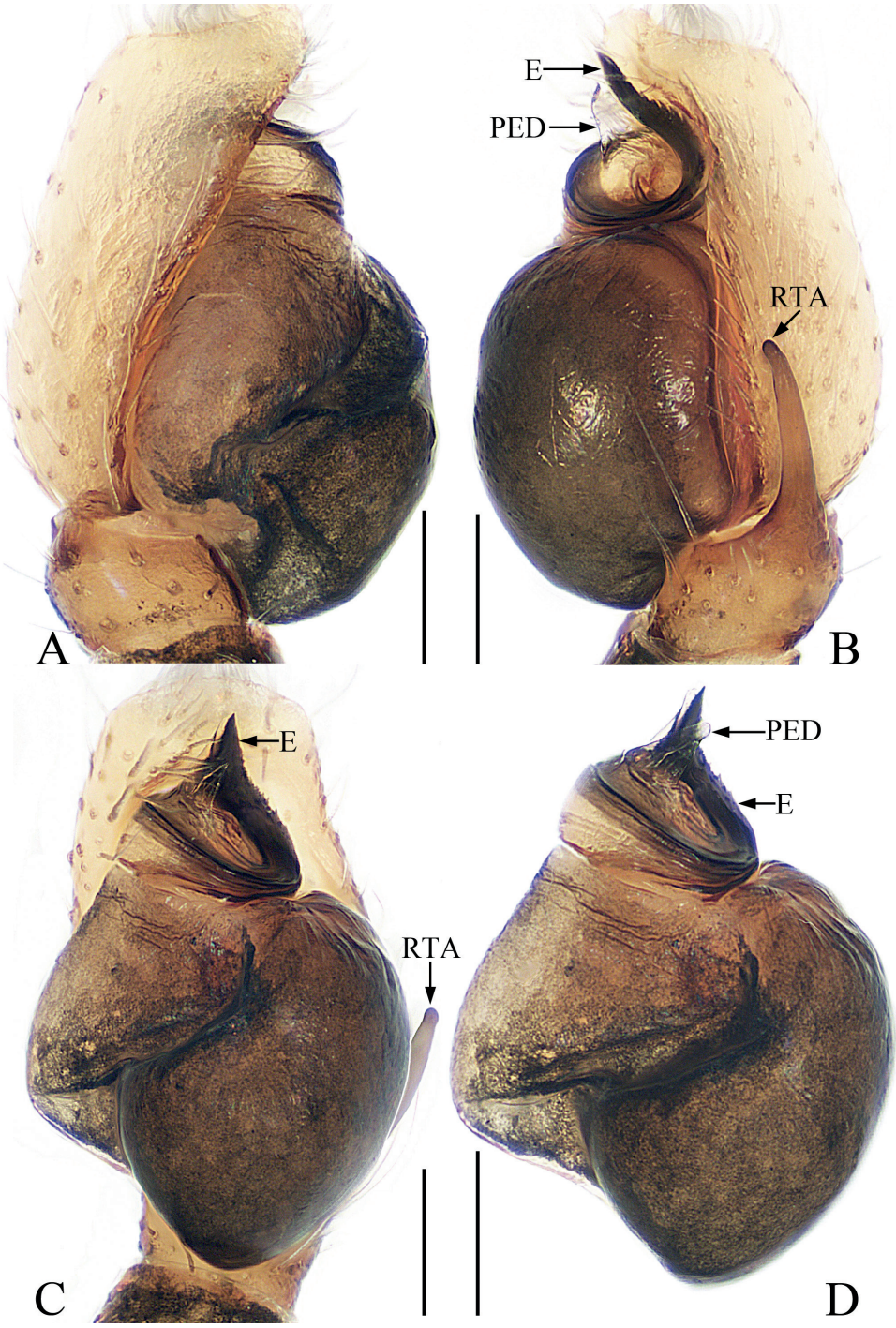

Figure 12. Male palp of *Pengmarengo yangi* sp. nov., holotype **A** prolateral **B** retrolateral **C** ventral **D** bulb, ventral. Scale bars: 0.1 mm. Abbreviations: E – embolus; PED – process of embolic disc; RTA – retrolateral tibial apophysis.

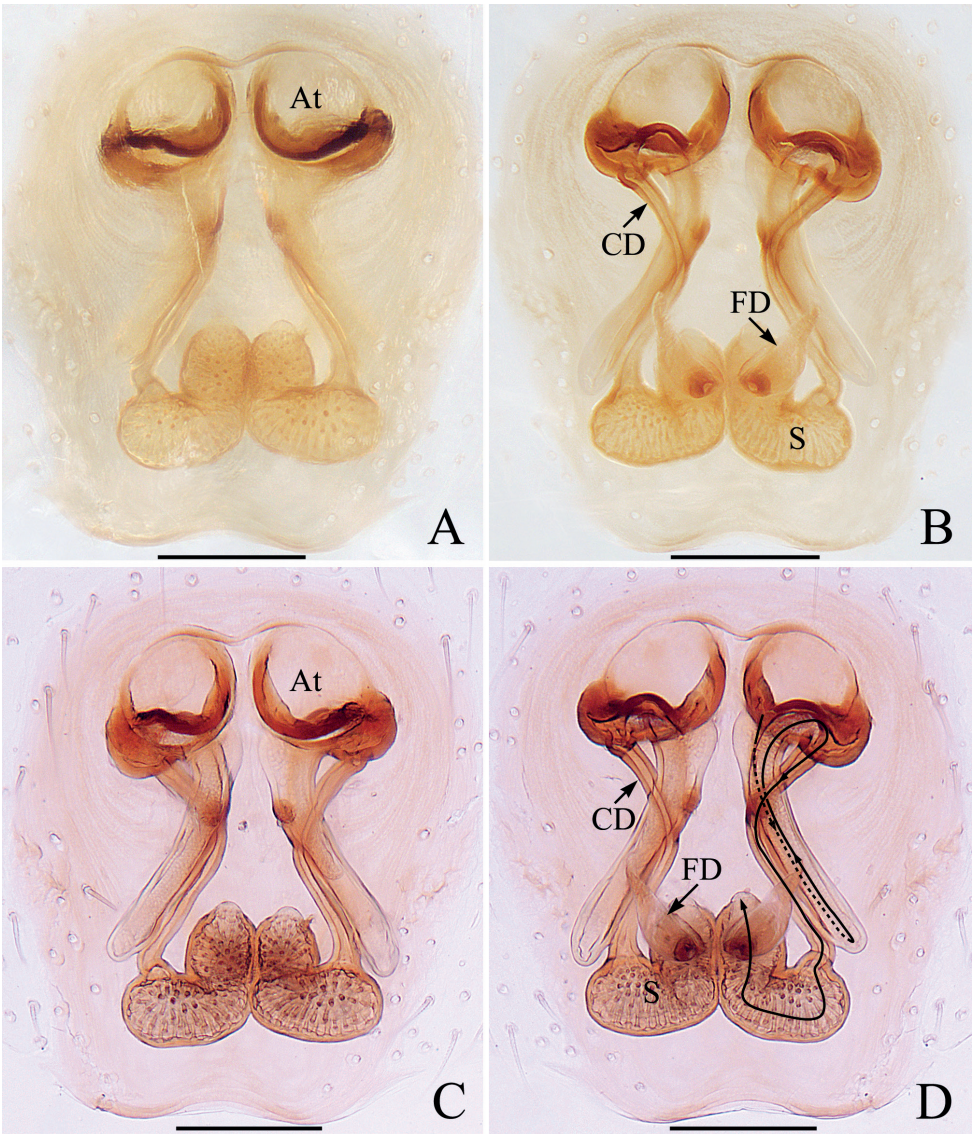

Figure 13. Epigyne-vulva of *Pengmarengo yangi* sp. nov., female paratype **A, C** epigyne, ventral **B, D** vulva, dorsal. Scale bars: 0.1 mm. Abbreviations: At – atrium; CD – copulatory duct; FD – fertilization duct; S – spermatheca.

Description. Male (Figs 12, 14A–C, E–G). Total length 3.07. Carapace 1.36 long, 0.82 wide. Abdomen 1.72 long, 0.64 wide. Eye sizes and inter-distances: AME 0.28, ALE 0.12, PLE 0.11, AERW 0.75, PERW 0.78, EFL 0.51. Leg measurements: I 3.08 (0.80, 0.45, 0.93, 0.70, 0.20), II 1.68 (0.50, 0.25, 0.38, 0.33, 0.20), III 1.55 (0.43, 0.23, 0.33, 0.33, 0.23), IV 2.01 (0.60, 0.28, 0.50, 0.40, 0.23). Carapace red-brown to dark brown, with two clusters of white setae near PLEs and two posteriorly, covered

with small papillae and thin setae. Chelicerae with two promarginal teeth and three retromarginal teeth fused basally. Legs I robust, with enlarged tibiae with dense, ventral, leaf-like scales, two prolatero-ventral and three retrolatero-ventral tibial macrosetae and two pairs of ventral metatarsal macrosetae, respectively; remaining legs yellow to pale yellow, with brown stripes on femora. Abdomen elongated, slightly constricted at anterior 1/3, dorsum brown to dark brown, with pair of oval white patches of setae on lateral margins behind constriction, entirely covered by large scutum and thin setae; venter dark brown. Palp (Fig. 12A–D): tibia wider than long; RTA ~ 1.6 × longer than tibia, slightly curved distally to a blunt tip; bulb swollen, divided by pale, oblique cleft; embolus short, coiled ca. a circle, pointed apically, with spine-shaped processes distally; process of embolic disc lamellar, membranous, with two parts.

Female (Figs 13, 14D). Total length 3.67. Carapace 1.33 long, 0.80 wide. Abdomen 2.02 long, 0.84 wide. Eye sizes and inter-distances: AME 0.29, ALE 0.11, PLE 0.11, AERW 0.75, PERW 0.78, EFL 0.51. Leg measurements: I 2.39 (0.63, 0.35, 0.70, 0.53, 0.18), II 1.59 (0.50, 0.25, 0.38, 0.28, 0.18), III 1.53 (0.45, 0.23, 0.35, 0.30, 0.20), IV 2.01 (0.63, 0.28, 0.50, 0.40, 0.20). Habitus (Fig. 14D) similar to that of male except lacks abdominal scutum, constriction, but with sub-trapeziform scutum near anterior margin. Epigyne (Fig. 13A–D): longer than wide, with pair of round atria anteriorly; copulatory openings beneath the posterior margins of atria; copulatory ducts long, posterolaterally extending before reversing direction at proximal 2/3, and followed by the S-shaped thinner portions connected to anterolateral edges of spermathecae; spermathecae L-shaped, touching; fertilization ducts originate from the center of longitudinal extended parts of spermathecae, extending anterolaterally.

Distribution. Only known from the type locality on Hainan Island, China.

Figure 14. *Pengmarengo yangi* sp. nov., male holotype and female paratype **A** holotype habitus, dorsal **B** ditto, lateral **C** ditto, ventral **D** female paratype habitus, dorsal **E** holotype carapace, frontal **F** holotype chelicera, posterior **G** holotype leg I, prolateral. Scale bars: 0.1 mm (**F**); 0.2 mm (**E, G**); 0.5 mm (**A–D**).

Genus *Philates* Simon, 1900

Type species. *Philates grammicus* Simon, 1900 from Philippines by original designation.

Comments. The genus *Philates* is belonging to the tribe Ballini and is represented by ten species distributed from Southeast Asia to Papua New Guinea (Maddison 2015; WSC 2022). A recent re-defined of the genus was also provided by Benjamin (2004), who diagnosed the genus by the absence of carapace protuberance, and the presence of leaf-like setae ventrally on tibiae I. However, certainly, the genus definition is too broad and that has also been noted by Benjamin (2004), who mentioned the Papuan New Guinea species could be divided into another genus. Herein, a proper definition of the genus is not discussed, and we placed *Philates zhoui* sp. nov. into the genus due to it possesses the leaf-like setae ventrally on tibiae I and shares a similar carapace shape with the generotype.

Philates zhoui sp. nov.

https://zoobank.org/54C7065F-031A-49BA-9CAE-C252FEC9DB1D
Figs 15, 16

Type material. ***Holotype*** ♂ (IZCAS-Ar43206), China: Hainan: Baisha County, Yinggeling National Nature Reserve (19°02.93'N, 109°33.65'E, ca. 730 m), 20.viii.2010, G. Zheng leg. ***Paratypes*** 20♂17♀ (IZCAS-Ar43207–43243), same data as holotype.

Etymology. The specific name is a patronym of Mr. Runbang Zhou, our guide in Jianfengling National Nature Reserve; noun (name) in genitive case.

Diagnosis. *Philates zhoui* sp. nov. resembles that of *P. grammicus* Simon, 1900 known from Philippines and Indonesia in the carapace sloping steeply at the posterior sub-margin, the enlarged femora I, and the dense setae ventrally on the enlarged tibia I, but it can be easily distinguished by the following characters: (1) the RTA is longer than the tibia (Fig. 15B), whereas it is ~ 1/2 the tibia length in *P. grammicus* (Wanless 1978: fig. 10J); (2) the copulatory ducts are separated from each other proximally by their width (Fig. 16A, B), whereas they are touching in *P. grammicus* (Wanless 1978: fig. 10D, H); (3) the male carapace lacks patches of scales (Fig. 16C, D), whereas there are patches of white scales behind the PMEs and on the slope of the thorax in *P. grammicus* (Wanless 1978: fig. 10D, H). The new species is also similar to *Colaxes sazailus* Paul, Prajapati, Joseph & Sebastian, 2020 known from India in having very similar copulatory organs, but it can be easily distinguished by the square cephalic region, which is trapeziform in *C. sazailus* (Paul et al. 2020: fig. 6, 15).

Description. Male (Figs 15, 16C–E, G, H). Total length 2.51. Carapace 1.30 long, 1.04 wide. Abdomen 1.28 long, 1.02 wide. Eye sizes and inter-distances: AME 0.33, ALE 0.19, PLE 0.15, AERW 0.98, PERW 0.98, EFL 0.57. Leg measurements: I 2.26 (0.75, 0.43, 0.55, 0.33, 0.20), II 1.61 (0.53, 0.25, 0.30, 0.33, 0.20), III 1.56 (0.50, 0.23, 0.30, 0.33, 0.20), IV 1.86 (0.63, 0.25, 0.40, 0.38, 0.20). Carapace red-brown, acutely sloped at posterior sub-margin, the square cephalic region with two

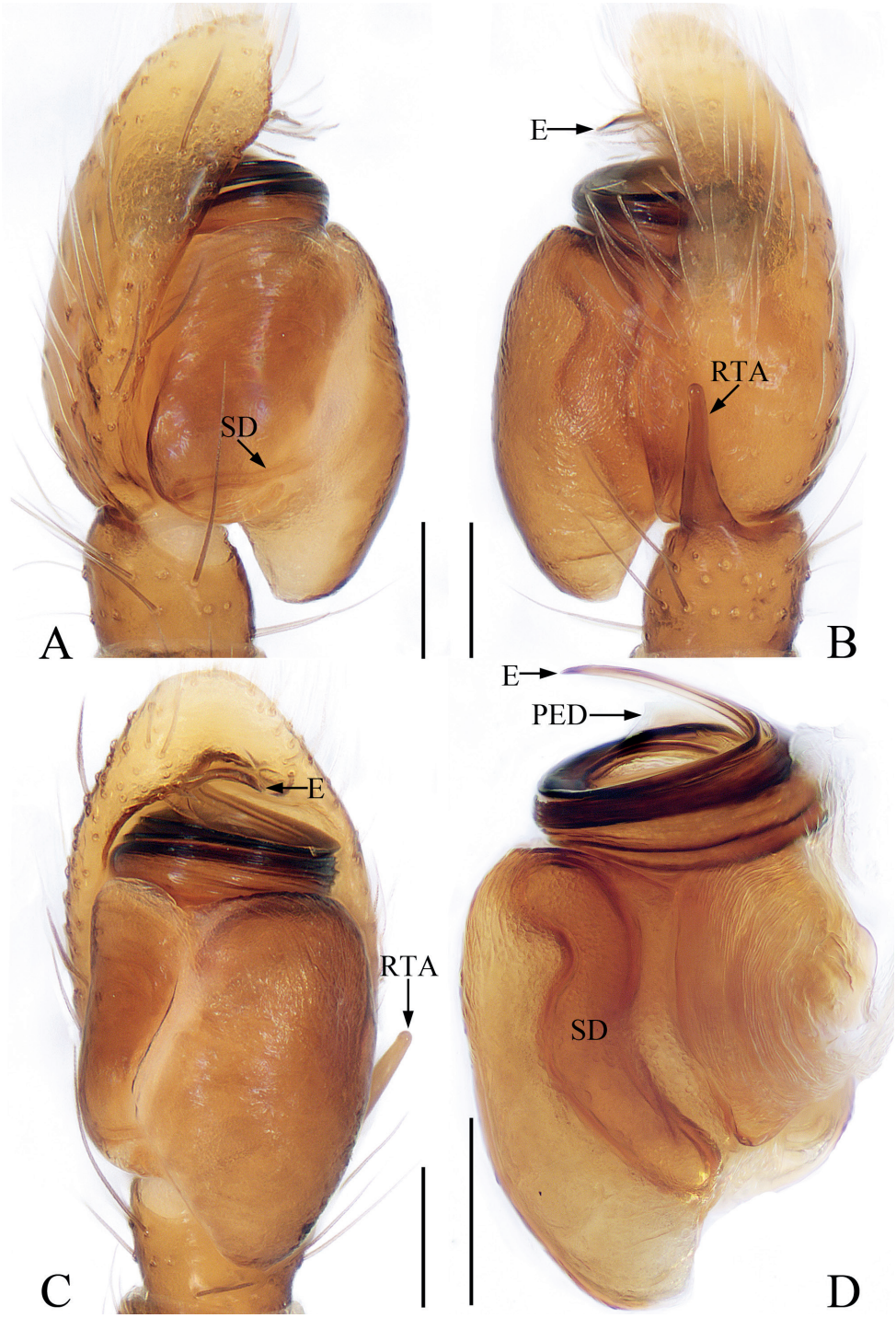

Figure 15. Male palp of *Philates zhoui* sp. nov., holotype **A** prolateral **B** retrolateral, **C** ventral **D** bulb, retrolateral. Scale bars: 0.1 mm. Abbreviations: E – embolus; PED – process of embolic disc; RTA – retrolateral tibial apophysis; SD – sperm duct.

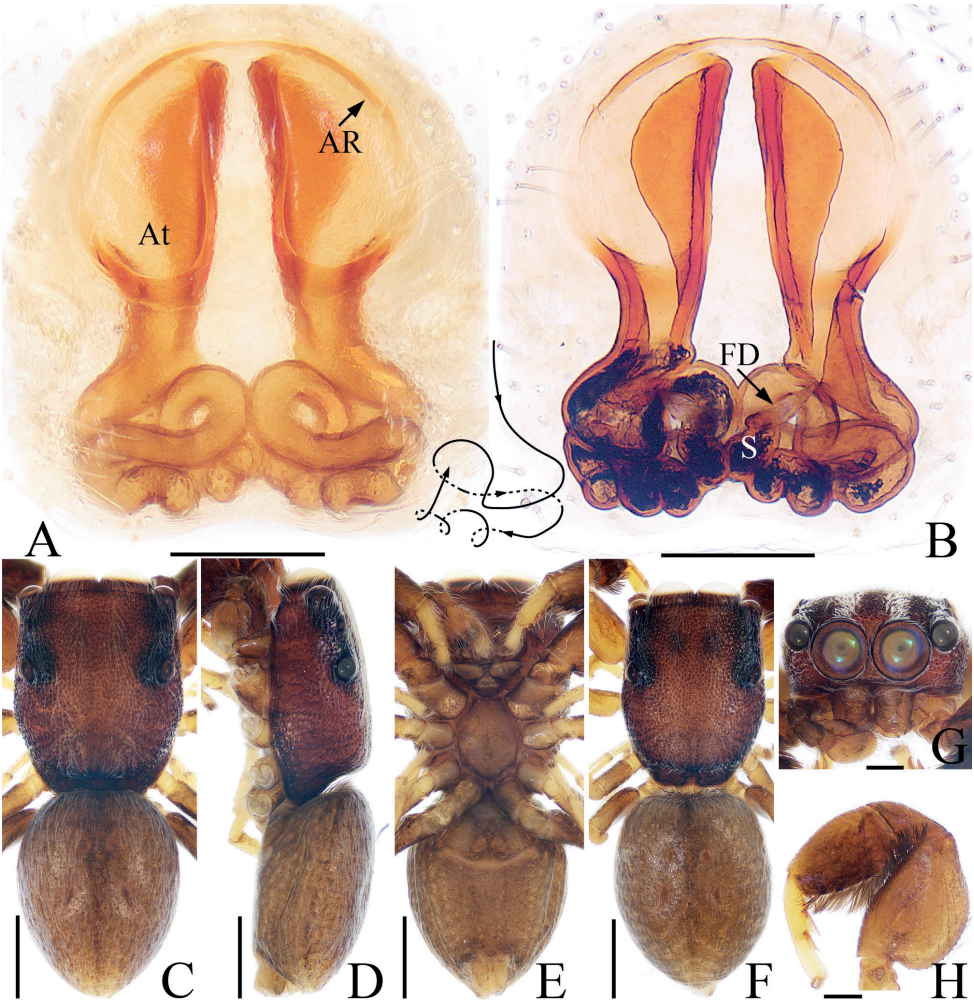

Figure 16. *Philates zhoui* sp. nov., male holotype and female paratype **A** epigyne, ventral **B** vulva, dorsal **C** holotype habitus, dorsal **D** ditto, lateral **E** ditto, ventral **F** female paratype habitus, dorsal **G** holotype carapace, frontal **H** holotype leg I, prolateral. Scale bars: 0.1 mm (**A, B**); 0.2 mm (**G, H**); 0.5 mm (**C–F**). Abbreviations: AR – atrial ridge; At – atrium; FD – fertilization duct; S – spermatheca.

longitudinal white streaks of setae medially. Chelicerae with two promarginal and four retromarginal teeth. Endites colored as chelicerae, broadened distally. Labium sub-linguiform, dark brown, paler apically. Sternum yellow-brown, slightly longer than wide. Legs I robust, with enlarged femora and tibiae, and dense, long, dark setae ventrally on femora, patellae and tibiae; other legs pale yellow to dark brown. Abdomen oval, dorsum red-brown, paler at terminus, with longitudinal, irregular dark streak centrally, two pairs of muscle depressions medially, covered entirely by scutum, with dense, thin setae; venter colored as dorsum. Palp (Fig. 15A–D): tibia slightly wider than long, with straight, tapered RTA ~ 1.5 × of its length, and blunt apically; bulb swollen, longer

than wide, sperm duct sinuous retrolaterally; embolus coiled ~ 2 ×, pointed at terminus; process of embolus disc lamellar.

Female (Fig. 16A, B, F). Total length 2.44. Carapace 1.17 long, 0.92 wide. Abdomen 1.23 long, 1.01 wide. Eye sizes and inter-distances: AME 0.31, ALE 0.16, PLE 0.15, AERW 0.87, PERW 0.87, EFL 0.51. Leg measurements: I 1.76 (0.58, 0.33, 0.40, 0.25, 0.20), II 1.41 (0.43, 0.25, 0.28, 0.25, 0.20), III 1.39 (0.43, 0.23, 0.28, 0.25, 0.20), IV 1.74 (0.58, 0.28, 0.38, 0.30, 0.20). Habitus (Fig. 16F) similar to that of male except with pair of dark spots medially in eye field. Epigyne (Fig. 16A, B): longer than wide; anteriorly located, oval atrium separated by broad, sub-oblong septum ~ 2 × longer than wide; copulatory openings beneath the lowest margin of atrium; copulatory ducts separated, widened proximally, with complex coils; spermathecae elongated; fertilization ducts lamellar, extending anterolaterally.

Distribution. Only known from the type locality in Hainan Island, China.

Genus *Toxeus* C.L. Koch, 1846

Type species. *Toxeus maxillosus* C. L. Koch, 1846 from Indonesia by original designation.

Comments. *Toxeus* is a Myrmarachnina genus and represented 12 species distributed from East to Southeast Asia (Maddison 2015; WSC 2022). The genus has always been considered a synonym of the genus *Myrmarachne* until was reinstated by Prószyński (2016), who separates nine genera from *Myrmarachne* based on the study of the morphology of copulatory organs and diagnosed *Toxeus* by the pipe-like sclerotized spermathecae. However, Prószyński's conclusion was denied by the molecular evidence (Yamasaki et al. 2018; Maddison and Szűts 2019) and so the validity of the genus is uncertain. Herein, we assigned the following new species to the genus due to its being morphologically similar to the known species of the genus.

Toxeus hainan sp. nov.

https://zoobank.org/7F0388AD-9659-4ABE-9EE6-542CBC555F32
Figs 17, 18

Type material. ***Holotype*** ♀ (IZCAS-Ar43196), China: Hainan: Lingshui County, Diaoluoshan National Nature Reserve (18°43.39'N, 109°51.27'E, ca. 930 m), 10.viii.2010, G. Zheng leg. ***Paratypes*** 1♂ (IZCAS-Ar43197), same data as holotype; 1♂ (IZCAS-Ar43198), Ledong County, Jianfengling National Nature Reserve, eastern ravine of Mingfenggu (18°64.69'N, 108°51.59'E, ca. 810 m), 17.xii.2007 morning, S. Li leg.; 1♀ (IZCAS-Ar43199), same locality and collector, 18.xii.2007 morning, S. Li leg.; 1♂ (IZCAS-Ar43200), Changjiang County, Bawangling National Nature Reserve, Dong'er Management Station (19°05.75'N, 109°10.56'E, ca. 830 m), 24.xii.2007, S. Li leg.; 1♂ (IZCAS-Ar43201), 5 km ahead of Dong'er Management Station (19°05.19'N, 109°11.80'E, ca. 1010 m), 25.xii.2007, S. Li leg.; 1♀ (IZCAS-Ar43202), Wangxia Village, 26.xii.2007, S. Li leg.; 1♀ (IZCAS-Ar43203), Qicha

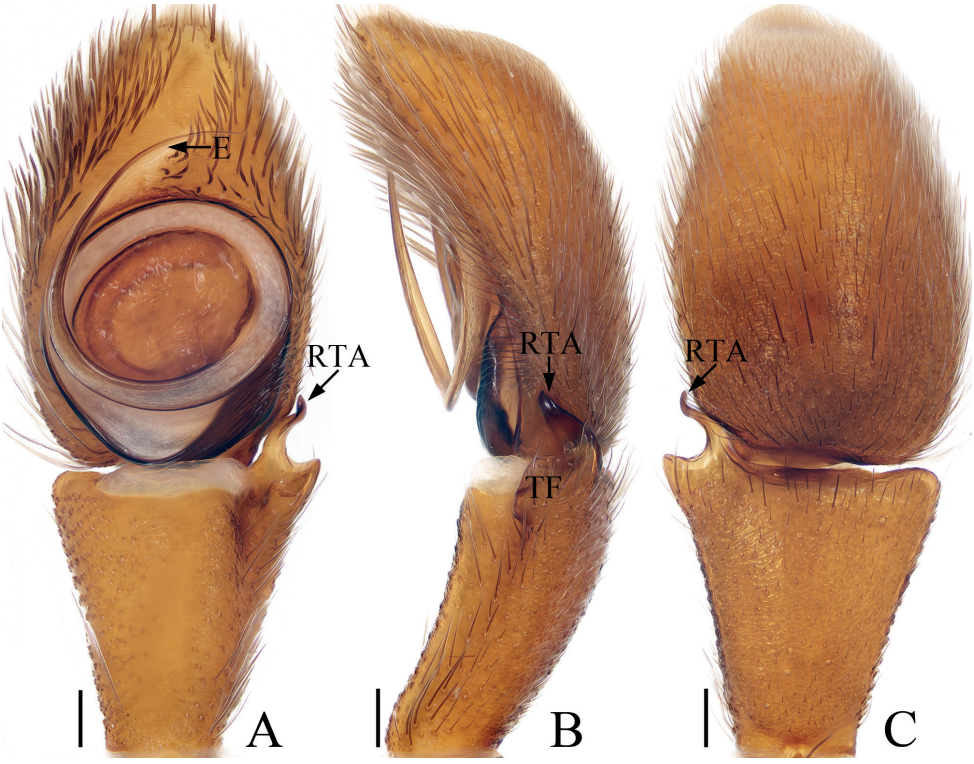

Figure 17. Male palp of *Toxeus hainan* sp. nov., paratype **A** ventral **B** retrolateral **C** dorsal. Scale bars: 0.1 mm. Abbreviations: E – embolus; RTA – retrolateral tibial apophysis; TF – tibial flange.

Township (19°01.95'N, 109°06.15'E, ca. 700 m), 29.xii.2007, S. Li leg.; 1♀ (IZCAS-Ar43204), Dong'er Management Station (19°05.75'N, 109°10.56'E, ca. 830 m), 30.xii.2007, S. Li leg.; 1♀ (IZCAS-Ar43205), Qiongzhong County, Limushan National Nature Reserve (19°11.98'N, 109°43.76'E, ca. 580 m), 13.viii.2007, S. Li leg.

Etymology. The specific name comes from the type locality, Hainan Island; noun in apposition.

Diagnosis. *Toxeus hainan* sp. nov. resembles *T. latithoracicus* (Yamasaki & Huang, 2012) known from Ryukyu Island by having short chelicerae in males, tapered embolus, and similarly shaped RTA, but it can be easily distinguished by the following characters: (1) the presence of proximal processes of the sclerotized portions of copulatory ducts (Fig. 18C, D), whereas they are absent in *T. latithoracicus* (Yamasaki and Huang 2012: figs 12, 13); (2) the spermathecae are ca. as long as wide (Fig. 18A–D), whereas they are longer than wide in *T. latithoracicus* (Yamasaki and Huang 2012: figs 12, 13); (3) the RTA is curved inward distally in ventral view (Fig. 17A), whereas it is straight in *T. latithoracicus* (Yamasaki and Huang 2012: fig. 5); (4) the sternum is > 3 × longer than wide (females only) (Fig. 18G), whereas it is < 2.8 × longer than wide in *T. latithoracicus* (Yamasaki and Huang 2012: fig. 11).

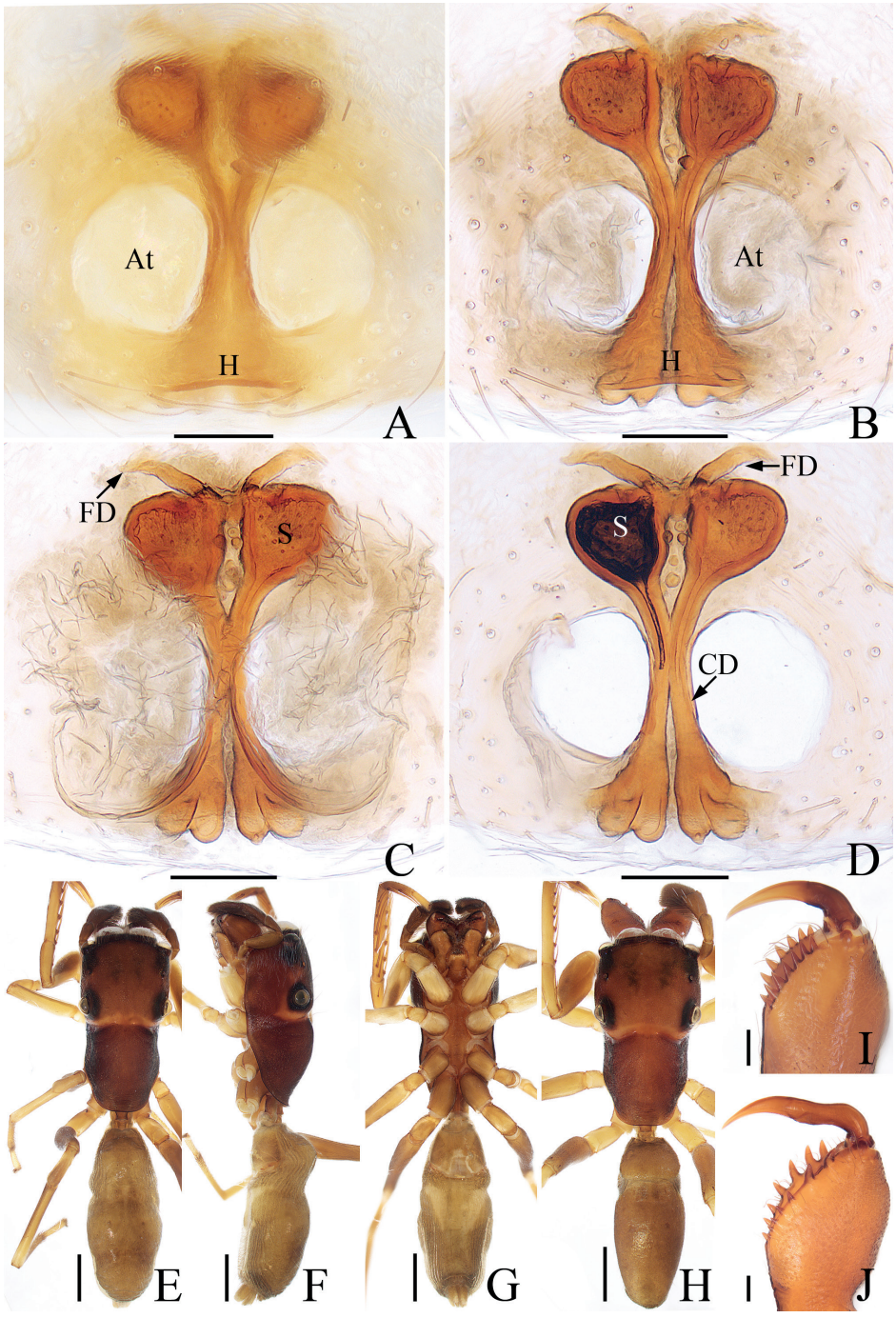

Figure 18. *Toxeus hainan* sp. nov., female holotype and male paratype **A, B** epigyne, ventral **C, D** vulva, dorsal **E** holotype habitus, dorsal **F** ditto, lateral **G** ditto, ventral **H** male paratype habitus, dorsal **I** holotype chelicera, posterior **J** male paratype chelicera, posterior. Scale bars: 0.1 mm (**A–D**); 0.2 mm (**I, J**); 1.0 mm (**E–H**). Abbreviations: At – atrium; CD – copulatory duct; FD – fertilization duct; H – epigynal hood; S – spermatheca.

Description. Male (Figs 17, 18H, J). Total length 6.83 Carapace 3.38 long, 1.97 wide. Abdomen 3.10 long, 1.31 wide. Eye sizes and inter-distances: AME 0.66, ALE 0.35, PLE 0.35, AERW 1.86, PERW 1.98, EFL 1.45. Leg measurements: I 6.89 (2.15, 1.08, 2.05, 1.01, 0.60), II 5.54 (1.65, 0.88, 1.40, 1.01, 0.60), III 5.60 (1.65, 0.75, 1.30, 1.30, 0.60), IV 7.90 (2.35, 0.90, 2.00, 2.00, 0.65). Habitus (Fig. 18H) similar to that of female except with longer chelicerae, covered entirely by dorsal scutum of abdomen. Palp (Fig. 17A–C): tibia > 2 × longer than wide, with tapered RTA curved into S-shape in ventral view, curved towards cymbium distally in retrolateral view, and lamellar flange near the base of RTA; cymbium longer than wide, setose; bulb almost round, with sperm duct extending along prolateral sub-margin; embolus flat, coiled ~ 1.5 ×, tapered distally, and pointed apically.

Female (Fig. 18A–D, E–G, I). Total length 7.82 Carapace 3.73 long, 1.91 wide. Abdomen 3.78 long, 1.64 wide. Eye sizes and inter-distances: AME 0.71, ALE 0.41, PLE 0.39, AERW 2.00, PERW 2.05, EFL 1.56. Leg measurements: I 7.01 (2.15, 1.08, 2.13, 1.05, 0.60), II 5.55 (1.65, 0.85, 1.45, 1.00, 0.60), III 6.03 (1.75, 0.80, 1.38, 1.50, 0.60), IV 8.40 (2.35, 1.00, 2.15, 2.15, 0.75). Carapace red-brown, pale yellow in cervical groove, with pair of indistinct dark patches medially on square cephalic region, covered with thin setae. Chelicerae red-brown, with seven teeth on both margins, respectively. Endites > 2 × longer than wide, with dense setae on inner margins of distal 1/2. Labium longer than wide, with dense antero-marginal setae. Sternum fusiform, > 3 × longer than wide. Legs pale to brown, with six and two pairs of ventral macrosetae on tibiae and metatarsi I, respectively. Abdomen elongated, constricted at anterior 2/5, dorsum brown, with indistinct patch medially, covered with thin setae, venter same color as dorsum, with pair of pale patches mediolaterally. Epigyne (Fig. 18A–D): longer than wide, with pair of round atria posteromedially, and inverted, cup-shaped hood posteriorly; sclerotized parts of copulatory ducts originate posteriorly, slightly curved medially, connect with posterior edges of oval spermathecae, with two pairs of proximal processes; fertilization ducts originate from antero-inner edges of spermathecae.

Distribution. Only known from the type locality, Hainan Island, China.

Acknowledgements

The manuscript benefited greatly from the comments by Dmitri V. Logunov (Manchester, UK), Galina N. Azarkina (Novosibirsk, Russia), Junxia Zhang (Baoding, China), and Zhiyuan Yao (Shenyang, China). Sarah Crews (San Francisco, USA) and Nathalie Yonow (Swansea, UK) checked the English of the manuscript. Guo Zheng, Guo Tang, Xiaoqi Mi, Jiahui Gan, Yuanfa Yang, and Feng'e Li helped with fieldwork. This research was supported by the National Natural Science Foundation of China (NSFC-31972869, 31660609), the Science and Technology Project Foundation of Guizhou Province ([2020]1Z014), the Key Laboratory Project of Guizhou Province ([2020]2003), the Open Project of Ministry of Education Key Laboratory for Ecology of Tropical Islands, Hainan Normal University, China, and the Doctoral Research Foundation of Tongren University (trxyDH2102).

References

Azarkina GN, Haddad CR (2020) Partial revision of the Afrotropical Ballini, with the description of seven new genera (Araneae: Salticidae). Zootaxa 4899(1): 15–92. https://doi.org/10.11646/zootaxa.4899.1.4

Benjamin SP (2004) Taxonomic revision and phylogenetic hypothesis for the jumping spider subfamily Ballinae (Araneae, Salticidae). Zoological Journal of the Linnean Society 142(1): 1–82. https://doi.org/10.1111/j.1096-3642.2004.00123.x

Guo J, Zhang F, Zhu M (2011) Two new species of the genus *Irura* Peckham & Peckham, 1901 (Araneae: Salticidae) from Hainan Island, China. Acta Arachnologica 60(2): 89–91. https://doi.org/10.2476/asjaa.60.89

Hong D, Zhuang W, Zhu M, Ma K, Wang X, Huang D, Zhang Y, Ren G, Bu W, Cai W, Ren D, Yang D, Liang A, Bai F, Zhang R, Lei F, Li S, Kong H, Cai L, Dai Y, Zhu C, Yang Q, Chen J, Sha Z, Jiang J, Che J, Wu D, Li J, Wang Q, Wei X, Bai M, Liu X, Chen X, Qiao G (2022) Positioning taxonomic research for the future. Zoological Systematics 47(3): 185–187. https://doi.org/10.11865/zs.2022301

Li S (2020) Spider taxonomy for an advanced China. Zoological Systematics 45(2): 73–77. https://doi.org/10.11865/zs.202011

Li J, Yan X, Lin Y, Li S, Chen H (2021) Challenging Wallacean and Linnean shortfalls: *Ectatosticta* spiders (Araneae, Hypochilidae) from China. Zoological Research 42(6): 791–794. https://doi.org/10.24272/j.issn.2095-8137.2021.212

Logunov DV (2022) On four species of *Irura* Peckham & Peckham, 1901 (Araneae: Salticidae) collected by John and Frances Murphy from south-east Asia. Arachnology 19(Special Issue): 229–237. https://doi.org/10.13156/arac.2022.19.sp1.229

Maddison WP (2015) A phylogenetic classification of jumping spiders (Araneae: Salticidae). The Journal of Arachnology 43(3): 231–292. https://doi.org/10.1636/arac-43-03-231-292

Maddison WP, Szűts T (2019) Myrmarachnine jumping spiders of the new subtribe Levieina from Papua New Guinea (Araneae, Salticidae, Myrmarachnini). ZooKeys 842: 85–112. https://doi.org/10.3897/zookeys.842.32970

Maddison WP, Beattie I, Marathe K, Ng PYC, Kanesharatnam N, Benjamin SP, Kunte K (2020) A phylogenetic and taxonomic review of baviine jumping spiders (Araneae, Salticidae, Baviini). ZooKeys 1004: 27–97. https://doi.org/10.3897/zookeys.1004.57526

Metzner H (2022) Jumping spiders (Arachnida: Araneae: Salticidae) of the world. Accessed 8 June 2022. [Online at] https://www.jumping-spiders.com

Mi X, Wang C (2016) A new species of *Irura* Peckham & Peckham, 1901 (Araneae: Salticidae) from Yunnan Province, China. Sichuan Journal of Zoology 35(3): 400–403. https://doi.org/10.11984/j.issn.1000-7083.20160008

Paul J, Prajapati DA, Joseph MM, Sebastian PA (2020) Description of a new species of *Colaxes* Simon, 1900 (Araneae: Salticidae: Ballinae) from the tropical montane cloud forests of Western Ghats, India. Arthropoda Selecta 29(2): 244–250. https://doi.org/10.15298/arthsel.29.2.10

Peng X (2020) Fauna Sinica, Invertebrata 53, Arachnida: Araneae: Salticidae. Science Press, Beijing, 612 pp.

Peng X, Kim J (1997) Three new species of the genus *Eupoa* from China (Araneae: Salticidae). Korean Journal of Systematic Zoology 13: 193–198.

Peng X, Li S (2006) Description of *Eupoa liaoi* sp. nov. from China (Araneae: Salticidae). Zootaxa 1285: 65–68. https://doi.org/10.11646/zootaxa.1285.1.5

Peng X, Yin C (1991) Five new species of the genus *Kinhia* from China (Araneae: Salticidae). Acta Zootaxonomica Sinica 16: 35–47.

Prószyński J (2016) Delimitation and description of 19 new genera, a subgenus and a species of Salticidae (Araneae) of the world. Ecologica Montenegrina 7: 4–32. https://doi.org/10.37828/em.2016.7.1

Wang C, Li S (2020) Seven new species of jumping spiders (Araneae, Salticidae) from Xishuangbanna, China. ZooKeys 968: 43–69. https://doi.org/10.3897/zookeys.968.55047

Wang C, Li S (2021) On ten species of jumping spiders from Xishuangbanna, China (Araneae, Salticidae). ZooKeys 1062: 123–155. https://doi.org/10.3897/zookeys.1062.72531

Wang C, Li S (2022) On eleven species of jumping spiders from Xishuangbanna, China (Araneae, Salticidae). ZooKeys 1116: 85–119. https://doi.org/10.3897/zookeys.1116.82858

Wang C, Li S, Zhu W (2020) Taxonomic notes on Leptonetidae (Arachnida, Araneae) from China, with descriptions of one new genus and eight new species. Zoological Research 41(6): 684–704. https://doi.org/10.24272/j.issn.2095-8137.2020.214

Wanless FR (1978) A revision of the spider genus *Marengo* (Araneae: Salticidae). Bulletin of the British Museum, Natural History. Zoology 33: 259–278. https://doi.org/10.5962/p.28739

WSC (2022) World Spider Catalog. Version 23.0. Natural History Museum Bern. [accessed on 8 June 2022] https://doi.org/10.24436/2

Yamasaki T, Huang JN (2012) A new species of the genus *Myrmarachne* (Araneae: Salticidae) from the central Ryukyus and Taiwan. Acta Arachnologica 61(1): 7–10. https://doi.org/10.2476/asjaa.61.7

Yamasaki T, Hashimoto Y, Endo T, Hyodo F, Itioka T, Meleng P (2018) New species of the ant-mimicking genus *Myrmarachne* MacLeay, 1839 (Araneae: Salticidae) from Sarawak, Borneo. Zootaxa 4521(3): 335–356. https://doi.org/10.11646/zootaxa.4521.3.2

Yao Z, Wang X, Li S (2021) Tip of the iceberg: Species diversity of *Pholcus* spiders (Araneae, Pholcidae) in Changbai Mountains, Northeast China. Zoological Research 42(3): 267–271. https://doi.org/10.24272/j.issn.2095-8137.2021.037

Żabka M (1985) Systematic and zoogeographic study on the family Salticidae (Araneae) from Vietnam. Annales Zoologici, Warszawa 39: 197–485.

Zhou Y, Li S (2013) Two new genera of jumping spiders from Hainan Island, China (Araneae, Salticidae). Zootaxa 3712(1): 1–84. https://doi.org/10.11646/zootaxa.3712.1.1

Zhu C, Luo A, Bai M, Orr MC, Hou Z, Ge S, Chen J, Hu Y, Zhou X, Qiao G, Kong H, Lu L, Jin X, Cai L, Wei X, Zhao R, Miao W, Wang Q, Sha Z, Lin Q, Qu M, Jiang J, Li J, Che J, Jiang X, Chen X, Gao L, Ren Z, Xiang C, Luo S, Wu D, Liu D, Peng Y, Su T, Cai C, Zhu T, Cai W, Liu X, Li H, Xue H, Ye Z, Chen X, Tang P, Wei S, Pang H, Xie Q, Zhang F, Zhang F, Peng X, Zhang A, Gao T, Zhou C, Shao C, Ma L, Wei Z, Luan Y, Yin Z, Dai W, Wei C, Huang X, Liu J, Chen X, Yi T, Zhang Z, Aishan Z, Li Q, Hu H (2022) A joint call for actions to advance taxonomy in China. Zoological Systematics 47(3): 188–197. https://doi.org/10.11865/zs.2022302

ZooKeys 1118: 73–95 (2022)
doi: 10.3897/zookeys.1118.84643
https://zookeys.pensoft.net

RESEARCH ARTICLE

A peer-reviewed open-access journal
ZooKeys
Launched to accelerate biodiversity research

Two new species of *Alainites* (Ephemeroptera, Baetidae) from the Mediterranean biodiversity hotspot

Zohar Yanai[1], Pavel Sroka[2], Jean-Luc Gattolliat[3,4]

1 *The Steinhardt Museum of Natural History, Tel Aviv University, Tel Aviv 6997801, Israel* **2** *Biology Centre of the Czech Academy of Sciences, Institute of Entomology, Branišovská 31, 37005 České Budějovice, Czech Republic* **3** *Musée cantonal de zoologie, Palais de Rumine, Place de la Riponne 6, 1014 Lausanne, Switzerland* **4** *University of Lausanne (UNIL), Department of Ecology and Evolution, 1015 Lausanne, Switzerland*

Corresponding author: Zohar Yanai (yanaizohar@gmail.com)

Academic editor: L. Pereira-da-Conceicoa | Received 31 March 2022 | Accepted 25 July 2022 | Published 24 August 2022

https://zoobank.org/704E06A1-0877-4307-A3E5-258FFB0D1E18

Citation: Yanai Z, Sroka P, Gattolliat J-L (2022) Two new species of *Alainites* (Ephemeroptera, Baetidae) from the Mediterranean biodiversity hotspot. ZooKeys 1118: 73–95. https://doi.org/10.3897/zookeys.1118.84643

Abstract

The mayfly genus *Alainites* Waltz & McCafferty, 1994 encompassed 20 species and was represented across the West Palaearctic region by six species. Based on morphological (nymphal characters) and molecular (mitochondrial COI sequences) evidence, two new species are described: *A. bengunn* **sp. nov.** from Sardinia and *A. gasithi* **sp. nov.** from Israel. Both species are confined to narrow distribution ranges, in line with most of their congeners from the region. The key nymphal traits are discussed and identified to distinguish species in the group.

Keywords

COI, Israel, Italy, mayfly, microendemics, Sardinia, systematics, West Palaearctic

Introduction

Baetis Leach, 1815 (Ephemeroptera: Baetidae) is one of the most diversified mayfly genera (Sroka 2012). In order to better understand its phylogenetic structure, as well as for practical reasons, attempts are made to divide it into monophyletic taxa, ranked as

either species groups, subgenera, or independent genera, siblings to *Baetis*. One of the first to suggest such a division for the European fauna was Müller-Liebenau (1969), who divided *Baetis* s.l. into eleven species groups. The concept of *Baetis* s. l. was subsequently recognised as polyphyletic, especially when considering taxa from other biogeographic regions (e.g., Novikova and Kluge 1987; Waltz et al. 1994; Waltz and McCafferty 1997; Fujitani 2008; Gattolliat et al. 2008). Most of the species groups were proven to correspond to independent lineages and part of them were raised to subgeneric or generic levels (Novikova and Kluge 1987; Waltz et al. 1994; McCafferty and Waltz 1995).

Nigrobaetis Novikova & Kluge, 1987 and *Alainites* Waltz & McCafferty, 1994 were erected for species mainly belonging to the species groups *niger* and *muticus*, respectively, sensu Müller-Liebenau (1974). *Takobia* Novikova & Kluge, 1987 was established for a single species originally described from Uzbekistan by Braasch and Soldán (1983) under the binomial combination "*Centroptilum maxillare*". The status of these three taxa was rather hectic as they were repeatedly subject to synonymies and rank changes between species groups, subgenera, and genera (Müller-Liebenau 1969; Novikova and Kluge 1987, 1994; Waltz et al. 1994; Waltz and McCafferty 1997; Jacob 2003; Kluge and Novikova 2014). This confusion is partly due to the fact that some of these acts lack solid morphological or molecular support; moreover, the revisions were not based on type material and detailed descriptions were missing (see Sroka et al. 2021).

When Waltz and McCafferty (in Waltz et al. 1994) established the genus *Alainites*, the *muticus* group sensu Müller-Liebenau (1974) included nine species; all of them were reassigned to the new genus (Waltz et al. 1994). Diagnostic nymphal characters of *Alainites* were: 1) paraproct with an elongated prolongation; 2) prostheca of the right mandible bifid, reduced to two bristle-like feathered appendages; 3) absence of villopore; and 4) body laterally compressed. At the imaginal stage: 1) hindwings, when present, with three longitudinal veins, the second being bifurcated; and 2) segment III of the male forceps spherical to slightly elongated and curved (Waltz et al. 1994; Zrelli et al. 2012). It is worth mentioning that none of the imaginal characters allows the separation of *Alainites* from its allied genus *Nigrobaetis* (Novikova & Kluge 2014). The *Alainites* concept was widely debated in the literature (Tong and Dudgeon 2000; Fujitani et al. 2003; Gattolliat 2011; Zrelli et al. 2012). In some studies focusing on European fauna, *Alainites* was still tentatively considered a synonym of *Baetis* s.l. (Jacob 2003) or *Nigrobaetis* (Bauernfeind and Soldán 2012). Kluge and Novikova (2014) considered *Alainites* as a junior synonym of *Takobia* Novikova & Kluge, 1987, and transferred de facto all the species of *Alainites* into *Takobia*. They justified this synonymy by a strict application of the principles of phylogenetic systematics (Hennig 1950), as they considered *Takobia maxillare* (Braasch & Soldán, 1983) as highly derived within the lineage and the remaining species previously assigned to *Alainites* as plesiomorphic. Therefore, to avoid keeping *Alainites* as a plesiomorphon, they synonymised it with *Takobia*. However, for a long time *T. maxillare* remained, as Kluge and Novikova 2014 wrote, a "single aberrant species". Recently Sroka et al. (2021) provided a redescription of the type species of *Takobia* based on the type material; important characters, such as the prosthecas and the paraprocts, were re-examined and corrected. Moreover, two new species were described form Central Asia which present-

ed derived characters similar to *T. maxillare*, namely a very elongated maxillary palp, the dorsal surface of the labrum covered with numerous setae (none of them arranged in a row), the peculiar setation of the dorsal margin of femora, and elongated claws.

Currently *Alainites* is widely distributed across the Palaearctic (represented by 13 species) as well as in the Oriental realm (7 species). In Oriental realm, *Alainites* is reported both from continental areas (mainly China and Malaysia) and from a few islands (Taiwan and Borneo). Ongoing studies in Thailand, Philippines, and Indonesia clearly indicate that the genus is more widely distributed in the region, but seems nowhere very common (J. Garces, C. Suttinun, pers. comm.). During the study of other Baetidae from South East Asia, it was never found eastern to Wallace Line (i.e. in New Guinea and nearby islands) (Kaltenbach and Gattolliat 2017, 2018, 2019a, 2019b). Unlike its closely related genus *Nigrobaetis*, *Alainites* is absent from Afrotropics including the Arabian Peninsula.

In Western Palaearctic, *Alainites muticus* (Linneaus, 1758) is the most common and widely distributed species of the genus. It has been reported across Europe, from Portugal to Ukraine and from Greece to Scandinavia (Bauernfeind and Soldán 2012), with highest densities exhibited in Central Europe, where it is often one of the most common mayfly species. It was also recently reported from Armenia (Hrivniak et al. 2018) and Iran (Bojková et al. 2018). Based on molecular evidence, *A. muticus* seems to represent in fact a complex of at least two cryptic species (Sroka 2012); however, no morphological studies have validated these species hypotheses to date.

Just behind the limit of distribution of *A. muticus*, species with restricted distribution were described over the last three decades. Sympatry amongst West Palaearctic *Alainites* species has very seldomly been recorded and is probably very rare, given the restricted distribution range of most species. In the Maghreb, *Alainites oukaimeden* (Thomas & Sartori, 1992) occurs in the High Atlas (Morocco), whilst *Alainites sadati* Thomas, 1994 is found from West Algeria to North Tunisia (Thomas and Gagneur 1994; Zrelli et al. 2012). The westernmost species is *A. navasi* (Müller-Liebenau, 1974), known from the Iberian Peninsula (Müller-Liebenau 1974). In the eastern border of the distribution of *A. muticus*, *Alainites kars* (Thomas & Kazancı, 1989) was described from Turkey (Kazancı and Thomas 1989), and *Nigrobaetis* (*Takobia*) *katerynae* Martynov & Godunko, 2017 was recently discovered from the Caucasus (Martynov and Godunko 2017); the latter species was never formally transferred to *Alainites*.

In Corsica, an endemic species, *Alainites albinatii* (Sartori & Thomas, 1989) was described based on nymphs and imagos (Sartori and Thomas 1989). In the sister island of Sardinia, a population of *Alainites* was firstly considered to be the continental *A. muticus* (Buffagni et al. 2003). In the barcoding of the Italian mayflies project, the Sardinian lineage was tentatively considered as *A.* sp. cf. *albinatii* without further explanations (Tenchini et al. 2018). However, morphological and molecular approaches proved that Sardinian specimens of *Alainites* noticeably differed from both the Corsican endemic and the continental lineages (Gattolliat et al. 2015; Tenchini et al. 2018). Gattolliat et al. (2015) noticed that the number of abdominal gills and the structure of the prolongation of the paraproct significantly differed between the Sardinian, Corsican and continental specimens; they even proposed that *Alainites* could

be the only lineage present on both Corsica and Sardinia which demonstrates more affinities between Sardinia and Maghreb than between the two islands. The Sardinian lineage was therefore considered as a species hypothesis without formal description (Gattolliat et al. 2015).

For the Levant area, Koch (1988) did not mention any species which could be assigned to *Alainites*. He only reported for the first time two species of the related genus *Nigrobaetis* (*N. niger* and *N. digitatus*) from Syria. In his unpublished master thesis, Samocha (1972) mentioned the presence in Israel of one unidentified species with some probability to be a representative of *Alainites*. The species L55 is characterised by having six pairs of gills and bifid, thin right prostheca (Samocha 1972).

In the current paper, we describe two species of *Alainites* that join the six species of *Alainites* distributed in the circum-Mediterranean region. The Mediterranean basin is recognised as a biodiversity hotspot (Myers et al. 2000). Mediterranean stream biota is unique and featuring a high rate of endemic species (Bonada et al. 2007), including over one third of its mayfly species (Tierno de Figueroa et al. 2013). Stream macroinvertebrates exhibit a clear set of traits that make them suitable for the typical Mediterranean climatic and hydrological conditions (Hershkovitz and Gasith 2013). The combination of specialised fauna, unique environment, and heavy anthropogenic pressure results in a constant threat to these fragile aquatic insects (Filipe et al. 2012).

Materials and methods

The material treated here includes nymphs, that have been collected using a hand net or picked manually from rocks and pebbles. All material is preserved in ethanol, except for a few specimens that have been mounted on microscope slides fixed in Canada Balsam, as specified in the material examined sections below. Ethanol-preserved specimens were studied under a Leica M205 stereomicroscope; microscope slides were drawn from a drawing tube mounted on an Olympus BX51 compound microscope. Material is deposited in the Musée Cantonal de Zoologie at Lausanne, Switzerland (**MZL**), Steinhardt Museum of Natural History at Tel Aviv University, Israel (**SMNH**), and Biology Centre of the Czech Academy of Sciences, Institute of Entomology (**IECA**).

DNA for species delineation was extracted using the non-destructive protocol outlined by Vuataz et al. (2011), which enabled post-extraction morphological study of specimens. The 'barcoding section' of the mitochondrial cytochrome *c* oxidase subunit I (**COI**) was PCR-amplified with the primers HCO2198 and LCO1490 (Folmer et al. 1994). Amplification followed the conditions and protocols outlined by Sroka et al. (2021). Automated sequencing was carried out in Microsynth (Balgach, Switzerland).

Molecular reconstruction was conducted on the four newly obtained sequences from Israel and three already published sequences from Sardinia (Suppl. material 1). Forty-six additional reference sequences of representative Palaearctic *Alainites* species and allied genera were obtained from GenBank (http://www.ncbi.nlm.nih.gov/), from the unpublished FREDIE database (http://wp.fredie.eu//), or sequenced for the first time (an individual of *A. sadati* from Algeria). GenBank ac-

cession numbers are available in Suppl. material 1. Sequence chromatograms were inspected and edited using Geneious v. 7.1.5 (Biomatters Ltd.). Alignment, reconstruction, and genetic distance calculations were conducted in MEGA-X v. 10.0.5 (Kumar et al. 2018). A maximum likelihood (**ML**) analysis was conducted in RAxML v. 8 (Stamatakis 2014; implemented in raxmlGUI v. 2.0.7, Edler et al. 2021), employing HKY+I as sequence evolution model, with 100 runs and 1000 bootstrap replicates.

Results

In comparison to COI sequences of other available taxa in *Alainites* and allied genera, the two newly described species demonstrate very low intraspecific variation (up to 0.7%) and very high interspecific distances (at least 19.2%).

***Alainites bengunn* Yanai & Gattolliat, sp. nov.**
https://zoobank.org/A4EA23BC-7DEE-4587-88E7-D27BCA64EE31
Figs 1–3

Alainites muticus in Buffagani et al. 2003
Alainites cf. *muticus* in Gattolliat et al. 2015
Takobia sp. cf. *albinatii* in Tenchini et al. 2018

Material examined. *Holotype*. 1 nymph, Italy, Sardinia, Loc near Fonni, trib. of Taloro (SA27), 40°09.05'N, 9°16.37'E, alt. 810 m a.s.l., 15.v.2009, L. Vuataz, E. Cavallo & Y. Chittaro leg., MZL (GBIFCH 00970536). ***Paratypes.*** Italy. 3 nymphs (2 on slide), same details as holotype, SMNH, IECA, MZL (GBIFCH 00280204, GBIFCH 00604446, GBIFCH 00604447) • 21 nymphs (2 on slide), Sardinia, Monti del Genargentu, near Monte Spada, 20.vi.2010, T. Soldán leg., MZL (7 nymphs), SMNH (7 nymphs), IECA (7 nymphs) • 33 nymphs (2 on slide), Sardinia, tributary of Fiume Taloro Riv., Fonni village, 20.vi.2010, T. Soldán leg., MZL (11 nymphs), SMNH (11 nymphs), IECA (11 nymphs) • 35 nymphs (2 on slide), Sardinia, Riu Pramaera River, Lotzorai village, 21.vi.2010, T. Soldán leg., MZL (11 nymphs), SMNH (11 nymphs), IECA (13 nymphs). **Additional non-type material.** Italy. 3 nymphs, Sardinia, Rio Rumine, vicinity of Mamoiada village, 20.vi.2010, T. Soldán leg., IECA • 1 nymph, Sardinia, Genna Stream, Auxi Pass, vicinity of Urzulei village, 21.vi.2010, T. Soldán leg., IECA.

Material not examined. Italy. Sardinia, Loc. Siligo village, 40°35.36'N, 8°43.55'E, alt. 240 m a.s.l., C. Belfiore leg.

Differential diagnosis. The species is distinct amongst other West Palaearctic *Alainites* species based on the combination of (1) six pairs of abdominal gills, (2) paraproct prolongation covered with spines on its entire surface, (3) serration between prostheca and mola, and (4) low number of dorsal setae on its fore-femora (14–20) and relatively many of them on the fore-tibiae (up to 17).

Figure 1. *Alainites bengunn* sp. nov., habitus: lateral view (top) and dorsal view (bottom).

Description of nymph. ***Length***. Female body 7.0–7.9 mm; cerci 4.5–5.5 mm; median caudal filament ca. 2/3 of cerci. Male body 6.0–6.7 mm; cerci 4.0–5.0 mm; median caudal filament ca. 2/3 of cerci.

Colouration (Fig. 1). General colouration brown. Head uniformly brown with vermiform marks on vertex and frons. Legs ecru except upper side of femora brown. Thorax brown with some paler area, but without clear pattern. Abdominal tergites brown with a central yellowish elongated dot; distal part of tergite IX and whole tergite X yellowish. Abdominal sternites I and II yellowish, III–IX pale brown. Cerci ecru to pale brown.

Head. Antennae (Fig. 2A) close to each other, with a narrow interantennal carina; scape with few deep scale insertions. Dorsal surface of labrum (Fig. 2B) with one central long seta and distolateral arc of four medium to long, simple, stout setae, and small fine setae scattered on surface; ventral surface with 5–6 submarginal small, pointed setae; distal margin fringed with ca. 20 short, followed by seven or eight long, feathered setae. Right mandible (Fig. 2C) slightly shagreened, with sparse fine setae and deep scale insertions; incisors composed of eight apically rounded, distinct denticles, outer- and innermost denticles smaller than others; prostheca reduced and bifid with numerous thin setae; space between prostheca and mola serrated, tuft of setae absent; apex of mola with tuft of two setae. Left mandible (Fig. 2D) slightly shagreened, with sparse fine setae and deep scale insertions; incisors composed of

eight rounded, distinct denticles, outer- and innermost denticles smallest, and small denticle in the middle; prostheca with few medium denticles and comb-shaped structure; margin between prostheca and mola serrated, without setae; tuft on apex of mola reduced to one seta. Hypopharynx (Fig. 2E) trilobed, apically sparsely covered with thin setae; lingua with no central protuberance; superlingua subequal to lingua. Maxillae (Fig. 2F) apex with three elongated and curved teeth and a tooth-like dentiseta; crown with two rows of setae, first row with small setae, second row with two long stout feathered dentisetae; palp two-segmented, extending the apex of galealacinia, length of segment I approximately 0.75 × segment II; segment II apically rounded, with sparse thin setae. Labium (Fig. 2G) with glossae slightly shorter than paraglossae; inner margins of glossae with eight or nine stout medium setae, apical margin with ca. nine long stout setae; ventral surface with few thin scattered setae; dorsal surface with row of ca. six medium setae; paraglossae with three rows of eight or nine long, stout, simple setae apically; labial palp three-segmented; segment I 0.75 × length of segments II and III combined; segment II with dorsal oblique row of five medium setae; segment III rounded, nearly symmetrical, slightly pointed apically, covered with few short thin setae.

Thorax. Forelegs (Fig. 3A). Trochanter with four or five marginal short stout pointed setae and few similar setae on surface. Femora dorsally with one row of 14–20 long, stout setae, and very few setae subparallel to dorsal margin; dorsoapical setal patch formed by two stout, long setae; ventrally several marginal and submarginal short stout pointed setae; lateral surface with scale bases, mainly on apical half and along subdorsal area. Tibiae dorsally with 9–17 short stout pointed setae, denser towards apical end, few proximal minute setae; ventrally with marginal and submarginal short stout pointed setae, denser towards apical end; tibiopatellar suture present; lateral surface with few short, stout, pointed setae and numerous scale bases. Tarsi bare dorsally; ventral margin with ca. 20 pointed medium setae; lateral surface with numerous scale bases. Tarsal claws (Fig. 3B) hooked with one row of 10–15 medium teeth, apical setae absent. Mid and hindlegs similar to forelegs except femora dorsally with 13–25 pointed setae and tibiae (Fig. 3C) with 11–18 similar setae dorsally. Hindwing pads present.

Abdomen. Terga (Fig. 3D) shagreened, with numerous scale bases, distal margin of tergite IV with triangular spines about twice longer than broad. Sterna shagreened with scales and scale bases; posterior margin smooth without spination. Gills (Fig. 3E) on segments II–VII, elliptical, almost symmetrical and with serrated margins, except proximal part; tracheation well visible and well branched; gill VII similar to gills II to VI. Paraproct (Fig. 3F) with abundant scale bases but almost no setae; margin with ca. seven broad, triangular spines inner to prolongation and numerous medium spines outer to prolongation; prolongation covered with numerous small spines; cercotractor with scattered scale bases, margin with ca. 20 small spines.

Imagos. Unknown.

Etymology. The species is endemic to an island, just like Ben Gunn who was deserted and isolated on an island by his crewmates in "Treasure Island" by R.L. Stevenson (1850–1894).

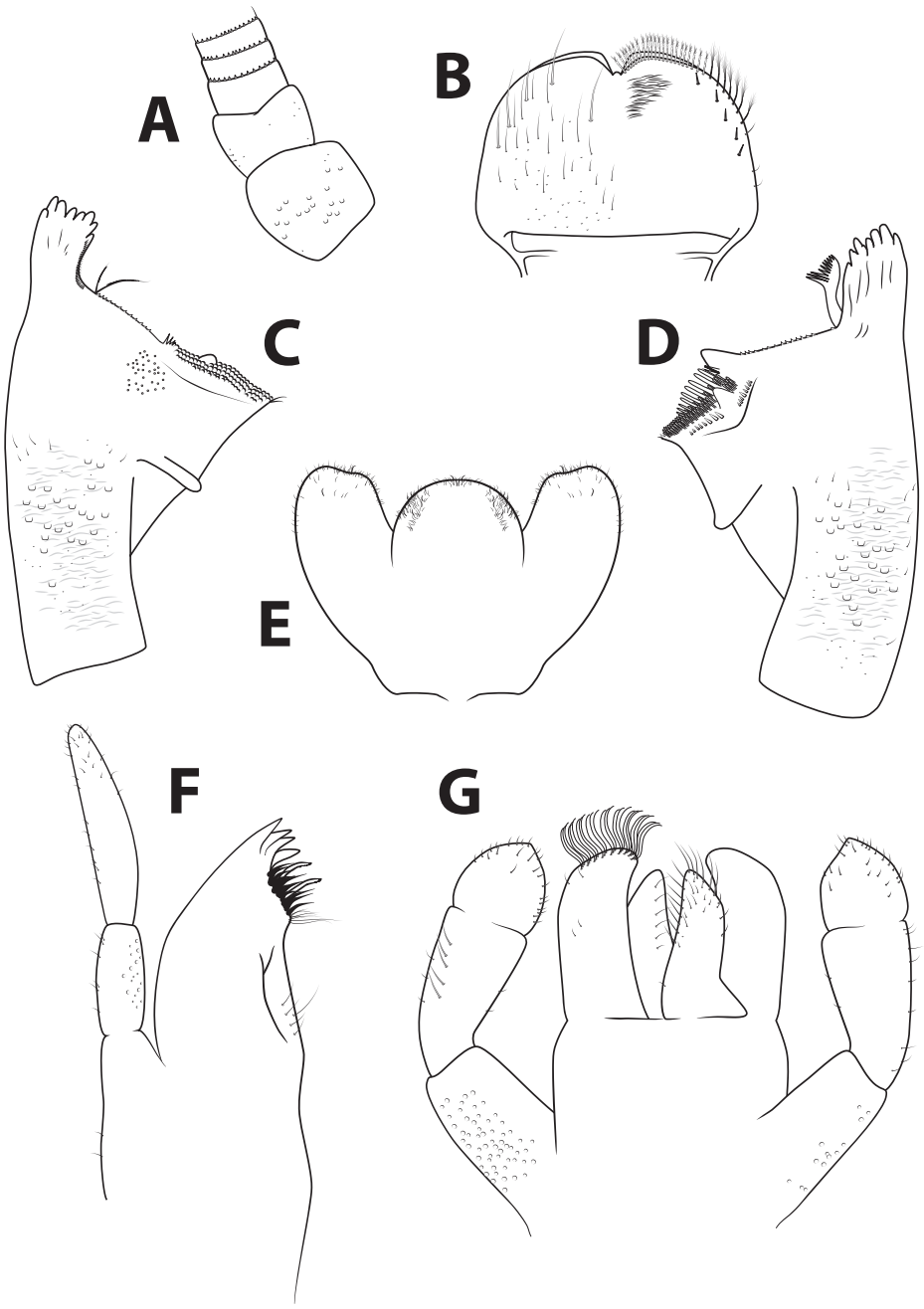

Figure 2. *Alainites bengunn* sp. nov., nymph, characters of the head **A** antenna base **B** labrum (left side dorsal view, right side ventral view) **C** right mandible (ventral view) **D** left mandible (ventral view) **E** hypopharynx **F** maxilla **G** labium (left side dorsal view, right side ventral view). **B–G** presented to the same scale.

Distribution and ecology. Little is known about the ecology and distribution of this species. The type locality is a small stream (less than three meters wide), shallow, and with medium current velocity. The species is only known from Sardinia where it is apparently not frequent and not very abundant.

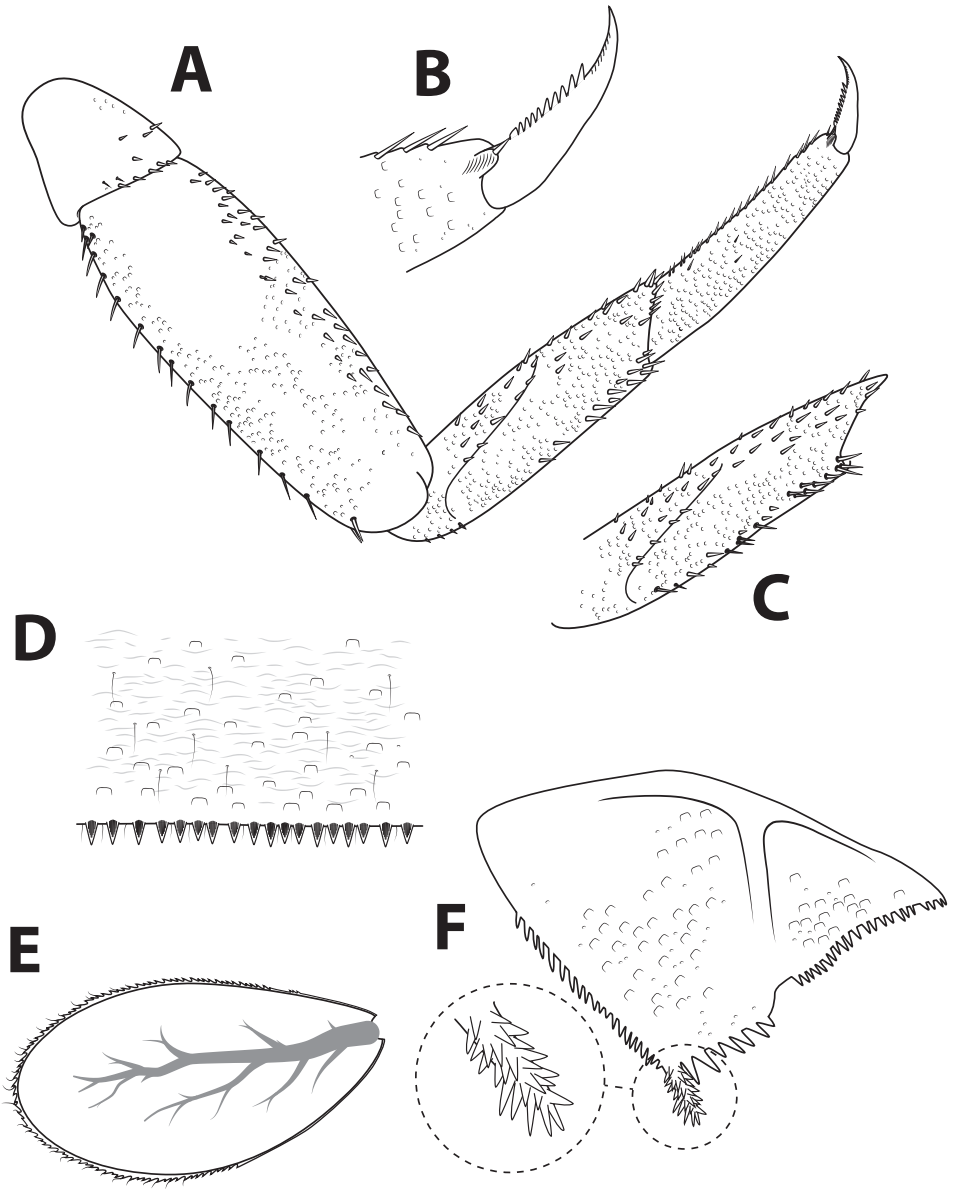

Figure 3. *Alainites bengunn* sp. nov., nymph, characters of the thorax and abdomen **A** foreleg **B** tarsal claw of foreleg **C** tibia of midleg **D** distal margin of tergum IV **E** gill IV **F** paraproct (with detail of prolongation).

***Alainites gasithi* Yanai & Gattolliat, sp. nov.**
https://zoobank.org/6445DE52-25A3-49AF-92A4-FCE665C57753
Figs 4–6

species L55 in Samocha 1972

Material examined. ***Holotype*.** Israel. 1 female nymph; Wadi Al-Qassab, Maymon Spring, 33°06.74'N, 35°39.62'E, 290 m a.s.l., 4.iv.2016, Z. Yanai leg., SMNH (385900). ***Paratypes*.** Israel. 9 nymphs, same data as holotype. 5 nymphs SMNH (385901), 2 nymphs MZL (GBIFCH 00972062), 2 nymphs IECA • 10 nymphs, Maymon Spring, 33°06.74'N, 35°39.62'E, 290 m a.s.l., 22.vi.2014, Z. Yanai leg., 7 nymphs SMNH (385895), 3 nymphs MZL (GBIFCH 00971882) • 2 nymphs, same locality, 13.iv.2018, Z. Yanai leg., SMNH (385896) • 4 nymphs (1 on slide), same locality, 26.iii.2019, Z. Yanai leg., SMNH (385892, 385893, 385894) • 10 nymphs (2 on slides), Tina (Nutra) Stream, 33°04.70'N, 35°38.63'E, 72 m a.s.l., 15.vii.2014, Z. Yanai leg., SMNH (385902, 385903, 385904, 385905) • 5 nymphs, same locality, 6.xi.2015, Z. Yanai & S. Cohen leg., SMNH (385898, 385899) • 1 nymph, same locality, 16.v.2016, Z. Yanai & A. Charvet leg., SMNH (385897) • 1 nymph, same locality, 10.iii.2017, Z. Yanai & J.-L. Gattolliat leg., MZL (GBIFCH 00971972) • 4 nymphs (1 on slide), same locality, 27.iii.2019, Z. Yanai leg., SMNH (385906, 385907) • 7 nymphs (1 on slides), Gilbon Stream, old mill, 33°02.45'N, 35°38.40'E, 76 m a.s.l., 29.x.2015, Z. Yanai leg., SMNH (385889, 385890) • 4 nymphs, Divsha Stream, 33°05.41'N, 35°38.90'E, 150 m a.s.l., 6.xi.2015, Z. Yanai & S. Cohen leg., SMNH (385887, 385888) • 1 nymph, ʻAyit Waterfall, 32°57.28'N, 35°45.23'E, 470 m a.s.l., 4.iv.2016, Z. Yanai leg., SMNH (385891). **Additional non-type material.** Israel. 1 nymph, Jordan River, ʻAteret Fortress, 33°00.19'N, 35°37.72'E, 63 m a.s.l., 16.v.2016, Z. Yanai & A. Charvet leg., SMNH (385908).

Differential diagnosis. The species is distinct amongst other West Palaearctic *Alainites* species based on the combination of (1) six pairs of abdominal gills, (2) paraproct prolongation with spines only along the border, (3) serration between prostheca and mola, and (4) low number of dorsal setae on its fore-femora (10–20) and foretibiae (6–12).

Description of nymph. ***Length*.** Female body 3.7–4.0 mm; cerci broken; median caudal filament 1.3–1.4 mm (ca. 2/3 of cerci); male body 3.7–3.9 mm; cerci broken; median caudal filament ca. 2/3 of cerci.

Colouration (Fig. 4). General colouration pale to medium brown. Head uniformly pale brown with vermiform marks faintly visible on vertex and frons. Turbinate eyes in male nymphs medium brown. Legs ecru, except a broad area on upper side of femora. Thorax medium brown without mark or pattern. Abdominal tergites medium brown without any pattern. Abdominal sternites pale to medium brown. Cerci ecru to pale brown without bands or pattern.

***Head*.** Antennae (Fig. 5A) close to each other, with a narrow interantennal carina; scape with few deep scale insertions and few setae. Dorsal surface of labrum (Fig. 5B)

Figure 4. *Alainites gasithi* sp. nov., habitus: lateral view (top) and dorsal view (bottom).

with one central long seta, distolateral arc of three or four simple medium to long, stout setae, and scattered small fine setae; ventral surface with 5–10 submarginal small pointed setae; distal margin fringed with ca. 20 short, followed by seven or eight long, feathered setae. Right mandible (Fig. 5C) smooth, not shagreened, with sparse fine setae; incisors composed of eight apically rounded, distinct denticles, outer- and innermost denticles smaller than others; prostheca reduced and bifid with numerous thin setae; outer half of margin between prostheca and mola serrated, tuft of setae absent; apex of mola with tuft of setae. Left mandible (Fig. 5D) smooth, with sparse fine setae; incisors composed of seven apically rounded, distinct denticles, outer- and innermost

denticles smallest; prostheca with medium denticles and comb-shaped structure; margin between prostheca and mola almost entirely serrated, without setae; apex of mola with tuft of setae. Hypopharynx (Fig. 5E) trilobed, apically covered with thin setae; lingua with small central protuberance; superlingua slightly longer than lingua. Maxillae (Fig. 5F) apex with three elongated and curved teeth and a tooth-like dentiseta; crown with two rows of setae, first row with small setae, second row with two long stout feathered dentisetae; palp two-segmented, reaching or slightly exceeding the apex of galealacinia, length of segment I subequal to segment II; segment II apically rounded, with few thin setae. Labium (Fig. 5G) with glossae subequal to paraglossae; inner margins of glossae with 7–10 stout medium setae, apical margin with 7–11 long stout setae, ventral surface with few thin scattered setae; dorsal surface with row of ca. 7 medium setae; paraglossae of constant width, with three rows of 10–12 long, stout, simple setae apically; labial palp three-segmented; segment I nearly half the length of segments II and III combined; segment II with dorsal oblique row of four medium setae; segment III conical, asymmetrical.

***Thorax*.** Forelegs (Fig. 6A). Trochanter with four or five marginal short stout pointed setae. Femora dorsally with one row of 10–20 medium, stout setae; dorsoapical setal patch formed by two stout, medium setae; ventral margin with pointed short setae; lateral margin with sparse scale bases, mainly on apical half. Tibiae dorsally with ca. six (rarely up to 10–12) setae and single apical seta; ventral margin with small pointed scales and apical patch formed of four or five stout setae; tibiopatellar suture present; lateral margins with few scales and numerous scale bases. Tarsi bare dorsally; ventral margin with 10–15 small pointed setae; lateral margins with numerous scale bases. Tarsal claws (Fig. 6B) hooked with one row of 7–13 (usually 10–11) medium teeth, apical setae absent. Mid and hindlegs similar to forelegs, except midtibiae (Fig. 6C) usually with 9–11 pointed setae on the dorsal margin and hind tibiae usually with 5–7 such setae. Hindwing pads present.

***Abdomen*.** Terga (Fig. 6D) with numerous scale bases, smooth, not shagreened, distal margin of tergite IV with triangular spines, at least twice longer than wide. Sterna shagreened with scales and scale bases; posterior margin smooth without spination. Gills (Fig. 6E) on segments II–VII, elliptic, symmetrical and serrated on margins of distal half; tracheation well visible and well divided; gill VII similar to gills II to VI. Paraproct (Fig. 6F) with abundant scale bases, no setae; margin with six or seven triangular spines of varying size inner to prolongation and numerous medium spines outer to prolongation; prolongation margined with about 15 elongated medium spines, without spines on ventral surface; cercotractor with scale bases, margin with medium spines.

Imagos. Unknown.

Etymology. The name is a noun in apposition. The first author dedicates the species to his former mentor Prof. Avital Gasith (1943–). He is, in many aspects, the founder of freshwater ecology research in Israel. He trained the majority of the local active experts and contributed significantly to our understanding of freshwater systems and taxa, and to their conservation.

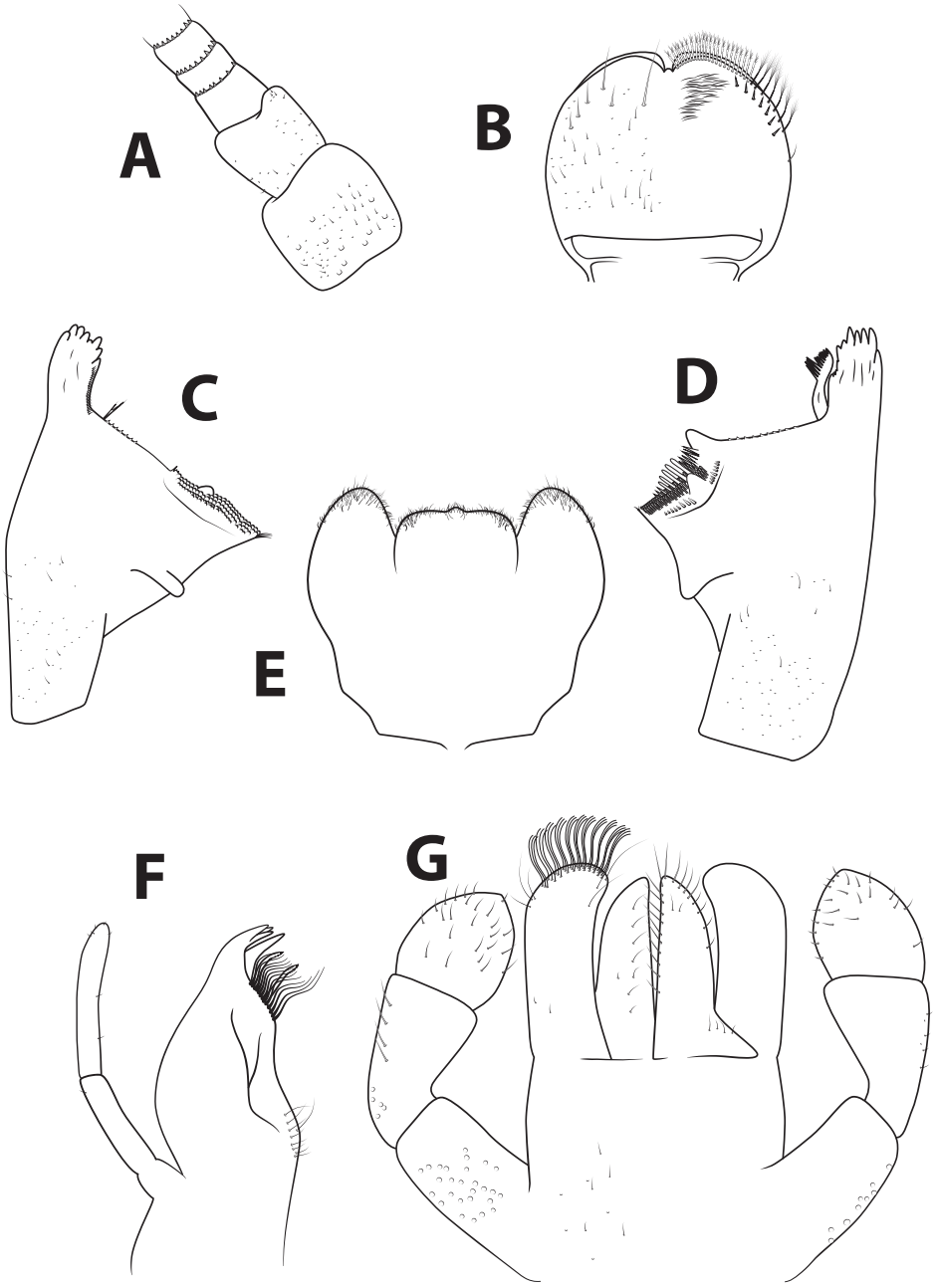

Figure 5. *Alainites gasithi* sp. nov., nymph, characters of the head **A** antenna base **B** labrum (left side dorsal view, right side ventral view) **C** right mandible (ventral view) **D** left mandible (ventral view) **E** hypopharynx **F** maxilla **G** labium (left side dorsal view, right side ventral view). **B–G** presented to the same scale.

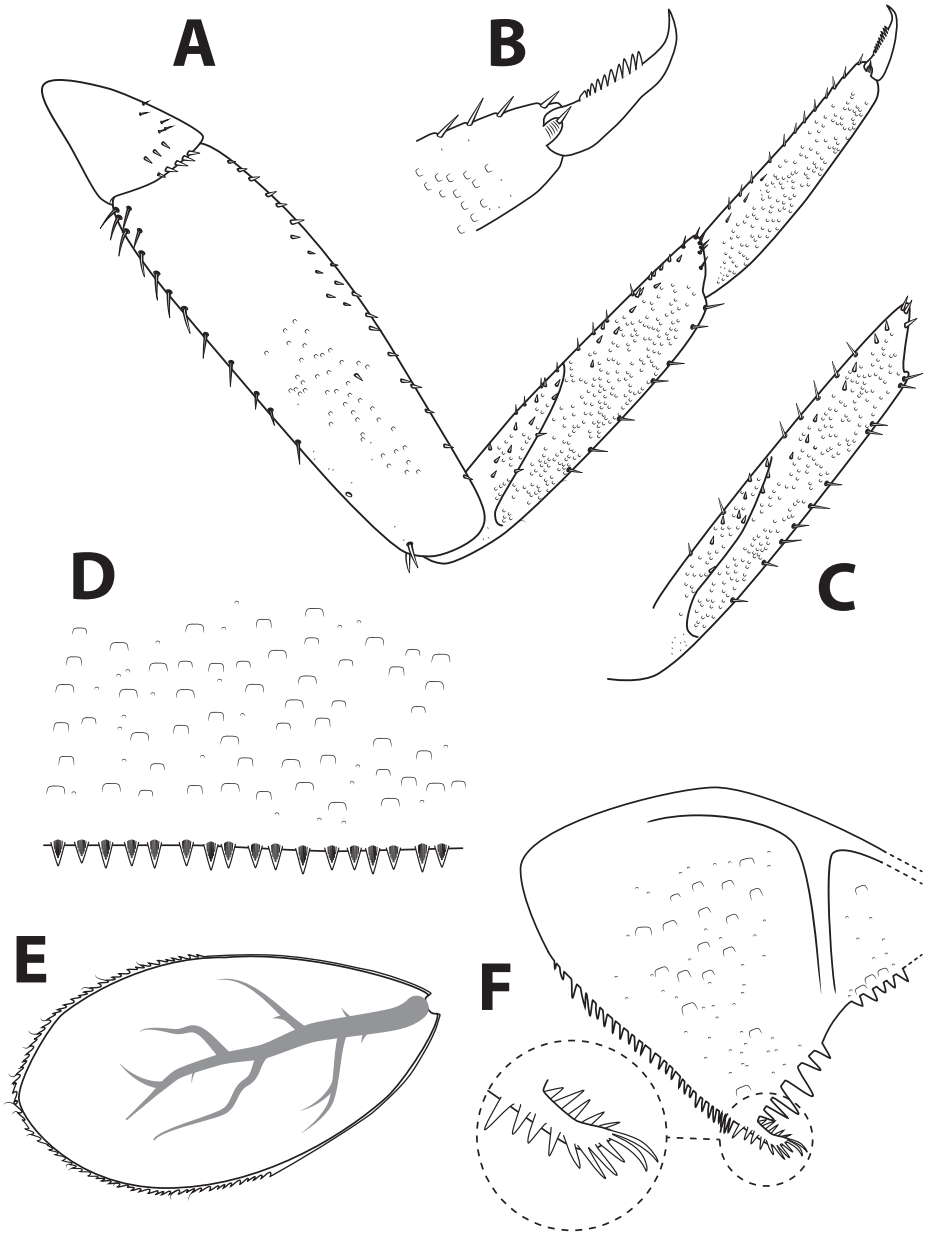

Figure 6. *Alainites gasithi* sp. nov., nymph, characters of the thorax and abdomen **A** foreleg **B** tarsal claw of foreleg **C** tibia of midleg **D** distal margin of tergum IV **E** gill IV **F** paraproct (with detail of prolongation).

Distribution and ecology. Typical habitats of *A. gasithi* sp. nov. include spring-fed brooks in the western slopes of the Golan Heights, with shallow running waters upon basalt bedding. Little is known about the seasonality of this species as it has been rarely collected. Mature nymphs were collected in the spring and early summer (late March

to June). Interestingly, the examined specimens were collected mainly in 2014–2019, and despite continuing research and much effort in the same sites, the species was not collected in 2020–2021, an observation that may indicate inter-annual fluctuations in population sizes. However, the species is very rare even in positive sampling event, suggesting that further research is needed for estimation of meta-population structure and stability.

Discussion

Morphological characters of *A. bengunn* sp. nov. and *A. gasithi* sp. nov.

The two newly described species are assigned to *Alainites* since they share all the synapomorphic characters of the genus, especially laterally compressed body, elongated paraproct prolongations, and prostheca of the right mandible composed of two feathered bristles (Waltz et al. 1994). Within *Alainites*, the nymphs of the two species are distinct from the most common species *A. muticus* by the number of gills (*A. muticus* is the only West Palearctic species of *Alainites* with seven pairs). They differ from other West Palaearctic congeners as follows (see also Table 1):

Alainites bengunn sp. nov. can be distinguished from *A. gasithi* sp. nov. based on a presence of spines on all the surface of the paraproct prolongation (spines only on margins in *A. gasithi* sp. nov.). Spines restricted to the prolongation margin were originally also reported for *A. kars* by Kazancı and Thomas (1989: fig. 7). It is worth mentioning, that later Martynov and Godunko (2017: figs 45, 46) depicted specimens of *A. kars* from Armenia with spines on all the surface of paraproct prolongation. Additionally, *A. kars* possesses many more setae on the dorsal margin of femora (more than 40 on the forefemur of *A. kars* according to Kazancı and Thomas 1989), and lacks the serration between the prostheca and mola. From *A. navasi*, occurring in the West Mediterranean, *A. bengunn* sp. nov. can be distinguished by the more shagreened surface of terga, together with fewer dorsal setae on femora and tibiae (ca. 26 and ca. 21 in *A. navasi*, respectively, according to Zrelli et al. 2012).

Alainites bengunn sp. nov. is rather similar to the Corsican *A. albinatii*. The main character to distinguish them is the presence of spines on the dorsal margin of foretibiae (ca. seven for *A. albinatii*, at least nine in *A. bengunn* sp. nov.), the shape of the spines of the distal margin of terga (slender and more pointed in *A. albinatii*) and the spines on the paraproct prolongation (the prolongation is completely covered by small spines in *A. bengunn* sp. nov., whilst only the apex is covered by spines in *A. albinatii*).

The North African species *A. sadati* and *A. oukaimeden* usually have more femoral setae and fewer tibial setae than *A. bengunn* sp. nov. (Table 1; Zrelli et al. 2012). *Alainites sadati* also exhibits more elongated labrum and apical segment of the labial palp compared to *A. bengunn* sp. nov. Furthermore, the length of maxillary palp does not exceed the apex of galealacinia in *A. sadati*, contrary to *A. bengunn* sp. nov. *Alainites oukaimeden* possesses a different arrangement of paraproct compared to *A. bengunn* sp. nov.: the prolongation in *A. oukaimeden* is broader, and

Table 1. Diagnostic characters of West Palaearctic *Alainites* species.

Species	Distribution	Left mandible: margin between prostheca and mola	Mandible lateral side	Fore-femur dorsal margin: number of spines	Fore-tibia dorsal margin: number of spines	Number of gill pairs	Cuticle abdominal terga and sterna	Tergite IV: spines on distal margin	Prolongation of paraproct
Alainites albinatii (Sartori & Thomas, 1989)	Corsica	10 small teeth	scale bases, shagreened	15	6	6	slightly shagreened	long triangular, pointed	apically covered by spines
Alainites bengunn sp. nov.	Sardinia	serrated	scale bases, slightly shagreened	14–20	9–17	6	shagreened	slightly lanceolate	covered by spines
Alainites gasithi sp. nov.	Israel	serrated	no scale bases, almost not shagreened	10–20	ca. 6, rarely 10–12	6	smooth	long triangular, pointed	spines only on border
Alainites kars (Thomas & Kazancı, 1989)	Turkey	only minute serration close to mola	no scale bases, almost not shagreened	> 40 in two rows	5–9	6	slightly shagreened	triangular, pointed	spines on entire surface (Martynov and Godunko 2017) or just on apex (Kazancı and Thomas 1989)
Alainites muticus (Linnaeus, 1758)	Palaearctic	10 small teeth	rare scale bases	14	8	7	slightly shagreened	short triangular, broad basally	spines only on border
Alainites navasi (Müller-Liebenau, 1974)	Iberian Peninsula	10 small teeth	?	26	21	6	smooth	short triangular	covered by spines
Alainites oukaimeden (Thomas & Sartori, 1992)	Morocco (High Atlas)	10 small teeth	shagreened	20	8	6	strongly shagreened	long, relatively narrow	covered by spines
Alainites sadati Thomas, 1994	Algeria, Tunisia	10 small teeth	no scale bases, almost not shagreened	ca. 25	6–9	6	slightly shagreened	medium triangular	covered by spines

marginal spines outer to prolongation are smaller and more numerous (Thomas et al. 1992: fig. 6).

Nigrobaetis (*Takobia*) *katerynae* from Georgia represents a species not formally assigned in *Alainites*, although complying with the definition of this genus used in the present study. Until a more extensive phylogenetic analysis is done, we refrain from introducing new combinations, therefore we treat *N. katerynae* under the name originally proposed by Martynov and Godunko (2017). *Nigrobaetis katerynae* can be distinguished from *A. bengunn* sp. nov. by multiple characters: a different structure of the area between incisors and mola of mandibles (no serration on left mandible and row of setae on right one in *N. katerynae*, whereas the space between prostheca and mola is serrated in both mandibles in *A. bengunn* sp. nov.); more elongated apical segment of labial palp in *N. katerynae*; and narrower spines on posterior margin of terga in *A. bengunn* sp. nov.

Alainites gasithi sp. nov. is more distinct amongst the West Palaearctic species, mainly due to the arrangement of spines on the paraproct prolongation, i.e., only along the lateral margin. The only two other species with similar spines arrangement are easily distinguished: *A. muticus* has seven pairs of gills, and *A. kars* has no serration between prostheca and mola, plus it has many more dorsal setae on its forefemora. Moreover, at least some populations of *A. kars* possess spines on all the surface of the paraproct prolongation (Martynov and Godunko 2017: figs 45, 46). *Alainites gasithi* sp. nov. may have the lowest number of dorsal setae on forefemora and foretibiae compared to all other West Palaearctic species, but this character should be treated with caution since it may vary to some extent and can overlap with numbers exhibited by other species.

Phylogenetic reconstruction

The ML analysis (Fig. 7) supports the monophyly of the two new species, *A. bengunn* sp. nov. and *A. gasithi* sp. nov. No further information can be gained regarding the relationships amongst close genera, since COI is a useful barcode segment for species delineation and identification, but not informative for deeper nodes. We therefore recommend on a more thorough investigation regarding the systematics of *Alainites*, *Nigrobaetis*, and *Takobia*, which should rely on morphological or wider genetic data. An analysis of the genetic distances amongst and between populations also supports the monophyly of the newly described species (Suppl. material 2). Intraspecific variation of the COI distances never exceeds 0.7%, as expected from populations that belong to the same species. For both species, the known populations are geographically restricted, and we expect higher differences only if additional, further populations are discovered. On the other hand, each of the sequences of the new species is at least 19% different from any other *Alainites*, *Nigrobaetis*, or *Takobia* species that we have analysed, a pattern that leaves no doubt regarding their specific independence. High variation amongst *A. muticus* samples is evident, and has already been noticed by Sroka (2012) and Sroka et al. (2021). As detailed therein, these are probably due to misidentified specimens that were contributed to GenBank, and, perhaps, it is another

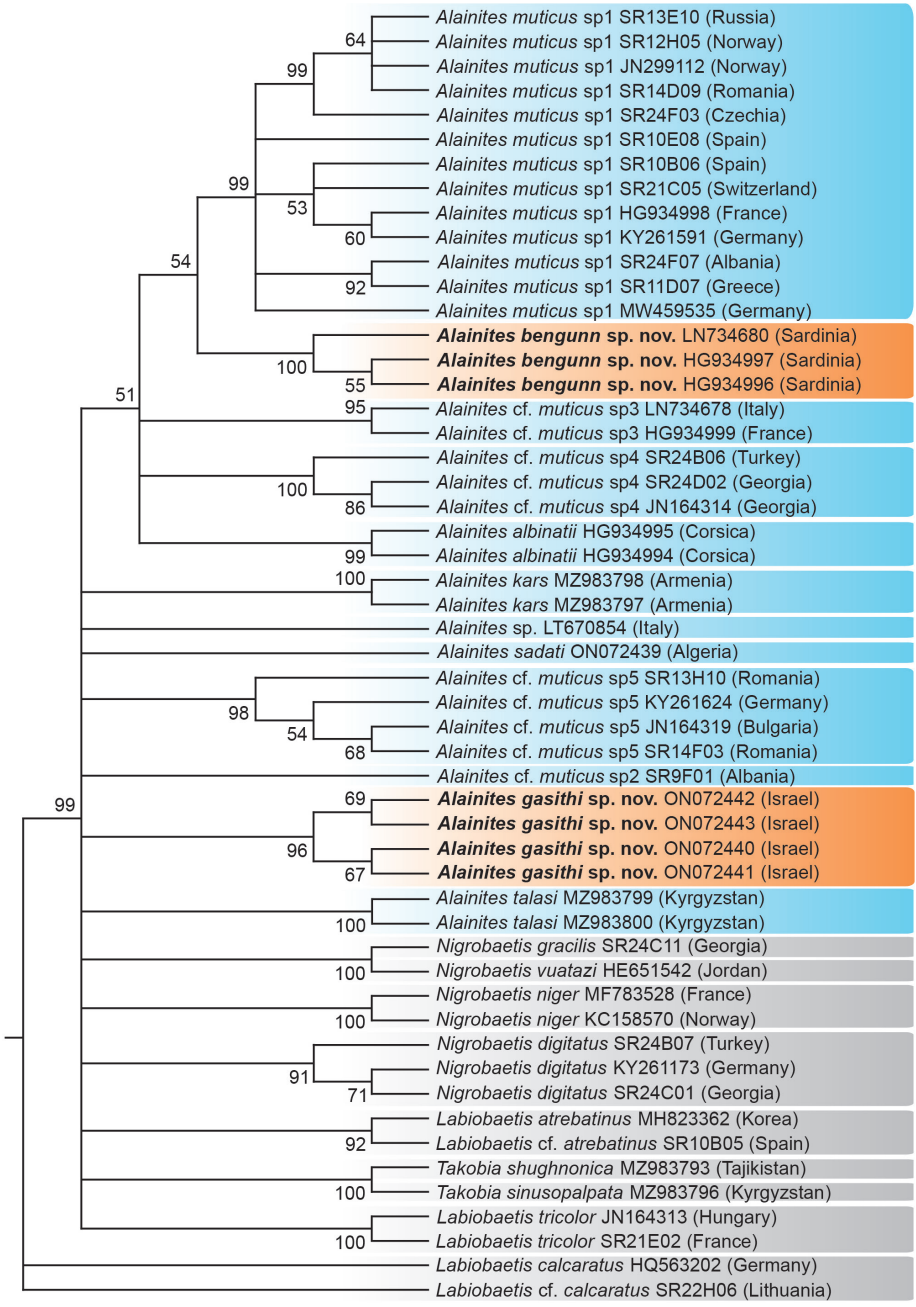

Figure 7. Phylogenetic reconstruction of *Alainites* species and allied taxa, based on maximum likelihood analysis of sequences of the mitochondrial COI gene. The reconstruction includes representatives of the two new *Alainites* species (displayed with orange background), all other sequenced *Alainites* species (blue), and representative species of *Nigrobaetis* and *Takobia* (grey). For full details of selected samples see Suppl. material 1. ML bootstrap values higher than 50% are indicated next to the nodes; lower than 50% are collapsed. Due to the wide polytomy in deeper nodes, branch lengths are in fact meaningless in this presentation. Taxa names are consistent with our findings, and may sometimes differ from names entered in GenBank.

clue for *A. muticus* being a complex of cryptic species. The latter explanation is of high importance for the resolution of *Alainites* systematics.

Distribution of *Alainites* species

Both *A. bengunn* sp. nov. and *A. gasithi* sp. nov. are known from very restricted ranges and are endemic to Sardinia and to Israel, respectively. It is possible that further research will reveal *A. gasithi* sp. nov. populations in Jordan, Syria, or Lebanon, although no suspicious species have been reported from there to date (e.g., Koch 1988, Gattolliat et al. 2012, Alhejoj et al. 2020). Being so geographically restricted, the two species follow the knowledge of the distribution of other West Palaearctic *Alainites* spp.: most of them are known from very limited areas, and almost no sympatry is recorded, i.e., two *Alainites* species are almost never found together.

In conclusion, identification of nymphs of *Alainites* based solely on morphology may be remarkably confusing. However, an integrative approach, including also molecular evidence and distribution, often allows an accurate species delimitation and a reliable identification. Similar approach should be applied to solve the potential presence of cryptic species within *Alainites muticus* s. l. and the assignment of populations from Sicily (Tenchini et al. 2018) and North Morocco (Khadri et al. 2017; Mabrouki et al. 2019).

Acknowledgements

We thank Marion Podolak (Museum of Zoology Lausanne) for her lab work, as well as Emilie Cavallo, Yannick Chittaro, and Laurent Vuataz for collecting material in Sardinia and Corsica. Material from Israel was collected under collecting permits 40223, 40720, 41168, 41587, 41897, and 42160 by the Israel Nature and Parks Authority. We thank Sereina Rutschmann and Laurent Vuataz for providing unpublished sequences from the FREDIE project. We also appreciate the meaningful insights and contributions made by Thomas Kaltenbach and Roman Godunko, which improved the manuscript significantly. Roman Godunko also contributed by linking the findings of this study to unpublished material collected by Tomáš Soldán, which provided richer and more accurate information about *A. bengunn* sp.nov. The study was funded by the Israel Taxonomy Initiative (ITI) and the Swiss Government Excellence Scholarship (FCS), both given to ZY; and by the institutional support of Institute of Entomology (Biology Centre of the Czech Academy of Sciences) RVO: 60077344 given to PS.

References

Alhejoj I, Sartori M, Gattolliat J-L (2020) Contribution to the mayflies (Insecta, Ephemeroptera) of Jordan. Check List 16: 237-242. https://doi.org/10.15560/16.2.237

Bauernfeind E, Soldán T (2012) The mayflies of Europe (Ephemeroptera). Apollo Books, Ollerup, 781 pp. https://doi.org/10.1163/9789004260887

Bojková J, Sroka P, Soldán T, Namin JI, Straniczek AH, Polášek M, Hrivniak Ľ, Abdoli A, Godunko RJ (2018) Initial commented checklist of the Iranian mayflies, with new area records and description of *Procloeon caspicum* sp. n. (Insecta, Ephemeroptera, Baetidae). ZooKeys 749: 87–123. https://doi.org/10.3897/zookeys.749.24104

Bonada N, Dole'dec S, Statzner B (2007) Taxonomic and biological trait differences of stream macroinvertebrate communities between Mediterranean and temperate regions: Implications for future climatic scenarios. Global Change Biology 13(8): 1658–1671. https://doi.org/10.1111/j.1365-2486.2007.01375.x

Braasch D, Soldán T (1983) Baetidae in Mittelasien III (Ephemeroptera). Entomologische Nachrichten und Berichte 27: 266–271.

Buffagni A, Belfiore C, Erba S, Kemp JL, Cazzola M (2003) A review of Ephemeroptera species distribution in Italy: Gains from recent studies and areas for future focus. In: Gaino E (Ed.) Research update on Ephemeroptera & Plecoptera. University of Perugia, Italy, 279–280.

Edler D, Klein J, Antonelli A, Silvestro D (2021) raxmlGUI 2.0: A graphical interface and toolkit for phylogenetic analyses using RAxML. Methods in Ecology and Evolution 12(2): 373–377. https://doi.org/10.1111/2041-210X.13512

Filipe AF, Lawrence JE, Bonada N (2012) Vulnerability of stream biota to climate change in Mediterranean climate regions: A synthesis of ecological responses and conservation challenges. Hydrobiologia 719: 331–351. https://doi.org/10.1007/s10750-012-1244-4

Folmer O, Black M, Hoeh W, Lutz R, Vrijenhoek R (1994) DNA primers for amplification of mitochondrial cytochrome *c* oxidase subunit I from diverse metazoan invertebrates. Molecular Marine Biology and Biotechnology 3: 294–299.

Fujitani T (2008) The family Baetidae from Japan. In: Hauer FR, Stanford JA, Newell RL (Eds) International advances in the ecology, zoogeography and systematics of mayflies and stoneflies. University of California Publications in Entomology 128: 205–218. https://doi.org/10.1525/california/9780520098688.003.0015

Fujitani T, Hirowatari T, Tanida K (2003) Genera and species of Baetidae in Japan: *Nigrobaetis*, *Alainites*, *Labiobaetis*, and *Tenuibaetis* n. stat. (Ephemeroptera). Limnology 4(3): 121–129. https://doi.org/10.1007/s10201-003-0105-2

Gattolliat J-L (2011) A new species of *Alainites* (Ephemeroptera: Baetidae) from Borneo (East Kalimantan, Indonesia). Mitteilungen der Schweizerischen Entomologischen Gesellschaft / Bulletin de la Société Entomologique Suisse 84: 185–192.

Gattolliat J-L, Monaghan MT, Sartori M, Elouard J-M, Barber-James H, Derleth P, Glaizot O, de Moor F, Vogler AP (2008) A molecular analysis of the Afrotropical Baetidae. International Advances in the Ecology, Zoogeography and Systematics of Mayflies and Stoneflies. University of California Press, Berkeley, 219–232. https://doi.org/10.1525/california/9780520098688.003.0016

Gattolliat J-L, Cavallo E, Vuataz L, Sartori M (2015) DNA barcoding of Corsican mayflies (Ephemeroptera) with implications on biogeography, systematics and biodiversity. Arthropod Systematics & Phylogeny 73: 3–18.

Gattolliat J-L, Vuataz L, Sartori M (2012) First contribution to the mayflies of Jordan. Zoology in the Middle East 56: 91-110. https://doi.org/10.1080/09397140.2012.10648945

Hennig W (1950) Grundzüge einer Theorie der Phylogenetischen Systematik. Deutscher Zentralveriag, Berlin, 370 pp.

Hershkovitz Y, Gasith A (2013) Resistance, resilience, and community dynamics in mediterranean-climate streams. Hydrobiologia 719(1): 59–75. https://doi.org/10.1007/s10750-012-1387-3

Hrivniak Ľ, Sroka P, Godunko RJ, Palatov D, Polášek M, Manko P, Oboňa J (2018) Diversity of Armenian mayflies (Ephemeroptera) with the description of a new species of the genus *Ecdyonurus* (Heptageniidae). Zootaxa 4500(2): 195–221. https://doi.org/10.11646/zootaxa.4500.2.3

Jacob U (2003) *Baetis* Leach 1815, sensu stricto oder sensu lato. Ein Beitrag zum Gattungskonzept auf der Grundlage von Artengruppen mit Bestimmungsschlüsseln. Lauterbornia 47: 59–129.

Kaltenbach T, Gattolliat J-L (2017) New species of *Indocloeon* Müller-Liebenau from South-East Asia (Ephemeroptera, Baetidae). ZooKeys 723: 43–60. https://doi.org/10.3897/zookeys.723.20578

Kaltenbach T, Gattolliat J-L (2018) The incredible diversity of *Labiobaetis* Novikova & Kluge in New Guinea revealed by integrative taxonomy (Ephemeroptera, Baetidae). ZooKeys 804: 1–136. https://doi.org/10.3897/zookeys.804.28988

Kaltenbach T, Gattolliat J-L (2019a) A new species of *Tenuibaetis* Kang & Yang, 1994 from Indonesia (Ephemeroptera, Baetidae). ZooKeys 820: 13–23. https://doi.org/10.3897/zookeys.820.31487

Kaltenbach T, Gattolliat J-L (2019b) The tremendous diversity of *Labiobaetis* Novikova & Kluge in Indonesia (Ephemeroptera, Baetidae). ZooKeys 895: 1–117. https://doi.org/10.3897/zookeys.895.38576

Kazancı N, Thomas AGB (1989) Compléments et corrections à la fauna des Ephéméroptères do Proche-Orient: 2. *Baetis kars* n. sp. de Turquie (Ephemeroptera, Baetidae). Bulletin de la Société Entomologique Suisse 62: 323–327.

Khadri O, El Alami M, El Bazi R, Slimani M (2017) Ephemeroptera's diversity and ecology in streams of the ultramafic massif of Beni Bousera and in the adjacent non-ultramafic sites (NW, Morocco). Journal of Materials & Environmental Sciences 8: 3508–3523.

Kluge NJ, Novikova EA (2014) Systematics of *Indobaetis* Müller-Liebenau & Morihara, 1982, and related implications for some other Baetidae genera (Ephemeroptera). Zootaxa 3835(2): 209–236. https://doi.org/10.11646/zootaxa.3835.2.3

Koch S (1988) Mayflies of the Northern Levant (Insecta: Ephemeroptera). Zoology in the Middle East 2(1): 89–112. https://doi.org/10.1080/09397140.1988.10637565

Kumar S, Stecher G, Li M, Knyaz C, Tamura K (2018) MEGA X: Molecular Evolutionary Genetics Analysis across computing platforms (Version 10.0.2). Molecular Biology and Evolution 35: 1547–1549. https://doi.org/10.1093/molbev/msy096

Mabrouki Y, Taybi AF, El Alami M, Berrahou A (2019) Biotypology of stream macroinvertebrates from North African and semi-arid catchment: Oued Za (Morocco). Knowledge and Management of Aquatic Ecosystems 420: e17. [11 pp] https://doi.org/10.1051/kmae/2019009

Martynov AV, Godunko RJ (2017) Mayflies of the Caucasus Mountains IV. New species of the genus *Nigrobaetis* Novikova & Kluge, 1987 (Ephemeroptera, Baetidae) from Georgia. Zootaxa 4231(1): 70–84. https://doi.org/10.11646/zootaxa.4231.1.4

McCafferty WP, Waltz RD (1995) *Labiobaetis* (Ephemeroptera: Baetidae): new status, new North American species, and related new genus. Entomological News 106: 19–28.

Müller-Liebenau I (1969) Revision der europäischen Arten der Gattung *Baetis* Leach, 1815 (Insecta, Ephemeroptera). Gewässer und Abwässer 48/49: 1–214.

Müller-Liebenau I (1974) Baetidae aus Südfrankreich, Spanien und Portugal (Insecta, Ephemeroptera). Gewässer und Abwässer 53/54: 7–42.

Myers N, Mittermeier RA, Mittermeier CG, da Fonseca GAB, Kent J (2000) Biodiversity hotspots for conservation priorities. Nature 403(6772): 853–858. https://doi.org/10.1038/35002501

Novikova EA, Kluge NJ (1987) Systematics of the genus *Baetis* (Ephemeroptera, Baetidae), with description of new species from Middle Asia. Vestnik Zoologii 1987: 8–19. [in Russian]

Novikova EA, Kluge NJ (1994) Mayflies of the subgenus *Nigrobaetis* (Ephemeroptera, Baetidae, *Baetis*). Entomologicheskoe Obozrenie 73: 623–644. [in Russian]

Samocha M (1972) Ephemeroptera of Israel. MSc thesis, Tel Aviv University, Tel Aviv, Israel, 111 pp.

Sartori M, Thomas AGB (1989) Contribution à la connaissance du genre *Baetis* Leach, 1815 en Corse (Ephemeroptera; Baetidae). *B. albinatii* nov. sp. du groupe *muticus* (L.). Annales de Limnologie-International Journal of Limnology 25(2): 131–137. https://doi.org/10.1051/limn/1989013

Sroka P (2012) Systematics and phylogeny of the West Palaearctic representatives of subfamily Baetinae (Insecta: Ephemeroptera): combined analysis of mitochondrial DNA sequences and morphology. Aquatic Insects 34(1): 23–53. https://doi.org/10.1080/01650424.2012.718081

Sroka P, Yanai Z, Palatov D, Gattolliat J-L (2021) Contribution to the knowledge of the genus *Takobia* Novikova & Kluge, 1987 (Ephemeroptera, Baetidae) in Central Asia. ZooKeys 1071: 127–154. https://doi.org/10.3897/zookeys.1071.71582

Stamatakis A (2014) RAxML version 8: A tool for phylogenetic analysis and post-analysis of large phylogenies. Bioinformatics 30(9): 1312–1313. https://doi.org/10.1093/bioinformatics/btu033

Tenchini R, Cardoni S, Piredda R, Simeone MC, Belfiore C (2018) DNA barcoding and faunistic criteria for a revised taxonomy of Italian Ephemeroptera. The European Zoological Journal 85(1): 254–267. https://doi.org/10.1080/24750263.2018.1480732

Thomas A, Gagneur J (1994) Compléments et corrections à la faune des Ephéméroptères d'Afrique du Nord. 6. *Alainites sadati* n. sp. d'Algérie (Ephemeroptera, Baetidae). Bulletin de la Société d'Histoire Naturelle de Toulouse 130: 43–45.

Thomas A, Bouzidi A, Sartori M, Assef S, Ajakane A (1992) Compléments et corrections à la faune des Ephéméroptères d'Afrique du Nord. 5. *Baetis oukaimeden* n. sp. du Haut Atlas marocain: Description et écologie (Ephemeroptera, Baetidae). Bulletin de la Société Entomologique Suisse 65: 369–377.

Tierno de Figueroa JM, López-Rodríguez MJ, Fenoglio S, Sánchez-Castillo P, Fochetti R (2013) Freshwater biodiversity in the rivers of the Mediterranean Basin. Hydrobiologia 719(1): 137–186. https://doi.org/10.1007/s10750-012-1281-z

Tong X, Dudgeon D (2000) Two new species of *Alainites* (Ephemeroptera: Baetidae) from Hong Kong, China. The Pan-Pacific Entomologist 46: 115–120.

Vuataz L, Sartori M, Wagner A, Monaghan MT (2011) Toward a DNA taxonomy of alpine *Rhithrogena* (Ephemeroptera: Heptageniidae) using a mixed yule-coalescent analysis of mi-

tochondrial and nuclear DNA. PLoS ONE 6(5): e19728. https://doi.org/10.1371/journal.pone.0019728

Waltz RD, McCafferty WP (1997) New generic synonymies in Baetidae (Ephemeroptera). Entomological News 108: 134–140.

Waltz RD, McCafferty WP, Thomas A (1994) Systematics of *Alainites* n. gen., *Diphetor*, *Indobaetis*, *Nigrobaetis* n. stat., and *Takobia* n. stat. (Ephemeroptera, Baetidae). Bulletin de la Société d'Histoire naturelle de Toulouse 130: 33–36.

Zrelli S, Gattolliat J-L, Boumaiza M, Thomas A (2012) First record of *Alainites sadati* Thomas, 1994 (Ephemeroptera: Baetidae) in Tunisia, description of the larval stage and ecology. Zootaxa 3497(1): 60–68. https://doi.org/10.11646/zootaxa.3497.1.6

Supplementary material 1

Table S1

Authors: Zohar Yanai, Pavel Sroka, Jean-Luc Gattolliat

Data type: docx file.

Explanation note: Taxa used for genetic distance analysis (mitochondrial COI sequences) with GenBank accession numbers or FREDIE reference codes (novel sequences are highlighted in bold font).

Link: https://doi.org/10.3897/zookeys.1118.84643.suppl1

Supplementary material 2

Table S2

Authors: Zohar Yanai, Pavel Sroka, Jean-Luc Gattolliat

Data type: docx file.

Explanation note: Kimura 2 parameter distance amongst sequences of the mitochondrial COI gene of selected Alainites, Takobia, and Nigrobaetis species.

Link: https://doi.org/10.3897/zookeys.1118.84643.suppl2

ZooKeys 1118: 97–109 (2022)
doi: 10.3897/zookeys.1118.86448
https://zookeys.pensoft.net

RESEARCH ARTICLE

A peer-reviewed open-access journal
ZooKeys
Launched to accelerate biodiversity research

A new species of giant *Eunice* (Eunicidae, Polychaeta, Annelida) from the east coast of Australia

Joana Zanol[1], Pat Hutchings[2,3]

1 *Departamento de Invertebrados, Museu Nacional, Universidade Federal do Rio de Janeiro, Av. Bartolomeu de Gusmão, 875, Rio de Janeiro, RJ 20941-160 Brazil* **2** *Australian Museum Research Institute, Australian Museum, 1 William Street, 2010, New South Wales, Australia* **3** *Department of Biological Sciences, Macquarie University, North Ryde 2109, Australia*

Corresponding author: Joana Zanol (joanazanol@mn.ufrj.br)

Academic editor: Christopher Glasby | Received 12 May 2022 | Accepted 5 July 2022 | Published 24 August 2022

https://zoobank.org/AD0EF3AA-6C9A-4988-B69B-FA9D2F6A7E7E

Citation: Zanol J, Hutchings P (2022) A new species of giant *Eunice* (Eunicidae, Polychaeta, Annelida) from the east coast of Australia. ZooKeys 1118: 97–109. https://doi.org/10.3897/zookeys.1118.86448

Abstract

A new giant species is described from New South Wales, Australia. *Eunice dharastii* **sp. nov.** differs from described Australian species and is most similar to *E. aphroditois* (Pallas, 1788), *E. flavopicta* Izuka, 1912, and *E. kinbergi* Ehlers, 1868. The unique combination of features that characterizes the new species is irregular articulated prostomial appendages; antennae reaching back beyond chaetiger 4; branchiae starting at chaetiger 10, initially button-shaped and distinctly longer than notopodial cirri where best developed; dorsal fleshy knobs on anterior chaetal lobes; notopodial cirri pendulous, abrupt tapering from inflated bases; bidentate compound falcigerous chaetae with both teeth directed laterally, distal tooth much shorter than proximal tooth in median and posterior chaetigers; and dark bidentate subacicular hooks starting at chaetiger 58, tapering to a small head with both teeth directed distally, and proximal tooth much larger than minute and spur-like distal tooth. This new species lives in sandy sediments in coastal waters 1–8 m deep. It is highly mobile and not easy to collect, which may explain why it was not described before.

Keywords

Bobbit worm, *Eunice aphroditois*, Port Stephens, taxonomy

Introduction

Eunice, type genus of Eunicidae, is polyphyletic and currently characterized by plesiomorphic characters, such as the presence of three antennae, a pair of palps and a pair of peristomial cirri, the absence of regular articulations on prostomial appendages, presence of limbate, thin pectinate, compound bidentate falciger or spiniger chaetae, and dark uni- or bidentate subacicular hooks (Zanol and Budaeva 2021). The genus includes around 250 valid species (Read and Fauchald 2021). However, this number is likely to be an over-estimate because some species of the revalidated genera *Leodice* and *Nicidion* are still formally classified within *Eunice* (Zanol et al. 2021). Species of *Eunice* are present in all oceans in soft and hard substrates and various depths, but they are more common in biogenic hard substrates in shallow tropical waters (Fauchald 1992). The length of specimens of the genus is highly variable with longest species reaching a few meters in length (Fauchald 1992). These long species are considered giant due to their enormous length in comparison to the average length of *Eunice* species (e.g., Pruvot and Racovitza 1895; Salazar-Vallejo et al. 2011). Here, we consider giant species those with complete specimens reaching at least 1 m in length and 1 cm in maximum width.

Giant species are found in subtidal and intertidal zones of tropical and temperate oceans. The classification of these species has a long history of confusion. Many species have been synonymized with *Eunice aphroditois* (Pallas, 1788) (e.g., Fauvel 1932), leading to the common association of this name with a certain morph (large specimens bearing branchiae with many filaments, dark aciculae and dark subacicular hooks), and the underestimation of species diversity within the large-bodied morph (Fauchald 1992; Salazar-Vallejo et al. 2011). A more restricted and clear characterization of the species was made available by Fauchald (1992), who maintained only *Leodice gigantea* Lamarck, 1818 (no type specimen available, type locality La Réunion, Indian Ocean) as a junior synonym of *E. aphroditois* (no type specimen available, type locality Sri Lanka, Indian Ocean) and described two specimens from La Réunion (for a different opinion on this synonym see Salazar-Vallejo et al. 2011). In future, giant morphs identified as *E. aphroditois* should be re-examined and their true identity confirmed (e.g., Parapar and Harto 2001; Zanol and Bettoso 2006; Salazar-Vallejo et al. 2011; Schulze 2011).

Giant morphs from Indian and Pacific Oceans are almost always identified as *E. aphroditois* (e.g., Lachat and Haag-Wackernagel 2016), which is the only giant species recorded from Australian waters. *Eunice aphroditois* has been reported from East, South and West Australia in habitats such as sand, sponges, coral rubble, and under rocks from intertidal to subtidal (Zanol et al. 2020). Such diversity of habitats and widespread distribution is unexpected for eunicid species and detailed taxonomic reanalyses of widespread eunicid species have shown that multiple species have been confused as one (Iannotta et al. 2007; Lewis and Karageorgopoulos 2008; Glasby and Hutchings 2010; Schulze and Timm 2011; Molina-Acevedo and Carrera-Parra 2015; Zanol et al. 2016; Kara et al. 2020).

In this study, we describe a new species of giant *Eunice* from the subtidal zone of the east Australian coast (Southwest Pacific Ocean).

Materials and methods

Specimens were collected during scuba dives at depths of 1–8 m by attracting an individual worm out of its tube through enticement with crushed pilchard, *Sardinops sagax* (Jenyns, 1842). Once the individual extended far enough out of the tube, it was quickly grabbed from behind the head and pulled out of its tube (see Suppl. material 1). Specific density was calculated during the scuba dive by a visual census of four transects, each 30 × 1 m.

Collected specimens were fixed and preserved in 95% ethanol. Preserved specimens were photographed with a Canon EOS 7D with a Macro EF 100 mm and the Spot Flex CCD 15.2 fitted on a Leica MZ16 Stereo microscope at the Australian Museum. The software Helicon Focus 5.3 was used for focus stacking. Parapodia (4, 15, 45,100, 200, 300, 400, 470) were removed from the holotype and paratype, dehydrated in ethanol, critically point dried, coated with 20 nm of gold, and examined under a JEOL JSM-6480 scanning electron microscope (SEM) at Macquarie University, Sydney. Additional parapodia (3, 80, 160, 240, 300, 380, 460) were removed, mounted in glycerine on a cavity slide and photographed using an Olympus DP 74 fitted on an Olympus Compound Microscope BX53, then the images were processed by Olympus cellSens software.

We describe the holotype and include values of paratype in parentheses. The general format of the description follows Fauchald (1992). Nomenclature used to describe articulation of prostomial appendages and cirri, and shape of chaetal lobe follows Zanol et al. (2014); shape of maxillae I and II follows Molina-Acevedo and Idris (2021); and shape of pectinate chaetae follows Carrera-Parra and Salazar-Vallejo (1998) and Zanol et al. (2016). Measurements of body length start at the anterior end of prostomium, they do not consider the length of prostomial appendages. All material is deposited in the Australian Museum, Sydney. The species is registered in ZooBank under urn:lsid:zoobank.org:act:63BC2367-9654-45DA-8021-FD17584DFFDC.

Results

Family Eunicidae
***Genus* Eunice**

***Eunice dharastii* sp. nov.**
https://zoobank.org/63BC2367-9654-45DA-8021-FD17584DFFDC
Figs 1, 2

Material examined. *Holotype*. Australia • New South Wales, Nelson Bay, Port Stephens Main Beach; 32°42'54.91"S, 152°9'1.12"E; 8 m depth; Aug. 2012; D. Harasti leg.; AM W.53870. ***Paratype*.** Australia • 1 same data as for holotype; AM W.41747.

Comparative material. Australia • 1 incomplete with 80 chaetigers, 120 mm in length and 20 mm maximum width *Eunice* cf. *aphroditois*; New South Wales, Nelson Bay, Port Stephens; AM W.140.

Description. Live specimens: iridescent reddish with lighter patches on prostomium, peristomium, and along the body (Fig. 1A, B). Prostomium appendages, peristomial cirri, and notopodial cirri red to brown, uniformly colored, with lighter areas close to proximal half and at distal ends. Dorsal and ventral buccal lips whitish at distal end, standing out from posterior part of prostomium (Fig. 1B; see Suppl. material 2).

Fixed specimens iridescent brown to purple with lighter patches. Only peristomial cirri and few notopodial cirri retain color pattern of live specimens, prostomial appendages beige (Fig. 1A–C). Specimens are very curled and rigid because of the 95% ethanol fixation, making measurement of length and width difficult.

Holotype incomplete, with 520 chaetigers, in two pieces; first with 300 chaetigers, 200 well preserved + 100 slightly flaccid, and second with 220 chaetigers, all slightly flaccid; total length 980 mm; length through chaetiger 10 20 mm; width at chaetiger 10 without/with parapodia 12/15 mm, maximum width at chaetiger 18 without/with parapodia 18/22 mm, from chaetiger 18 width fairly uniform for following 200 chaetigers. Many parapodia with broken chaetae.

Paratype incomplete with 782 chaetigers in three pieces, first with 250 chaetigers, second with 222, all slightly flaccid, and third with 310 chaetigers; total length 1170 mm; length through chaetiger 10 20 mm; width at chaetiger 10 without/with parapodia 16/19 mm; maximum width at chaetiger 100 without/with parapodia 18/23 mm. Body almost semicircular anteriorly, becoming more flattened around chaetiger 70–80.

Prostomium with dorsal buccal lips as paired median dorsal ridges, obliquely truncate, with thickened lateral margins and median sulcus narrow (Fig. 1B). Dark eyes present outside lateral antennae. Median, lateral antennae and palps reaching back, respectively, to chaetigers 4 (9), 5 (9) and at least until middle of first peristomium ring (3) (antennae and palps are very rigid and difficult to manipulate in holotype; measurements are estimates). Prostomial appendages not evenly spaced, palps isolated by a small gap from lateral antennae; arranged in semicircle, palps partially in front of lateral antennae (Fig. 1B). Ceratophores of median and lateral antennae and palpophores short and ring-shaped. Ceratostyles of median and lateral antennae and palpostyles irregularly articulated; tapering (Fig. 1E). Peristomium cylindrical; separation between first and second rings only visible on dorsal and ventral sides; ventrally second ring much shorter than dorsally (Fig. 1C–E). Dorsally first ring 5/6 of total length of peristomium. Ventrolateral lips muscular and inflated (Fig. 1D). Peristomial cirri reaching a little more anterior than middle of first peristomial ring; irregularly articulated; tapering (Fig. 1C, E).

Maxillary formula 1+1, 7+7, 7+0, 4+7, 1+1, 1+1 (Fig. 2A). Carrier with lateral anterior sclerotized margins almost parallel to each other, abrupt tapering after initial 1/3 of its length. MxI about 2.5 times longer than carrier, lacking a curvature at internal basal edge, with a curvature at outer basal edge, falcal arch extended. MxII with teeth distributed along more than half its length, posterior end wide with distinct thickened outer ridge. MxIII short; part of distal arc with left MxIV and V. MxVI ridge like with a narrow distal tooth. Mandibles calcareous cutting plates with ellipsoid shape (Fig. 2B).

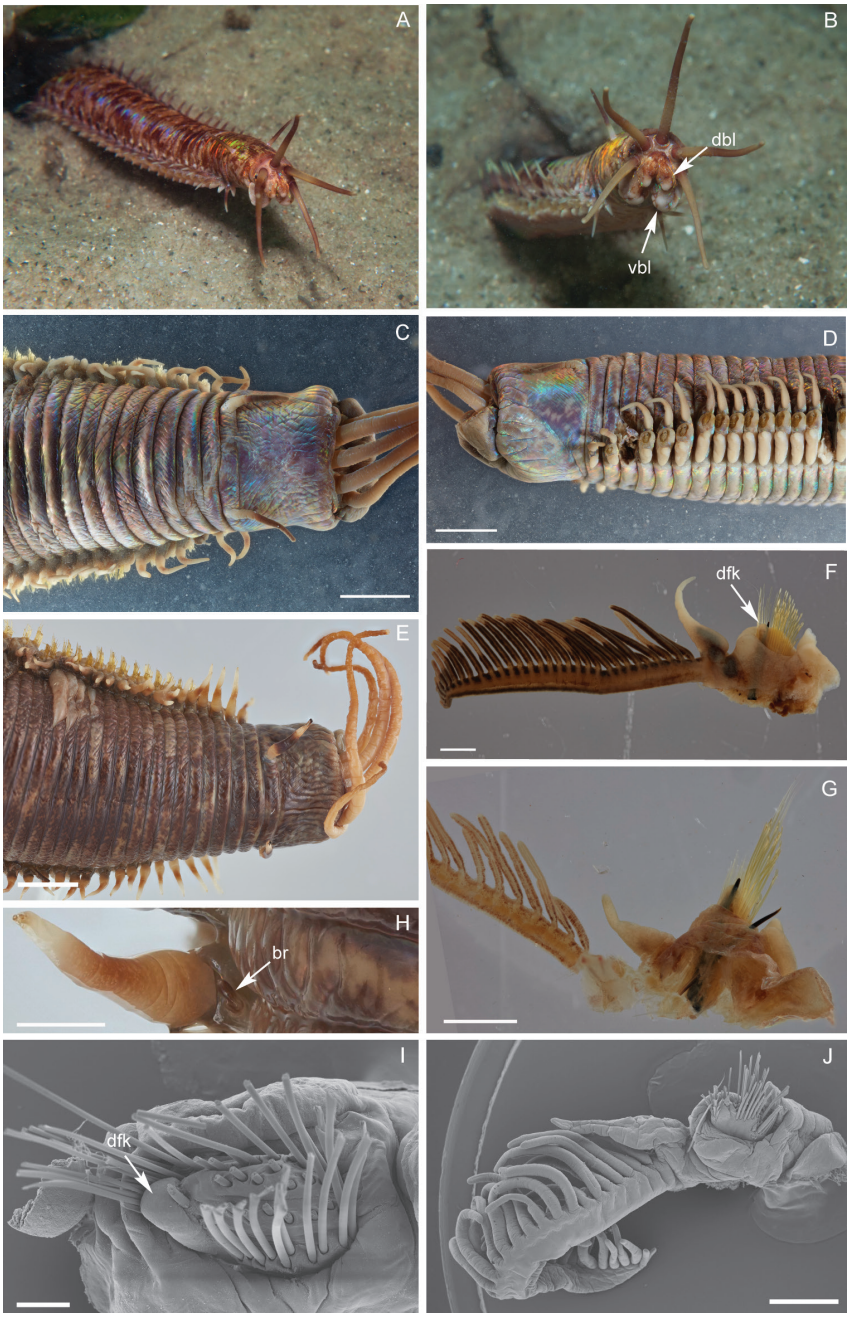

Figure 1. *Eunice dharastii* sp. nov. **A** anterior end of live specimen coming out of its burrow, dorsal view **B** anterior end of live specimen coming out of its burrow, anterior view **C** anterior end, dorsal view **D** anterior end, lateral **E** anterior end, dorsal view **F** parapodia, chaetiger 34, anterior view **G** parapodia from posterior chaetiger of the fragment, anterior view **H** branchiae and notopodial cirrus, chaetiger 10 **I** parapodia, chaetiger 4, upper view **J** parapodia, chaetiger 90, anterior view. br, branchiae; dbl, dorsal buccal lip; dfk, dorsal fleshy knob, vbl, ventral buccal lip. **I, J** scanning electron microscopy. **C, D** holotype AM W.53870 **E–J** paratype AM W.41747. Scale bars: 0.2 mm (**I**); 1 mm (**F, G, H, J**); 5 mm (**C, D, E**).

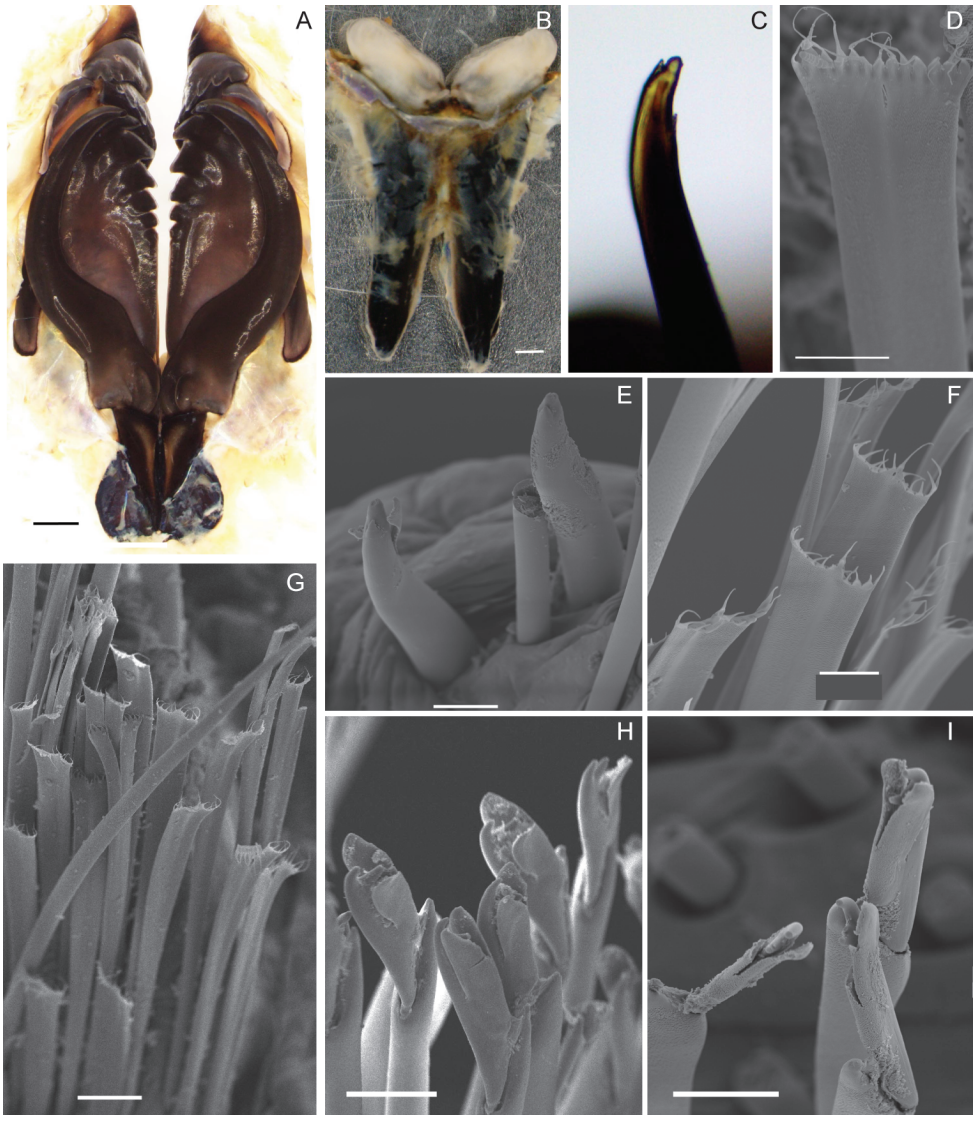

Figure 2. *Eunice dharastii* sp. nov. (paratype AM W.41747) **A** maxillae, dorsal view **B** mandible, ventral view **C** subacicular hook from posterior chaetiger of the fragment **D** pectinate chaeta, chaetiger 200 **E** subacicular hook, chaetiger 300 **F** pectinate chaetae, chaetiger 300 **G** pectinate chaetae, chaetiger 240 **H** falciger chaetae, chaetiger 300 **I** falciger chaetae, chaetiger 4. Scale bars: 20 µm (**D, F**); 50 µm (**C, E, G, H, I**); 1 mm (**A, B**).

Branchiae present from 10 (10) until at least chaetiger 520, end of branchiae not recorded (branchiae ends well before pygidium on chaetiger 492); first with just 1 button-shaped filament around 1/5 of dorsal cirri length (Fig. 1H), around chaetiger 22 as long as notopodial cirri, number of filaments rapidly increasing to 38 (26); best developed branchiae from about chaetiger 40 through subsequent chaetigers with

thick tapering stems, around 2.5 to 4 times longer than longest filament and notopodial cirri (Fig. 1F, J); becoming shorter at end of most posterior fragment (becoming shorter at end of distribution).

Chaetal lobes truncate along whole fragment, posterior increasingly oblique; anterior with dorsal fleshy knob and neuroaciculae emerging posterior to it (Fig. 1F, I); neuroaciculae near dorsal edge in all parapodia. Prechaetal lobe low transverse fold until end of fragment. Postchaetal lobes round/truncate, longer than chaetal lobe at anterior end (Fig. 1D), decreasing along the body, low transverse fold shorter than chaetal lobe by end of fragment. Anteriormost ventral cirri thumb-shaped to tapering, becoming basally inflated from about chaetiger 4 or 5; inflated bases elongate, ridge-like decreasing towards posterior end; free tip round to slightly tapering in all chaetigers, clearly separated from base (Fig. 1D, F). Notopodial cirri pendulous, abrupt tapering from inflated bases, irregularly articulated (Fig. 1D–F, H).

Slender, tapering limbate chaetae longer than all other chaetae present in all chaetigers. Pectinate chaetae thin anodont with flattened shafts; tapering smoothly subdistally or near proximal end along whole fragment (Fig. 2D, F, G). Numbers of teeth variable, 10–14 ($N = 21$, mode = 11); each tooth flattened, distally tapering abruptly to slender hair-like tip; all with similar lengths. Distal ends of compound falciger chaetae shafts a little wider than proximal ends along whole fragment. Appendages of compound falciger chaetae with variable lengths within a chaetal bundle of anterior parapodia, longest in anterior parapodia; shortest appendages of anterior chaetigers as long as appendages in median and posterior chaetigers, all with similar lengths; bidentate with both teeth directed laterally; both teeth about same length in anterior chaetigers, distal tooth much shorter than proximal tooth in median and posterior chaetigers; guards asymmetrically blunt (Fig. 2H, I). Neuroaciculae distinctly dark along all its length, double in most parapodia, some posterior parapodia with single acicula; tapering to blunt or sharp tips (Fig. 1F, G). Subacicular hooks present from chaetiger 58 (53); initially one per parapodium, increasing to two, reaching a maximum of four at chaetiger 81 (85) subsequent parapodia with three or four, most posterior with two; distinct, dark along all its length, with distinct dark core and clear sheath at distal end; bidentate tapering to small head, distal tooth minute, spur-like, proximal tooth much larger, both teeth directed distally (Fig. 2C, E). In both types many chaetae broken.

Posterior end of body and pygidium missing.

Habitat and specific density. Water depth, 1–8 m, in tubes in coarse sand substrates; also occurs in sandy habitats to the west and east of the type locality in same depth range. Average specific density in Nelson Bay main beach 3.5 ± 0.6 individuals per 30 m^2.

Type locality. Nelson Bay Main Beach (32°42'54.91"S, 152°9'1.12"E), Port Stephens, New South Wales, Australia.

Etymology. The species is named in honor of Dr David Harasti, who collected the specimens, donated them to the Australian Museum, and first suspected they were a species new to science.

Remarks. *Eunice dharastii* sp. nov. is most similar to *E. aphroditois*, *E. flavopicta* Izuka, 1912 and *E. kinbergi* Ehlers, 1868 in having the prostomium with dorsal buccal

lips as paired median dorsal ridges; MxVI present; branchiae longer than notopodial cirri, with stem much longer and thicker than filaments; pectinate chaetae thin anodonts with flattened shafts tapering smoothly subdistally or near proximal end; bidentate compound falcigers, dark paired tapering/blunt neuroaciculae and dark bidentate subacicular hooks (Izuka 1912; Fauchald 1992). The unique combination of features that characterizes *Eunice dharastii* sp. nov. and differentiate it from these three species are: irregular articulated prostomial appendages; antennae reaching back beyond chaetiger 4; branchiae starting at chaetiger 10, initially button-shaped; best developed branchiae distinctly longer than notopodial cirri; dorsal fleshy knob on anterior chaetal lobe; notopodial cirri pendulous (sensu Fauchald 1992), abrupt tapering from inflated bases; bidentate compound falciger chaetae with both teeth directed laterally, distal tooth much shorter than proximal tooth in median and posterior chaetigers; and dark bidentate subacicular hooks starting at chaetiger 58, tapering to small head with both teeth directed distally, proximal tooth much larger than minute and spur-like distal tooth (Table 1). The unusual shape of the subacicular teeth is shared only with *E. aphroditois*, *E. borneensis* Grube, 1878 (type locality North Borneo), and *E. mutabilis* Gravier, 1900 (type locality Djibouti; Fauchald 1992). The latter two are clearly distinct from *E. dharastii* sp. nov. in several features, such as the absence of MxVI, shape of branchiae and chaetae.

The examined specimen from Port Stephens identified as *E.* cf. *aphroditois* (Zanol et al. 2020) differs from the new species in the length of the prostomial appendages, median and lateral antennae folding back to chaetiger 1 and palps to the first peristomial ring; and the start of branchiae at chaetiger 11 with five short filaments. Thus, it is here considered a different species. At least three *Eunice* species live in sympatry in the vicinity of the type locality (Port Stephens), *E.* cf. *aphroditois*, *E. impexa* Grube, 1878 (Zanol et al. 2020), and *E. dharastii* sp. nov. Besides *E. aphroditois*, *E. confusus* Zanol, Hutchings & Fauchald, 2020 is the most similar species to *E. dharastii* sp. nov. reported from Australian waters. Nevertheless, they only share a similar shape of the prostomium, peristomium and peristomial cirri, the prostomial appendages are irregularly articulated, maxillary formula (but not shape of plates and carrier), shape of anterior pectinate chaetae and aciculae. Considering previous knowledge on the diversity of morphological features, the observed differences are enough to consider the analyzed specimens a new species to science. Molecular data for this species will be available in a subsequent paper.

Discussion

Here we describe a new *Eunice* species to science, which is at least 1 m long. Despite the large size and the shallow water habitat of some giant *Eunice* species, their diversity is not fully understood. This is due to the wide synonymizing of species, poor understanding of their biology and morphological variation, their concealed habitats, and difficulty in sampling (Fauchald 1992; Parapar and Harto 2001; Salazar-Vallejo et al. 2011; Schulze 2011; Escobar-Ortega et al. 2022).

Table 1. Main morphological features that differentiate *Eunice dharastii* sp. nov. from the closest species.

	***Eunice dharastii* sp. nov.**	***Eunice aphroditois* (Pallas, 1788)**	***Eunice flavopicta* Izuka, 1912**	***Eunice kinbergi* Ehlers, 1868**
Data source	Present description	Fauchald 1992	Izuka 1912; Fauchald 1992	Fauchald 1992
Type locality	Australia, New South Wales Nelson Bay, Port Stephens Main Beach	Sri Lanka	Japan[1]	South Africa, Cape of Good Hope
Irregular articulation of prostomial appendages (antennae and palps)	Present	Absent	Present	Present
Region median and lateral antennae reach when folded back	holotype- chaetiger 4 (M), 5 (L)paratype- chaetiger 9 (M), 9 (L)	posterior end of peristomium (M, L)	chaetiger 2 (M), chaetiger 1 (L)[2]	chaetiger 1 or 4 (M), chaetiger 1 (L)
Branchiae present from chaetiger	10	6	5[2]	8–9
Length of best developed branchiae in relation to notopodial cirri	Distinctly longer	Distinctly longer	Distinctly longer	About as long as
Dorsal fleshy knob on anterior chaetal lobe	Present	Absent	Absent	Absent
Shape of notopodial cirri	Pendulous (sensu Fauchald 1992); abrupt tapering from inflated bases	Smooth tapering from inflated bases	Pendulous (sensu Fauchald 1992); smooth tapering from with inflated bases	Smooth tapering from slightly inflated bases
Direction of teeth of compound chaetae	Both directed laterally	Not described	Proximal directed laterally, distal directed distally	Both directed laterally
Relative length of distal and proximal teeth of compound chaetae	Anterior both similar in length, median and posterior distal tooth much shorted than proximal tooth	Not described	Distal tooth shorter than proximal tooth[3], variation not described	Both similar in length or distal tooth longer than proximal tooth
Shape of the distal end and direction of teeth of the subacicular hook	Tapering to small head with both teeth directed distally	Tapering to small head with both teeth directed distally	Head bent with both teeth directed laterally	Distinct head with proximal tooth directed laterally, distal tooth directed distally
Shape and relative size of proximal and distal teeth of subacicular hook	Proximal tooth distally blunt, distal tooth minute spur-like, much smaller than proximal tooth	Both teeth distally blunt, distal tooth smaller than proximal tooth	Both teeth triangular, distal tooth much smaller than proximal tooth	Both teeth triangular, distal tooth smaller than proximal tooth
Subacicular hook present from chaetiger, distribution	53 or 58, uniform present in all chaetigers thereafter	200, scattered missing in several chaetigers thereafter	Not described	123, scattered missing in several chaetigers thereafter

[1]The original description contains two localities in Japan: Misaki in Sagami Province (currently Kanagawa Prefecture) and Ushibuka in Higo Province (currently Kumamoto Prefecture) (Izuka 1912). [2]Numbers differ from those in Izuka (1912), because he considered peristomial rings as two segments. [3]Izuka (1912) described denticles between proximal and distal teeth. In the illustration (Plate XIV, fig. 4 in Izuka 1912), these denticles appear to be the distal end of the guards. The presence of these denticles needs to be revised. M, median antenna. L, lateral antennae.

Specimens from Australia identified and described as *E. aphroditois* (Ehlers 1868; McIntosh 1885; Augener 1913; Fauvel 1917; Monro 1931) assume a high intraspecific diversity and may in fact represent more than one species (Fauchald 1992; Salazar-Vallejo et al. 2011). Despite the diversity found in these descriptions, they all contrast from *E. dharastii* sp. nov. in the shape of the chaetae and, in some cases, in the start of branchiae (e.g., McIntosh 1885). However, we cannot rule out that at least some of the previous records of *E. aphroditois* from Australian waters are in fact *E. dharastii* sp.

nov. and that online photographs of the species may have been available prior to this description (e.g., Salazar-Vallejo et al. 2011). The name *E. aphroditois* may, therefore, have obscured other undescribed species.

However, the large variation in size may lead to the identification of one species as belonging to several species. Giant species are described from large specimens, but which were once small during earlier life stages (Pruvot and Racovitza 1895; Schulze 2011). Thus, the identification of giant specimens should also include comparisons with species described from smaller specimens bearing in mind that some features vary with size. Subacicular hooks tend to appear for the first time in more posterior chaetigers and to be irregularly distributed in giant species (Fauchald 1992), which is probably due to a progressive loss with size increase (Miura 1977). Maximum number of branchial filaments tend to increase with size (Parapar and Harto 2001). On the other hand, the shape of prostomium and dorsal buccal lips, branchiae with more than 10 filaments where best developed, a type A pattern of branchial distribution (sensu Miura 1986), the dark color of aciculae and subacicular hooks all appear to be useful in recognizing similar species within this group of *Eunice* despite their size. By contrast, for the identification of species, it appears to be more informative to consider the relative length of prostomial appendages, morphology of the jaws, shape of ventral cirri, start of branchiae, shape and relative size (length and width) of branchial stem and filaments, shape and relative size of notopodial cirri, and shape and variation along the body of compound falciger chaetae, pectinate chaetae, and teeth of bidentate subacicular hooks, fewer features than those suggested by Pruvot and Racovitza (1895). The consideration of the shape of pectinate chaetae and its variation along the body in the diagnosis of species of the eunicid genera such as *Marphysa* have improved the identification and differentiation of species (e.g., Martin et al. 2020).

Despite the large size of giant species, they are concealed in deep burrows from which the anterior end emerges for feeding. Other than by dredging, regular substrate sampling is unlikely to sample them. They can rapidly retreat back into their extensive burrow when sensing any vibration. Many of the reports of these large species come from dredged samples (e.g., McIntosh 1885), washed up specimens (e.g., Pruvot and Racovitza 1895), or hand-collected specimens (not an easy task; Escobar-Ortega et al. 2022), usually, from places with high numbers of scuba divers or where giant species are used as bait (e.g., Bettoso et al. 1998). Thus, we can expect that the diversity of giant species is underestimated and that even places where the *Eunice* fauna is relatively well studied hide new giant species. Knowledge of these large species will aid to improve our understanding of their diversity, morphological variation, and evolution of body size in Eunicidae.

Acknowledgements

We are thankful to Dr David Harasti for calculating specific density, collecting the specimens, and donating them to the Australian Museum; Sue Lindsay for making SEM and light micrographs possible; Dr Hannelore Paxton for the dissection of the

jaws; Dr Carol Simon, Dr Julio Parapar, and Dr Chris Glasby for their valuable suggestions. Funding to JZ came from FAPERJ (proc. E-26/201.329/2021 and proc. E-26/010.002252/2019).

References

Augener H (1913) IV Die Fauna südwest-australiens. Ergebnisse der Hamburger südwest-australischen Forschungsreise 1905 herausgegeben von Prof. Dr. W. Michaelsen und Dr. R. Hartmeyer. Polychaeta I, Errantia. Verlag von Gustva Fischer, Jena, 302 pp.

Bettoso N, Faverio G, Orel G (1998) Note sulla biologia e sulla pesca del verme de rimini (*Eunice aphroditois* Pallas) in alto Adriatico. Hydrores 16: 24–34.

Carrera-Parra LF, Salazar-Vallejo SI (1998) A new genus and 12 new species of Eunicidae (Polychaeta) from the Caribbean Sea. Journal of the Marine Biological Association of the United Kingdom 78(1): 145–182. https://doi.org/10.1017/S0025315400040005

Ehlers E (1868) Die Borstenwürmer (Annelida Chaetopoda) nach systematischen und anatomischen Untersuchungen dargestellt. Volume II. Wilhelm Engelmann, Leipzig, 748 pp.

Escobar-Ortega D, Fernández N, Muíño R, Parapar J, Bettoso N, Couceiro L (2022) On the presence of a giant bristle worm (*Eunice roussaei*) in NW Iberian Peninsula: Comments on its taxonomy and reproductive cycle. Estuarine, Coastal and Shelf Science 274: 107899. https://doi.org/10.1016/j.ecss.2022.107899

Fauchald K (1992) A review of the genus *Eunice* (Eunicidae: Polychaeta) based upon type material. Smithsonian Contributions to Zoology 523: 1–422. https://doi.org/10.5479/si.00810282.523

Fauvel P (1917) Annélides polychètes de l'Australie meridionale. Archives de Zoologie Expérimentale et Générale 56: 159–277.

Fauvel P (1932) Annelida Polychaeta of the Indian Museum, Calcutta. Memoirs of the Indian Museum 12: 1–262.

Glasby CJ, Hutchings PA (2010) A new species of *Marphysa* Quatrefages, 1865 (Polychaeta: Eunicida: Eunicidae) from northern Australia and a review of similar taxa from the Indo-west Pacific, including the genus *Nauphanta* Kinberg, 1865. Zootaxa 2352(1): 29–45. https://doi.org/10.11646/zootaxa.2352.1.2

Iannotta MA, Patti FP, Ambrosino M, Procaccini G, Gambi M (2007) Phylogeography of two species of *Lysidice* (Polychaeta, Eunicidae) associated to the seagrass *Posidonia oceanica* in the Mediterranean Sea. Marine Biology 150(6): 1115–1126. https://doi.org/10.1007/s00227-006-0405-2

Izuka A (1912) The errantia Polychaeta of Japan. Journal of the College of Science. Imperial University of Tokyo 30: 1–262.

Kara J, Molina-Acevedo IC, Zanol J, Simon C, Idris I (2020) Morphological and molecular systematic review of *Marphysa* Quatrefages, 1865 (Annelida: Eunicidae) species from South Africa. PeerJ 8: e10076. https://doi.org/10.7717/peerj.10076

Lachat J, Haag-Wackernagel D (2016) Novel mobbing strategies of a fish population against a sessile annelid predator. Scientific Reports 6(1): e33187. https://doi.org/10.1038/srep33187

Lewis C, Karageorgopoulos P (2008) A new species of *Marphysa* (Eunicidae) from the western Cape of South Africa. Journal of the Marine Biological Association of the United Kingdom 88(2): 277–287. https://doi.org/10.1017/S002531540800009X

Martin D, Gil J, Zanol J, Meca MA, Pérez Portela R (2020) Digging the diversity of Iberian bait worms *Marphysa* (Annelida, Eunicidae). Rubal García M (Ed.) PLoS ONE 15: e0226749. https://doi.org/10.1371/journal.pone.0226749

McIntosh WC (1885) Report on the Annelida Polychaeta collected by H.M.S. *Challenger* during the years 1873–1876. Report on the Scientific Results of the Voyage of H.M.S. *Challenger* during the years 1872–76 12: 1–554.

Miura T (1977) Eunicid polychaetous annelids from Japan – I. La Mer (Bulletin de la Société Franco-Japonaise d'Océanographie) 15: 1–20.

Miura T (1986) Japanese polychaetes of the genera *Eunice* and *Euniphysa*: Taxonomy and branchial distribution patterns. Publications of the Seto Marine Biological Laboratory 31(3–6): 269–325. https://doi.org/10.5134/176125

Molina-Acevedo IC, Carrera-Parra LF (2015) Reinstatement of three species of the *Marphysa sanguinea* complex (Polychaeta: Eunicidae) from the Grand Caribbean Region. Zootaxa 3925(1): 37–55. https://doi.org/10.11646/zootaxa.3925.1.3

Molina-Acevedo IC, Idris I (2021) Revision of abranchiate species of *Marphysa* de Quatrefages, 1865 and their transference to *Nicidion* Kinberg, 1865 (Eunicidae: Annelida) with redescription of the type species *N. cincta* Kinberg, 1865. Marine Biodiversity 51(2): 30. https://doi.org/10.1007/s12526-020-01157-6

Monro CCA (1931) Polychaeta, Oligochaeta, Echiuroidea and Sipunculoidea. Scientific Reports of the Great Barrier Reef Expedition British Museum Natural History 4: 1–37.

Parapar J, Harto I (2001) On the presence in the Iberian waters and morphological variability in *Eunice roussaei* Quatrefages, 1866 (Polychaeta, Eunicidae). Boletin de la Real Sociedad Espanola de Historia Natural. Seccion Biologica 96: 165–174.

Pruvot G, Racovitza ÉG (1895) Matériaux pour la faune des annélides de Banyuls. Archives de Zoologie Expérimentale et Générale 3: 339–342.

Read G, Fauchald K [Eds] (2021) World Polychaeta Database. *Eunice* Cuvier, 1817. http://marinespecies.org/polychaeta/aphia.php?p=taxdetails&id=129278 [Accessed on 2022-06-22]

Salazar-Vallejo SI, Carrera-Parra LF, de León-González JA (2011) Giant eunicid Polychaetes (Annelida) in shallow tropical and temperate seas. Revista de Biología Tropical 59: 1463–1474. https://doi.org/10.15517/rbt.v59i4.3411

Schulze A (2011) The bobbit worm dilemma: A case for DNA. Revista de Biología Tropical 59: 1475–1477. https://orcid.org/10.15517/rbt.v59i4.3411

Schulze A, Timm LE (2011) Palolo and *un*: distinct clades in the genus *Palola* (Eunicidae: Polychaeta). Marine Biodiversity 42(2): 161–171. https://doi.org/10.1007/s12526-011-0100-5

Zanol J, Bettoso N (2006) Identity of *Eunice roussaei* (Eunicidae: Polychaeta: Annelida) from the Adriatic and Mediterranean Seas. Journal of the Marine Biological Association of the United Kingdom 86(5): 1017–1024. https://doi.org/10.1017/S0025315406013993

Zanol J, Budaeva N (2021) Eunicidae. In: Purschke G, Westheide W, Böggemann M (Eds) Handbook of Zoology Annelida, Volume 3: Sedentaria III, Errantia I. De Gruyter, Berlin–Boston, 414–452. https://doi.org/10.1515/9783110291704

Zanol J, Halanych KM, Fauchald K (2014) Reconciling taxonomy and phylogeny in the bristleworm family Eunicidae (polychaete, Annelida). Zoologica Scripta 43(1): 79–100. https://doi.org/10.1111/zsc.12034

Zanol J, da Silva TSC, Hutchings P (2016) *Marphysa* (Eunicidae, polychaete, Annelida) species of the Sanguinea group from Australia, with comments on pseudo-cryptic species. Invertebrate Biology 135(4): 328–344. https://doi.org/10.1111/ivb.12146

Zanol J, Hutchings PA, Fauchald K (2020) *Eunice sensu lato* (Annelida: Eunicidae) from Australia: Description of seven new species and comments on previously reported species of the genera *Eunice*, *Leodice* and *Nicidion*. Zootaxa 4748: 1–43. https://doi.org/10.11646/zootaxa.4748.1.1

Zanol J, Carrera-Parra LF, Steiner TM, Amaral ACZ, Wiklund H, Ravara A, Budaeva N (2021) The current state of Eunicida (Annelida) systematics and biodiversity. Diversity 13(2): 74. https://doi.org/10.3390/d13020074

Supplementary material 1

Video S1

Author: David Harastii

Data type: Video file.

Explanation note: Attempt to catch a specimen of *E. dharastii* sp. nov.

Link: https://doi.org/10.3897/zookeys.1118.86448.suppl1

Supplementary material 2

Video S2

Author: David Harastii

Data type: Video file.

Explanation note: Anterior end of *E. dharastii* sp. nov. live specimen coming out of burrow.

Link: https://doi.org/10.3897/zookeys.1118.86448.suppl2

ZooKeys 1118: 111–118 (2022)
doi: 10.3897/zookeys.1118.84686
https://zookeys.pensoft.net

CHECKLIST

A peer-reviewed open-access journal
ZooKeys
Launched to accelerate biodiversity research

A checklist of black flies (Diptera, Simuliidae) from India

Arka Mukherjee[1], Atanu Naskar[1], Oishik Kar[1], Debdeep Pramanik[1], Dhriti Banerjee[1]

1 *Zoological Survey of India, Prani Vigyan Bhawan, M-Block, New Alipore, Kolkata, 700053, West Bengal, India*

Corresponding author: Atanu Naskar (atanu.diptera@gmail.com)

Academic editor: Fabio Laurindo da Silva | Received 31 March 2022 | Accepted 18 June 2022 | Published 24 August 2022

https://zoobank.org/8A0DE6D0-FC3A-4D09-93FA-ACFCE27890D6

Citation: Mukherjee A, Naskar A, Kar O, Pramanik D, Banerjee D (2022) A checklist of black flies (Diptera, Simuliidae) from India. ZooKeys 1118: 111–118. https://doi.org/10.3897/zookeys.1118.84686

Abstract

An updated checklist of the family Simuliidae from India is presented. A total of 79 species of *Simulium* belonging to eight different subgenera are listed. Eleven species that were not reported in the previous checklist are added here. The present list contributes to a better understanding of the diversity of Simuliidae in India, as well as the impact of *Simulium* species on the public health of this mega-diverse country.

Keywords

Diversity, inventory, onchocerciasis, public health

Introduction

Black flies (Diptera, Nematocera, Simuliidae) are infamous as vectors for transmitting onchocerciasis (river blindness) in many countries throughout the world (Datta 1997). However, in India, onchocerciasis is still not a serious concern despite some sporadic cases in North-east India (Barua et al. 2011). The total number of simuliid species throughout the world is estimated to be 2,415, of which 2,398 species are living and 17 are fossil species (Adler 2022). An inventory of world Simuliidae was first published by Crosskey (1988) and has since been updated almost every year. The beginning of simuliid research was in the early 19th century when Latreille (1802) described *Simulium* Latreille, 1802. The family Simuliidae Newman, 1834 was established by Newman (1834) with the inclusion of only the genus *Simulium*. According to Mitra et al. (2017), the first description of *Simulium* from India was probably by Becher (1885), and since then, researchers have described new species of simuliids

from the country (Brunetti 1911; Senior-White 1922a, 1922b; Edwards 1927; Puri 1932a, 1932b, 1932c, 1932d, 1932e, 1933a, 1933b, 1933c). In the second half of the 20th century, the simuliid research was mainly undertaken by Datta (1973, 1974a, 1974b, 1975, 1978, 1980, 1983, 1985, 1992a, 1992b, 1997). He extensively studied the Indian simuliid fauna, described several new species of *Simulium*, and provided new distributional records. His review of the family in the Oriental realm (Datta 1983) is an exceptional piece of work in its understanding of the biology of black flies. Datta and Pal (1975); Datta et al. (1975) described a few additional rare species of the subgenus *Simulium*, especially from the Darjeeling area of West Bengal state, and provided taxonomic identification keys to simuliid species found in that region. Later, in the 21st century, several researchers discovered many new species (Mitra et al. 2006; Takaoka and Somboon 2008; Shrestha and Takaoka 2009; Mitra and Sharma 2010; Takaoka et al. 2010, 2011; Henry et al. 2011; Borah et al. 2012; Dutta Saha et al. 2012; Anbalagan et al. 2014, 2015a, 2015b). The first checklist of Simuliidae of India was published by Mitra et al. (2017). The most recent publications are by Anbalagan et al. (2020a, 2020b) in which they described three new species of the *Simulium*—two in the subgenus *Gomphostilbia* and one in the subgenus *Nevermannia*.

The present work documents 79 species of Simuliidae belonging to eight subgenera of *Simulium*, based on a review of the World Catalog of Simuliidae (Adler 2022) and other literature. The binomial names are based on the valid nomenclature of Systema Dipterorum (Evenhuis and Pape 2022). Eleven species have been added here to those species already included in the earlier checklist of Indian Simuliidae by Mitra et al. (2017). The inclusion of these previously unreported species will help us to better understand the taxonomy and diversity of the black flies in India. It will also lead to the assessment of the newly reported species as potential vectors of onchocerciasis in India.

Results

Order Diptera Linnaeus, 1758
Infraorder Culicomorpha Hennig, 1948
Superfamily Chironomoidea Newman, 1834
Family Simuliidae Newman, 1834
Subfamily Simulinae Newman, 1834
Tribe Simuliini Newman, 1834
Genus *Simulium* Latreille, 1802

Subgenus *Eusimulium* Roubaud, 1906

1. *Simulium* (*Eusimulium*) *aureum* Fries, 1824
2. *Simulium* (*Eusimulium*) *weiningense* Chen & Zhang, 1997

Subgenus *Gomphostilbia* Enderlein, 1973

3. *Simulium* (*Gomphostilbia*) *bucolicum* Datta, 1975

4. *Simulium* (*Gomphostilbia*) *darjeelingense* Datta, 1973
5. *Simulium* (*Gomphostilbia*) *fidum* Datta, 1975
6. *Simulium* (*Gomphostilbia*) *litoreum* Datta, 1975
7. *Simulium* (*Gomphostilbia*) *metatarsale* Brunetti, 1911
8. *Simulium* (*Gomphostilbia*) *pattoni* Senior-White, 1922
9. *Simulium* (*Gomphostilbia*) *sundaicum* Edwards, 1934
10. *Simulium* (*Gomphostilbia*) *tenuistylum* Datta, 1973
11. *Simulium* (*Gomphostilbia*) *unum* Datta, 1975
    In the revised inventory of Adler (2022), this species was documented from Java (Indonesia) and Malaysia. However, Datta (1991) reported its occurrence in the Bankura and Purulia districts (23°14'28.7"N, 87°3'42.6"E and 23°19'57.1"N, 86°21'46.8"E) in West Bengal, India. It was not included in Mitra et al.'s (2017) checklist.
12. *Simulium* (*Gomphostilbia*) *agasthyamalaiense* Vijayan, Anbalagan, Rekha, Dinakaran & Krishnan, 2019
    This species was described by Vijayan et al. (2019) from reared pupa collected in Agasthyamalai Biosphere Reserve, Tamil Nadu (8°55'4.1"N, 77°36'1.6"E), India.
13. *Simulium* (*Gomphostilbia*) *barnesi* Takaoka & Suzuki, 1984
14. *Simulium* (*Gomphostilbia*) *cauveryense* Anbalagan, 2015
15. *Simulium* (*Gomphostilbia*) *decuplum* Takaoka & Davies, 1995
16. *Simulium* (*Gomphostilbia*) *dinakarani* Anbalagan, 2020
    This species was described by Anbalagan et al. (2020a) and occurs in Tamil Nadu (10°27'30.7"N, 78°01'15.7"E), India.
17. *Simulium* (*Gomphostilbia*) *kottoorense* Anbalagan, 2015
18. *Simulium* (*Gomphostilbia*) *krishnani* Anbalagan, 2020
    This species was reported from Karnataka (14°58'36"N, 74°46'40"E), India, by Anbalagan et al. (2020a).
19. *Simulium* (*Gomphostilbia*) *kumbakkaraiense* Anbalagan, 2019
20. *Simulium* (*Gomphostilbia*) *panagudiense* Anbalagan 2015
    This species was recently described by Anbalagan et al. (2019) with distributional records in Tamil Nadu (10°18'30.3"N, 77°53'35.8"E), India.
21. *Simulium* (*Gomphostilbia*) *parahiyangum* Takaoka & Sigit, 1992
22. *Simulium*(*Gomphostilbia*) *peteri* Anbalagan, 2014
23. *Simulium* (*Gomphostilbia*) *sachini* Takaoka & Henry, 2010
24. *Simulium* (*Gomphostilbia*) *takaokai* Anbalagan, 2014
25. *Simulium* (*Gomphostilbia*) *williei* Takaoka & Thapa, 2010

Subgenus *Montisimulium* Rubstov, 1974

26. *Simulium* (*Montisimulium*) *dasguptai* Datta, 1974
27. *Simulium* (*Montisimulium*) *dattai* Takaoka & Somboon, 2008
28. *Simulium* (*Montisimulium*) *ghoomense* Dutta, 1973
29. *Simulium* (*Montisimulium*) *nemorivagum* Datta, 1973
30. *Simulium* (*Montisimulium*) *yuntaiense* Chen, Wen & Wei, 2006

Subgenus *Nevermannia* Enderlein, 1921

31. *Simulium* (*Nevermannia*) *aureohirtum* Brunetti, 1911
32. *Simulium* (*Nevermannia*) *gracilis* Datta, 1973
33. *Simulium* (*Nevermannia*) *karavalliense* Anbalagan, Rekha, Vijayan, Balachandran, Dinakaran & Krishnan, 2020
    This species was reared from pupae collected in Tamil Nadu (11°20'03.8"N, 78°19'19.6"E), India and described by Anbalagan et al. (2020b).
34. *Simulium* (*Nevermannia*) *praelargum* Datta, 1973
35. *Simulium* (*Nevermannia*) *purii* Datta, 1973
36. *Simulium* (*Nevermannia*) *rufithorax* Brunetti, 1911
37. *Simulium* (*Nevermannia*) *senile* Brunetti, 1911
38. *Simulium* (*Nevermannia*) *subratai* Takaoka, Thapa & Henry, 2011
39. *Simulium* (*Nevermannia*) *wichaii* Takaoka, 2010

Subgenus *Tetisimulium* Rubtsov, 1960

40. *Simulium* (*Tetisimulium*) *stevensoni* Edwards, 1927

Subgenus *Himalayum* Lewis, 1973

41. *Simulium* (*Himalayum*) *indicum* Becher, 1885

Subgenus *Simulium* Latreillie, 1802

42. *Simulium* (*Simulium*) *alajense* Rubtsov, 1938
43. *Simulium* (*Simulium*) *asishi* Datta, 1985
44. *Simulium* (*Simulium*) *adventicium* Datta, 1985
45. *Simulium* (*Simulium*) *barraudi* Puri, 1932
46. *Simulium* (*Simulium*) *biforaminiferum* Datta, 1974
47. *Simulium* (*Simulium*) *consimile* Puri, 1932
48. *Simulium* (*Simulium*) *christophersi* Puri, 1932
49. *Simulium* (*Simulium*) *dentatum* Puri, 1932
50. *Simulium* (*Simulium*) *digitatum* Puri, 1932
51. *Simulium* (*Simulium*) *ephemerophilum* Rubstov, 1947
52. *Simulium* (*Simulium*) *gravelyi* Puri, 1933
53. *Simulium* (*Simulium*) *griseifrons* Brunetti, 1911
54. *Simulium* (*Simulium*) *grisescens* Brunetti, 1911
55. *Simulium* (*Simulium*) *gurneyae* Senior-White, 1922
56. *Simulium* (*Simulium*) *himalayense* Puri, 1932
57. *Simulium* (*Simulium*) *hirtipannus* Puri, 1932
58. *Simulium* (*Simulium*) *howletti* Puri, 1932
59. *Simulium* (*Simulium*) *kapuri* Datta, 1975

60. *Simulium* (*Simulium*) *lineothorax* Puri, 1932
61. *Simulium* (*Simulium*) *nigrifacies* Datta, 1974
62. *Simulium* (*Simulium*) *nilgiricum* Puri, 1932
63. *Simulium* (*Simulium*) *nitidithorax* Puri, 1932
64. *Simulium* (*Simulium*) *novolineatum* Puri, 1933
65. *Simulium* (*Simulium*) *nodosum* Puri, 1933
66. *Simulium* (*Simulium*) *pallidum* Puri, 1932
67. *Simulium* (*Simulium*) *palmatum* Puri, 1932
68. *Simulium* (*Simulium*) *palniense* Puri, 1932
69. *Simulium* (*Simulium*) *pradyai* Takaoka & Somboon, 2008
70. *Simulium* (*Simulium*) *pothigaiense* Anbalagan, 2018
71. *Simulium* (*Simulium*) *ramosum* Puri, 1932
72. *Simulium* (*Simulium*) *rashidi* Lewis, 1973
73. *Simulium* (*Simulium*) *rufibasis* Brunetti, 1911
74. *Simulium* (*Simulium*) *singtamense* Datta & Pal, 1975
75. *Simulium* (*Simulium*) *striatum* Brunetti, 1912
76. *Simulium* (*Simulium*) *tenuitarsus* Puri, 1933
77. *Simulium* (*Simulium*) *valparaiense* Anbalagan, 2018
78. *Simulium* (*Simulium*) *yanaense* Anbalagan, 2019
    This species was described from Karnataka (14°31'19.2"N, 74°19'12"E), India by Anbalagan et al. (2019).

Subgenus *Wilhelmia* Enderlein, 1921

79. *Simulium* (*Wilhelmia*) *pseudequinum* Séguy, 1921

References

Adler PH (2022) World blackflies (Diptera: Simuliidae): a comprehensive revision of the taxonomic and geographical inventory [2022]. Inventory Revision, South Carolina. https://biomia.sites.clemson.edu/pdfs/blackflyinventory.pdf [Accessed on: 2022-4-5]

Anbalagan S, Prasanna VA, Dinakaran S, Krishnan M (2014) Two new species of *Simulium* (*Gomphostilbia*) (Diptera: Simuliidae) from Peninsular India with keys to Peninsular Indian members of the genus *Simulium*. Zootaxa 3861(5): 451–465. https://doi.org/10.11646/zootaxa.3861.5.3

Anbalagan S, Arunprasanna V, Kannan M, Dinakaran S, Krishnan M (2015a) *Simulium* (*Gomphostilbia*) (Diptera: Simuliidae) from Southern Western Ghats, India: two new species and DNA barcoding. Acta Tropica 149: 94–105. https://doi.org/10.1016/j.actatropica.2015.05.015

Anbalagan S, Balachandran C, Arunprasanna V, Kannan M, Dinakaran S, Krishnan M (2015b) A new species of *Simulium* (*Gomphostilbia*) (Diptera: Simuliidae) from South India, with keys to Indian members of the subgenus Gomphostilbia. Zootaxa 3974(4): 555–563. https://doi.org/10.11646/zootaxa.3974.4.6

Anbalagan S, Vijayan S, Balachandran C, Dinakaran S (2019) A new species of *Simulium* (*Simulium*) (Diptera: Simuliidae), with keys to S. striatum species-group from India. Journal of Threatened Taxa 11(5): 13573–13578. https://doi.org/10.11609/jott.4318.11.5.13573-13578

Anbalagan S, Vijayan S, Balachandran C, Thiyonila B, Surya A (2020a) Two new species of *Simulium* (*Gomphostilbia*) (Diptera: Simuliidae) from South India. Zootaxa 4742(1): 57–72. https://doi.org/10.11646/zootaxa.4742.1.3

Anbalagan S, Rekha K, Vijayan S, Balachandran C, Dinakaran S, Krishnan M (2020b) A new black fly species of *Simulium* (*Nevermannia*) (Simuliidae: Diptera) from the Southern Eastern Ghats, India. Zootaxa 4768(3): 374–382. https://doi.org/10.11646/zootaxa.4768.3.4

Barua P, Sharma A, Hazarika NK, Barua N, Bhuyan S, Alam ST (2011) A rare case of ocular onchocerciasis in India. The Southeast Asian Journal of Tropical Medicine and Public Health 42(6): 1359–1364.

Becher E (1885) A new species of *Simulium* from Assam. Journal of the Asiatic Society of Bengal 53(2): 199–200.

Borah S, Rahman I, Goswami S, Deka M, Takaoka H (2012) Notes on black flies (Diptera: Simuliidae) from North-East India: new records of five species from Arunachal Pradesh and Roubaud and *Gomphostilbia* Enderlein from the Darjeeling area, India. Oriental Insects 7(3): 363–401. https://doi.org/10.1080/00305316.1973.10434099

Datta M (1974a) Some black flies (Diptera: Simuliidae) of the subgenus *Simulium* Latreille (s. str.) from the Darjeeling area (India). Oriental Insects 8(1): 15–27. https://doi.org/10.1080/00305316.1974.10434435

Datta M (1974b) New species of black flies (Diptera: Simuliidae) from the Darjeeling area, India. Oriental Insects 8(4): 457–468. https://doi.org/10.1080/00305316.1974.10434877

Datta M (1975) Simuliidae (Diptera) from Assam foot-hills, India. Japanese Journal of Sanitary Zoology 26(1): 31–40. https://doi.org/10.7601/mez.26.31

Datta M (1978) Simuliidae (Diptera) from Sikkim, India. Bulletin of the Zoological Survey of India 1(3): 253–256.

Datta M (1980) Collection and preservation of blackflies (Diptera: Simuliidae). In: Proceedings of the Workshop on Techniques in Parasitology, Zoological Survey of India 75–82.

Datta M (1983) A review of Simuliidae (Diptera) from the Oriental Region. Oriental Insects 17(1): 215–267. https://doi.org/10.1080/00305316.1983.10433696

Datta M (1985) Notes on black flies (Diptera: Simuliidae) from Kashmir, India. Bulletin of the Zoological Survey of India 7(2–3): 231–236.

Datta M (1991) Occurence of blackflies in Bankura and Purulia districts in West Bengal, India (Diptera: Simuliidae). Journal of Bengal Natural History Society 10(1): 11–15.

Datta M (1992a) An overview of the Simuliidae (Diptera) of West Bengal, India. Journal of Bengal Natural History Society 11: 41–62.

Datta M (1992b) Contribution to the knowledge on the black fly fauna (Diptera: Simuliidae) of Himachal Pradesh, India. Proceedings of the Zoological Society, Calcutta 45(1): 39–52.

Datta M (1997) Insecta: Diptera: Simuliidae. In: Zoological Survey of India, Fauna of West Bengal, State Fauna Series 3(7): 127–162.

Datta M, Pal TK (1975) Few rare black fly species (Diptera: Simuliidae) of the subgenus *Latreille* (s. str.) from the Darjiling area. Proceedings of the Indian Academy of Sciences (B) 81(4): 154–161. https://doi.org/10.1007/BF03050757

Datta M, Dey RK, Pal AK, Pal TK (1975) Ecology of the black flies in (Diptera: Simuliidae) in Darjeeling area. Proceedings of the Indian Academy of Sciences (B) 81(1): 7–19. https://doi.org/10.1007/BF03050742

Dutta Saha P, Sharma RM, Mitra B (2012) Insecta: Diptera. In: Zoological Survey of India, Fauna of Maharashtra, State Fauna Series 20: 531–538.

Edwards FW (1927) Two new *Simulium* from Kashmir. Bulletin of Entomological Research 18(2): 169–170. https://doi.org/10.1017/S0007485300019866

Evenhuis NL, Pape T [Eds] (2022) Systema Dipterorum, Version (3.6). http://diptera.org/ [Accessed on: 2022-4-5]

Henry W, Thapa S, Adler PH, Dey SK, Varma R (2011) Cytotaxonomy of *Simulium* (*Montisimulium*) *ghoomense* (Diptera: Simuliidae) from the Darjeeling Hills, India. Zootaxa 2872(1): 49–57. https://doi.org/10.11646/zootaxa.2872.1.4

Latreille PA (1802) Histoire naturelle: générale et particulière des crustacés et des insectes. Tome troisième. Dufart, Paris, [i–xii +] 13–467 [+ 1 pp]. https://doi.org/10.5962/bhl.title.15764

Mitra B, Sharma RM (2010) Checklist of Indian Black flies (Insecta: Diptera: Simuliidae). Zoological survey of India. https://www.zsi.gov.in/WriteReadData/userfiles/file/Checklist/blackflies.pdf

Mitra B, Lahiri AR, Mukherjee M (2006) Insecta: Diptera: Nematocera. In: Zoological Survey of India, Fauna of Arunachal Pradesh, State Fauna Series 13(2): 225–255.

Mitra B, Roy S, Roy S, Halder S, Chattopadhyay U, Bhaumik S (2017) A current status on diversity and distribution of black flies (Insecta: Diptera: Simuliidae) in India. Ambient Science 4(1): 21–26. https://doi.org/10.21276/ambi.2017.04.1.rv01

Newman E (1834) Attempted division of British insects into natural orders. The Entomological Magazine 2: 379–431.

Puri IM (1932a) Studies on Indian Simuliidae. Part-I. *Simulium himalayense* sp. n.; *Simulium gurneyae* Senior-White; and *Simulium nilgiricum* sp. n. The Indian Journal of Medical Research 19: 883–898.

Puri IM (1932b) Studies on Indian Simuliidae. Part-II. Description of males, females and pupae of *Simulium rufibasis* Brunetti, its variety fasciatum nov. var. and of three new species from the Himalayas. The Indian Journal of Medical Research 19: 899–913.

Puri IM (1932c) Studies on Indian Simuliidae. Part-III. Description of males, females and pupae of *S. griseifrons* Brunetti (1911) and of four new species with striped thorax. The Indian Journal of Medical Research 19: 1125–1143.

Puri IM (1932d) Studies on Indian Simuliidae. Part IV. Descriptions of two new Species from North-east India, *Simulium howletti* sp. n. and *Simulium hirtipannus* sp. n., with a note on *S. ornatum* Meigen. The Indian Journal of Medical Research 20: 505–514.

Puri IM (1932e) Studies on Indian Simuliidae. Part-V. Species and varieties of the striatum series. The Indian Journal of Medical Research 20: 515–532.

Puri IM (1933a) Studies on Indian Simuliidae. Part VI. Descriptions of males, females and pupae of two new species from Palni Hills and of male and pupa of sp. n. from Bengal Terai. The Indian Journal of Medical Research 20(3): 803–812.

Puri IM (1933b) Studies on Indian Simuliidae. Part VII. Description of larvae, pupa and females of *Simulium nodosum* sp. nov., with an appendix dealing with *S. novolineatum*. nov. nom. (= *S. lineatum* Puri). The Indian Journal of Medical Research 20: 813–817.

Puri IM (1933c) Studies on Indian Simuliidae. Part VIII. Description of larvae, pupa, male & females of *S. aureohirtum* Brunetti and *S. aureumflies*. The Indian Journal of Medical Research 21: 1–10.

Senior-White RA (1922a) Notes on Indian Diptera. 1. Diptera from the Khasia Hills. 2. Tabanidae in the collection of the forest zoologist. 3. New species of Diptera from the Indian Region. Memoirs of the Department of Agriculture in India, Entomological Series 7: 83–170.

Senior-White RA (1922b) New species of Diptera from the Indian Region. Memoirs of the Department of Agriculture in India, Entomological Series 7: 107–169, pls 11–15.

Shrestha S, Takaoka H (2009) New records of ten species of black flies (Diptera: Simuliidae) from Nepal. Japanese Journal of Sanitary Zoology 60(4): 253–258. https://doi.org/10.7601/mez.60.253

Takaoka H, Somboon P (2008) Eleven new species and one new record of black flies (Diptera: Simuliidae) from Bhutan. Japanese Journal of Sanitary Zoology 59(3): 213–262. https://doi.org/10.7601/mez.59.213

Takaoka H, Thapa S, Henry W (2010) Description of two new species of *Simulium* (Gomphostilbia) (Diptera: Simuliidae) from Darjeeling, India. Japanese Journal of Sanitary Zoology 61(2): 105–110. https://doi.org/10.7601/mez.61.105

Takaoka H, Thapa S, Henry W (2011) A new species of black fly (Diptera: Simuliidae) with an entirely yellow thorax from Darjeeling, India. Zootaxa 2824(1): 62–68. https://doi.org/10.11646/zootaxa.2824.1.5

Vijayan S, Anbalagan S, Rekha K, Dinakaran S, Krishnan M (2019) A new black fly species of the subgenus *Gomphostilbia* (*Simulium*: Simuliidae: Diptera) from India. Journal of Asia-Pacific Entomology 22(2): 568–574. https://doi.org/10.1016/j.aspen.2019.04.003

ZooKeys 1118: 119–131 (2022)
doi: 10.3897/zookeys.1118.84403
https://zookeys.pensoft.net

RESEARCH ARTICLE

A peer-reviewed open-access journal
ZooKeys
Launched to accelerate biodiversity research

The genus *Hercostomus* Loew (Diptera, Dolichopodidae, Dolichopodinae) from Inner Mongolia, China, with the description of two new species

Xingyang Qian[1], Ning Wang[1], Ding Yang[2]

1 *Institute of Grassland Research, Chinese Academy of Agricultural Sciences, Hohhot, Inner Mongolia 010010, China* **2** *Department of Entomology, College of Plant Protection, China Agricultural University, Beijing 100193, China*

Corresponding authors: Ning Wang (wangningis@163.com), Ding Yang (dyangcau@126.com, dyangcau@aliyun.com)

Academic editor: Marija Ivković | Received 27 March 2022 | Accepted 7 June 2022 | Published 24 August 2022

https://zoobank.org/862064A3-0C52-401A-AA0C-10D33D626A66

Citation: Qian X, Wang N, Yang D (2022) The genus *Hercostomus* Loew (Diptera, Dolichopodidae, Dolichopodinae) from Inner Mongolia, China, with the description of two new species. ZooKeys 1118: 119–131. https://doi.org/10.3897/zookeys.1118.84403

Abstract

Previously, only two species of *Hercostomus* Loew were known to occur in Inner Mongolia. Here two species from Inner Mongolia are described as new to science, namely *Hercostomus chifengensis* **sp. nov.** and *Hercostomus triangulatus* **sp. nov.** Three new records of *Hercostomus* in Inner Mongolia are added. A key to the species of *Hercostomus* in Inner Mongolia is provided.

Keywords

Identification key, long-legged flies, new records, taxonomy

Introduction

Hercostomus Loew is one of the largest genera in the family Dolichopodidae with 475 known species worldwide, of which 300 species have been recorded from China (Yang et al. 2006; Yang et al. 2011; Qilemoge et al. 2017, 2020; Grichanov 2020). Members

of *Hercostomus* can be identified by the following features: eyes separated at the lower margin; thorax lacking a distinct dark spot above the notopleuron, pleural surface in front of the posterior spiracle bare; mid femora with an anterior preapical bristle; hind femora with the anterior bristle positioned at the apex, usually slightly flattened laterally, or not; fore tarsus usually simple; wing rarely darkened in the anterior half; vein M_{1+2} weakly sinuate, flexion at the basal third or at the middle of the distal part and sometimes with subapical flexion; sometimes the basiventral epandrial lobe of the epandrium and hypandrium forming complex entangled asymmetrical lobes (Brooks 2005; Grichanov 2011; Yang et al. 2011).

Inner Mongolia is located in a narrow region extending northeast to southwest in northern China. The climate of Inner Mongolia is temperate continental with greater precipitation in the northeast compared to the southwest and higher temperatures in the southwest compared to the northeast. Natural vegetation types range from forests, meadow steppe, typical steppe, desert steppe and the Gobi Desert from the northeast to the southwest, respectively.

Previously, only two species, *Hercostomus neimengensis* Yang, 1997 and *H. sinicus* Stackelberg, 1934, were recorded from Inner Mongolia (Yang et al. 2011). Here two new species of *Hercostomus* are described from Inner Mongolia, namely *H. chifengensis* sp. nov. and *H. triangulatus* sp. nov. The following three species are newly recorded from Inner Mongolia: *Hercostomus beijingensis* Yang, 1996, *Hercostomus dilatitarsis* Stackelberg, 1949 and *Hercostomus shennongjiensis* Yang, 1997. A key to species of *Hercostomus* in Inner Mongolia is provided. All of the updated records are distributed in mountains of nature reserves in Inner Mongolia: Jiufeng Mountain, Helan Mountain, Daqinggou. *Hercostomus neimengensis* Yang, 1997 is also distributed in grasslands of Keerqin. We discovered that all *Hercostomus* species in Inner Mongolia are distributed in grasslands near creeks and damp areas of mountains (Fig. 1). Currently, the genus comprises 300 species in China and is distributed widely around China. The low level of diversity of the genus in Inner Mongolia is probably the result of few investigations (Yang et al. 2011). Thus, it is promising to find more *Hercostomus* species in Inner Mongolia, especially in forests of northeast part of Inner Mongolia.

Materials and methods

The specimens on which this study is based were collected from Inner Mongolia in 2013 and 2014 by sweeping net. All specimens are deposited in the Entomological Museum of China Agricultural University (CAU), Beijing. Morphological terminology follows Cumming and Wood (2017). The following abbreviations are used: **acr** = acrostichal bristle (s), **ad** = anterodorsal bristle (s), **av** = anteroventral bristle (s), **dc** = dorsocentral bristle (s), **sc** = scutellars, **pd** = posterodorsal bristle (s), **v** = ventral bristle (s), **LI** = fore leg, **LII** = mid leg, **LIII** = hind leg, **CuAx ratio** = length of dm–cu / length of distal portion of CuA.

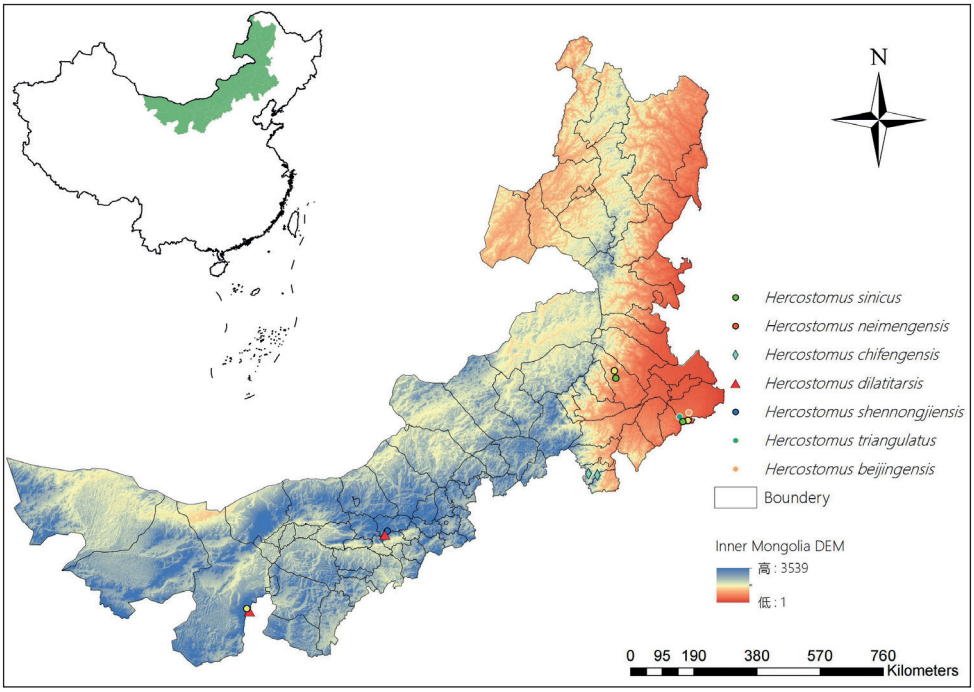

Figure 1. Distribution of *Hercostomus* in Inner Mongolia.

Taxonomy

Key to species (males) of *Hercostomus* from Inner Mongolia

1 Antenna entirely black **2**
– Antenna yellow or partly dark yellow **4**
2 Abdominal tergites (Figs 3, 7) wholly metallic green; male cercus (Figs 10, 11) with distinct denticles **3**
– Abdominal tergites 1–3 (Fig. 2) yellow at lateral margin; male cercus with indistinct or weak denticles ..... ***H. beijingensis* Yang**
3 Postpedicel (Fig. 9) 1.8 times longer than wide, blunt at tip; male cercus (Fig. 10) lobate, slightly shorter than epandrium, distinctly longer than wide, with several short finger-like marginal processes ..... ***H. chifengensis* sp. nov.**
– Postpedicel 1.3 times longer than wide, sharp at tip; male cercus (Fig. 11) long strip-like, geniculate, apical half with long marginal bristles hook-like apically ..... ***H. sinicus* Stackelberg**
4 Epandrial lobe very long finger-like; male cercus very narrow, long strip-like with indistinct or weak digitations ..... ***H. shennongjiensis* Yang**
– Epandrial lobe (Fig. 14) very short or absent; male cercus (Fig. 14) rather wide, somewhat quadrate or triangular with distinct digitations **5**

5 Fore tarsomeres 2–5 flattened; epandrium slightly longer than wide, with nearly truncate apical margin ..... ***H. dilatitarsis*** **Stackelberg**

– Fore tarsus simple; epandrium (Fig. 14) distinctly longer than wide, with convex apical margin **6**

6 Postpedicel blackish at base, obtuse at tip; male cercus band-like with some marginal denticles at tip ..... ***H. neimengensis*** **Yang**

– Postpedicel (Fig. 12) blackish with basal ventral surface dark yellow, acute at tip; male cercus (Fig. 14) nearly triangular with weak denticles and 3 relatively long finger-like processes ..... ***H. triangulatus*** **sp. nov.**

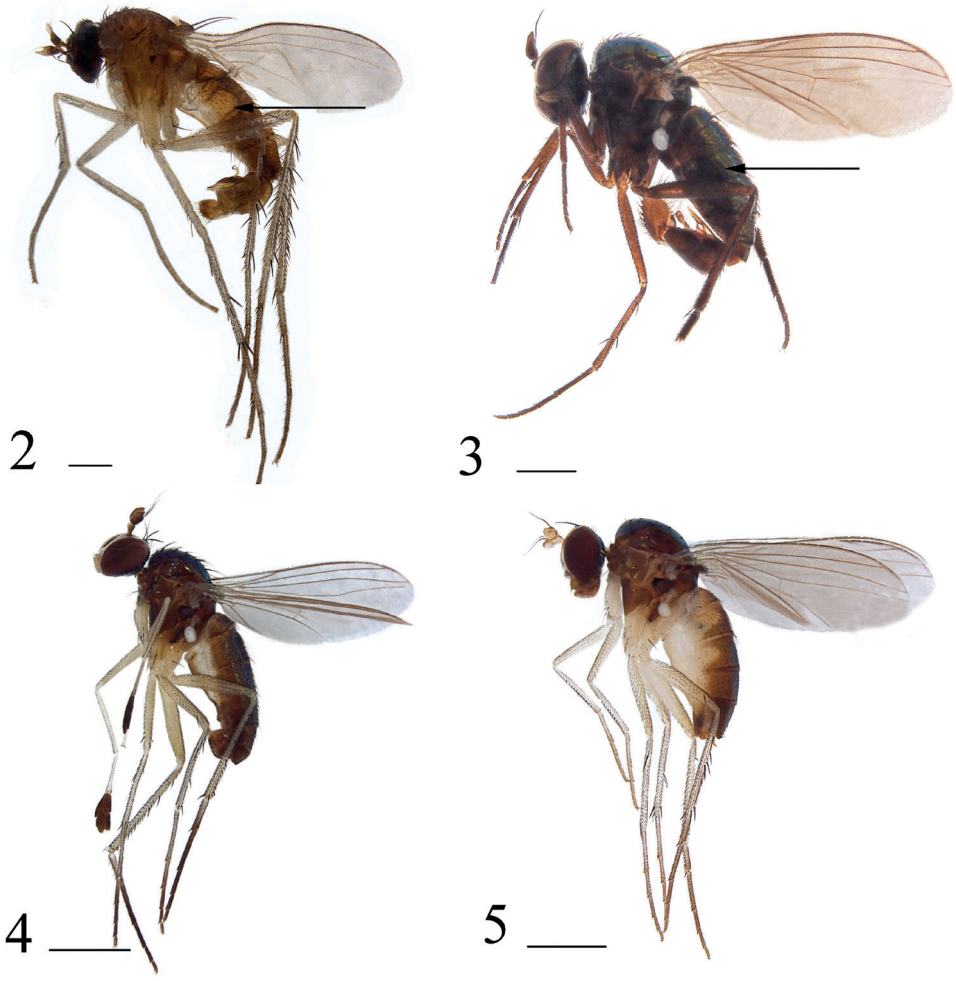

Figures 2–5. Habitus, lateral view **2** *Hercostomus beijingensis* Yang, 1966, male **3** *Hercostomus chifengensis* sp. nov., holotype male **4** *Hercostomus dilatitarsis* Stackelberg, 1949, male **5** *Hercostomus neimengensis* Yang, 1997, female. Scale bars: 1 mm.

***Hercostomus beijingensis* Yang, 1996**
Fig. 2

Hercostomus beijingensis Yang, 1996: 318. Type locality: China: Beijing, Yingtaogou.

Diagnosis. Antenna entirely black; postpedicel 1.8 times longer than wide, blunt at tip. Metapleuron yellow. Abdominal tergites 1–3 yellow at lateral margin. All coxae entirely yellow. Male cercus nearly quadrate. Phallus thin and long, apically geniculate.

Specimens examined. ***Holotype*:** male, China, Beijing, Xiangshan, Yingtaogou, 1987.V.30, Ding Yang (CAU). **Other material:** 2 males, China, Inner Mongolia, Tongliao, Daqinggou, 200–300m, 2014.VII.22, Ning Wang & Ding Yang (CAU).

Distribution. China (Inner Mongolia, Beijing, Henan, Shanxi, Hubei).

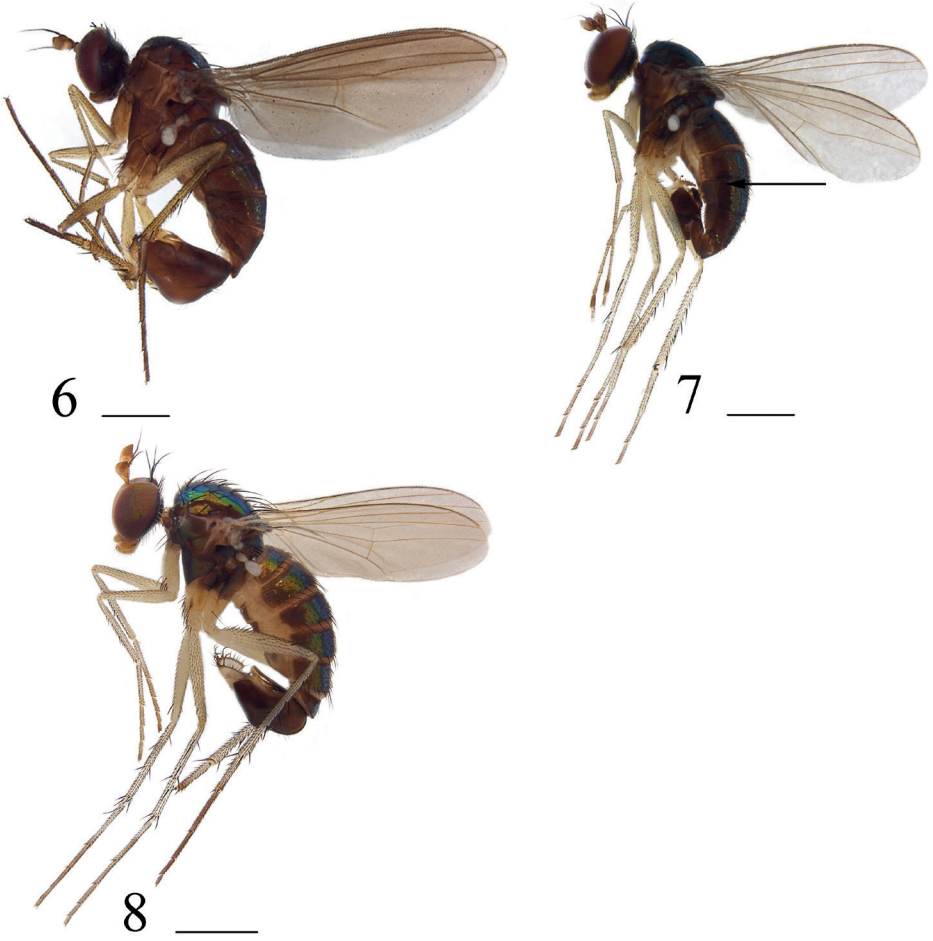

Figures 6–8. Habitus, lateral view **6** *Hercostomus shennongjiensis* Yang, 1997, male **7** *Hercostomus sinicus* Stackelberg, 1934, male **8** *Hercostomus triangulatus* sp. nov., holotype male. Scale bars: 1 mm.

***Hercostomus chifengensis* sp. nov.**
https://zoobank.org/BAA059A0-E3CE-4AF2-AEDD-61689F5F5270
Figs 3, 9–10

Diagnosis. Antenna entirely black; postpedicel 1.8 times longer than wide, blunt at tip; basal segment of arista 0.55 times as long as apical segment. Legs entirely black. Wings slightly tinged brown. Male cercus nearly lobate, distinctly longer than wide, with short finger-like marginal processes.

Description. Male (Fig. 3). Body length 3.1–3.2 mm, wing length 3.5–4.1 mm.

Head metallic green with pale grey pollinosity. Hairs and bristles on head black, but middle and lower postocular bristles and posteroventral hairs yellow. Ocellar tubercle with 2 strong oc and 2 short posterior hairs. Antenna (Fig. 9) black; postpedicel 1.8 times longer than wide, blunt at tip; arista black, basal segment 0.55 times as long as apical segment. Proboscis brownish with black hairs; palpus black with black hairs and 1 black apical bristle.

Thorax metallic green with pale grey pollinosity. Hairs and bristles on thorax black; 7–8 irregularly biseriate acr short hair-like, 6 long strong dc. Scutellum with 2 pairs of sc and several short marginal hairs, basal pair hair-like.

Legs entirely black. Hairs and bristles on legs black. Mid and hind coxae each with 1 outer bristle; mid and hind femora each with 1 preapical bristle; fore tibia with 3 short ad, 2 short pd and 2 apical bristles; mid tibia with 4 ad, 2 pd, 1 av and 3 apical bristles; hind tibia with 3 ad, 2 pd, 1 short av and 3 apical bristles; hind tarsomere 1 with 1 short v at base. Relative lengths of tibia and 5 tarsomeres of legs LI: 1.8: 0.8: 0.4: 0.3: 0.2: 0.2; LII: 2.7: 1.15: 0.6: 0.5: 0.3: 0.2; LIII: 3.4: 0.85: 1.0: 0.7: 0.45: 0.3. ***Wing*** nearly hyaline, slightly tinged brownish; veins brown; R_{4+5} and M_{1+2} distinctly convergent apically; CuAx ratio 0.55. Squama yellow with blackish hairs. Halter yellow.

Abdomen metallic green with pale grey pollinosity. Hairs and bristles on abdomen black. Male genitalia (Fig. 10): Epandrium distinctly longer than wide, narrowed at tip; inner epandrial lobe relatively small, outer epandrial lobe long finger-like with somewhat swollen tip. Subepandrial process with two long processes branched, one blunt at tip, one sharp at tip. Male cercus large, lobate, slightly shorter than epandrium, distinctly longer than wide, with several short finger-like marginal processes. Hypandrium tubular at tip, with a hook-like projection near middle.

Female. Unknown

Type material examined. ***Holotype*:** male, China, Inner Mongolia, Chifeng, Wangyedian, Binlanggoumen, 1223 m, 2014.VIII.25, Li Shi (CAU). ***Paratype*:** 1 male, China, Inner Mongolia, Chifeng, Saihanwula, 1200 m, 2013.VII.24, Xiumei Lu (CAU).

Distribution. China (Inner Mongolia).

Remarks. The new species is somewhat similar to *H. subrusticus* Zhang, Yang & Grootaert, 2008 from Xinjiang of China, but can be distinguished from the latter by the arista located at middle of the dorsal margin of the postpedicel and the male

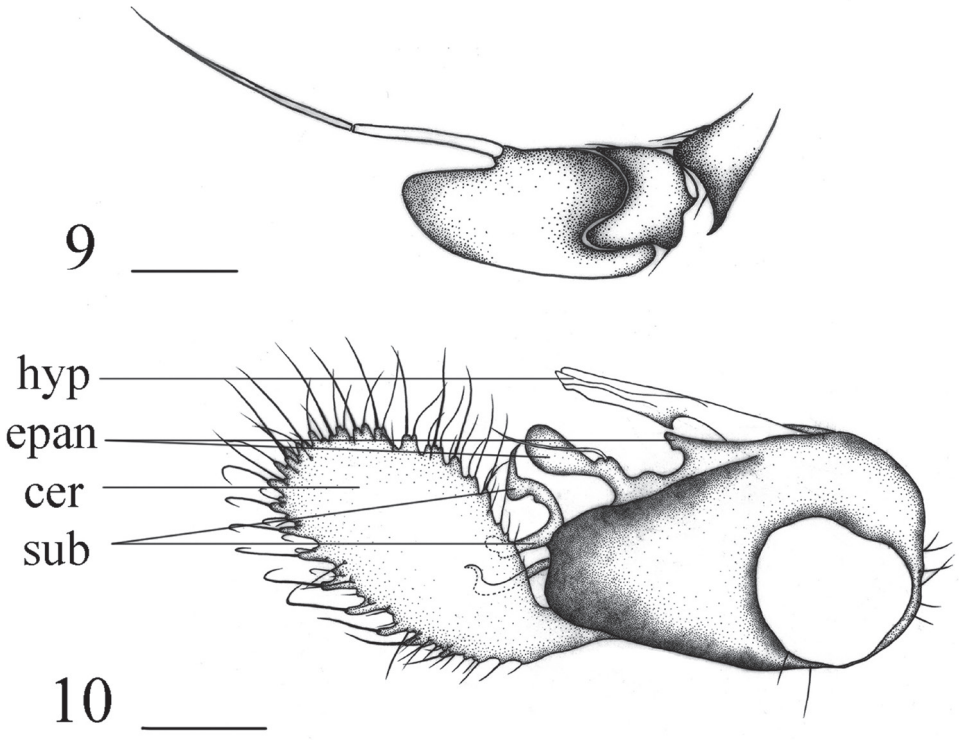

Figures 9, 10. *Hercostomus chifengensis* sp. nov., male. **9** antenna, lateral view **10** genitalia, lateral view. Abbreviations: hyp = hypandrium, epan = epandrial lobe, cer = cercus, sub = subepandrial process. Scale bars: 0.1 mm.

cercus long and narrow. In *H. subrusticus*, the arista is located at the apical one-third of the dorsal margin of the postpedicel, and the male cercus is relatively short and wide (Zhang et al. 2008).

Etymology. The species is named after the type locality Chifeng.

Hercostomus dilatitarsis Stackelberg, 1949

Fig. 4

Hercostomus dilatitarsis Stackelberg, 1949: 687. Type locality: Tajikistan: Kondara. Valley Varzob. Gissar Ridge.

Diagnosis. Postpedicel entirely black. Coxae entirely yellow, but mid coxa tinged blackish. Fore tarsomere 1 yellow, tarsomeres 2–3 distinctly flattened and black, tarsomeres 4–5 weakly flattened and white.

Specimens examined. 1 male, China, Inner Mongolia, Mount Jiufeng, Toudaogou, 1500–1600 m, 2013.VIII.4, Xiao Zhang (CAU). 3 males 3 females, China,

Inner Mongolia, Helan Mountain, Shuimogou, 1800–1900 m, 2010.VIII.6, Lihua Wang (CAU).

Distribution. China (Inner Mongolia, Hebei); Tajikistan.

Hercostomus neimengensis Yang, 1997

Fig. 5

Hercostomus (*Hercostomus*) *neimengensis* Yang, 1997: 138. Type locality: China: Inner Mongolia, Tuyouqi.

Diagnosis. Antenna yellow with postpedicel blackish at tip and 1.1 times longer than wide. Thorax metallic green, except hypopleuron partly yellow and metapleuron entirely yellow. Legs including coxae yellow; hairs and bristles on coxae yellowish. Male cercus band-like with some marginal denticles at tip.

Specimens examined. ***Holotype*:** male, China, Inner Mongolia, Tumoteyouqi, 1978.VII.21, Heming Chen (CAU). **Other material:** 1 male 8 females, China, Inner Mongolia, Helan Mountain, Xiangchizigou, 1900 m, 2013.VII.30, Xiao Zhang (CAU).

Distribution. China (Inner Mongolia, Gansu).

Hercostomus shennongjiensis Yang, 1997

Fig. 6

Hercostomus (*Hercostomus*) *shennongjiensis* Yang, 1997: 118. Type locality: China: Hubei, Shennongjia.

Diagnosis. Postpedicel dark yellow at basal ventral portion, 1.2 times longer than wide, somewhat acute at tip. All coxae entirely black or blackish. Wing slightly brownish. Male cercus long strip-like with short hairs. Epandrial lobe long finger-like with very long apical bristles.

Specimens examined. 1 male 1 female, China, Inner Mongolia, Mount Jiufeng, Erdaogou, 1400–1500 m, 2013.VIII.3, Xiumei Lu (CAU).

Distribution. China (Inner Mongolia, Hubei, Shanxi, Henan).

Hercostomus sinicus Stackelberg, 1934

Figs 7, 11

Hercostomus sinicus Stackelberg, 1934: 174. Type locality: China: "Dyn-uan-in, Nord-Alashan".

Diagnosis. Postpedicel 1.3 times longer than wide, sharp at tip. Fore tarsomeres 1–3 relatively thin, tarsomeres 4–5 weakly thickened, tarsomere 4 dark brown, tarsomere

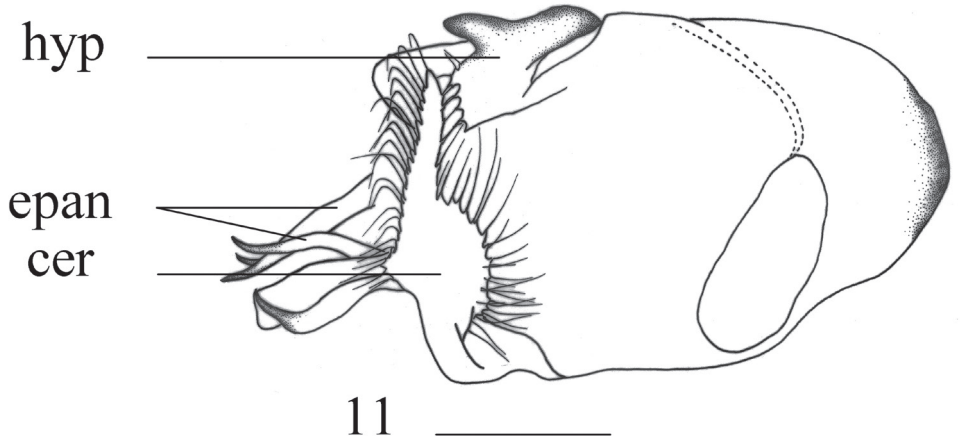

Figure 11. *Hercostomus sinicus* Stackelberg, 1934, male genitalia, lateral view. Abbreviations: hyp = hypandrium, epan = epandrial lobe, cer = cercus. Scale bars: 0.1 mm.

5 white. Male cercus long strip-like, geniculate, apical half with long marginal bristles hook-like apically.

Description. Male (Fig. 7). Body length 3.1–3.2 mm, wing length 3.0–3.2 mm.

Head metallic green with pale grey pollinosity. Hairs and bristles on head black, but middle and lower postocular bristles and posteroventral hairs yellow. Antenna black; postpedicel nearly square, 1.3 times longer than wide, sharp at tip; arista black with short hairs, basal segment 0.2 times as long as apical segment. Proboscis brownish yellow with brownish yellow hairs; palpus blackish with brownish yellow hairs and 1 blackish apical bristle.

Thorax metallic green with pale grey pollinosity. Hairs and bristles on thorax black; 6 irregularly biseriate acr slightly long and strong, 6 long strong dc. Scutellum with 2 pairs of sc, basal pair hair-like. Propleuron with yellowish hairs and 1 bristle on lower portion.

Legs mostly yellow. Fore coxa yellow, mid coxa blackish, hind coxa brownish yellow; fore tarsomere 4 dark brown, tarsomere 5 white; mid and hind tarsus brown or dark brown from tip of tarsomere 1 onwards. Fore tarsomeres 1–3 relatively thin, tarsomeres 4–5 weakly thickened. Hairs and bristles on legs black, but some hairs and bristles on coxae yellow; mid and hind coxae each with 1 outer bristle; mid and hind femora each with 1 preapical bristle. Fore tibia with 1 ad, 2 pd and 3 apical bristles (apico-ventral bristle brown, 1/4 as long as tarsomere 1); mid tibia with 2–3 ad, 2 pd and 4 apical bristles; hind tibia with 2 ad, 3 pd and 4 apical bristles (including 1 subapical pd). Relative lengths of tibia and 5 tarsomeres of legs LI: 2.25: 1.1: 0.85: 0.6: 0.35: 0.3; LII: 2.75: 1.45: 0.8: 0.65: 0.4: 0.3; LIII: 3.2: 0.9: 1.2: 0.7: 0.5: 0.3. ***Wing*** nearly hyaline, veins dark brown; R_{4+5} and M_{1+2} distinctly convergent apically; CuAx ratio 0.4. Squama yellow with brown hairs. Halter yellow.

Abdomen metallic green with pale grey pollinosity except hypogygium brownish yellow at tip. Hairs and bristles on abdomen black. Male genitalia (Fig. 11): Epandrium distinctly longer than wide; epandrial lobe weakly bulged. Male cercus long strip-like, geniculate, apical half with long marginal bristles hook-like apically. Hypandrium irregularly branched, right process short, left process long and hook-like.

Female. Body length 3.2–3.5 mm, wing length 3.0–3.2 mm.

Specimens examined. 2 males, China, Inner Mongolia, Tongliao, Daqinggou, 180 m, 2014.VII.22, Ning Wang & Ding Yang (CAU).

Distribution. China (Inner Mongolia).

Remarks. This species is redescribed with illustrations of male genitalia for the first time.

Hercostomus triangulatus sp. nov.

https://zoobank.org/76823345-6706-4FC3-BBAF-D3087E4E34C4

Figs 8, 12–14

Diagnosis. Antenna mainly dark yellow; postpedicel blackish with basal ventral surface dark yellow, 1.2 times longer than wide, obtuse at tip; arista black, basal segment 0.25 times as long as apical segment. All coxae dark yellow. Male cercus nearly triangular with weak denticles and 3 relatively long finger-like processes.

Description. Male (Fig. 8). Body length 3.7–4.1 mm, wing length 3.3–3.6 mm.

Head metallic green with dense pale grey pollinosity. Hairs and bristles on head black, middle and lower postocular bristles and posteroventral hairs yellow. Antenna (Fig. 12) dark yellow except scape blackish at base and postpedicel blackish with base and ventral surface dark yellow; postpedicel 1.2 times longer than wide, somewhat acute at tip; arista blackish with short pubescence, basal segment 0.25 times as long as apical segment. Proboscis brownish yellow with black hairs; palpus brownish, with dark yellow hairs and 1 dark yellow apical bristle.

Thorax metallic green with pale grey pollinosity. Hairs and bristles on thorax black; 6~8 irregularly biseriate acr short hair-like; 6 long strong dc. Scutellum with 2 pairs of sc, basal pair short hair-like. Propleuron with yellowish hairs and 1 black bristle on lower portion.

Legs yellow; all coxae yellow; all tarsi brown to dark brown from tip of tarsomere 1 onwards. Hairs and bristles on legs black; mid and hind coxae each with 1 outer bristle; mid and hind femora each with 1 preapical bristle; fore tibia with 1 ad, 2 pd and 2 short apical bristles; mid tibia with 4 ad, 2 short pd, 1 av and 4 short apical bristles; hind tibia with 3 ad, 3 pd, 4 short av (2 inner bristles thin, 2 outer bristles thick) and 3 apical bristles. Hind tarsomere 1 with 1 short ventral bristle at base. Relative lengths of tibia and 5 tarsomeres of legs LI: 2.0: 1.1: 0.5: 0.4: 0.3: 0.2; LII: 2.8: 1.5: 0.8: 0.7: 0.4: 0.3; LIII: 3.4: 1.0: 1.2: 0.5: ?: ?. ***Wing*** nearly hyaline, veins dark brown; R_{4+5} and M distinctly convergent apically; CuAx 0.5. Squama yellow with dark yellowish hairs. Halter yellow.

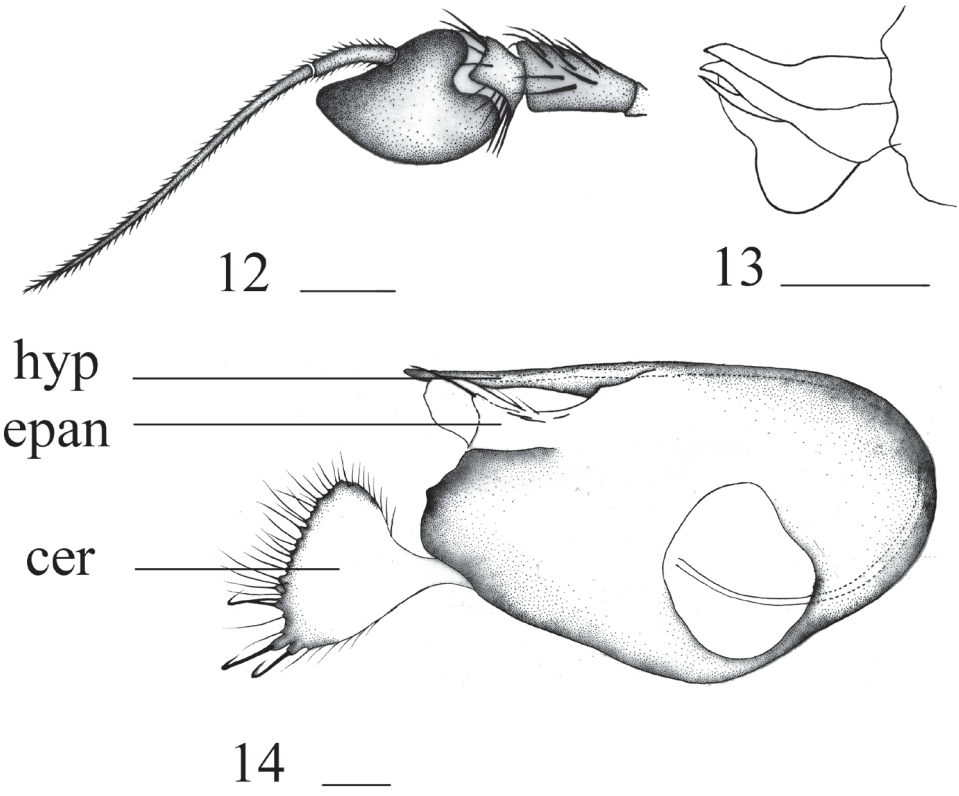

Figures 12–14. *Hercostomus triangulatus* sp. nov., male **12** antenna, lateral view **13** subepandrial processess and postgonite, lateral view **14** genitalia, lateral view. Abbreviations: hyp = hypandrium, epan = epandrial lobe, cer = cercus. Scale bars: 0.1 mm.

Abdomen metallic green with pale grey pollinosity. Hairs and bristles on abdomen black; tergite 1 with several short yellow hairs; sternites 2–3 with short yellow hairs. Male genitalia (Fig. 14): Epandrium distinctly longer than wide, narrowed at tip; epandrial lateral lobe relatively short and thick. Subepandrial process (Fig. 13) with two processes separated, narrowed at tip. Male cercus nearly triangular with some weak denticles and 3 relatively long finger-like processes bearing long bristles on apical margin. Hypandrium somewhat acute at tip.

Female. Body length 3.0–3.6 mm, wing length 3.6–3.7 mm.

Type material examined. *Holotype*: male, China, Inner Mongolia, Tongliao, Daqinggou, 180m, 2014.VII.24, Ning Wang & Ding Yang (CAU). ***Paratypes*:** 3 males 1 female, same data as holotype (CAU); 8 males 3 females, China, Inner Mongolia, Tongliao, Daqinggou, 180 m, 2014.VII.23, Ning Wang & Ding Yang (CAU); 1 male 1 female, China, Tongliao, Daqinggou, 180 m, 2014.VII.22, Ning Wang & Ding Yang (CAU).

Distribution. China (Inner Mongolia).

Remarks. The new species is somewhat similar to the members of *H. crassivena* group, but the veins of *H. triangulatus* are not thickened (Zhang and Yang 2007).

Etymology. This species is named after the triangular cercus.

Discussion

Hercostomus Loew is probably polyphyletic and not a monophyletic genus as it is poorly defined (Brooks 2005; Yang et al. 2011). Currently 300 species of *Hercostomus* are distributed in China, of which seven species are distributed in Inner Mongolia. Twenty-four species groups of *Hercostomus* distributed in China were recognized (Yang et al. 2011; Grichanov 2020), namely *H. crassivena* group, *H. abnormis* group, *H. longicercus* group, *H. quadriseta* group, *H. takagii* group, *H. fatuus* group, *H. ulrichi* group, *H. flavimaculatus* group, *H. subnovus* group, *H. flaviventris* group, *H. curvus* group, *H. albidipes* group, *H. apiculatus* group, *H. baishanzuensis* group, *H. nanlingensis* group, *H. absimilis* group, *H. intactus* group, *H. longus* group, *H. fluvius* group, *H. prolongatus* group, *H. digitiformis* group, *H. biancistrus* group, *H. incisus* group, *H. digitatus* group. As to the seven species distributed in Inner Mongolia, *H. shennongjiensis* Yang, 1997 belongs to the *H. digitiformis* group, *H. chifengensis* sp. nov. belongs to the *H. nanlingensis* group, and *H. beijingensis* Yang, 1996 belongs to the *Hercostomus subnovus* group, while *H. dilatitarsis* Stackelberg, 1949, *H. neimengensis* Yang, 1997, *H. sinicus* Stackelberg, 1934, and *H. triangulatus* sp. nov. were not assigned to any species group. Further studies are necessary in order to clarify their systematic placement.

Acknowledgements

We are very grateful to Dr. Xiao Zhang (Qingdao), Dr. Li Shi (Hohhot) and Dr. Xiumei Lu (Shanghai) for collecting specimens. This research was funded by Natural Science Foundation of Inner Mongolia (2020JQ04), National Science & Technology Fundamental Resources Investigation Program of China (Grant No. 2019FY100400) and Key Science and Technologies Program of Inner Mongolia (No. 2021ZD0011-2).

References

Brooks SE (2005) Systematics and phylogeny of the Dolichopodidae (Diptera: Dolichopodidae). Zootaxa 857(1): 1–158. https://doi.org/10.11646/zootaxa.857.1.1

Cumming JM, Wood DM (2017) Adult morphology and terminology. In: Kirk-Spriggs AH, Sinclair BJ (Eds) Manual of Afrotropical Diptera. Volume 1. Introductory Chapters and Keys to Diptera Families: 89–134. Suricata 4, SANBI Graphics & Editing, Pretoria.

Grichanov IY (2011) An illustrated synopsis and keys to Afrotropical genera of the epifamily Dolichopodidae (Diptera: Empidoidea). Priamus (Supplement 24): 1–98.

Grichanov IY (2020) New records of Dolichopodidae (Diptera) from Russian Primorye and notes on some Chinese species. Russian Entomological Journal 29(4): 432–438. https://doi.org/10.15298/rusentj.29.4.12

Qilemoge, Liu XY, Yang D (2017) A review of the *Hercostomus ulrichi* group (Diptera: Dolichopodidae) from China, with descriptions of two new species. Transactions of the American Entomological Society 143: 701–711. https://doi.org/10.3157/061.143.0301

Qilemoge, Zhang LL, Yang D (2020) A key to species groups of the genus *Hercostomus* (Diptera: Dolichopodidae) from China, with description of one new species. Transactions of the American Entomological Society 146(2): 305–312. https://doi.org/10.3157/061.146.0202

Stackelberg AA (1934) Dolichopodidae. Die Fliegen der Palaearktischen Region Lief 82: 129–176.

Stackelberg AA (1949) Species of the genus *Hercostomus* Lw. (Diptera, Dolichopodidae) of the Middle-Asiatic fauna. Trudy Zoologicheskogo Instituta 8(4): 669–687.

Yang D (1996) New species of Dolichopodidae from China (Diptera, Dolichopodidae). Entomofauna 17(18): 317–324.

Yang D, Zhu YJ, Wang MQ, Zhang LL (2006) World catalog of Dolichopodidae (Insecta: Diptera). China Agricultural University Press, Beijing, 147–180.

Yang D, Zhang LL, Wang MQ, Zhu YJ (2011) Fauna Sinica Insecta Vol. 53. Diptera Dolichopodidae. Science Press, Beijing, 651–976.

Zhang LL, Yang D (2007) Species of *Hercostomus crassivena*-group (Diptera: Dolichopodidae). Transactions of the American Entomological Society 133(1): 155–159. https://doi.org/10.3157/0002-8320(2007)133[155:SOHCDD]2.0.CO;2

Zhang LL, Yang D, Grootaert P (2008) New species of *Hercostomus* (Diptera: Dolichopodidae) from China. Bulletin de l'Institut Royal des Sciences Naturelles de Belgique Entomologique 78: 259–274.

ZooKeys 1118: 133–180 (2022)
doi: 10.3897/zookeys.1118.83156
https://zookeys.pensoft.net

RESEARCH ARTICLE

A peer-reviewed open-access journal
ZooKeys
Launched to accelerate biodiversity research

Three new species of the genus *Biasticus* Stål, 1867 (Insecta, Heteroptera, Reduviidae, Harpactorinae) from Central Highlands, Vietnam

Ngoc Linh Ha[1,2], Xuan Lam Truong[2,3], Tadashi Ishikawa[4], Weeyawat Jaitrong[5], Chi Feng Lee[6], Bounsanong Chouangthavy[7], Katsuyuki Eguchi[1]

1 *Department of Biological Sciences, Graduate School of Science, Tokyo Metropolitan University, Minami-osawa 1-1, Hachioji, Tokyo 192-0397, Japan* **2** *Institute of Ecology and Biological Resources, Vietnam Academy of Science and Technology, 18 Hoang Quoc Viet Road, Nghia Do, Cau Giay, Hanoi, Vietnam* **3** *Graduate University of Science and Technology, Vietnam Academy of Science and Technology, 18 Hoang Quoc Viet Road, Nghia Do, Cau Giay, Hanoi, Vietnam* **4** *Faculty of Agriculture, Tokyo University of Agriculture, Atsugi, Kanagawa, Japan* **5** *Office of Natural Science Research, National Science Museum, 39 Moo 3, Khlong 5, Khlong Luang, Pathum Thani, 12120 Thailand* **6** *Applied Zoology Division, Taiwan Agricultural Research Institute, Taichung 413, Taiwan* **7** *Plant Protection Unit, Department of Plant Science, Faculty of Agriculture, National University of Laos, P.O. Box 7322, Vientiane, Lao People's Democratic Republic*

Corresponding author: Ngoc Linh Ha (linh.hangoc02@gmail.com)

Academic editor: Jader Oliveira | Received 5 March 2022 | Accepted 27 July 2022 | Published 24 August 2022

https://zoobank.org/43714075-E832-4248-9916-38E5AEFA9F71

Citation: Ha NL, Truong XL, Ishikawa T, Jaitrong W, Lee CF, Chouangthavy B, Eguchi K (2022) Three new species of the genus *Biasticus* Stål, 1867 (Insecta, Heteroptera, Reduviidae, Harpactorinae) from Central Highlands, Vietnam. ZooKeys 1118: 133–180. https://doi.org/10.3897/zookeys.1118.83156

Abstract

Three new assassin bug species of the genus *Biasticus* Stål, 1867 are recognized in Vietnam based on morphological examination, morphometric and molecular phylogenetic analyses, and described as *Biasticus taynguyenensis* Ha, Truong & Ishikawa, **sp. nov.**, *Biasticus griseocapillus* Ha, Truong & Ishikawa, **sp. nov.**, and *Biasticus luteicollis* Ha, Truong & Ishikawa, **sp. nov.** The conspecific male and female associations of the new species were confirmed by phylogenetic analyses and DNA barcoding of the mitochondrial 16S rDNA and COI genes. All three new species are presently restricted to the Central Highlands, Vietnam (Kon Chu Rang NR, Gia Lai Province, and Chu Yang Sin NP, Dak Lak Province).

Keywords

Assassin bugs, Indo-China, molecular phylogeny, morphometry, taxonomy

Introduction

The assassin bug genus *Biasticus* Stål, 1867 was established by monotypy with *Reduvius impiger* Stål, 1863, which was described based on a single female specimen from Cambodia and is currently assigned to the subfamily Harpactorinae of the family Reduviidae (Stål 1863, 1867; Maldonado 1990). *Biasticus* currently includes 20 valid named species known exclusively from the Oriental and Sino-Japanese realms (Stål 1863; Reuter 1887; Distant 1903; Bergroth 1913; Matsumura 1913; Miller 1941, 1948, 1949, 1954a, 1954b; Hsiao 1979; Hsiao and Ren 1981; Cai and Yang 2002; Ishikawa 2003; Afzal and Ahmad 2019). There has been no notable modification to the genus classification since Hsiao and Ren (1981) added three new species. According to Truong et al. (2015), three species have been recorded from Vietnam, i.e., *B. confusus* Hsiao et al., 1979, *B. flavinotus* (Matsumura, 1913), and *B. flavus* (Distant, 1903).

We discovered dozens of *Biasticus* specimens in Central Highlands, Vietnam, during recent field surveys and examinations of Reduviidae specimens owned by research organizations in Vietnam, Thailand, Laos, Taiwan, and Japan, but they were not identifiable as valid species of the genus. Therefore, this study aims to confirm the taxonomic status of those *Biasticus* specimens using an integrated approach that includes morphological examination, morphometric analyses, molecular phylogenetic analyses, and molecular-based species delimitation analyses, i.e., Assemble Species by Automatic Partitioning (ASAP) (Puillandre et al. 2021) and Bayesian implementation of the Poisson Tree Processes model (bPTP) (Zhang et al. 2013) for species delimitation, as well as the necessary taxonomic treatments.

Materials and methods

Material examined

This study included 31 specimens (10 male and 21 female adults) collected from Central Highlands, Vietnam (Kon Chu Rang Nature Reserve, Gia Lai Province, and Chu Yang Sin National Park, Dak Lak Province), which are in accordance with the diagnosis of *Biasticus* but were not assigned to any validly named species. The following species that were previously recorded from Vietnam were also herein examined: *B. confusus* Hsiao et al., 1979 (six specimens from Northern Vietnam), *B. flavinotus* (Matsumura, 1913) (eight from Northern Thailand, Northern Vietnam, and Taiwan, including the lectotype), and *B. flavus* (Distant, 1903) (11 from Northern Laos and Northern Thailand). Furthermore, specimens of *Sphedanolestes pubinotus* Reuter, 1881, *Rhynocoris mendicus* (Stål, 1867), and *Coranus* sp. collected from Vietnam were used as outgroups in molecular phylogenetic analysis (Table 1). The voucher samples of this investigation are housed in the following institutions:

HU	Matsumura Collection at the Laboratory of Systematic Entomology, Department of Agriculture, Hokkaido University, Sapporo, Japan;
IEBR	Institute of Ecology and Biological Resources, Vietnam Academy of Science and Technology, Vietnam;
NSMT	National Museum of Nature and Science, Tokyo, Japan;
NSM	Department of Entomology, Zoological Research Division, Office of Natural Science Research, National Science Museum, Thailand;
NUOL-FA	Faculty of Agriculture, National University of Laos, Laos P.D.R.;
TARI-AZ	Applied Zoology Division, Taiwan Agricultural Research Institute, Taiwan;
VNMN	Vietnam National Museum of Nature, Vietnam Academy of Science and Technology, Vietnam.

This study followed the description of the genus *Biasticus* slightly modified by Distant (1904): "Body elongate; head subelongate, almost as long as the pronotum, postocular a little longer than anteocular area; rostrum with the first segment shorter than second, a little longer than anteocular area of head; first segment of antennae a little longer than pronotum; anterior lobe of pronotum longitudinally impressed, posterior lobe with a distinct, central, anterior, longitudinally elevation; scutellum not apically produced; hemelytra passing the abdominal apex; legs moderately long and slender; femora apically moderately nodulose, anterior femora very slightly incrassated."

Examination at the species level was executed by referring to the original descriptions and other taxonomic publications (Stål 1863; Reuter 1887; Distant 1903; Bergroth 1913; Matsumura 1913; Miller 1941, 1948, 1949, 1954a, 1954b; Hsiao 1979; Hsiao and Ren 1981; Cai and Yang 2002; Ishikawa 2003; Afzal and Ahmad 2019) of the following congeners known from Vietnam and adjacent areas: *B. abdominalis* (Reuter, 1887), type location: India and Myanmar; *B. abjectus* Miller, 1941, Borneo; *B. breddin* Miller, 1948, Indonesia; *B. chersonesus* (Distant, 1903), Malaysia and Myanmar; *B. confusus* Hsiao et al., 1979, South China (see also Table 1); *B. dilectus* Miller, 1954, Indonesia; *B. eburneus* Miller, 1941, Borneo; *B. flavinotus* (Matsumura, 1913), Taiwan (see also Table 1); *B. flavus* (Distant, 1903), Hong Kong and Myanmar (see also Table 1); *B. fuliginosus* Reuter, 1887, North India; *B. gagatinus* Breddin, 1903, Indonesia; *B. horfieldi* Distant, 1903, Indonesia; *B. impiger* (Stål, 1863), Cambodia; *B. insignis* (Miller, 1941), Indonesia; *B. lutescens* Breddin, 1903, Indonesia; *B. moultoni* Bergroth, 1913, Malaysia; *B. nigricollis* (Dallas, 1850), Indonesia; *B. obfuscatus* Miller, 1949, Malaysia; *B. princeps* Miller, 1949, Malaysia; *B. ventralis* Hsiao et al., 1979, South China.

Newly obtained specimens were labeled with their specimen IDs and locality information before being individually preserved in vials containing 99% ethanol. Each specimen's right hind leg was cut off in the lab and used for DNA extraction (then for molecular phylogenetic analysis and DNA barcoding). The rest of the body was pinned or preserved in 99% ethanol for morphological and morphometric study.

Table 1. The data of specimens used in this study. Abbreviations and symbols: n/a: no data; HU, Matsumura Collection at the Laboratory of Systematic Entomology, Department of Agriculture, Hokkaido University, Sapporo, Japan; IEBR, Institute of Ecology and Biological Resources, Vietnam Academy of Science and Technology, Vietnam; NSMT, National Museum of Nature and Science, Tokyo, Japan; NSM, Department of Entomology, Zoological Research Division, Office of Natural Science Research, National Science Museum, Thailand; NUOL-FA, Faculty of Agriculture, National University of Laos, Laos P.D.R; TARI-AZ, Applied Zoology Division, Taiwan Agricultural Research Institute Insect Collection, Taiwan Agricultural Research Institute, Taiwan; VNMN, Vietnam National Museum of Nature, Vietnam Academy of Science and Technology, Vietnam; *, tentatively held by HNL (first author); bA–bF, morphospecies code (see in the text).

Morphospecies	Specimen code	Collecting date	Locality	Sex	Accession numbers			Depository
					16S	Uni-Minibar (COI)	COI	
***Biasticus* (ingroups)**								
B. taynguyenensis Ha, Truong & Ishikawa, sp. nov. [bA]	HNL2018-036	09, v, 2018	Vietnam, Dak Lak	♀	OM908207	ON542864	OM868188	IEBR*
B. taynguyenensis Ha, Truong & Ishikawa, sp. nov. [bA]	HNL2018-072	08, v, 2018	Vietnam, Gia Lai	♀	OM908210	ON542867	OM868178	IEBR*
B. taynguyenensis Ha, Truong & Ishikawa, sp. nov. [bA]	HNL2018-073	08, v, 2018	Vietnam, Gia Lai	♀	OM908211	ON542868	OM868192	NSMT
B. taynguyenensis Ha, Truong & Ishikawa, sp. nov. [bA]	HNL2018-074	08, v, 2018	Vietnam, Gia Lai	♀	OM908212	ON542869	OM868193	NSMT
B. taynguyenensis Ha, Truong & Ishikawa, sp. nov. [bA]	HNL2018-075	08, v, 2018	Vietnam, Gia Lai	♀	OM908213	ON542870	OM868194	VNMN
B. taynguyenensis Ha, Truong & Ishikawa, sp. nov. [bA]	HNL2018-076	08, v, 2018	Vietnam, Gia Lai	♀	ON554765	ON542871	n/a	IEBR
B. taynguyenensis Ha, Truong & Ishikawa, sp. nov. [bA]	TXL2016-545	28, iv, 2016	Vietnam, Gia Lai	♂	OM908227	ON542894	OM868177	NSMT
B. griseocapillus Ha, Truong & Ishikawa, sp. nov. [bB]	HNL2018-007	05, v, 2018	Vietnam, Gia Lai	♀	OM908197	ON542854	OM868176	IEBR*
B. griseocapillus Ha, Truong & Ishikawa, sp. nov. [bB]	HNL2018-037	09, v, 2018	Vietnam, Dak Lak	♀	OM908208	ON542865	OM868189	VNMN
B. griseocapillus Ha, Truong & Ishikawa, sp. nov. [bB]	HNL2018-038	09, v, 2018	Vietnam, Dak Lak	♀	OM908209	ON542866	OM868191	NSMT
B. griseocapillus Ha, Truong & Ishikawa, sp. nov. [bB]	TXL2016-546	28, iv, 2016	Vietnam, Gia Lai	♂	OM908228	ON542895	OM868190	NSMT
B. luteicollis Ha, Truong & Ishikawa, sp. nov. [bC]	HNL2018-017	09, v, 2018	Vietnam, Dak Lak	♀	OM908198	ON542855	OM868179	VNMN
B. luteicollis Ha, Truong & Ishikawa, sp. nov. [bC]	HNL2018-018	09, v, 2018	Vietnam, Dak Lak	♀	OM908199	ON542856	OM868180	IEBR*
B. luteicollis Ha, Truong & Ishikawa, sp. nov. [bC]	HNL2018-019	09, v, 2018	Vietnam, Dak Lak	♀	OM908200	ON542857	OM868181	IEBR*
B. luteicollis Ha, Truong & Ishikawa, sp. nov. [bC]	HNL2018-020	09, v, 2018	Vietnam, Dak Lak	♀	OM908201	ON542858	OM868182	IEBR*
B. luteicollis Ha, Truong & Ishikawa, sp. nov. [bC]	HNL2018-021	09, v, 2018	Vietnam, Dak Lak	♀	OM908202	ON542859	OM868183	NSMT
B. luteicollis Ha, Truong & Ishikawa, sp. nov. [bC]	HNL2018-022	09, v, 2018	Vietnam, Dak Lak	♂	OM908203	ON542860	OM868184	NSMT
B. luteicollis Ha, Truong & Ishikawa, sp. nov. [bC]	HNL2018-023	09, v, 2018	Vietnam, Dak Lak	♀	OM908204	ON542861	OM868185	NSMT
B. luteicollis Ha, Truong & Ishikawa, sp. nov. [bC]	HNL2018-024	09, v, 2018	Vietnam, Dak Lak	♀	OM908205	ON542862	OM868186	NSMT
B. luteicollis Ha, Truong & Ishikawa, sp. nov. [bC]	HNL2018-025	09, v, 2018	Vietnam, Dak Lak	♂	OM908206	ON542863	OM868187	NSMT
B. luteicollis Ha, Truong & Ishikawa, sp. nov. [bC]	HNL2018-078	08, v, 2018	Vietnam, Gia Lai	♀	OM908214	ON542872	OM868195	IEBR*
B. luteicollis Ha, Truong & Ishikawa, sp. nov. [bC]	HNL2018-079	08, v, 2018	Vietnam, Gia Lai	♂	OM908215	ON542873	OM868196	IEBR*
B. luteicollis Ha, Truong & Ishikawa, sp. nov. [bC]	HNL2018-080	08, v, 2018	Vietnam, Gia Lai	♀	OM908216	ON542874	OM868197	IEBR*

Morphospecies	Specimen code	Collecting date	Locality	Sex	Accession numbers			Depository
					16S	Uni-Minibar (COI)	COI	
B. luteicollis Ha, Truong & Ishikawa, sp. nov. [bC]	HNL2018-081	08, v, 2018	Vietnam, Gia Lai	♀	OM908217	ON542875	OM868198	IEBR*
B. luteicollis Ha, Truong & Ishikawa, sp. nov. [bC]	HNL2018-082	08, v, 2018	Vietnam, Gia Lai	♀	OM908218	ON542876	OM868199	IEBR*
B. luteicollis Ha, Truong & Ishikawa, sp. nov. [bC]	HNL2018-083	08, v, 2018	Vietnam, Gia Lai	♂	OM908219	ON542877	OM868200	IEBR*
B. luteicollis Ha, Truong & Ishikawa, sp. nov. [bC]	HNL2018-084	08, v, 2018	Vietnam, Gia Lai	♂	OM908220	ON542878	OM868201	IEBR*
B. luteicollis Ha, Truong & Ishikawa, sp. nov. [bC]	HNL2018-085	08, v, 2018	Vietnam, Gia Lai	♂	OM908221	ON542879	OM868202	IEBR*
B. luteicollis Ha, Truong & Ishikawa, sp. nov. [bC]	HNL2018-086	08, v, 2018	Vietnam, Gia Lai	♂	OM908222	ON542880	OM868203	NSMT
B. luteicollis Ha, Truong & Ishikawa, sp. nov. [bC]	TXL2016-616	05, v, 2018	Vietnam, Dak Lak	♀	OM908229	ON542896	OM868208	IEBR
B. luteicollis Ha, Truong & Ishikawa, sp. nov. [bC]	TXL2016-617	05, v, 2018	Vietnam, Dak Lak	♂	OM908230	ON542897	OM868209	IEBR
B. confusus Hsiao et al., 1979 [bE]	NSMT-I-He-8263	15.v.1998	Vietnam, Cao Bang	♂	n/a	n/a	n/a	NSMT
B. confusus Hsiao et al., 1979 [bE]	NSMT-I-He-73786	18.v.2003	Vietnam, Lao Cai	♂	n/a	n/a	n/a	NSMT
B. confusus Hsiao et al., 1979 [bE]	VN-Hem-1998-010	15.v.1998	Vietnam, Cao Bang	♀	ON554779	ON542898	n/a	IEBR*
B. confusus Hsiao et al., 1979 [bE]	VN-Hem-1998-011	15.v.1998	Vietnam, Cao Bang	♀	n/a	ON542899	n/a	IEBR*
B. confusus Hsiao et al., 1979 [bE]	VN-Hem-1998-012	22-27.v.1998	Vietnam, Cao Bang	♀	n/a	ON542900	n/a	IEBR*
B. confusus Hsiao et al., 1979 [bE]	ADNg2020-027	6.vi.2020	Vietnam, Cao Bang		ON554766	ON542882	n/a	IEBR*
B. flavinotus (Matsumura, 1913) [bD] (lectotype)			Taiwan, Gyochi (Yuechih)	♀	n/a	n/a	n/a	HU
B. flavinotus (Matsumura, 1913) [bD]		iv-v.1928	Taiwan	♂	n/a	n/a	n/a	HU
B. flavinotus (Matsumura, 1913) [bD]	HNL2018-117	12, v, 2018	Vietnam, Lang Son	♀	OM908223	ON542881	OM868204	IEBR*
B. flavinotus (Matsumura, 1913) [bD]	TXL2000-006	20, x, 2000	Vietnam, Son La	♀	n/a	n/a	n/a	IEBR
B. flavinotus (Matsumura, 1913) [bD]	HEM-TH1999-002	25, iii, 1999	Thailand, Chiang Mai	♀	n/a	n/a	n/a	NSM
B. flavinotus (Matsumura, 1913) [bD]	HEM-TH2004-022	3, vi, 2004	Thailand, Chiang Rai	♀	n/a	ON542892	n/a	NSM
B. flavinotus (Matsumura, 1913) [bD]	TW-Redu-2014-001	3, vii, 2014	Taiwan, Nantou	♀	ON554776	ON542893	n/a	TARI-AZ
B. flavinotus (Matsumura, 1913) [bD]	TW-Redu-2019-001	3, v, 2019	Taiwan, Taitung	♀	ON554777	n/a	n/a	TARI-AZ
B. flavus (Distant, 1903) [bF]	LA-Redu-2004-006	15, v, 2004	Laos, Houaphan	♀	ON554778	ON542883	n/a	NUOL-FA
B. flavus (Distant, 1903) [bF]	LA-Redu-2004-011	21, v, 2004	Laos, Houaphan	♂	n/a	n/a	n/a	NUOL-FA
B. flavus (Distant, 1903) [bF]	LA-Redu-2004-014	22, v, 2004	Laos, Houaphan	♂	n/a	n/a	n/a	NUOL-FA
B. flavus (Distant, 1903) [bF]	HEM-TH2004-016	24, v, 2004	Thailand, Chiang Mai	♂	ON554770	ON542887	n/a	NSM
B. flavus (Distant, 1903) [bF]	HEM-TH2004-017	24, v, 2004	Thailand, Chiang Mai	♀	ON554771	ON542888	n/a	NSM
B. flavus (Distant, 1903) [bF]	HEM-TH2004-018	25, v, 2004	Thailand, Chiang Mai	♂	ON554772	ON542889	n/a	NSM
B. flavus (Distant, 1903) [bF]	HEM-TH2004-019	25, v, 2004	Thailand, Chiang Mai	♂	ON554773	ON542890	n/a	NSM

Morphospecies	Specimen code	Collecting date	Locality	Sex	Accession numbers			Depository
					16S	Uni-Minibar (COI)	COI	
B. flavus (Distant, 1903) [bF]	HEM-TH2004-021	3, vi, 2004	Thailand, Chiang Rai	♀	ON554774	ON542891	n/a	NSM
B. flavus (Distant, 1903) [bF]	LA-Redu-2008-005	4, v, 2008	Laos, Xieng Khouang	♀	ON554767	ON542884	n/a	NUOL-FA
B. flavus (Distant, 1903) [bF]	LA-Redu-2010-004	11, v, 2010	Laos, Xieng Khouang	♀	ON554768	ON542885	n/a	NUOL-FA
B. flavus (Distant, 1903) [bF]	LA-Redu-2010-005	11, v, 2010	Laos, Xieng Khouang	♂	ON554769	ON542886	n/a	NUOL-FA
Outgroups								
Sphedanolestes pubinotus Reuter, 1881	HNL2019-002	11, iii, 2019	Vietnam, Quang Tri	♀	OP106594	OP103647	n/a	IEBR
Rhynocoris mendicus (Stål, 1867)	HNL2018-040	9, v, 2018	Vietnam, Gia Lai	♂	OP106592	OP103646	n/a	IEBR*
Coranus sp.	TXL2018-128	15, vi, 2018	Vietnam, Son La	♀	OP106593	OP103648	n/a	IEBR*

Morphological examination and imaging

External structural characteristics were observed for dry-mounted and ethanol-preserved specimens using a Nikon SMZ1270 stereomicroscope. The genitalia were prepared for examination as described below. Firstly, each male specimen was relaxed by soaking for 3 days in 70% ethanol. After that, the male genitalia was detached from the body and then soaked in hot 10% KOH for five minutes until body fat and muscle was released. The endosoma was pulled out of the phallosoma by fine tweezers after removing the phallus from the pygophore. All parts of male genitalia were preserved in a genitalia vial filled with propylene glycol and subsequently associated with the pinned specimens. Next, the female genitalia were inspected without being detached from the body. A Nikon SMZ1270 stereomicroscope was used to examine the male and female genital morphology.

Focus stacking was executed using Helicon Focus Pro 7.5.3 software (Helicon Soft Ltd., Ukraine) based on a sequence of the source pictures photographed by a Canon EOS Kiss X9 digital camera connected to a Nikon AZ100 stereomicroscope, and artifacts were removed using the retouch function of the software. After that, the contrast, brightness, color balance, and intensity were adjusted using Adobe Photoshop Elements 10.0 software (Adobe Systems Incorporated, San Jose, CA, USA) using a color corresponding sticker (CASMATCH, Bear Medic Corporation, Japan).

Measurement, indices, and terminology

Morphological terminology (Figs 1–3) followed that of Schuh and Weirauch (2020), Forero and Weirauch (2012), and Rosa et al. (2005). The following parts of the bodies were measured for 52 out of 56 *Biasticus* samples (Table 1; Fig. 4), using the software Image-J (http://imageJ.nih.gov/ij/) based on the direct stacking pictures designed as stated above. The assessment features were stated below (Fig. 4), and all dimensions were given in mm:

BL body length excluding hemelytra;
HL head length;
AoL length of anteocular area of head;
AoW width of anteocular area of head, measured immediately in front of compound eyes;
PoL length of postocular area of head;
PoW maximum width of postocular area of head;
OE maximum distance measured between outer margins of compound eyes;
IE width of synthlipsis, minimum distance measured between inner margins of compound eyes;
ED maximum diameter of left compound eye;
OD maximum diameter of left ocellus;
OCD minimum distance measured between inner margins of lateral ocelli;
COD minimum distance between postero-inner margin of left compound eye and antero-outer margin of left lateral ocellus;
R1L length of first visible labial segment;
R2L length of second visible labial segment;
R3L length of third visible labial segment;
A1L length of scape;
A2L length of pedicel;
A3L length of first flagellomere;
A4L length of second flagellomere;
PnL pronotal length;
PnW maximum pronotal width;
APL length of anterior pronotal lobe;
PPL length of posterior pronotal lobe;
HeL length of right hemelytron;
HeW maximum width of right hemelytron;
Sc length of Sc of right hemelytron;
R+M length of R + M of right hemelytron;
HWL length of right hind wing;
HWW maximum width of right hind wing;
AFL length of left fore femur;
ATL length of left fore tibia;
MFL length of left mid femur;
MTL length of left mid tibia;
PFL length of left hind femur;
PTL length of left hind tibia.

The RGB color values were produced using Adobe Photoshop Elements 10.0 software from a virtual circle in the center of the posterior pronotal lobe with a diameter equal to the anteromedian and posteromedian edges of the posterior pronotal lobe (blue circle in Fig. 4A). The average blur function was then used to calculate mean color values, such as mR (red), mG (green), and mB (blue).

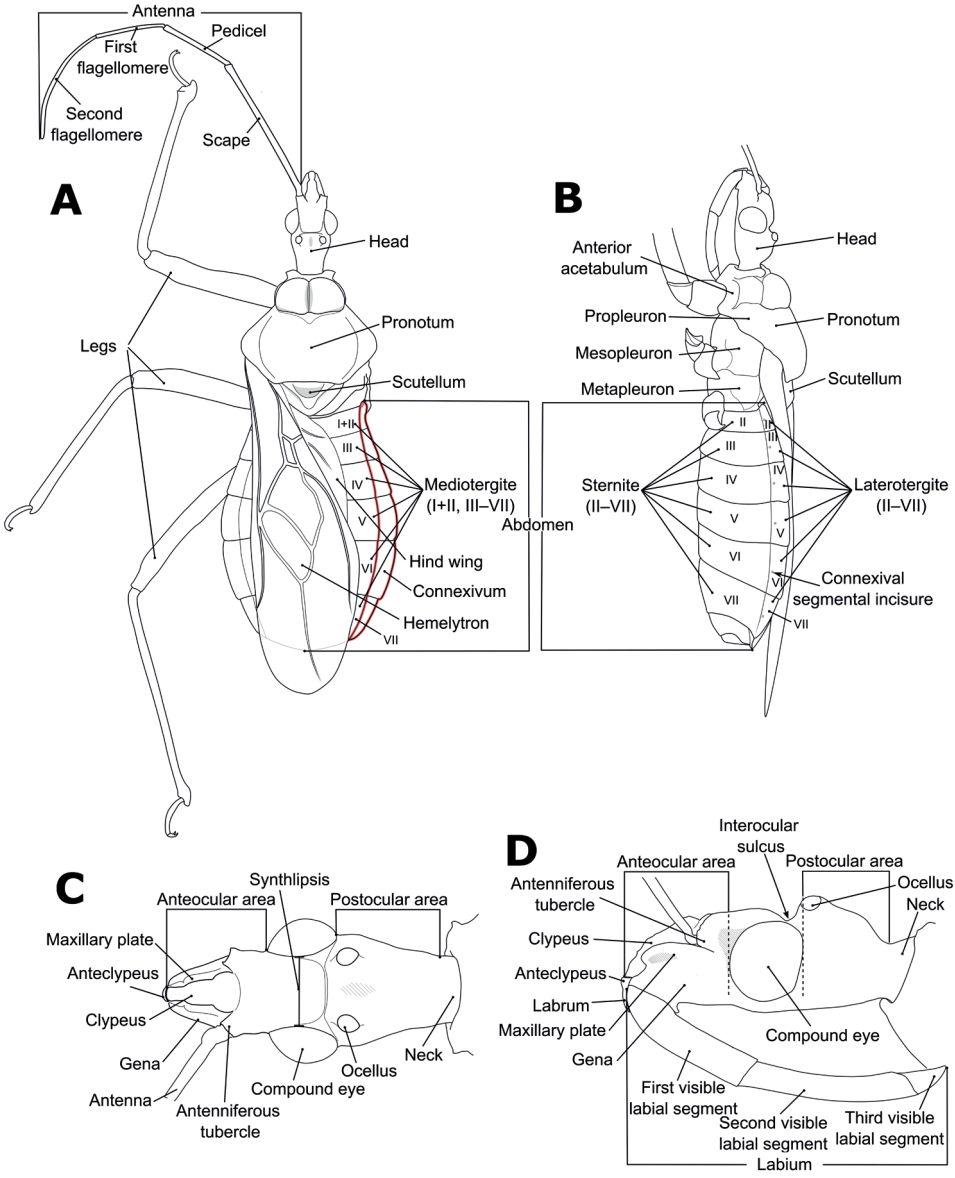

Figure 1. Structure and morphological terms of *Biasticus* species. Drawing based on *Biasticus luteicollis* Ha, Truong & Ishikawa, sp. nov., paratype, ♀, HNL2018-024 **A** 4 body in dorsal view **B** body in lateral view **C** head in dorsal view **D** head in lateral view.

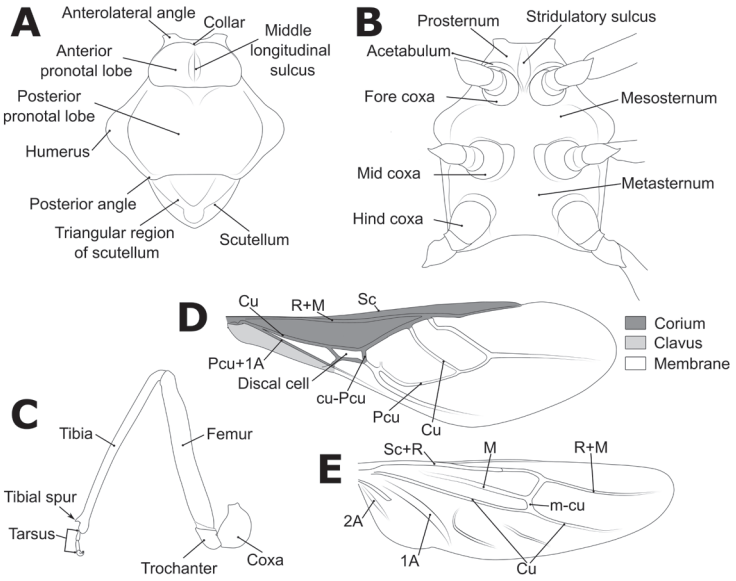

Figure 2. Structure and morphological terms of *Biasticus* species. Drawing based on *Biasticus luteicollis* Ha, Truong & Ishikawa, sp. nov., paratype, ♀, HNL2018-024 **A** pronotum and scutellum in dorsal view **B** thorax in ventral view **C** right fore leg in anterior view **D** right hemelytron in dorsal view **E** right hind wing in dorsal view.

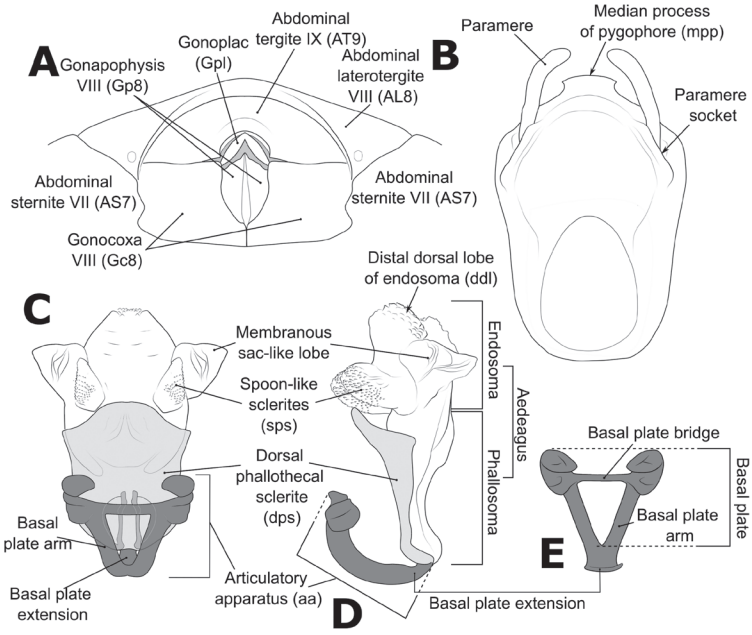

Figure 3. Structure and morphological terms of *Biasticus* species. Drawing based on *Biasticus luteicollis* Ha, Truong & Ishikawa, sp. nov. **A** paratype ♀ HNL2018-024 **B–E** holotype ♂ HNL2018-025. **A** female external genitalia in ventral view **B** pygophore with parameres of male genitalia in dorsal view **C** phallus in dorsal view **D** phallus in lateral view **E** articulatory apparatus in ventral view.

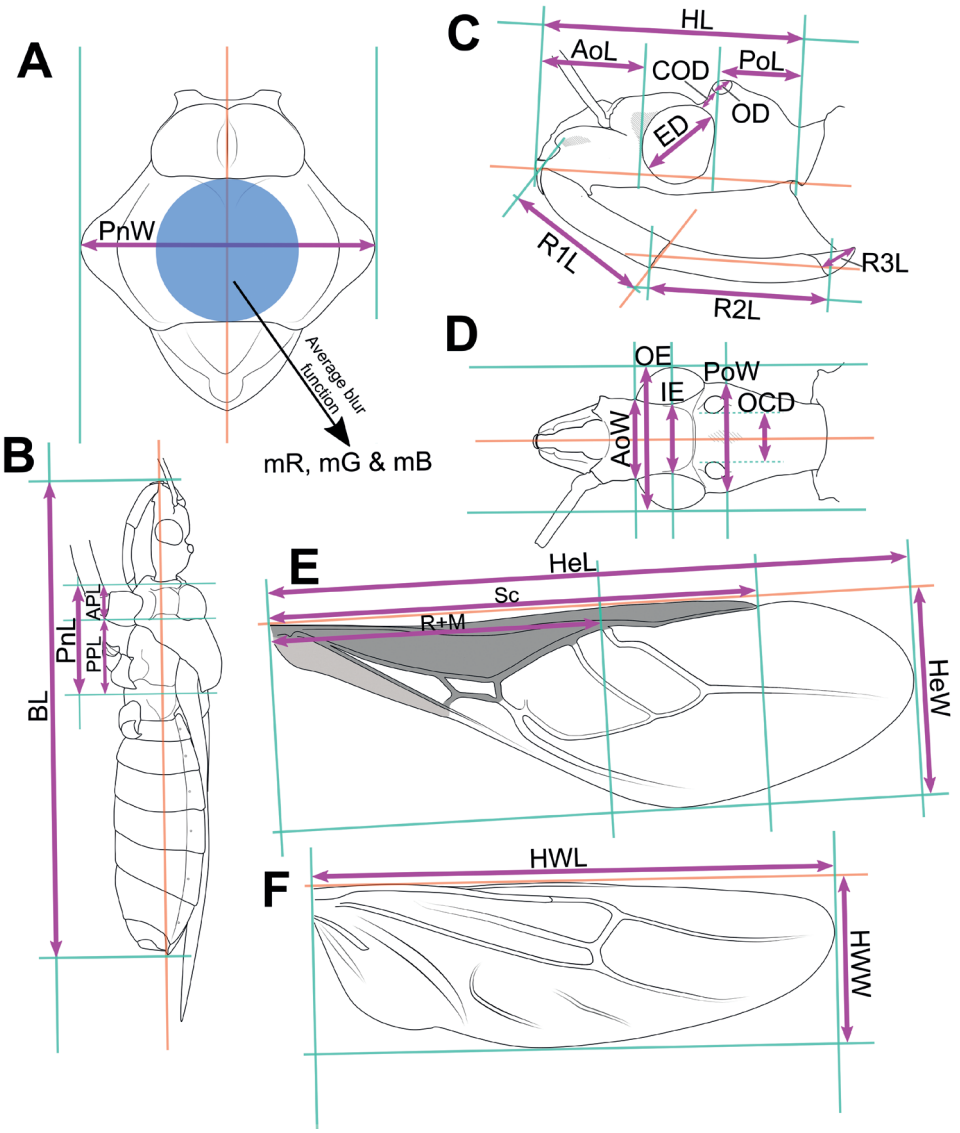

Figure 4. Measurement characters of *Biasticus* species. Drawing based on *Biasticus luteicollis* Ha, Truong & Ishikawa, paratype, sp. nov., ♀, HNL2018-024. **A** pronotum and scutellum in dorsal view, the circle in the center of posterior pronotal lobe with the diameter equal to the minimum length of posterior pronotal lobe, at which the RBG color information was measured for calculating the average RBG color information in the form "mR", "mG", "mB" **B** body in lateral view **C** head in lateral view **D** head in dorsal view **E** hemelytron in dorsal view **F** hind wing in dorsal view.

Morphometric analyses

Considering the weak to moderate sexual dimorphism of external morphology, the Principal Component Analyses (**PCA**) were performed separately for the female adult and male adult datasets using R software 4.1.2 (R core team 2021). The morphometric

dataset comprised 31 morphological features (head length (HL), length of anteocular area of head (AoL), length of postocular area of head (PoL), width of anteocular area of head (AoW), maximum width of postocular area of head (PoW), maximum distance measured between outer margins of compound eyes (OE), width of synthlipsis (IE), maximum diameter of left compound eye (ED), maximum diameter of left ocellus (OD), minimum distance measured between inner margins of lateral ocelli (OCD), minimum distance between postero-inner margin of left compound eye and antero-outer margin of left lateral ocellus (COD), length of first visible labial segment (R1L), length of second visible labial segment (R2L), length of scape (A1L), length of pedicel (A2L), length of first flagellomere (A3L), length of second flagellomere (A4L), length of right hemelytron (HeL), maximum width of right hemelytron (HeW), length of Sc of right hemelytron (Sc), length of R + M of right hemelytron (R+M), length of left fore femur (AFL), length of left fore tibia (ATL), length of left mid femur (MFL), length of left mid tibia (MTL), length of left hind femur (PFL), and length of left hind tibia (PTL)), and proportion of mean values of three color indices (mR, mG, and mB) of the central region of posterior pronotal lobe to sum of mR, mG, and mB (mRr = mR/(mR + mG + mB), mGr = mG/(mR + mG + mB), and mBr = mB/(mR + mG + mB)). The function "fviz_pca_ind" (factoextra package) (Kassambara and Mundt 2020) was used to graph the 2D plot of PCA. To determine the most prominent contributing morphometric characters in each male and female dataset, we used the "get_pca_var" (factoextra package) function to test the contribution of variables to the dimensions of PCA (Kassambara and Mundt 2020).

Raw morphometric datasets and the R-scripts used for the data design and analyses are presented in additional files (Suppl. materials 1–3).

Molecular data preparation

DNA was isolated from the right or left hind tibia of each specimen by the Chelex-TE-ProK protocol (Satria et al. 2015). The mitochondrial 16S and COI gene fragments were examined using the primers presented in Table 2. Polymerase chain reaction (PCR) amplification, cycle sequencing reaction, sequencing using ABI PRISM 3130xl (Applied Biosystems), and sequence assembly using ChromasPro 1.7.6 (Technelysium Pty Ltd., Australia) were executed using the methods of Satria et al. (2015), Simon et al. (1994), Cognato and Vogler (2001), Meusnier et al. (2008), Shekhovtsov et al. (2013), Bely and Wray (2004), and Zhang and Weirauch (2013). The PCR thermal situation for the two gene fragments, 16S and COI, comprised of initial denaturation 94 °C (2 min), denaturation 94 °C (30 s), annealing at appropriate annealing temperature (30 s) (Table 2), and extension 72 °C (45 s) for 35 cycles, with final extension at 72 °C (7 min). COI sequences were effectively obtained from 31 out of the 56 *Biasticus* samples and 16S sequences were effectively derived from 45 of the 56 *Biasticus* samples. The PCR thermal cycles for the mini-barcode of COI, i.e., Uni-Minibar, comprised of initial denaturation 95 °C (2 min), denaturation 95 °C (1 min), annealing 46 °C (1 min), and extension 72 °C (30 s) for 5 cycles, then denaturation 95 °C (1 min), annealing 53 °C (1 min), and extension 72 °C (30 s) for 35 cycles, with final

Table 2. Primers used for PCR amplification and Sanger sequencing.

Gene	Forward	Reverse	Annealing temperature	Source
16S	16sa: 5'-CGC CTG TTT ATC AAA AAC AT-3'	16sb: 5'-CTC CGG TTT GAA CTC AGA TCA-3'	48 °C	Kessing et al. (1989)
	LR-J-12961 (F): 5'- TTT AAT CCA ACA TCG AGG -3'	LR-J-13417 (R): 5'- CGC CTG TTT AAC AAA AAC AT -3'	47 °C	Simon et al. (1994) Cognato and Vogler (2001)
COI	Uni-Minibar (F1): 5'- TCC ACT AAT CAC AAR GAT ATT GGT AC -3'	Uni-Minibar (R): 5'- GAA AAT CAT AAT GAA GGC ATG AGC -3'	53 °C	Meusnier et al. (2008)
	LCO1490m: 5'-TAC TCA ACA AAT CAC AAA GAT ATT GG-3'	3' COI-E: 5'-TAT ACT TCT GGG TGT CCG AAG AAT CA-3'	48.5 °C	Shekhovtsov et al. (2013) Bely & Wray (2004)
	COI_Harp_F: 5'-ATT GGA AAT GAY CAA ATY TAT A-3'	COI_Harp_R: 5'-GAD GTA TTA AAR TTW CGR TCW-3'	48.5 °C	Zhang & Weirauch (2013)

extension at 72 °C (5 min). Uni-Minibar sequences were successfully derived from 47 of the 56 *Biasticus* samples.

Test for association was performed using MUSCLE implemented in MEGA X (Kumar et al. 2018) with default setting (Gap Open = -400.00; Gap Extend = 0.00; Cluster Method [Iterations 1,2 and Other iterations] = UPGMA; Min Diag Length [Lambda] = 24) for COI and 16S sequences while including and excluding outgroups (OG+ or OG–): $16S^{(OG+)}$ (487 bp), and $16S^{(OG-)}$ (487 bp), $COI^{(OG-)}$ (603 bp), Uni-$Minibar^{(OG+)}$ (174 bp), Uni-$Minibar^{(OG-)}$ (174 bp) datasets. The $16S^{(OG+)}$ and Uni-$Minibar^{(OG+)}$ datasets were aggregated to produce a concatenated 16S + Uni dataset (661 bp). The FASTA-configured files derived from MEGA X were then converted to NEXUS layout or PHYLIP design, which were suitable input layouts for molecular phylogenetic examination and estimation of genetic distances and species delimitation analysis by ClustalX 2.0.11 (Larkin et al. 2007).

Molecular phylogenetic analyses

Molecular phylogenetic analyses were done based on the concatenated 16S + Uni dataset since the number of specimens that were successfully obtained 16S gene fragment and Uni-Minibar gene fragment were the highest. The substitution models, K3Pu + F + I + G4, TIM2e + G4, and (K3Pu + F + I + G4, TIM2e + G4), were selected respectively for the $16S^{(OG+)}$, Uni-$Minibar^{(OG+)}$, and the concatenated 16S + Uni datasets by Model Finder (Kalyaanamoorthy et al. 2017) executed in IQ-TREE 2.1.2 (Minh et al. 2020). Maximum likelihood (**ML**) examinations were then carried out using IQ-TREE 2.1.2 (Chernomor et al. 2016; Minh et al. 2020); bootstrap values (**BP**) were estimated from 1,000 replications. The generalized time-reversible (**GTR**) + Gamma model was chosen for the 16S + Uni dataset using Model Finder (Kalyaanamoorthy et al. 2017) under the Bayesian information criterion. The Bayesian inference (**BI**) evaluations were then executed for the data using MrBayes v. 3.2.6 (Ronquist and Huelsenbeck 2003) with 20,000,000 production and statutory parameter configuration (examining every 500 generations and tuning constraints every 100 generations,

with a burn-in of 25%). The effective sampling size (ESS) of each constraint was verified to be > 200 using Tracer 1.7.1 (Rambaut et al. 2018). The nodes were designated as "well supported" when posterior probability (**PP**) ≥ 0.95 and BP ≥ 80.

Species delimitation analyses

To create species partitions, two different protocols, i.e., Assemble Species by Automatic Partitioning (**ASAP**) (Puillandre et al. 2021) and Bayesian implementation of the Poisson Tree Processes model (**bPTP**) for species delimitation (Zhang et al. 2013), were used with pairwise genetic distances. For ASAP, the FASTA-configured files of 16S$^{(OG-)}$, Uni-Minibar$^{(OG-)}$, and COI$^{(OG-)}$ datasets were used and executed on the ASAP website (https://bioinfo.mnhn.fr/abi/public/asap), with two replacement samples to estimate the distances, i.e., simple p-distance model and K2P model. The bPTP were executed in the bPTP online server (https://species.h-its.org) based on the NEXUS formatted input files of 16S$^{(OG-)}$, Uni-Minibar$^{(OG-)}$ and COI$^{(OG-)}$ datasets, with default values (100,000 Markov chain Monte Carlo [MCMC] generations, thinning = 100, burn-in = 0.1, and Seed = 123).

Results and discussion

Examination of genital morphology in the female and male

Thirty-five female specimens were grouped into six female-based morphospecies (fA–fF) based on the characteristics observed in the externally visible part of genitalia. The type fA (= *Biasticus taynguyenensis* sp. nov.) (6 specimens) was characterized by the following features: abdominal sternite VII (AS7) forming a semicircular or broad subpentagonal median concavity, with inner posterolateral margin very weakly sinuate; gonocoxa VIII (Gc8) with posterior margin gently slanting anteromesad, with apical inner corner weakly produced mesad and forming an acute apex, with inner margin weakly incurved in rear 2/3; abdominal laterotergite VIII (AL8) visible as a thin bridge above the posteromedian part of abdominal tergite IX (AT9) (Figs 5A, 15A). The type fB (= *B. griseocapillus* sp. nov.) (3 specimens) was characterized by the following features: AS7 forming a broad subpentagonal posteromedian concavity, with inner posterolateral margin almost straight; Gc8 with posterior margin gently slanting anteromesad, with an apical inner corner but not formed, with inner margin strongly slanting anteromesad and slightly incurved; AL8 visible as a thin bridge above the posteromedian part of AT9 (Figs 5B, 18A). The type fC (= *B. luteicollis* sp. nov.) (12 specimens) was characterized by the following features: AS7 producing a wide subrectangular concavity, with posteromedian margin almost straight, with inner posterolateral margin poorly sinuous; Gc8 with almost horizontal and poorly sinuous posterior margin, with apical inner corner weakly and formed posteromesad and forming a blunt apex, with inner margin strongly incurved in its posterior 2/3; AL8 visible as a relatively thick bridge above the

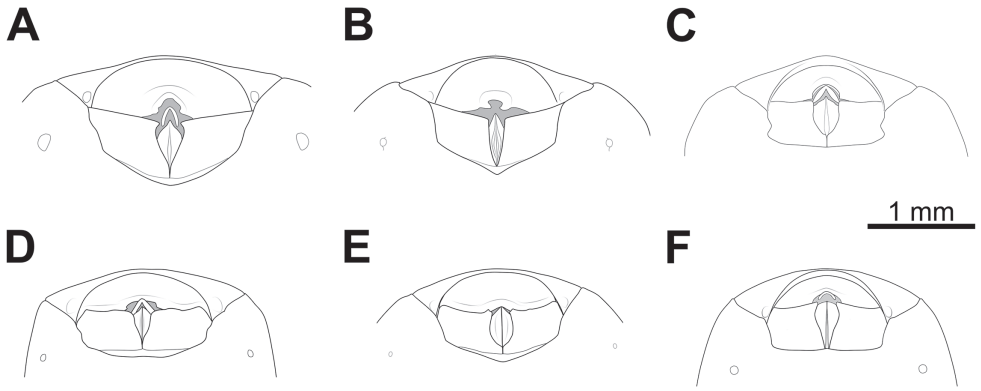

Figure 5. Female external genitalia of six morphospecies in ventral view **A** type fA, *Biasticus taynguyenensis* Ha, Truong & Ishikawa, sp. nov., holotype, ♀, HNL2018-073 **B** type fB, *B. griseocapillus* Ha, Truong & Ishikawa, sp. nov., holotype, ♀, HNL2018-038 **C** type fC, *B. luteicollis* Ha, Truong & Ishikawa, sp. nov., paratype, ♀, HNL2018-024 **D** type fD, *B. flavinotus* (Matsumura, 1913), ♀, HNL2018-117 **E** type fE, *B. confusus* Hsiao et al., 1979, ♀, VN-Hem-1998-012 **F** type fF, *B. flavus* (Distant, 1903), ♀, LA-Redu-2004-006.

posteromedian part of AT9 (Figs 5C, 21A). The type fD (= *B. flavinotus*) (7 specimens, including lectotype) was characterized by the following features: AS7 forming a wide subrectangular concavity, with posteromedian margin poorly incurved, with inner posterolateral margin poorly sinuous; Gc8 with almost horizontal and poorly sinuous rear margin, with rounded apical inner corners, with inner margin considerably slanting anteromesad in rear 2/3; AL8 visible as a thin bridge above the posteromedian part of AT9 (Figs 5D, 7F). The type fE (= *B. confusus*) (3 specimens) was characterized by the following features: AS7 forming a wide subpentagonal concavity, with inner posterolateral margin almost straight; Gc8 with rear margin slightly slanting anteromesad and almost incurved, with apical inner corner poorly formed posteromesad and producing a blunt apex, with inner margin considerably incurved in its rear 2/3; AL8 apparent as a thin linkage above the posteromedian part of AT9 (Figs 5E, 8F). The type fF (= *B. flavus*) (5 specimens) was characterized by the following features: AS7 forming a wide subrectangular concavity, with posteromedian margin nearly straight, with inner posterolateral margin almost straight; Gc8 with posterior margin slightly slanting posteromesad and slightly incurved, with apical inner corner poorly developed posteromesad and producing an acute apex, with inner margin weakly sinuous; AL8 visible as a thin bridge above the posteromedian part of AT9 (Figs 5F, 10A).

In contrast, based on characteristics present in male genitalia (pygophore and aedeagus), 17 adult male specimens were divided into four male-based morphospecies (mA–mC, mF). The type mA (= *B. taynguyenensis* sp. nov.) (1 specimen) was characterized by the following features: the median process of pygophore (mpp) broad and low, with apical margin weakly and progressively concave, with apicolateral corner specifically formed posterolaterad and emarginated (Figs 6A, 15B–E); endosoma with spoon-like sclerites (sps) hyaline and glabrous (Figs 6B, 15I); distal dorsal lobe of

endosoma (ddl) round, with membranous surface roughly lumpy; dorsal phallothecal sclerite (dps) in lateral view with posteromedian part poorly formed posterodorsad (Figs 6C, 15K); articulatory apparatus (aa) in ventral view with comparatively slender basal plate arms that mutually form a U-shape (Figs 6D, 15H), in lateral view arched

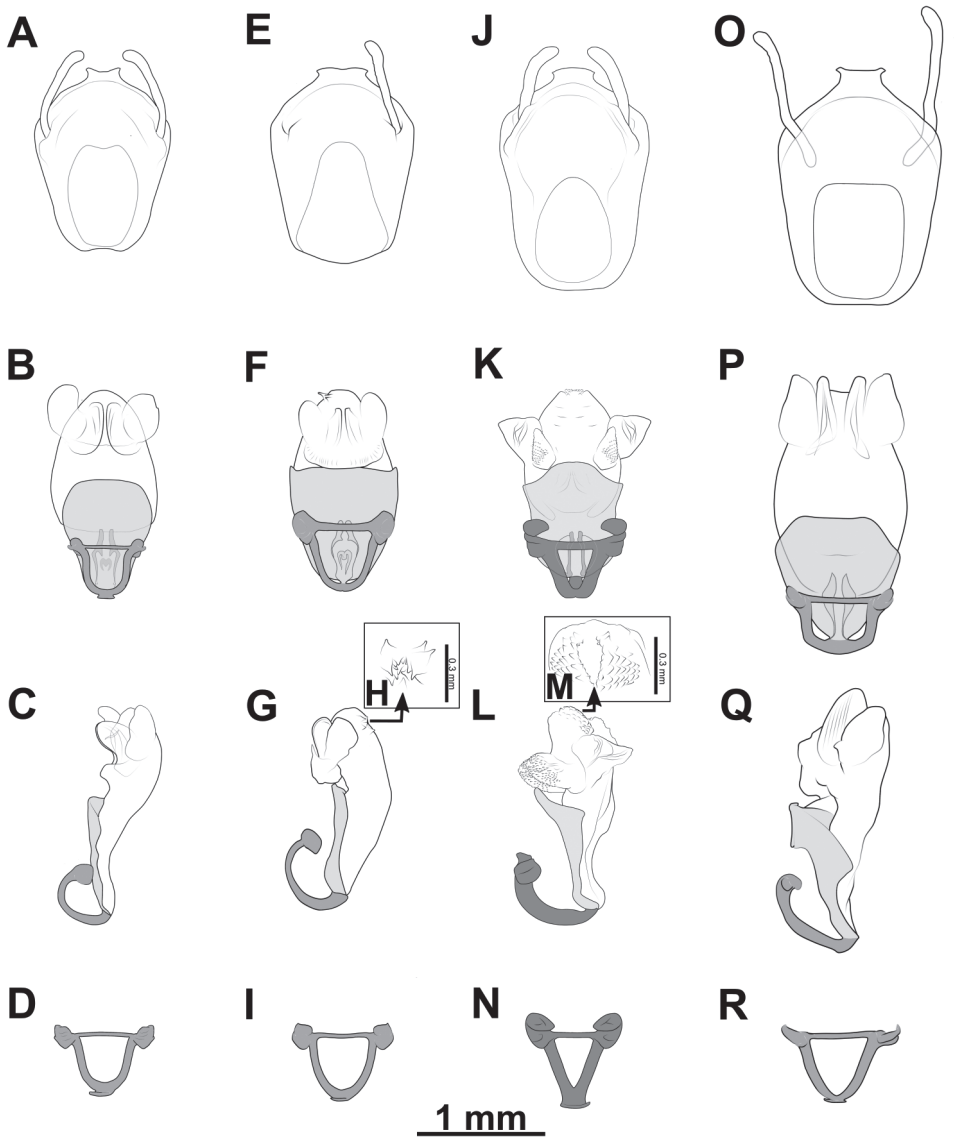

Figure 6. Male genitalia of four morphospecies **A–D** type mA, *Biasticus taynguyenensis* Ha, Truong & Ishikawa, sp. nov., paratype, ♂, TXL2016-545 **E–I** type mB, *B. griseocapillus* Ha, Truong & Ishikawa, sp. nov., paratype, ♂, TXL2016-546 **J–N** type mC, *B. luteicollis* Ha, Truong & Ishikawa, sp. nov., holotype, ♂, HNL2018-025 **O–R** mF, *B. flavus* (Distant, 1903), ♂, HEM-TH2004-018. **A, E, J, O** pygophore with paramere(s) in dorsal view **B, F, K, P** phallus in dorsal view **C, G, L, Q** phallus in lateral view **D, I, N, R** articulatory apparatus **H, M** distal dorsal lobe of endosoma.

intensely (Figs 6C, 15G). The type mB (*B. griseocapillus* sp. nov.) (1 specimen) was characterized by the following features: mpp broad and low, with apical margin slightly convex and emarginate medially, with apicolateral corner slightly formed laterad and not emarginated (Figs 6E, 18B–E); sps hyaline and glabrous (Fig. 6F, 18J); ddl round, with membranous surface enclosed with large hyaline prickles (Figs 6G, H, 18L, M); dps in lateral view with posteromedian part slightly formed posterodorsad (Figs 6G, 18L); aa in ventral view with comparatively slender basal plate arms that mutually form a U-shape (Figs 6I, 18I), in lateral view arched intensely (Figs 6G, 18H). The type mC (= *B. luteicollis* sp. nov.) (8 specimens) was characterized by the following features: mpp broad and low, with apical margin slightly and constantly convex and did not emarginate, with apicolateral corner slightly formed laterad and emarginated (Figs 6J, 21B–E); sps semi-hyaline and enclosed with tiny blunt spikes (Figs 6K, 21F); ddl round, with a membranous surface covered with small but distinctive spikes (Figs 6L, M, 21G, J); dps in lateral view with posteromedian part very strongly developed posterodorsad (Figs 6L, 21G); aa in ventral view with comparatively broad basal plate arms that mutually formed a V-shape (Figs 6N, 21I), in lateral view arched slightly (Figs 6L, 21G). The type mF (= *B. flavus*) (6 specimens) was characterized by the following features: mpp broad and low, with apical margin weakly and progressively concave, with apicolateral corner specifically formed posterolaterad and blunt at the apex (Figs 6O, 10B–E); sps hyaline and glabrous (Figs 6P, 10I); ddl round, with membranous surface roughly lumpy (Figs 6Q, 10K); dps in lateral view with posteromedian part poorly formed posterodorsad, producing a flat dorsal outline (Figs 6Q, 10K); aa in ventral view with comparatively slender basal plate arms that mutually form a U-shape (Figs 6R, 10H), in lateral view arched poorly (Figs 6Q, 10G, K).

Examination of other morphological features in the female and the male

Fifty-six *Biasticus* specimens were sorted into six morphospecies (bA–bF) based on external body morphology. The type bA (= *B. taynguyenensis* sp. nov.) consisting of fA and mA was characterized by the following features: body shiny blackish brown (Fig. 13A); base of first visible labial segment yellowish brown, remaining of labium black, tips of first and second visible labial segments pale luteous (Fig. 13D); scape ~ 1.5 × as long as head, pedicel slightly longer than first flagellomere and ~ equal in length to second flagellomere; proportional average length of scape, pedicel, first and second flagellomeres 3.1:1.6:1.4:1.6; anterior pronotal lobe blackish brown or black with some rows of short bent cream-yellow setae (Fig. 14A, B); posterior pronotal lobe blackish brown or dark brown, densely covered with short bent cream-yellow setae, interspersed with long erect setae (Fig. 14A, C, D); scutellum wholly black or blackish brown (Fig. 14A); abdominal mediotergites I+II to IV and middle of mediotergite V blackish brown; posterior half of mediotergite V to apex of abdomen, and abdominal sternites sanguineous (Fig. 13A, B); laterotergites II–IV luteous, anterior half of laterotergite V suffused with brown, posterior half of laterotergite V to

apex of abdomen sanguineous (Fig. 13B); femora and tibiae blackish brown (Fig. 13A, B). The type bB (= *B. griseocapillus* sp. nov.) consisting of fB and mB was characterized by the following features: body shiny blackish brown (Fig. 16A); first visible labial segment brown, second and third visible labial segments blackish brown, tips of first and second visible labial segments yellowish brown (Fig. 16D); scape ~ 1.5 × as long as head; pedicel slightly longer than first flagellomere and nearly equal in length to second flagellomere; proportional average length of scape, pedicel, first and second flagellomeres 3.0:1.6:1.4:1.6; anterior pronotal lobe black or blackish brown with some rows of long bent griseous setae (Fig. 17A, B); posterior pronotal lobe blackish brown or brown and densely covered with short bent griseous setae somewhat interspersed with long griseous setae (Fig. 17A, C, D); scutellum black in basal half and dark brown or brown in lateral margin and apical half (Fig. 17A); abdominal mediotergites I+II to V reddish brown or sanguineous, somewhat suffused with blackish brown, mediotergite VI suffused with reddish brown and irregularly suffused with sanguineous, mediotergite VII to posterior apex of abdomen sanguineous; abdominal sternites shiny sanguineous (Fig. 16B); laterotergites II–VI luteous, segmentally suffused with dark brown spots or blackish brown spots, laterotergite VII sanguineous (Fig. 16B); femora and tibiae blackish brown. The type bC (= *B. luteicollis* sp. nov.) consisting of fC and mC was characterized by the following characters: body shiny luteous (Fig. 19A); first visible labial segment and base of second visible labial segment luteous, apical 2/3 of second visible labial segment to third visible labial segment yellowish brown or brown (Fig. 19D); scape ~ 1.3 × as long as head; pedicel ~ as long as first flagellomere and ~ 0.7 × as long as second flagellomere; proportional average length of scape, pedicel, first and second flagellomeres 2.7:1.3:1.3:1.7; pronotum covered with long thick erect setae (Fig. 20A, C); anterior pronotal lobe, except lateral margin, shiny dark brown, sometimes with luteous suffusion centrally (Fig. 20B); posterior pronotal lobe luteous (Fig. 20A); scutellum dark brown in basal half and luteous in apical half, with median pale brownish luteous portion (Fig. 20A); abdominal mediotergites, except posterior half of mediotergite VII, dark brown and darker backward, posterior half of mediotergite VII luteous; abdominal sternites pale luteous (Fig. 19B); connexivum pale luteous, with segmentally dark brown suffusions (Fig. 19B); femora luteous with dark brown or yellowish brown suffusions at apex and sometimes at middle (Fig. 19A). The type bD consisting of fD only was characterized by the following features: body black (Fig. 7A); first and third visible labial segments and base of second visible labial segment black, remaining of second visible labial segment blackish brown (Fig. 7D); scape nearly 1.5 × as long as head; pedicel ~ 0.6 × as long as first flagellomere and ~ 0.4 × as long as second flagellomere; proportional average length of scape, pedicel, first and second flagellomeres 2.9:1.1:1.7:2.4; pronotum covered with short bent cream-yellow setae (Fig. 7E); anterior pronotal lobe black, posterior pronotal lobe luteous (Fig. 7E); scutellum wholly blackish brown to black (Fig. 7E); abdominal mediotergites, except lateral margins of mediotergite VII, blackish brown or dark reddish brown, lateral margins of mediotergite VII luteous; abdominal sternites luteous with some blackish brown or black segmental transverse stripes laterally (Fig. 7B);

Figure 7. *Biasticus flavinotus* (Matsumura, 1913), ♀, TW-Redu-2014-001 **A** body in dorsal view **B** body in lateral view **C** head in dorsal view **D** head in lateral view **E** pronotum in dorsal view **F** female external genitalia in ventral view.

connexivum yellow to sanguineous (Fig. 7B); femora and tibiae black (Fig. 7A). This morphospecies corresponded to *B. flavinotus*. The type bE consisting of fE only was characterized by the following features: body shiny black (Fig. 8A); labium dark brown (Fig. 8D); scape ~ 1.7 × as long as head, pedicel approximately equal in length to first flagellomere and shorter than second flagellomere; proportional average length of scape, pedicel, first and second flagellomeres 3.5:1.6:1.6:2.1; pronotum dark brown to blackish brown (Fig. 8E); central disc of scutellum blackish brown, remaining of scutellum dark brown (Fig. 8E); abdominal mediotergites and sternites luteous to pale sanguineous (Fig. 8B); connexivum sanguineous (Fig. 8B); femora and tibiae dark brown to blackish brown (Fig. 8A). This morphospecies corresponded to *B. confusus*. The type bF consisting of fF and mF was characterized by the following features: body shiny black (Fig. 9A); labium blackish brown, paler apically (Fig. 9D); scape ~ 1.5 × as long as head, pedicel slightly longer than first flagellomere and subequal in length to second flagellomere; proportional average length of scape, pedicel, first and second flagellomeres 3.2:1.7:1.4:1.7; pronotum densely covered with long thick yellow erect setae (Fig. 9E); anterior pronotal lobe blackish brown to black with some rows of short yellow bent setae (Fig. 9E); posterior pronotal lobe luteous, somewhat anteriorly centrally suffused with blackish brown (Fig. 9E); scutellum blackish brown to black, except posterior halves of lateral margins and posterior apex luteous (Fig. 9E); abdominal mediotergites luteous with irregular brown suffusion, sometimes mediotergites wholly brown; abdominal sternites luteous with some blackish brown or black segmental transverse stripes laterally (Fig. 9B); connexivum pale luteous to luteous (Fig. 9B); femora and tibiae blackish brown to black (Fig. 9A). This morphospecies corresponded to *B. flavus*.

Morphometric analyses

The six female-based morphospecies (fA–fF) were discriminated from each other by PCA based on the morphometric dataset of female adults (Fig. 11A). Similarly, PCA based on the morphometric dataset of male adults, also revealed a significant separation of two groups, i.e., mC and *B. flavus* (mF) and three singletons, i.e., mA, mB, and *B. confusus* (mE) (Fig. 11B). For *B. flavinotus*, the mature male specimen was unavailable.

Phylogenetic analyses and DNA barcoding

Based on the concatenated 16S + Uni dataset (Fig. 12), each of the six morphospecies (bA–bF) was recovered as an independent clade with high supporting values (PP = 1; BP ≥ 93) and long basal branches in both BI and ML trees. The phylogenetic portioning was supported consistently by ASAP and bPTP based on the $COI^{(OG-)}$, $Uni\text{-}Minibar^{(OG-)}$, and $16S^{(OG-)}$ datasets (Fig. 12).

That is to say that the conspecific female and male association was presumed for the following cases: bA (fA = mA), bB (fB = mB), bC (fC = mC) and bF (fF = mF; *B. flavus*). The males of *B. flavinotus* and *B. confusus* have not yet been collected by us.

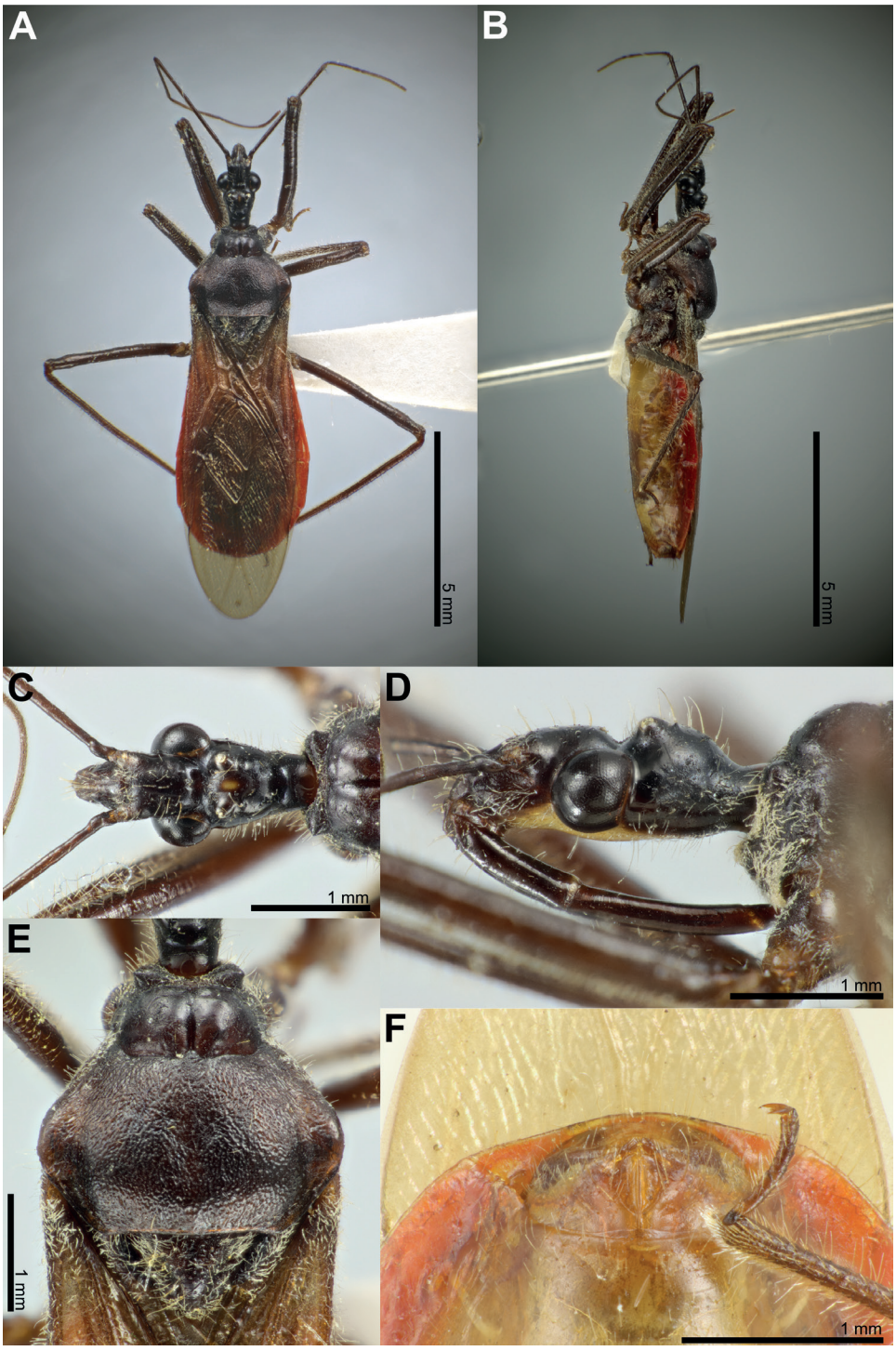

Figure 8. *Biasticus confusus* Hsiao et al., 1979, ♀, VN-Hem-1998-012 **A** body in dorsal view **B** body in lateral view **C** head in dorsal view **D** head in lateral view **E** pronotum in dorsal view **F** female external genitalia in ventral view.

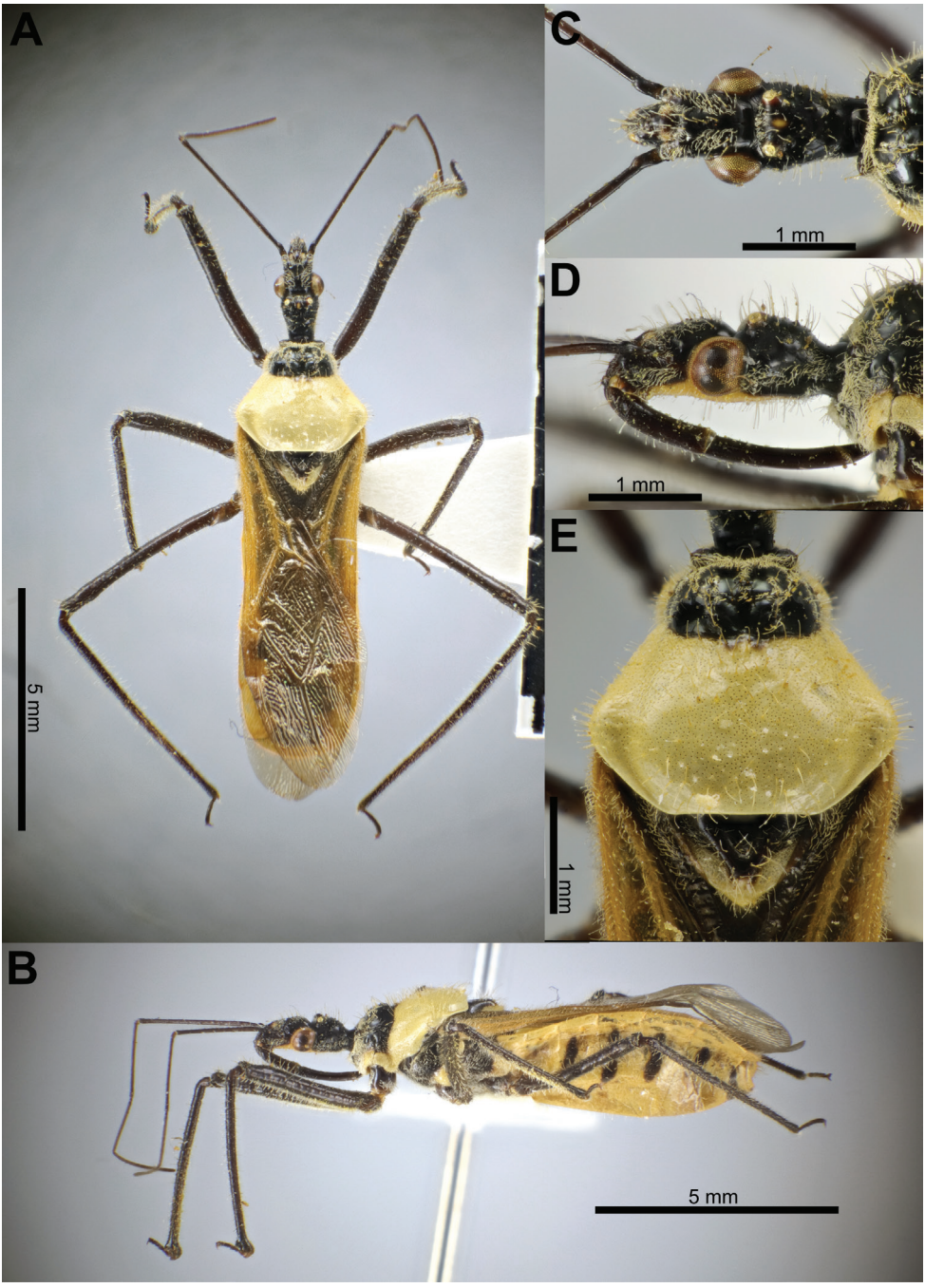

Figure 9. *Biasticus flavus* (Distant, 1903), ♀, LA-Redu-2004-006 **A** body in dorsal view **B** body in lateral view **C** head in dorsal view **D** head in lateral view **E** pronotum in dorsal view.

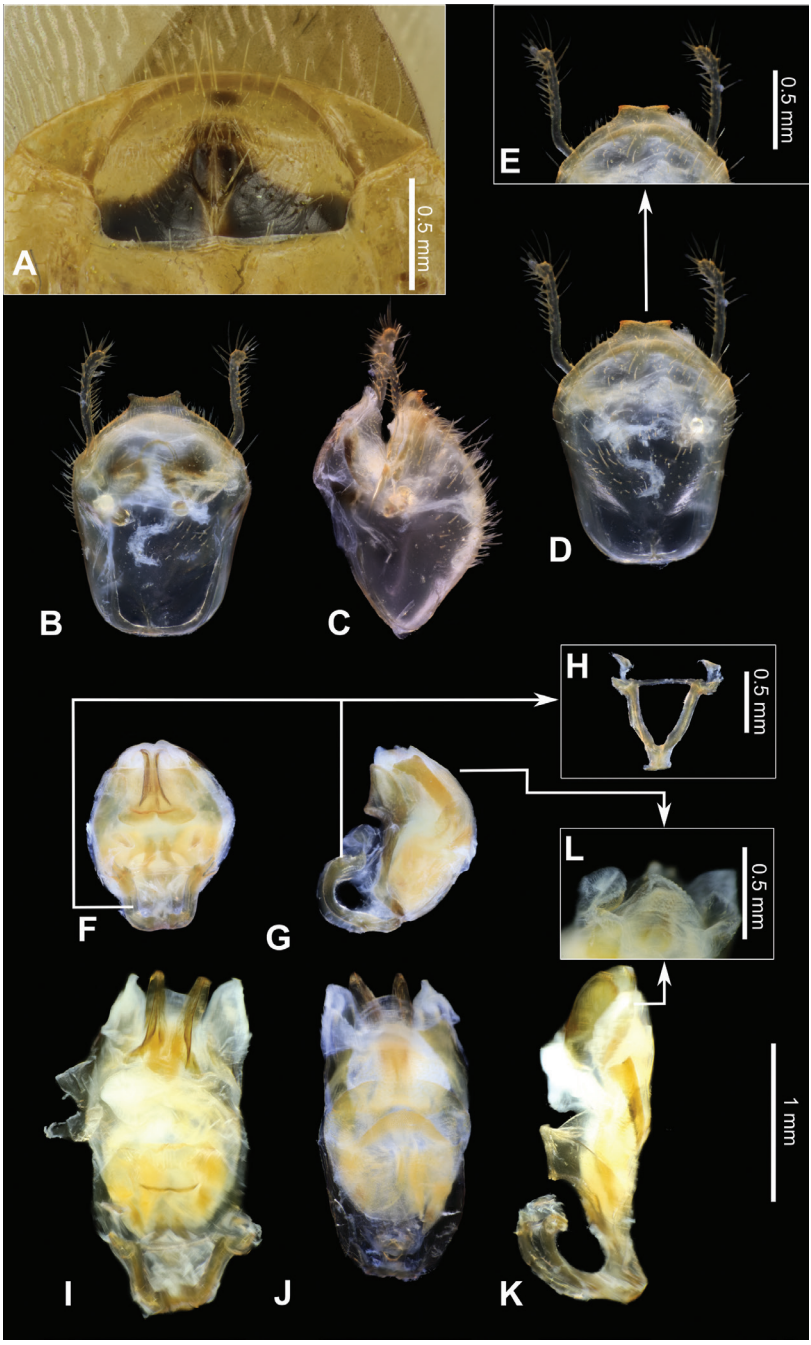

Figure 10. *Biasticus flavus* (Distant, 1903) **A** female genitalia in ventral view, ♀, LA-Redu-2004-006 **B–L** male genitalia, paratype, ♂, HEM-TH2004-018 **B–E** pygophore with parameres **B** dorsal view **C** lateral view **D** ventral view **E** apical portion of pygophore showing median process (mpp) and parameres **F–L** phallus **F** dorsal view **G** lateral view **H** articulatory apparatus (aa) **I** phallus with endosoma semi-everted, dorsal view **J** aedeagus with endosoma semi-everted, ventral view **K** phallus with endosoma semi-everted, lateral view **L** distal dorsal lobe of endosoma (ddl).

Table 3. Correlation and contribution in the percentage for the first and second dimensions (PC1 and PC2) of Principle Component Analysis (PCA) of the 10 most contributing morphometric characters based on female and male datasets (upper and lower tables, respectively).

Female dataset										
	A2L	HeL	Sc	A4L	mGr	mBr	HL	AFL	AoL	A1L
Dim.1 (PC1)	0.855	0.947	0.872	-0.783	-0.732	0.842	-0.235	0.102	-0.109	0.413
Dim.2 (PC2)	-0.139	0.189	0.412	-0.428	0.182	-0.008	0.689	-0.512	0.833	-0.542
Contribution (%)	4.720	4.701	4.650	4.614	4.612	4.531	4.494	4.428	4.326	4.229
Male dataset										
	PTL	PFL	mGr	MFL	A1L	AFL	ATL	OD	R2L	OE
Dim.1 (PC1)	0.940	0.891	-0.060	0.921	0.926	0.824	0.747	-0.737	0.685	-0.318
Dim.2 (PC2)	0.243	0.166	0.880	0.190	-0.117	0.390	0.535	-0.148	0.600	0.727
Contribution (%)	4.130	4.109	4.083	4.061	4.051	3.983	3.942	3.940	3.913	3.895

Species discrimination and identification

The bA, bB, and bC, of which each was confirmed to be an independent species, were distinguished also from 20 named congeners including the following three species already known from Vietnam, namely, *B. confusus* Hsiao et al., 1979 (= bE), *B. flavinotus* (Matsumura, 1913) (= bD), and *B. flavus* (Distant, 1903) (= bF), based on the features of external and genital morphology that have been used in diagnosing species of *Biasticus* and other related genera. The species bA, bB, and bC are therefore named and described as *Biasticus taynguyenensis* Ha, Truong & Ishikawa, sp. nov., *B. griseocapillus* Ha, Truong & Ishikawa, sp. nov., and *B. luteicollis* Ha, Truong & Ishikawa, sp. nov., respectively.

The present study effectively identified a set of morphological features in female and male adults that can be used to classify aged specimens in existing collections that are not suitable for molecular phylogenetic analysis: the morphology of the posterior margin of AS7 and of the apical inner corner and the posterior and inner margins of Gc8 in the female genitalia; the morphology of mpp, sps, ddl, and dps and aa in the male genitalia; length of scape (A1L), length of pedicel (A2L), length of second flagellomere (A4L), length of right hemelytron (HeL), length of Sc in the right hemelytron (Sc), proportions of mean values of green and blue color indicators (mG and mB) of the central region of rear pronotal lobe to sum of mR, mG, and mB (mGr = mG/(mR + mG + mB), and mBr = mB/(mR + mG + mB)), head length (HL), and length of anteocular area of head (AoL) of the female adult (Table 3); length of left fore and hind tibiae (ATL, PTL), length of left femora (AFL, MFL, PFL), proportion of mean value of green color indicators (mG) of the central region of rear pronotal lobe to sum of mR, mG, and mB (mGr = mG/(mR + mG + mB)), length of scape (A1L), and maximum diameter of left ocellus (OD) of the male adult (Table 3).

Taxonomic account

Family Reduviidae Latreille, 1807
Subfamily Harpactorinae Amyot & Serville, 1843

Genus *Biasticus* Stål, 1867

Biasticus taynguyenensis Ha, Truong & Ishikawa, sp. nov.

https://zoobank.org/290765E6-63AE-49F4-B835-B22A034E4DE7
Figs 5A, 6A–D, 13–15

Type material. ***Holotype.*** ♀; HNL2018-073; Vietnam, Gia Lai Province, Kon Chu Rang Nature Reserve; 08.v.2018; X. L. Truong leg.; NSMT. ***Paratypes.*** 1♀; HNL2018-036; Vietnam, Dak Lak Province, Chu Yang Sin National Park; 09.v.2018; X. L. Truong leg.; IEBR. 2♀; HNL2018-072; HNL2018-076; Vietnam, Gia Lai Province, Kon Chu Rang Nature Reserve; 08.v.2018; X. L. Truong leg.; IEBR. 1♀; HNL2018-074; Vietnam, Gia Lai Province, Kon Chu Rang Nature Reserve; 08.v.2018; X. L. Truong leg.; NSMT. 1♀; HNL2018-075; Vietnam, Gia Lai Province, Kon Chu Rang Nature Reserve; 08.v.2018; X. L. Truong leg.; VNMN. 1♂; TXL2016-545; Vietnam, Gia Lai Province, Kon Chu Rang Nature Reserve; 28.iv.2016; X. L. Truong leg.; NSMT.

Diagnosis. Body shiny blackish brown; anterior pronotal lobe blackish brown or black with some rows of short bent cream-yellow setae; posterior pronotal lobe blackish brown or dark brown, densely covered with short bent cream-yellow setae, interspersed with long erect setae; scutellum black or blackish brown; abdominal sternites sanguineous; laterotergites II–IV luteous; anterior half of laterotergite V suffused with brown; posterior half of laterotergite V to apex of abdomen sanguineous.

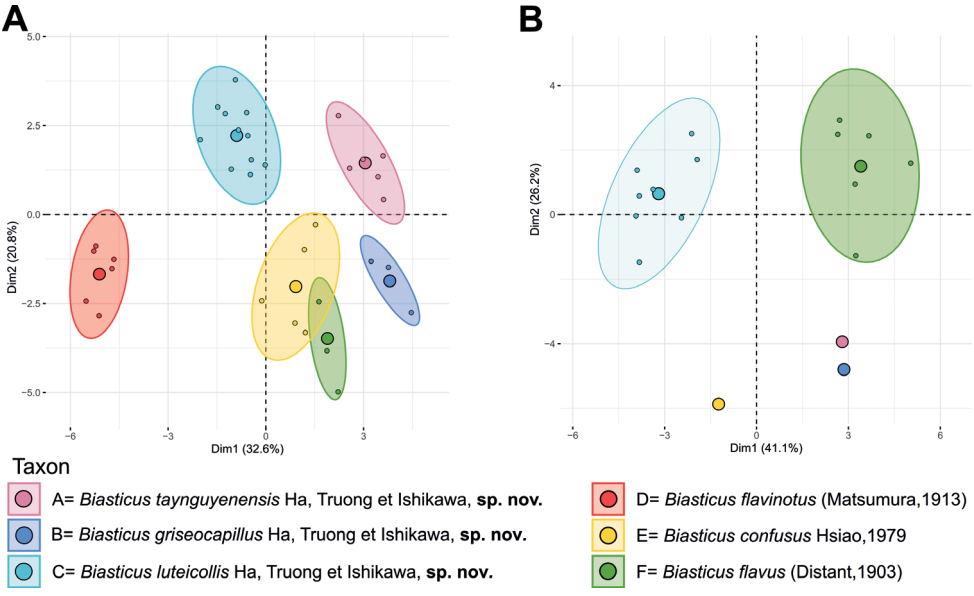

Figure 11. 2D PCA-plots from morphological dataset of the female adults (**A**) and male adults (**B**) of *Biasticus* collected from Vietnam and its surrounding areas.

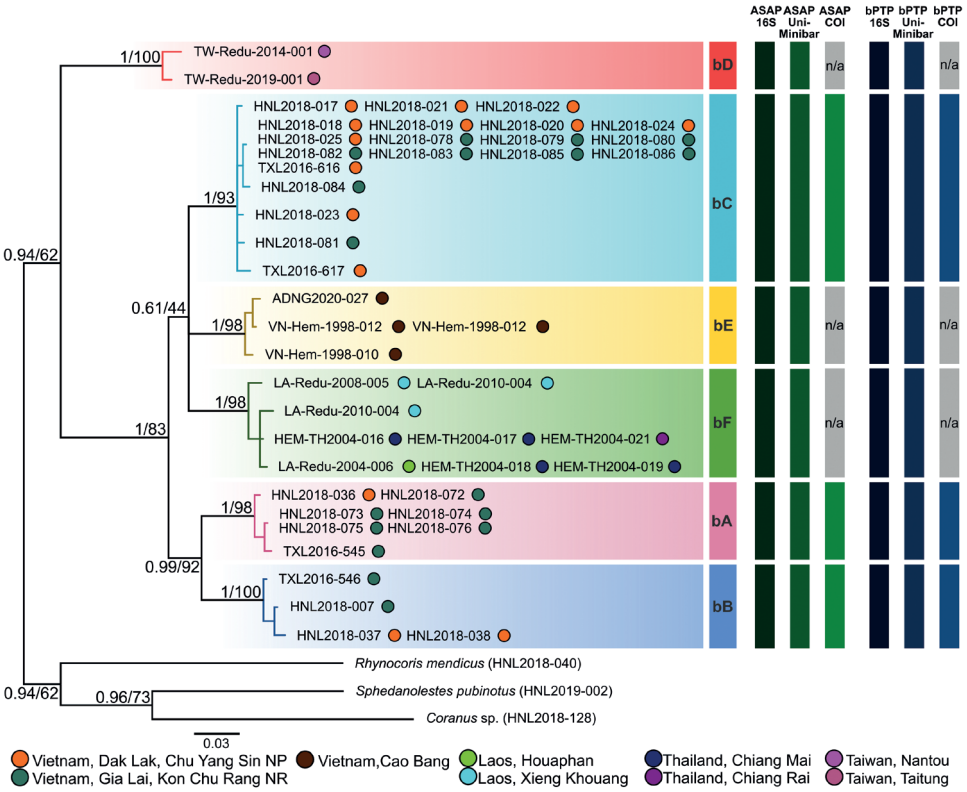

Figure 12. Bayesian inference phylogenetic tree based on the concatenated 16S + Uni dataset (661 bp) of *Biasticus* species collected from Vietnam and its surrounding areas. Posterior probability values and bootstrap values (in %) were given beside the basal nodes. The tips are labeled with the specimen IDs. The circles after specimen IDs showed the collecting localities.

This species is similar to *B. confusus* Hsiao et al., 1979 in general appearance, especially in body color, pronotum, and thoracic sterna. But the new species can be distinguished from *B. confusus* by a combination of the following characters: antennal pedicel longer than first flagellomere (in *B. confusus* pedicel as long as first flagellomere), second flagellomere as long as pedicel (in *B. confusus* second flagellomere longer than pedicel), proportional average length of first to third labial segments 1.1:1.4:0.3 (in *B. confusus* 0.9:1.2:0.3), anterior pronotal lobe with some rows of bent setae (in *B. confusus* without row of bent setae), posterior pronotal lobe ~ 2.3 × as long as anterior pronotal lobe (in *B. confusus* 2.0 ×), and apical margin of median process of pygophore weakly and continuously concave (in *B. confusus* weakly and continuously convex).

Furthermore, this species is somewhat similar to *B. ventralis* Hsiao et al., 1979 in general colors of body, pronotum, and sterna but the new species can be distinguished from *B. ventralis* by a combination of the following characters: antennal pedicel longer than first flagellomere (in *B. ventralis* pedicel ~ 1/2 as long as first flagellomere), second

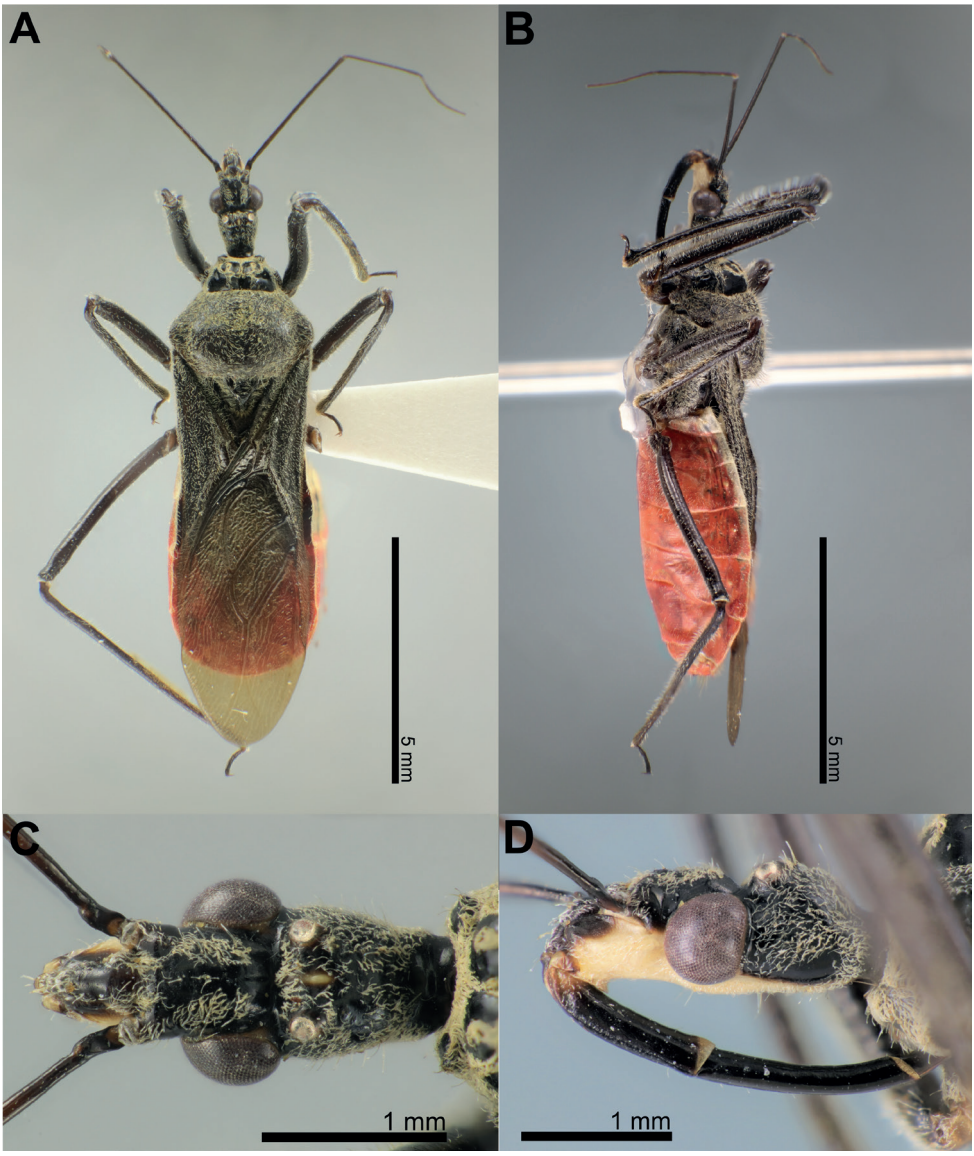

Figure 13. *Biasticus taynguyenensis* Ha, Truong & Ishikawa, sp. nov., holotype, ♀, HNL2018-073 **A** body in dorsal view **B** body in lateral view **C** head in dorsal view **D** head in lateral view.

flagellomere as long as pedicel (in *B. ventralis* second flagellomere 2.5 × as long as pedicel), proportional average length of antennal scape, pedicel, first and second flagellomeres 3.1:1.6:1.4:1.6 (in *B. ventralis* 3.3:1.1:2.0:2.8), and proportional average length of first to third labial segments 1.1:1.4:0.3 (in *B. ventralis* 1.0:1.3:0.3).

Description. Female description. ***Coloration.*** Body shiny blackish brown. Head dorsum shiny black or blackish brown; clypeus blackish brown; antenniferous tubercle, base of

neck, maxillary plate, and base of first visible labial segment yellowish brown; central fascia to head venter, gena, tips of first and second visible labial segments pale luteous; labium, except base of first visible labial segment, black; a brown stripe present after postero-upper corner of compound eye; area around lateral ocellus with reddish brown suffusion; a longitudinally elongated yellowish brown spot present between lateral ocelli. Base of scape dark brown; remaining of scape brown; pedicel, first and second flagellomeres brown, darker toward tip. Collar, anterior pronotal lobe, thoracic sterna, and pleura blackish brown or black; posterior pronotal lobe blackish brown; scutellum black or blackish brown; stridulatory sulcus, intersecting area of coxa and trochanter yellowish brown; coxae, trochanters, femora, and tibiae blackish brown. Corium and clavus blackish brown, apically brownish yellow; membrane bronzy brown, semi-hyaline. Hind wings faintly semi-hyaline. Abdominal mediotergites I+II to IV and middle of mediotergite V blackish brown; posterior half of mediotergite V to apex of abdomen and abdominal sternites sanguineous; laterotergites II–IV luteous; anterior half of laterotergite V suffused with brown; posterior half of laterotergite V to apex of abdomen sanguineous. Female external genitalia sanguineous.

Structure. Body medium-sized (BL = 10.38–11.35 mm), elongate, and somewhat robust. Head subelongate and robust (HL/PoW = 2.40–2.59), shorter than pronotum (HL/PnL = 0.80–0.86); postocular area of head sub-globose (PoL/PoW = 0.84–0.96), distinctly wider than anteocular area (PoW/AoW = 1.38–1.43), approximately as long as anteocular area (PoL/AoL = 0.95–1.08), constricted behind compound eyes, with a wide and deep interocular sulcus; neck short. Compound eyes protruding laterally, nearly globose, with posterior margin sub-straight; lateral ocelli produced, elevated behind interocular sulcus, widely separated from each other (OCD/PoW = 0.44–0.49);

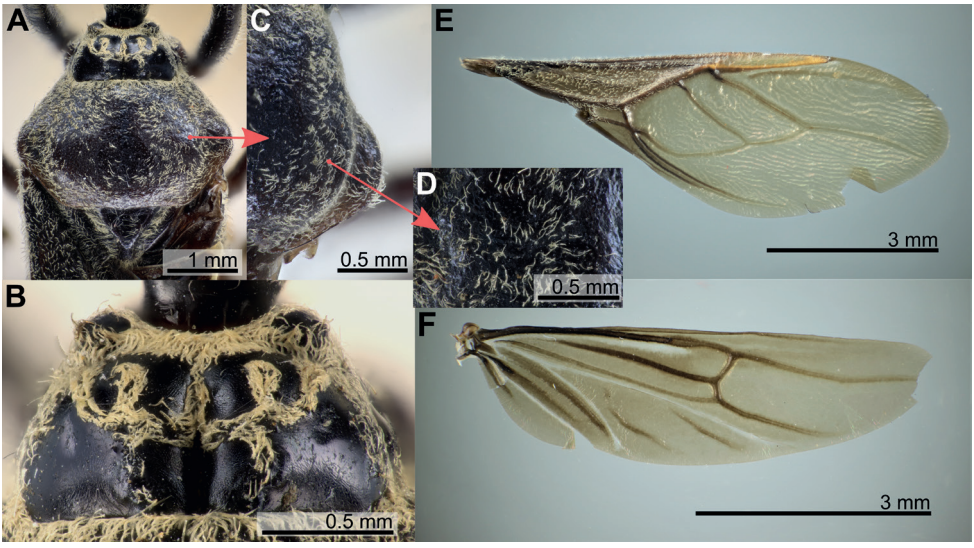

Figure 14. *Biasticus taynguyenensis* Ha, Truong & Ishikawa, sp. nov., holotype, ♀, HNL2018-073 **A** pronotum in dorsal view **B** anterior pronotal lobe in dorsal view **C, D** setae on posterior pronotum **E** right hemelytron **F** right hind wing.

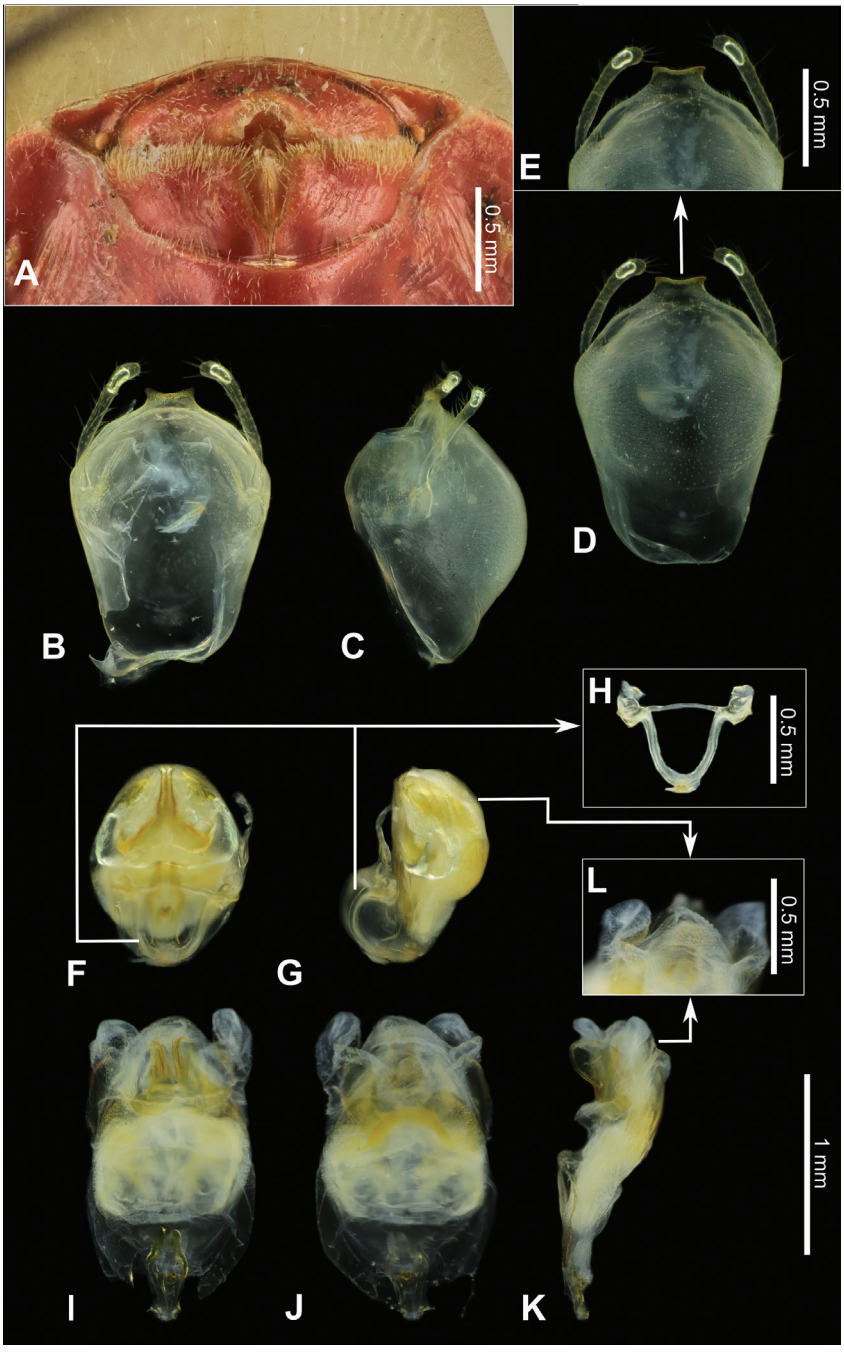

Figure 15. *Biasticus taynguyenensis* Ha, Truong & Ishikawa, sp. nov. **A** female genitalia in ventral view, holotype, ♀, HNL2018-073 **B–L** male genitalia, paratype, ♂, TXL2016-545 **B–E** pygophore with parameres **B** dorsal view **C** lateral view **D** ventral view **E** apical portion of pygophore, showing median process (mpp) and parameres **F–L** phallus **F** dorsal view **G** lateral view **H** articulatory apparatus (aa) **I** aedeagus with endosoma semi-everted dorsal view **J** aedeagus with endosoma semi-everted, ventral view **K** aedeagus with endosoma semi-everted, lateral view **L** distal dorsal lobe of endosoma (ddl).

interspace between lateral ocelli wider than distance between compound eye and lateral ocellus (OCD/COD = 2.03–2.06). First visible labial segment shorter than second segment (R1L/R2L = 0.76–0.84), longer than anteocular area of head (R1L/AoL = 1.42–1.60), extending beyond level of middle of compound eye when labium laid backward; proportional average length of first to third visible labial segments 1.1:1.4:0.3. Scape ~ 1.5 × as long as head; pedicel slightly longer than first flagellomere and nearly equal in length to second flagellomere; proportional average length of scape, pedicel, first and second flagellomeres 3.1:1.6:1.4:1.6. Collar very short in dorsal view, with anterolateral angle weakly and roundly produced; anterior pronotal lobe round and bulged, slightly rough, with middle longitudinal sulcus deep and narrow posteriorly; posterior pronotal lobe with slightly swollen anteromedial elevation; humerus roughly triangular, with round apex; posterior margin of pronotum straight; posterior angles round, not exceeded to posterior margin of pronotum. Scutellum triangular, somewhat triangularly depressed basally, apically produced, and sloping downward; posterior apex round; anterior margin slightly convex. Femora thick, apically moderately nodulose; fore femora very slightly incrassated, thicker than mid and hind femora. Hemelytra surpassing apex of abdomen when fully closed, 0.8 × as long as body length; discal cell nearly parallelogram-shaped, twice as long as width; Sc 0.8 × as long as hemelytron length, 1.5 × as long as R + M. Hind wing ~ 3.4 × as long as maximum width. Connexivum slightly dilated and ascending with segmental incisures; abdominal laterotergite VIII (AL8) with thin posterior margin (0.03 mm); abdominal sternite VII (AS7) forming a semi-circular or wide sub-pentagonal median concavity, with posteromedian margin gently U-shaped, with inner posterolateral margin almost straight; gonocoxa VIII (Gc8) ~ 1.3 × wider than length, gently slanting anteromesad along posterior margin, weakly produced mesad and forming an acute apex at apical inner corner, and with inner margin weakly incurved in posterior 2/3; gonapophysis (Gp8) small and subtriangular, 3.2 × longer than width; gonoplac (Gpl) V-shaped, thin, with maximum thick ~ 0.025 mm.

Vestiture. Body clothed with cream-yellow setation. Head, except interocular sulcus and area along anterior margin of compound eye, covered with short bent cream-yellow pubescence, and sparsely with long erect setae; labium with a few bent setae; scape without setae and pubescence; pedicel, first and second flagellomeres with short vertical setae; neck glabrous. Collar, anterior margin, lateral area of anterior pronotal lobe, posterior pronotal lobe, scutellum, pleura, thoracic sterna, and coxae densely covered with short bent cream-yellow pubescence; posterior pronotal lobe, pleura, thoracic sterna, and coxae interspersed with long erect setae; scutellum with long bent slender setae, especially in lateral slopes and in posterior apex; trochanters, femora, and tibiae with short erect setae; corium with short bent setae. Abdomen (including connexivum), except segment VII, with short slender vertical setae; gonocoxa VIII (Gc8) with long slender bent setae.

Male description. General external morphology similar to that of the female.

Coloration. Almost similar to female but slightly brighter than female. Clypeus dark brown; anteclypeus, base of first visible labial segment pale yellowish brown; first and third visible labial segments brown; second visible labial segment dark brown; area around ocellus with pale brown suffusion. Prosternum and propleuron blackish brown;

posterior pronotal lobe dark brown; scutellum blackish brown; meso- and metapleura brown or yellowish brown; meso- and metasterna yellowish brown; fore coxa pale yellowish brown; coxae and trochanters of mid and hind legs yellowish brown; femora and tibiae dark brown or blackish brown. Pygophore ventrally orangish sanguineous; paramere semi-hyaline, pale orange.

Structure. Almost same as female except for the following characters. Scape 1.7 × as long as head; pedicel, first and second flagellomeres missing. Hemelytra surpassing apex of abdomen when fully closed, nearly 0.9 × as long as body length. Pygophore elliptic; median process of pygophore (mpp) broad and low, 0.3 × as long as wide, with apical margin weakly and continuously concave, with apicolateral corner distinctly produced posterolaterad and pointed; paramere long, slender, clavate, somewhat incurved in apical part, with round apex (Figs 6A, 15B–E). Aedeagus in dorsal view ovoid, dorsally sclerotized (Figs 6B, 15F, I) and in lateral view long and narrow (Figs 6C, 15G, K); articulatory apparatus (aa) in ventral view with basal plate arms relatively slender and jointly forming a U-shape, and in lateral view arched very strongly (Figs 6C, D, 15G, H); dorsal phallothecal sclerite (dps) in lateral view with posteromedian part weakly produced posterodorsad (Figs 6C, 15G, K); spoon-like sclerites (sps) hyaline and glabrous; both membranous sac-like lobes posterolaterally produced; distal dorsal lobe of endosoma (ddl) round, with membranous surface roughly lumpy (Fig. 15L).

Vestiture. Almost same as female except for the following characters. Head covered with short bent cream-yellow pubescence, and sparsely with long bent setae; pedicel with short vertical setae; first and second flagellomeres missing; neck without setae. Scutellum densely covered with short bent cream-yellow pubescence interspersed with long erect setae; trochanters, femora, and tibiae with long erect setae; connexivum with long vertical thick setae; abdominal venter with vertical setae; pygophore with oblique setae; paramere with long erect setae.

Measurements. All dimensions are given in mm. ***Holotype*** (♀): BL 11.35; HL 2.12; AoL 0.76; AoW 0.58; PoL 0.76; PoW 0.82; OE 1.11; IE 0.57; ED 0.65; OD 0.17; OCD 0.41; COD 0.19; R1L 1.22; R2L 1.45; R3L 0.33; A1L 3.13; A2L 1.67; A3L 1.55; A4L n/a; PnL 2.52; PnW 3.01; APL 0.72; PPL 1.80; HeL 8.61; HeW 2.97; Sc 6.59; R+M 4.43; HWL 6.06; HWW 1.84; AFL 3.32; ATL 4.02; MFL 2.76; MTL 3.41; PFL 4.02; PTL 5.53. ***Paratype*** (♂): BL 9.86; HL 1.98; AoL 0.68; AoW 0.56; PoL 0.78; PoW 0.79; OE 1.03; IE 0.54; ED 0.61; OD 0.14; OCD 0.38; COD 0.21; R1L 1.11; R2L 1.39; R3L 0.31; A1L 3.28; A2L n/a; A3L n/a; A4L n/a; PnL 2.31; PnW 2.60; APL 0.70; PPL 1.60; HeL 8.48; HeW 2.72; Sc 6.56; R+M 4.34; HWL 5.60; HWW 1.70; AFL 3.30; ATL 3.91; MFL 2.73; MTL 3.29; PFL 4.00; PTL 5.45. ***Paratypes*** (♀). BL 10.38–10.81; HL 2.00–2.06; AoL 0.72–0.75; AoW 0.58–0.60; PoL 0.70–0.78; PoW 0.82–0.86; OE 1.06–1.09; IE 0.54–0.58; ED 0.62–0.63; OD 0.15–0.17; OCD 0.37–0.41; COD 0.17–0.19; R1L 1.07–1.13; R2L 1.37–1.42; R3L 0.31–0.32; A1L 2.99–3.13; A2L 1.52–1.60; A3L 1.25–1.52; A4L 1.44–1.74; PnL 2.36–2.51; PnW 2.73–2.87; APL 0.66–0.81; PPL 1.64–1.82; HeL 8.63–8.98; HeW 2.78–3.04; Sc 6.59–6.71; R+M 4.51–4.62; HWL 6.03–6.18; HWW 1.77–1.87; AFL 3.11–3.41; ATL 3.79–3.93; MFL 2.64–2.77; MTL 3.30–3.42; PFL 3.73–4.00; PTL 5.35–5.50.

Distribution. Vietnam, Central Highlands (Gia Lai, Dak Lak).

Type locality. Vietnam, Central Highlands, Gia Lai Province, Kon Chu Rang Nature Reserve.

Etymology. This new species is named after the Tay Nguyen region, the local name of Central Highlands.

***Biasticus griseocapillus* Ha, Truong & Ishikawa, sp. nov.**

https://zoobank.org/BDAB0B60-64D5-4529-8715-2E1B010AD57B

Figs 5B, 6E–I, 16–18

Type material. ***Holotype*.** 1♀; HNL2018-038; Vietnam, Dak Lak Province, Chu Yang Sin National Park; 09.v.2018; X. L. Truong leg.; NSMT. ***Paratypes*.** 1♀; HNL2018-007; Vietnam, Gia Lai Province, Kon Chu Rang Nature Reserve; 05.v.2018; X. L. Truong leg.; IEBR. 1♀; HNL2018-037; Vietnam, Dak Lak Province, Chu Yang Sin National Park; 09.v.2018; X. L. Truong leg.; VNMN. 1♂; TXL2016-546; Vietnam, Gia Lai Province, Kon Chu Rang Nature Reserve; 28.iv.2016; X. L. Truong leg.; NSMT.

Diagnosis. Body shiny blackish brown; anterior pronotal lobe black or blackish brown with some rows of long bent griseous setae; posterior pronotal lobe blackish brown or brown and densely covered with short bent griseous setae somewhat interspersed with long griseous setae; scutellum black in basal half and dark brown or brown in lateral margin and apical half; abdominal sternites shiny sanguineous; laterotergites II–VI luteous, segmentally suffused with dark brown spots or blackish brown spots; laterotergite VII sanguineous.

In general appearance, *Biasticus griseocapillus* sp. nov. resembles *B. confusus* Hsiao et al., 1979, especially in general colors of body, pronotum, and sterna. But the new species can be distinguished from *B. confusus* by a combination of the following characters: antennal pedicel longer than first flagellomere (in *B. confusus* pedicel as long as first flagellomere), second flagellomere of antenna as long as pedicel (in *B. confusus* second flagellomere longer than pedicel), proportional average length of first to third visible labial segments 1.1:1.4:0.3 (in *B. confusus* 0.9:1.2:0.3), anterior pronotal lobe with some rows of bent setae (in *B. confusus* without row of bent setae), posterior pronotal lobe 2.6 × as long as anterior pronotal lobe (in *B. confusus* 2.0 ×), and apical margin of median process of pygophore weakly convex and emarginate at middle (in *B. confusus* weakly convex without such emargination).

Furthermore, this species is similar to *B. ventralis* Hsiao et al., 1979 in general colors of body, pronotum, and sterna but the new species can be distinguished from *B. ventralis* by a combination of the following characters: antennal pedicel longer than first flagellomere (in *B. ventralis* pedicel ~ 1/2 as long as first flagellomere), second flagellomere as long as pedicel (in *B. ventralis* second flagellomere 2.5 × as long as pedicel), proportional average length of antennal scape, pedicel, first and second flagellomeres 3.0:1.6:1.4:1.6 (in *B. ventralis* 3.3:1.1:2.0:2.8), and proportional average length of first to third visible labial segments 1.1:1.4:0.3 (in *B. ventralis* 1.0:1.3:0.3).

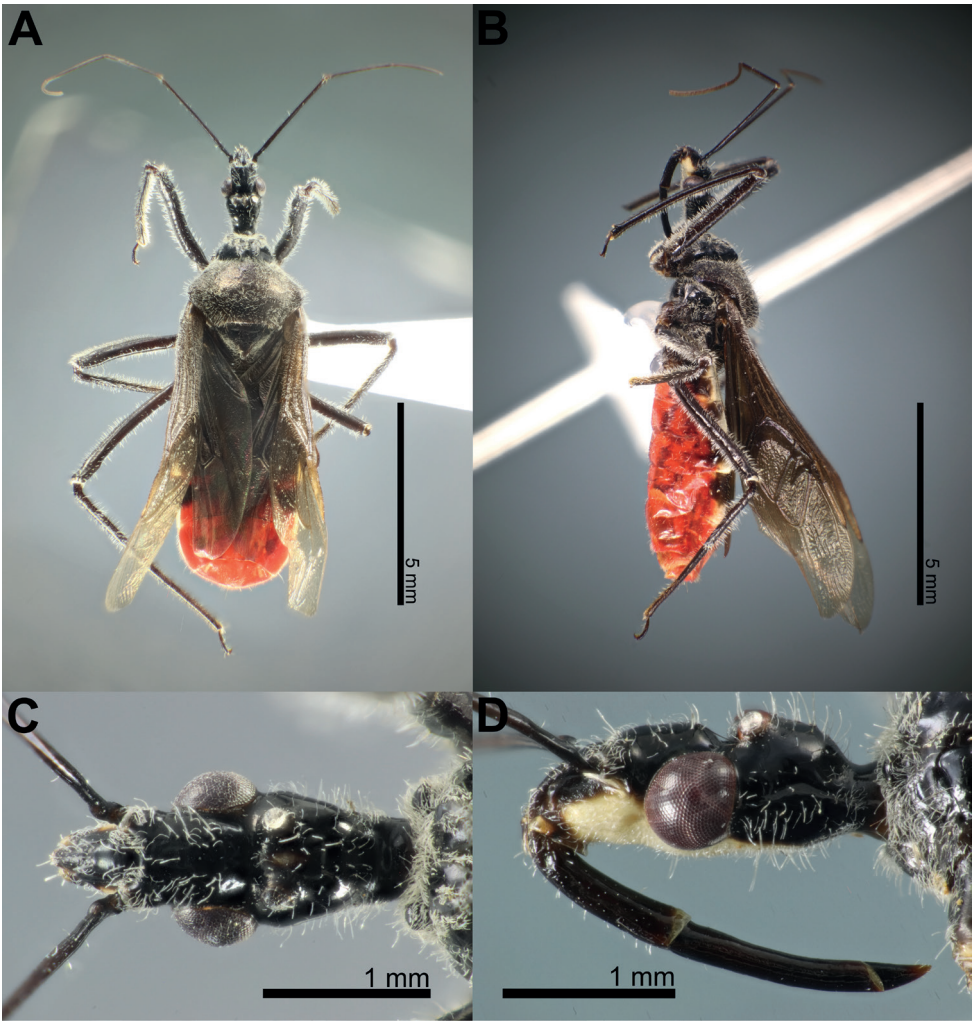

Figure 16. *Biasticus griseocapillus* Ha, Truong & Ishikawa, sp. nov., holotype, ♀, HNL2018-038 **A** body in dorsal view **B** body in lateral view **C** head in dorsal view **D** head in lateral view.

Also, *Biasticus griseocapillus* sp. nov. is similar to *B. taynguyenensis* sp. nov. in the body color pattern, the proportion average length of the antenna segments, and the proportion average length of the visible labial segments. However, *B. griseocapillus* can be distinguished from the latter by a combination of the following characters: collar, anterior pronotal lobe, and posterior pronotal lobe covered with long bent griseous setae (in *B. taynguyenensis* short bent cream-yellow setae), and median process of pygophore (mpp) 0.2 × as long as wide, with apical margin weakly convex and emarginate medially, and with apicolateral corner slightly produced laterad and pointed (in *B. taynguyenensis*, 0.3 × as long as wide, with apical margin weakly and continuously concave, and with apicolateral corner distinctly produced posterolaterad and pointed).

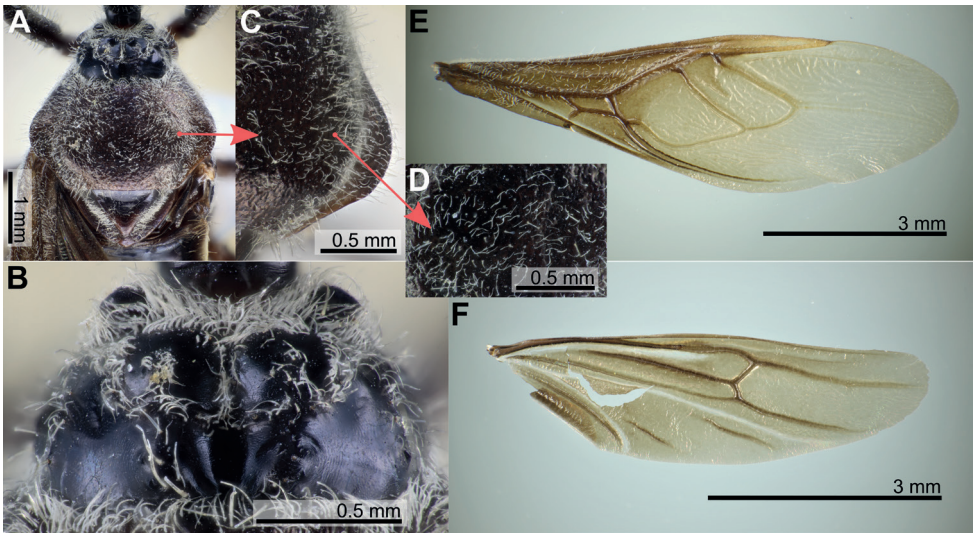

Figure 17. *Biasticus griseocapillus* Ha, Truong & Ishikawa, sp. nov., holotype, ♀, HNL2018-038 **A** pronotum in dorsal view **B** anterior pronotal lobe in dorsal view **C, D** setae on posterior pronotum **E** right hemelytron **F** right hind wing.

Description. Female description. ***Coloration.*** Body shiny blackish brown. Head dorsum (except anteclypeus, maxillary plate, and gena) black; anteclypeus, labrum, maxillary plate, and anterior region of gena brown; central fascia to head venter, and posterior region of gena pale luteous; first visible labial segment brown; second and third visible labial segments blackish brown; tips of first and second visible labial segments yellowish brown; area around lateral ocellus with reddish brown suffusion; a longitudinally elongated yellowish brown spot present between lateral ocelli. Base of scape brownish black; remaining of scape and pedicel, first and second flagellomeres blackish brown. Collar, anterolateral angles, anterior pronotal lobe, and anterior acetabulum black; posterior pronotal lobe, pleura, and thoracic sterna blackish brown; scutellum black in basal half and dark brown in lateral margin and apical half; stridulatory sulcus luteous; coxae and trochanters yellowish brown; intersecting area of fore coxae and fore trochanters luteous; femora, tibiae, and tarsi blackish brown. Corium and clavus darkish brown, apically brownish yellow; membrane bronzy brown, semi-hyaline. Hind wings faintly semi-hyaline. Abdominal mediotergites I+II to V reddish brown or sanguineous, somewhat suffused with blackish brown; mediotergite VI suffused with reddish brown and irregularly suffused with sanguineous; mediotergite VII and laterotergite VII to apex of abdomen sanguineous; abdominal sternite shiny sanguineous; laterotergites II–VI luteous, segmentally suffused with dark brown spots; laterotergite VII sanguineous. External genitalia sanguineous.

Structure. Body medium-sized (BL = 10.61–10.84 mm), elongate, and somewhat robust. Head subelongate and robust (HL/PoW = 2.37–2.45), shorter than pronotum (HL/PnL = 0.81–0.82); postocular area of head sub-globose (PoL/PoW = 0.85–1.03),

distinctly wider than anteocular area (PoW/AoW = 1.44–1.47), slightly longer than anteocular area (PoL/AoL = 1.05–1.27), constricted behind compound eyes, with a wide and deep interocular sulcus; neck short. Compound eyes protruding laterally, nearly globose, with posterior margin sub-straight; lateral ocelli produced, elevated behind interocular sulcus, widely separated from each other (OCD/PoW = 0.43–0.46); interspace between lateral ocelli wider than distance between compound eye and lateral ocellus (OCD/COD = 1.93–2.17). First visible labial segment shorter than second segment (R1L/R2L = 0.80–0.84), longer than anteocular area of head (R1L/AoL = 1.58–1.63), extending beyond level of middle of compound eye when labium laid backward; proportional average length of first to third visible labial segments 1.1:1.3:0.3. Scape ~ 1.5 × as long as head; pedicel slightly longer than first flagellomere and nearly equal in length to second flagellomere; proportional average length of scape, pedicel, first and second flagellomeres 3.0:1.6:1.4:1.6. Collar very short in dorsal view, with anterolateral angle weakly and roundly produced; anterior pronotal lobe round and bulged, slightly rough, with middle longitudinal sulcus deep and narrow posteriorly; posterior pronotal lobe with slightly swollen anteromedial elevation; humerus roughly triangular, with round apex; posterior margin of pronotum straight; posterior angles round, not exceeded to posterior margin of pronotum. Scutellum triangular, somewhat triangularly depressed basally, apically produced and sloping downward; posterior apex round; anterior margin slightly convex. Femora thick, apically moderately nodulose; fore femora very slightly incrassated, thicker than mid and hind femora. Hemelytra surpassing apex of abdomen when fully closed, 0.8 × as long as body length; discal cell nearly parallelogram-shaped, twice as long as width; Sc 0.7 × as long as hemelytron length, 1.4 × as long as R + M. Hind wing ~ 3.2 × as long as maximum width. Connexivum slightly dilated and ascending with segmental incisures; abdominal laterotergite VIII (AL8) with thin posterior margin (0.01 mm); abdominal sternite VII (AS7) forming a wide subpentagonal posteromedian concavity, with inner posterolateral margin almost straight; gonocoxa VIII (Gc8) broad, ~ 1.4 × wider than length, slightly opened inward for gonapophyses VIII (Gp8), with posterior margin gently slanting anteromesad, and with apical inner corner not produced; Gp8 small and subtriangular, 3.9 × longer than width; gonoplac (Gpl) V-shaped, thin, with maximum thick ~ 0.025 mm.

Vestiture. Body clothed with griseous setation. Head, except interocular sulcus and posterior margin of clypeus, covered with long erect setae; posterior margin of clypeus, head venter, anterolateral area of neck with short bent setae and sparsely with long erect setae; anteclypeus, labium, scape with a few short setae; pedicel, first and second flagellomeres covered with short erect to recumbent setae; dorsum of neck without setae. Collar, anterior margin of anterior pronotal lobe with dense bent pubescence; anterior pronotal lobe with some rows of long bent griseous setae; lateral area of anterior pronotal lobe with long erect setae; posterior pronotal lobe densely covered with short bent griseous setae somewhat interspersed with long griseous setae; lateral slope area and posterior apex of scutellum with dense short to long setae; posterior area of posterior pronotal lobe with long erect setae; pleura, thoracic sterna, and coxae

with short bent setae; trochanters, femora, and tibiae with long erect setae; corium with bent griseous pubescence. Anterior margin of abdominal mediotergite I+II with some long slender erect yellowish brown setae; mediotergites and dorsal laterotergites sparsely covered with a few short vertical setae; abdominal sternites interspersed with long vertical setae; posterior margin of abdominal laterotergite VIII (AL8) with long erect slender setae; gonocoxa VIII (Gc8) with long slender bent setae; apex of external genitalia with long thick erect setae.

Male description. General external morphology similar to that of the female.

Coloration. Almost similar to female but brighter than female. Gena brown in anterior half and luteous in posterior half; labium blackish brown; tips of first and second visible labial segments luteous. Collar, anterolateral angles, anterior pronotal lobe, and anterior acetabulum blackish brown; posterior pronotal lobe, pleura, and thoracic sterna brown; scutellum black in basal half and brown in lateral margin and apical half; stridulatory sulcus pale gray. Laterotergites II–VI pale luteous, segmentally suffused with blackish brown spots; laterotergite VII sanguineous. Pygophore ventrally orpiment-orange; paramere semi-hyaline, pale orange.

Structure. Almost similar to female except for the following characters. Scape 1.8 × as long as head and more than twice as long as pedicel; pedicel slightly longer than first flagellomere; second flagellomere missing; proportional length of scape, pedicel, and first flagellomere 3.5:1.6:1.4. Hemelytra surpassing apex of abdomen when fully closed, 0.9 × as long as body; Sc 0.8 × as long as hemelytron, and 1.5 × as long as R + M. Pygophore ovoid; median process of pygophore (mpp) broad and low, 0.2 × as long as wide, with apical margin weakly convex and emarginate medially, with apicolateral corner slightly produced laterad and pointed; paramere long, slender, clavate, somewhat curved medially, and apically subnodulose and round (Figs 6E, 18B–F). Aedeagus in dorsal view ovoid, dorsally sclerotized (Figs 6F, 18G, J) and in lateral view long and narrow (Figs 6G, 18H, L); articulatory apparatus (aa) in ventral view with basal plate arms relatively slender and jointly forming a U-shape, and in lateral view arched strongly (Figs 6G, I, 18H, I); dorsal phallothecal sclerite (dps) in lateral view with posteromedian part weakly produced posterodorsad (Figs 6G, 18L); spoon-like sclerites (sps) hyaline and glabrous; both membranous sac-like lobes posterolaterally produced; distal dorsal lobe of endosoma (ddl) round, with membranous surface covered with large hyaline prickles (Figs 6H, 18M).

Vestiture. Almost similar to female except for the following characters. Posterior margin of clypeus with short bent pubescence; anteclypeus and scape without setae. Collar and anterior margin of anterior pronotal lobe with short bent setae and some long bent setae; anterior pronotal lobe with some rows of long bent griseous setae; posterior pronotal lobe with bent griseous setae; scutellum with long slender erect setae abundantly, especially in lateral slopes; posterior apex of scutellum with a pinch of long slender erect and bent setae; pleura, thoracic sterna, and coxae with short bent setae, with a few long slender setae; trochanters sparsely with short bent pubescence and a few long setae; corium with bent pubescence. Pygophore ventrally covered with a few bent pubescence, more abundant laterally; paramere with a few long erect thick setae.

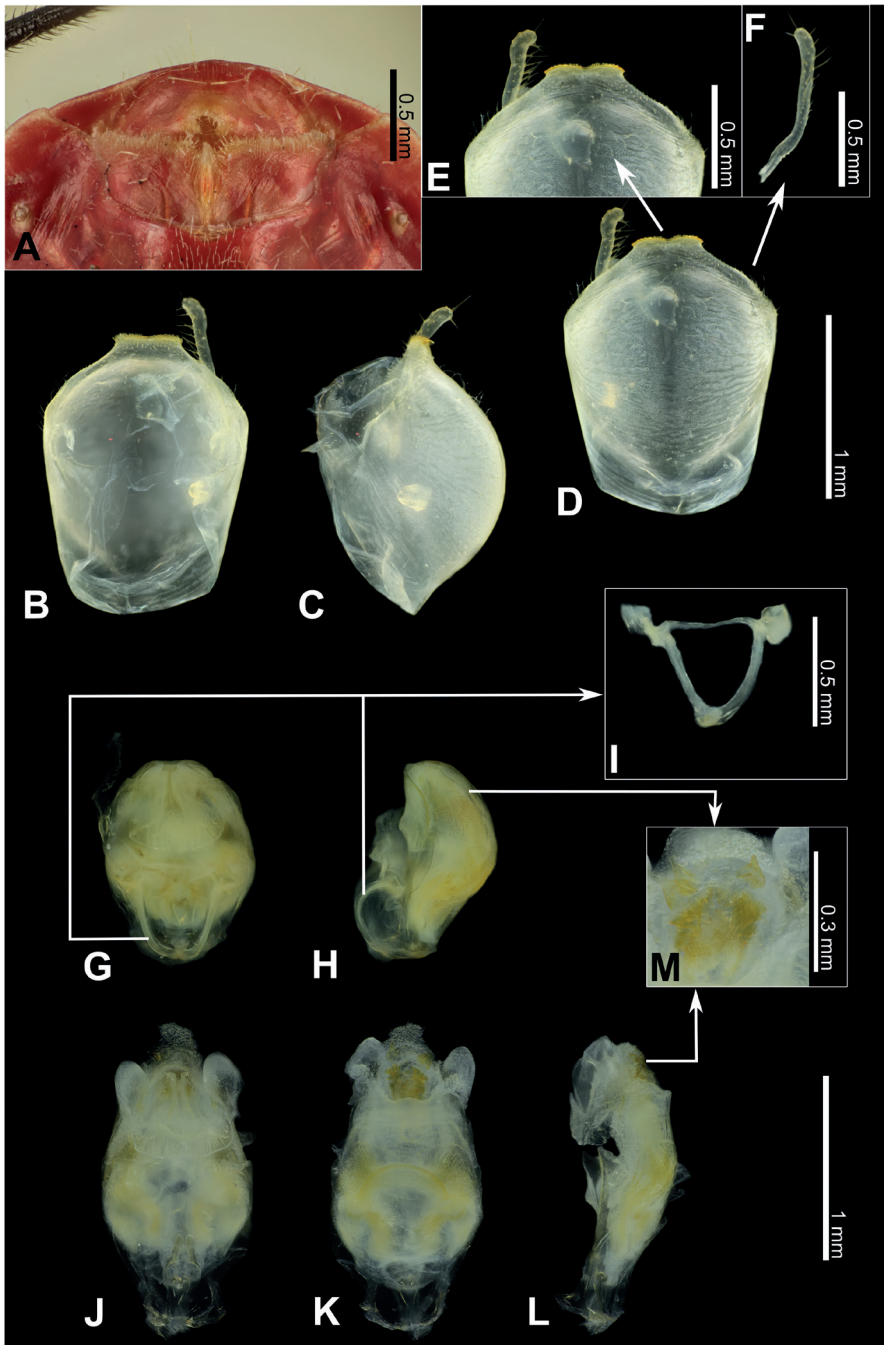

Figure 18. *Biasticus griseocapillus* Ha, Truong & Ishikawa, sp. nov. **A** female genitalia in ventral view, holotype, ♀, HNL2018-038 **B–M** male genitalia, paratype, ♂, TXL2016-546 **B–F** pygophore with paramere **B** dorsal view **C** lateral view **D** ventral view **E** apical portion of pygophore, showing median process (mpp) and paramere **F** left paramere **G–M** phallus **G** dorsal view **H** lateral view **I** articulatory apparatus (aa) **J** aedeagus with endosoma semi-everted, dorsal view **K** aedeagus with endosoma semi-everted, ventral view **L** aedeagus with endosoma semi-everted, lateral view **M** distal dorsal lobe of endosoma (ddl).

Measurements. All dimensions are given in mm. ***Holotype*** (♀): BL 10.84; HL 1.99; AoL 0.67; AoW 0.56; PoL 0.85; PoW 0.82; OE 1.05; IE 0.56; ED 0.60; OD 0.17; OCD 0.36; COD 0.18; R1L 1.09; R2L 1.31; R3L 0.32; A1L 3.01; A2L 1.59; A3L 1.52; A4L 1.56; PnL 2.45; PnW 2.74; APL 0.79; PPL 1.67; HeL 8.56; HeW 2.67; Sc 6.69; R+M 4.67; HWL 5.68; HWW 1.68; AFL 3.37; ATL 4.00; MFL 2.77; MTL 3.47; PFL 3.94; PTL 5.44. ***Paratype*** (♂): BL 9.77; HL 1.91; AoL 0.64; AoW 0.54; PoL 0.78; PoW 0.79; OE 1.05; IE 0.53; ED 0.63; OD 0.14; OCD 0.38; COD 0.19; R1L 1.05; R2L 1.31; R3L 0.29; A1L 3.48; A2L 1.62; A3L 1.49; A4L n/a; PnL 2.12; PnW 2.57; APL 0.59; PPL 1.52; HeL 8.45; HeW 2.79; Sc 6.78; R+M 4.52; AFL 3.44; ATL 4.06; MFL 2.90; MTL 3.52; PFL 3.99; PTL 5.36. ***Paratypes*** (♀). BL 10.61–10.75; HL 1.94–1.95; AoL 0.67; AoW 0.54–0.57; PoL 0.70–0.76; PoW 0.79–0.82; OE 1.05; IE 0.54–0.55; ED 0.58–0.62; OD 0.16; OCD 0.36–0.38; R1L 1.05–1.06; R2L 1.27–1.31; R3L 0.31–0.34; A1L 2.92–2.97; A2L 1.57–1.61; A3L 1.36–1.43; A4L 1.60–1.64; PnL 2.36–2.38; PnW 2.58–2.74; APL 0.72–0.84; PPL 1.52–1.66; HeL 8.65–8.88; HeW 2.75–2.98; Sc 6.30–6.49; R+M 4.40–4.48; HWL 5.78–5.89; HWW 1.79–1.91; AFL 3.31–3.33; ATL 3.78–3.93; MFL 2.70–2.78; MTL 3.42–3.51; PFL 3.69–3.87; PTL 4.91–5.35.

Distribution. Vietnam, Central Highlands (Gia Lai, Dak Lak).

Type locality. Vietnam, Central Highlands, Dak Lak Province, Chu Yang Sin National Park.

Etymology. This new species is named after griseous pubescence on the pronotum.

Biasticus luteicollis **Ha, Truong & Ishikawa, sp. nov.**
https://zoobank.org/752E02B7-586A-4A9C-8D70-09DE6199F2EE
Figs 5C, 6J–N, 19–21

Type material. ***Holotype.*** ♂; HNL2018-025; Vietnam, Dak Lak Province, Chu Yang Sin National Park; 09.v.2018; X. L. Truong leg.; NSMT. ***Paratypes.*** 1♀; TXL2016-616; Vietnam, Dak Lak Province, Chu Yang Sin National Park; 05.v.2016; X. L. Truong leg.; IEBR. 1♂; TXL2016-617; Vietnam, Dak Lak Province, Chu Yang Sin National Park; 05.v.2016; X. L. Truong leg.; IEBR. 4♀; HNL2018-078; HNL2018-080; HNL2018-081; HNL2018-082; Vietnam, Gia Lai Province, Kon Chu Rang Nature Reserve; 08.v.2018; X. L. Truong leg.; IEBR. 4♂; HNL2018-079; HNL2018-083; HNL2018-084; HNL2018-085; Vietnam, Gia Lai Province, Kon Chu Rang Nature Reserve; 08.v.2018; X. L. Truong leg.; IEBR. 1♂; HNL2018-086; Vietnam, Gia Lai Province, Kon Chu Rang Nature Reserve; 08.v.2018; X. L. Truong leg.; NSMT. 1♀; HNL2018-017; Vietnam, Dak Lak Province, Chu Yang Sin National Park; 09.v.2018; X. L. Truong leg.; VNMN. 3♀; HNL2018-018; HNL2018-019; HNL2018-020; Vietnam, Dak Lak Province, Chu Yang Sin National Park; 09.v.2018; X. L. Truong leg.; IEBR. 3♀; HNL2018-021; HNL2018-023; HNL2018-024; Vietnam, Dak Lak Province, Chu Yang Sin National Park; 09.v.2018; X. L. Truong leg.; NSMT. 1♂; HNL2018-022; Vietnam, Dak Lak Province, Chu Yang Sin National Park; 09.v.2018; X. L. Truong leg.; NSMT.

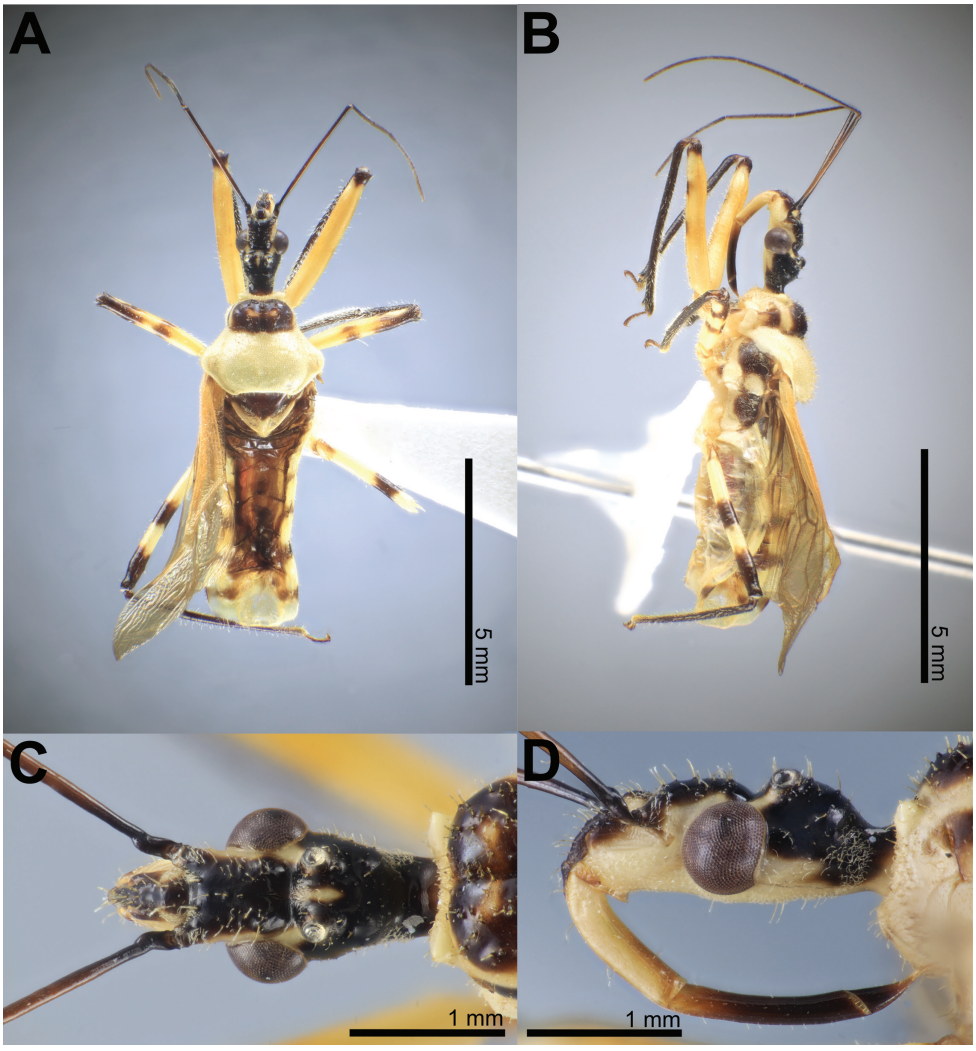

Figure 19. *Biasticus luteicollis* Ha, Truong & Ishikawa, sp. nov., holotype, ♂, HNL2018-025 **A** body in dorsal view **B** body in lateral view **C** head in dorsal view **D** head in lateral view.

Diagnosis. Body shiny luteous; first visible labial segment and base of second visible labial segment luteous; apical 2/3 of second visible labial segment to third visible labial segment yellowish brown or brown; posterior pronotal lobe luteous; scutellum dark brown in basal half and luteous in apical half, with median pale brownish luteous portion; femora luteous with dark brown or yellowish brown suffusions at apex and sometimes at middle.

This species is most similar to *Biasticus flavus* (Distant, 1903) in general appearance, especially in coloration and color pattern of the pronotum, scutellum, and abdomen. However, the new species can be easily separated from the latter by a combination of the following characters: femora luteous with some dark brown or yellowish brown suffu-

sions at apex and sometimes at middle (in *B. flavus* uniformly blackish brown) and abdominal sternites luteous without blackish brown or black suffusion (in *B. flavus* abdominal sternites luteous with blackish brown or black segmental transverse stripes laterally).

Description. Male description. ***Coloration.*** Body shiny luteous. Head dorsum, except antenniferous tubercle and neck, black; clypeus, antenniferous tubercle, and labrum brown; maxillary plate, gena, and head venter (except anterior margin of maxillary plate and anterior margin of gena) pale yellowish brown; anterior margin of maxillary plate and anterior margin of gena yellowish brown; first visible labial segment and base of second visible labial segment luteous; apical two-thirds of second visible labial segment to third visible labial segment yellowish brown or brown; a luteous suffusion present above upper margin of compound eye; a luteous stripe running along dorsal margin of compound eye and between postero-upper corner of compound eye and ocellus; area around lateral ocellus with yellowish brown suffusion; a longitudinally elongated luteous suffusion present between lateral ocelli; neck yellowish brown. Scape, except base, yellowish brown; base of scape blackish brown; pedicel, first and second flagellomeres dark brown. Collar, anterolateral angle, and posterior pronotal lobe pale luteous; anterior pronotal lobe, except lateral margin, shiny dark brown, sometimes with luteous suffusion centrally; lateral margin of anterior pronotal lobe, acetabulum, thoracic sterna, stridulatory sulcus, coxae, and trochanters pale luteous; coxae and trochanters sometimes with dark brown or yellowish brown spots; pleura, except lower half of propleuron, dark brown; lower half of propleuron pale luteous; scutellum dark brown in basal half and luteous in apical half, with median pale brownish luteous portion; femora luteous; fore femora apically dark brown, sometimes with dark brown or yellowish brown suffusion; mid and hind femora apically and medially yellowish brown; tibiae dark brown. Corium and clavus yellow or brownish yellow; membrane bronzy brown, semi-hyaline. Hind wings faintly semi-hyaline. Abdominal mediotergites, except posterior half of mediotergite VII, brownish yellow; posterior half of mediotergite VII luteous; abdominal sternites pale luteous; connexivum pale luteous, with segmentally dark brown suffusions. Pygophore ventrally luteous; paramere semi-hyaline, luteous.

Structure. Body medium-sized (BL = 9.19–10.21 mm), elongate, and somewhat robust. Head subelongate and robust (HL/PoW = 2.35–2.48), as long as or a little shorter than pronotum (HL/PnL = 0.84–1.03); postocular area of head sub-globose (PoL/PoW = 0.77–0.93), distinctly wider than anteocular area (PoW/AoW = 1.36–1.43), nearly as long as anteocular area (PoL/AoL = 0.84–1.03), constricted behind compound eyes, with a wide and deep interocular sulcus; neck short. Compound eyes protruding laterally, nearly globose, with posterior margin sub-straight and sometimes concave; lateral ocelli produced, elevated behind interocular sulcus, widely separated from each other (OCD/PoW = 0.42–0.48); interspace between lateral ocelli wider than distance between compound eye and lateral ocellus (OCD/COD = 1.95–2.36). First visible labial segment shorter than second segment (R1L/R2L = 0.79–0.82), longer than anteocular area of head (R1L/AoL = 1.39–1.51), not extending beyond level of middle of compound eye when labium laid backward; proportional average length of first to third visible labial segments 1.1:1.3:0.4. Scape ~ 1.4 × as long as

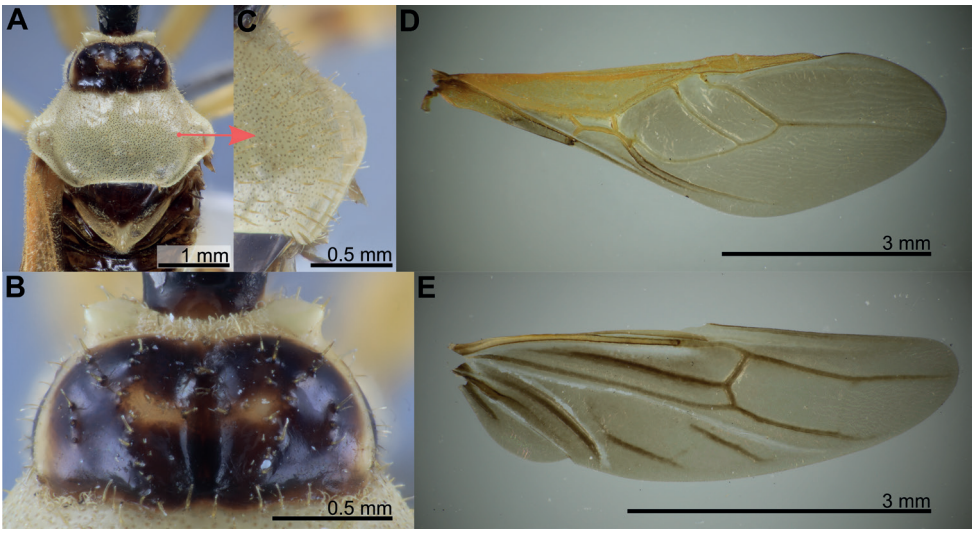

Figure 20. *Biasticus luteicollis* Ha, Truong & Ishikawa, sp. nov., holotype, ♂, HNL2018-025 **A** pronotum in dorsal view **B** anterior pronotal lobe in dorsal view **C** setae on posterior pronotum **D** right hemelytron **E** right hind wing.

head; pedicel slightly shorter than first flagellomere and nearly 0.7 × as long as second flagellomere; proportional average length of scape, pedicel, first and second flagellomeres 2.9:1.4:1.5:2.0. Collar very thick in dorsal view, with anterolateral angle roundly produced laterad; anterior pronotal lobe round and bulged, slightly rough, with middle longitudinal sulcus deep and narrow posteriorly; posterior pronotal lobe shallowly depressed on disc, abundantly punctured, with slightly swollen anteromedial elevation (never sulcate or concave); humerus roughly triangular, with round apex; posterior margin of pronotum concave; posterior angles round, slightly exceeded to posterior margin of pronotum. Scutellum triangular, somewhat triangularly depressed basally, apically produced and sloping downward; posterior apex round; anterior margin slightly convex. Femora thick, apically moderately nodulose; fore femora very slightly incrassated, thicker than mid and hind femora. Hemelytra surpassing beyond apex of abdomen when fully closed, 0.8 × as long as body length; discal cell nearly parallelogram-shaped, twice as long as width; Sc 0.8 × as long as hemelytron length, 1.5 × as long as R + M. Hind wing ~ 3.3 × as long as maximum width. Connexivum slightly dilated and ascending with segmental incisures; pygophore ovoid; median process of pygophore (mpp) broad and low, 0.2 × as long as wide, with apical margin weakly and continuously convex, and with apicolateral corner slightly produced laterad and pointed; paramere long, slender, clavate, somewhat curved medially, and apically subnodulose and round (Figs 6J, 21B–E). Aedeagus in dorsal view ovoid, dorsally sclerotized (Figs 6K, 21F) and in lateral view long and narrow (Figs 6L, 21G); articulatory apparatus (aa) in ventral view with relatively broad basal plates jointly forming a V-shape, and in lateral view arched moderately (Figs 6L, N, 21G, I); dorsal phallothecal sclerite (dps) in lateral view with posteromedian part strongly produced posterodorsad (Figs 6L, 21G);

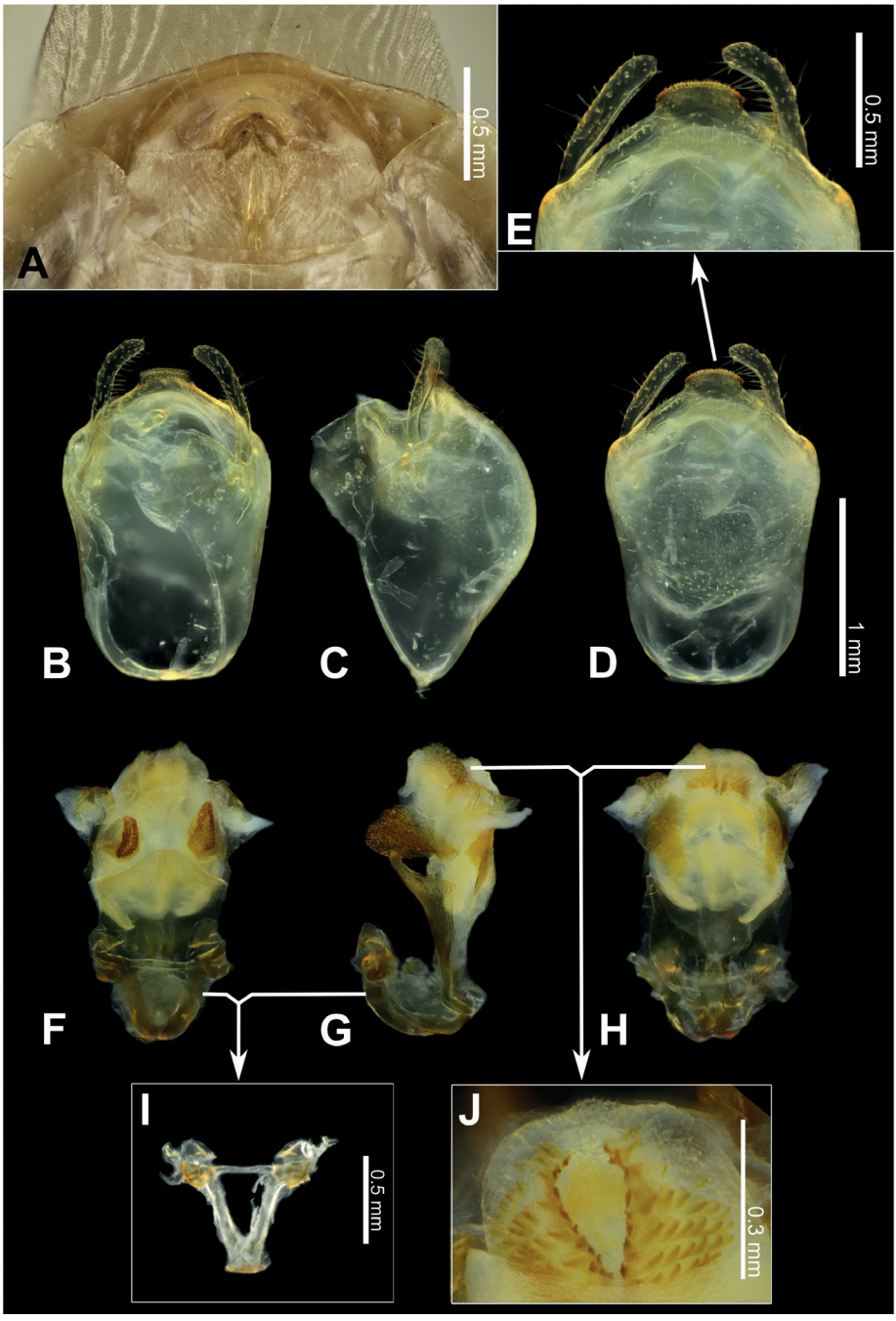

Figure 21. *Biasticus luteicollis* Ha, Truong & Ishikawa, sp. nov. **A** female external genitalia in ventral view, paratype, ♀, HNL2018-024 **B–J** male genitalia, holoype, ♂, HNL2018-025 **B–E** pygophore with parameres **B** dorsal view **C** lateral view **D** ventral view **E** apical portion of pygophore, showing median process (mpp) and parameres **F–H** phallus **F** phallus with endosoma semi-everted, dorsal view **G** phallus with endosoma semi-everted, lateral view **H** phallus with endosoma semi-everted, ventral view **I** articulatory apparatus (aa) **J** distal dorsal lobe of endosoma (ddl).

spoon-like sclerites (sps) semi-hyaline and covered with tiny blunt prickles; both membranous sac-like lobes laterally produced; distal dorsal lobe of endosoma (ddl) round, with membranous surface covered with small but distinct prickles (Figs 6M, 21J).

***Vestiture*.** Body clothed with cream-yellow setation. Head dorsum (except antenniferous tubercle, posterior base of clypeus, and gena) covered with short thick erect setae; area around antenniferous tubercle, posterior margin of clypeus, head venter, and lateral area of postocular area of head covered with short bent pubescence; head venter somewhat with a few long bent setae; maxillary plate without setae; first visible labial segment basally covered with a few erect setae; second and third visible labial segments without setae; scape with a few tiny erect setae; pedicel, first and second flagellomeres densely covered with short slender oblique setae. Anterior margin of collar densely covered with very short erect setae; dorsum of collar with bent cream-yellow pubescence; anterolateral angle and lateral region of collar with long thick erect setae, one of them placed at tip of anterolateral angle; pronotum and scutellum with long thick erect setae; lateral region of slopes of scutellum covered with long slender bent setae; posterior apex of scutellum with a pinch of long slender bent setae and long thick vertical setae; prosternum, except posterior margin, covered with long thick erect setae; posterior margin of prosternum, meso- and metasterna, pleura, and coxae abundantly covered with short bent pubescence. Corium densely covered with bent setae along anterior margin, centrally covered with short slender oblique setae. Abdomen sometimes with erect setae, slightly denser in posterior margin of abdomen; anterior margin of mediotergite I+II, anterior margin of sternite II, and lateral region of laterotergite II with very long slender erect setae; pygophore posteroventrally with some long erect setae and some bent slender setae; paramere with long thick erect setae.

Female description. General external morphology similar to that of the male.

***Coloration*.** Almost similar to male but slightly darker than male. Abdominal mediotergites, except posterior half of mediotergite VII, dark brown and darker backward; posterior half of mediotergite VII luteous; external genitalia pale luteous.

***Structure*.** Almost similar to male but slightly larger than male. Body medium-sized (BL = 10.11–10.91 mm). Proportional average length of first to third visible labial segments 1.1:1.4:0.4. Scape ~ 1.3 × as long as head; pedicel ~ as long as first flagellomere and ~ 0.8 × as long as second flagellomere; proportional average length of scape, pedicel, first and second flagellomeres 2.7:1.3:1.3:1.7. Sc 0.8 × as long as hemelytron length, and 1.5 × as long as R + M. Hind wing ~ 3.1 × as long as maximum width. Abdominal laterotergite VIII (AL8) with very thick posterior margin (0.09 mm); abdominal sternite VII (AS7) forming a wide subrectangular concavity, with posteromedian margin almost straight, with inner posterolateral margin weakly sinuous; gonocoxa VIII (Gc8) broad, ~ 1.2 × wider than length, slightly opened inward for gonapophyses VIII (Gp8), sinuate along outer lateral margin, almost horizontal or weakly sinuate along posterior margin, weakly produced posteromesad and forming a blunt apex at apical inner corner, and with inner margin strongly incurved in its posterior 2/3; Gp8 small and subtriangular, ~ 3 × longer than width; gonoplac (Gpl) V-shaped, with maximum thick ~ 0.05 mm.

Vestiture. Almost similar to male. Abdominal laterotergite VIII (AL8) and tergite IX (AT9) with some long thick erect setae and with shorter setae; apex of abdomen with some very long thick erect setae.

Measurements. All dimensions are given in mm. ***Holotype*** (♂): BL 9.29; HL 2.01; AoL 0.75; AoW 0.60; PoL 0.62; PoW 0.81; OE 1.12; IE 0.58; ED 0.63; OD 0.16; OCD 0.35; COD 0.18; R1L 1.03; R2L 1.30; R3L 0.32; A1L 2.85; A2L 1.41; A3L 1.55; A4L 2.07; PnL 2.21; PnW 2.64; APL 0.90; PPL 1.31; HeL 7.26; HeW 2.47; Sc 5.66; R+M 3.84; HWL 4.92; HWW 1.54; AFL 3.33; ATL 3.87; MFL 2.46; MTL 3.24; PFL 3.58; PTL 4.84. ***Paratypes*** (♂): BL 9.19–10.45; HL 1.94–2.12; AoL 0.70–0.79; AoW 0.57–0.62; PoL 0.64–0.77; PoW 0.80–0.86; OE 1.08–1.17; IE 0.55–0.59; ED 0.60–0.64; OD 0.14–0.19; OCD 0.34–0.41; COD 0.15–0.18; R1L 1.03–1.14; R2L 1.26–1.41; R3L 0.32–0.46; A1L 2.68–3.06; A2L 1.30–1.55; A3L 1.37–1.61; A4L 1.74–2.17; PnL 1.95–3.10; PnW 2.42–2.74; APL 0.74–0.99; PPL 1.22–2.25; HeL 7.26–7.88; HeW 2.23–2.63; Sc 5.32–6.09; R+M 3.44–4.08; HWL 4.92–5.22; HWW 1.46–1.62; AFL 3.15–3.46; ATL 3.78–4.08; MFL 2.33–2.69; MTL 2.73–3.50; PFL 3.56–3.91; PTL 4.80–5.10. ***Paratypes*** (♀): BL 10.11–10.91; HL 2.00–2.10; AoL 0.73–0.79; AoW 0.60–0.63; PoL 0.67–0.76; PoW 0.82–0.87; OE 1.06–1.15; IE 0.55–0.60; ED 0.59–0.63; OD 0.15–0.19; OCD 0.36–0.46; COD 0.18–0.20; R1L 1.08–1.15; R2L 1.31–1.41; R3L 0.32–0.37; A1L 2.52–2.83; A2L 1.26–1.35; A3L 1.23–1.41; A4L 1.61–1.87; PnL 2.09–2.47; PnW 2.24–3.65; APL 0.70–0.88; PPL 1.39–1.65; HeL 7.66–8.21; HeW 2.60–2.92; Sc 5.86–6.32; R+M 4.01–4.45; HWL 5.25–6.82; HWW 1.67–2.15; AFL 3.00–3.33; ATL 3.63–4.07; MFL 2.31–3.13; MTL 2.94–3.83; PFL 3.33–3.80; PTL 4.61–5.13.

Distribution. Vietnam, Central Highlands (Dak Lak, Gia Lai).

Type locality. Vietnam, Central Highlands, Dak Lak Province, Chu Yang Sin National Park.

Etymology. The new species is named after its yellow posterior pronotal lobe.

Key to the species of the genus *Biasticus* Stål, 1867 from Vietnam

1 Posterior pronotal lobe pale luteous to yellow **2**

– Posterior pronotal lobe brown to black **4**

2 Connexivum sanguineous; scutellum blackish brown or black with posterior apex blackish brown or black ..... ***Biasticus flavinotus*** **(Matsumura, 1913)**

– Connexivum pale luteous to luteous; scutellum dark brown with posterior apex luteous **3**

3 Abdominal sternites luteous with some blackish brown or black segmental transverse stripes laterally; femora uniformly blackish brown or brown ..... ***Biasticus flavus*** **(Distant, 1903)**

– Abdominal sternites pale luteous without blackish brown or black segmental transverse stripes laterally; femora luteous with some dark brown or yellowish brown suffusions..... ***Biasticus luteicollis*** **Ha, Truong & Ishikawa, sp. nov.**

4 Abdominal sternites luteous to sanguineous; anterior pronotal lobe without row of bent setae; pedicel as long as first flagellomere and shorter than second flagellomeres ..... ***Biasticus confusus*** **Hsiao et al., 1979**

– Abdominal sternites sanguineous; anterior pronotal lobe with some rows of bent setae; pedicel slightly longer than first flagellomere and as long as second flagellomere **5**

5 Posterior pronotal lobe densely covered with short bent cream-yellow setae, interspersed with long erect setae; apical margin of median process of pygophore weakly concave as a whole..... ..... ***Biasticus taynguyenensis*** **Ha, Truong & Ishikawa, sp. nov.**

– Posterior pronotal lobe densely covered with short bent griseous setae, sometimes interspersed with long griseous setae; apical margin of median process of pygophore weakly convex as a whole and slightly emarginate at middle.... .....***Biasticus griseocapillus*** **Ha, Truong & Ishikawa, sp. nov.**

Acknowledgements

The authors would like to thank Dr. Nguyen Van Sinh (Director, Institute of Ecology and Biological Resources [IEBR], Vietnam Academy of Science and Technology, Vietnam), Dr. Nguyen Duc Anh (IEBR), Dr. Nguyen Dac Dai (IEBR), director and staff in Kon Chu Rang Nature Reserve (Gia Lai Province), and Chu Yang Sin National Park (Dak Lak Province) for their kind assistance during our field activities, as well as Dr. Yoshida Takahiro (Tokyo Metropolitan University [TMU], Japan), Dr. Namiki Kikuchi (TMU), Dr. Francesco Ballarin (TMU), Msc. Aiki Yamada (TMU), Msc. Sho Tsukamoto (TMU), and Dr. Liao Hau-chuan (TMU) for their valuable assistance in lab experiments and specimen imaging. We also thank Dr. Wei Song Hwang (Lee Kong Chian Natural History Museum [LKCNHM], National University of Singapore, Singapore), Dr. Wendy Y. Wang (LKCNHM), and Dr. Takuya Kiyoshi (National Museum of Nature and Science [NMNS], Japan) for their generous hosting when the first author visited LKCNHM in January 2020 and NSMN in October 2021. Furthermore, we appreciate Dr. Kazunori Yoshizawa (Research Faculty of Agriculture, Hokkaido University, Japan) for his kind supports in taking photos of the lectotype specimen of *Biasticus flavinotus* (Matsumura, 1913) at Hokkaido University in July 2021. This research was funded by the following foundations and societies: Tokyo Human Resources Fund for City Diplomacy; Tokyo Metropolitan University Fund for TMU Strategic Research (Leader: Prof. Noriaki Murakami; FY2020–FY2022); Asahi Glass Foundation (Leader: Katsuyuki Eguchi; FY2017–FY2020). Furthermore, the authors would like to thank Enago (www.enago.jp) for the English language review. We are grateful to Dr. Cai Wanzhi of China Agricultural University, China, Dr. Hélcio R Gil-Santana of Laboratório de Diptera, Instituto Oswaldo Cruz, Av. Brasil, and an anonymous reviewer for their valuable comments on the manuscript.

References

Afzal H, Ahmad I (2019) A new record of the predatory bug *Biasticus flavus* (Distant) (Hemiptera: Reduviidae: Harpactorinae) from Pakistan and its redescription with reference to its unknown male and female genitalia. International Journal of Biology and Biotechnology 16(1): 205–210.

Bely AE, Wray GA (2004) Molecular phylogeny of naidid worms (Annelida: Clitellata) based on cytochrome oxidase I. Molecular Phylogenetics and Evolution 30(1): 50–63. https://doi.org/10.1016/S1055-7903(03)00180-5

Bergroth E (1913) New genera and species of Reduviidae from Borneo. The Sarawak Museum Journal 3: 25–38.

Cai W, Yang S (2002) Insect from Maolan landscape. Guizhou Science and Technology Publishing House, Guiyang, 208–230.

Chernomor O, von Haeseler A, Minh BQ (2016) Terrace aware data structure for phylogenomic inference from supermatrices. Systematic Biology 65(6): 997–1008. https://doi.org/10.1093/sysbio/syw037

Cognato AI, Vogler AP (2001) Exploring data interaction and nucleotide alignment in a multiple gene analysis of Ips (Coleoptera: Scolytinae). Systematic Biology 50(6): 758–780. https://doi.org/10.1080/106351501753462803

Distant WL (1903) Rhynchotal notes. XVI. Heteroptera: Family Reduviidae (continued). Apiomerinae, Harpactorinae and Nabidae. Annals & Magazine of Natural History 11(7): 203–213. https://doi.org/10.1080/00222930308678751

Distant WL (1904) Rhynchotal notes. XXII. Heteroptera from North Queensland. Annals & Magazine of Natural History 18(7): 286–293. https://doi.org/10.1080/03745480409443011

Forero D, Weirauch C (2012) Comparative genitalic morphology in the New World resin bugs Apiomerini (Hemiptera, Heteroptera, Reduviidae, Harpactorinae). Deutsche Entomologische Zeitschrift 59(1): 5–41. https://doi.org/10.1002/mmnd.201200001

Hsiao TY (1979) New species of Harpactorinae from China. II. (Hemiptera: Reduviidae). Acta Zootaxonomica Sinica 4: 238–295.

Hsiao TY, Ren SZ (1981) Reduviidae. In: Hsiao et al., A handbook for the determination of the Chinese Hemiptera-Heteroptera (II). Science Press, Beijing, 390–538.

Ishikawa T (2003) Taxonomic study on the Tribe Harpactorini (Heteroptera, Reduviidae) from Indochina, with Zoogeographical considerations. Ph.D. Thesis, Tokyo University of Agriculture, Kanagawa, Japan.

Kalyaanamoorthy S, Minh BQ, Wong T, von Haeseler A, Jermiin LS (2017) ModelFinder: Fast model selection for accurate phylogenetic estimates. Nature Methods 14(6): 587–589. https://doi.org/10.1038/nmeth.4285

Kassambara A, Mundt F (2020) Package 'factoextra': Extract and Visualize the Results of Multivariate Data Analyses. Version 1.0.7. https://cran.r-project.org/package=factoextra

Kumar S, Stecher G, Li M, Knyaz C, Tamura K (2018) MEGA X: Molecular Evolutionary Genetics Analysis across Computing Platforms. Molecular Biology and Evolution 35(6): 1547–1549. https://doi.org/10.1093/molbev/msy096

Larkin MA, Blackshields G, Brown NP, Chenna R, McGettigan PA, McWilliam H, Valentin F, Wallace IM, Wilm A, Lopez R, Thompson JD, Gibson TJ, Higgins DG (2007) Clustal W and Clustal X version 2.0. Bioinformatics 23(21): 2947–2948. https://doi.org/10.1093/bioinformatics/btm404

Maldonado J (1990) Systematic catalogue of the Reduviidae of the World. Caribbean Journal of Science, Special publication No. 1: 171–172.

Matsumura S (1913) Additions to Thousand Insects of Japan 1: 1–184.

Meusnier I, Singer GAC, Landry JF, Hickey DA, Hebert PDN, Hajibabaei M (2008) A universal DNA mini-barcode for biodiversity analysis. BMC Genomics 9(1): 214. https://doi.org/10.1186/1471-2164-9-214

Miller NCE (1941) New genera and species of Malaysian Reduviidae (continued). Part II. Journal of the Federated Malay States Museums 18: 601–773.

Miller NCE (1948) New genera and species of Reduviidae from the Philippines, Celebes, and Malaysia. The Transactions of the Entomological Society of London 99(13): 411–473. https://doi.org/10.1111/j.1365-2311.1948.tb01228.x

Miller NCE (1949) A new genus and new species of Malaysian Reduviidae. Proceedings of the Royal Entomological Society of London (B) 18(11–12): 229–237. https://doi.org/10.1111/j.1365-3113.1949.tb01417.x

Miller NCE (1954a) Reduviidae (Hemiptera-Heteroptera). Synonymic notes and corrections. Annals & Magazine of Natural History 7(12): 639–640. https://doi.org/10.1080/00222935408651764

Miller NCE (1954b) New genera and species of Reduviidae from Indonesia and the description of a new subfamily (Hemiptera-Heteroptera). Tijdschrift voor Entomologie 97: 75–114.

Minh BQ, Schmidt HA, Chernomor O, Schrempf D, Woodhams MD, von Haeseler A, Lanfear R (2020) IQ-TREE 2: New models and efficient methods for phylogenetic inference in the genomic era. Molecular Biology and Evolution 37(5): 1530–1534. https://doi.org/10.1093/molbev/msaa015

Puillandre N, Brouillet S, Achaz G (2021) ASAP: Assemble species by automatic partitioning. Molecular Ecology Resources 21(2): 609–620. https://doi.org/10.1111/1755-0998.13281

Rambaut A, Drummond AJ, Xie D, Baele G, Suchard MA (2018) Posterior summarisation in Bayesian phylogenetics using Tracer 1.7. Systematic Biology 67(5): 901–904. https://doi.org/10.1093/sysbio/syy032

Reuter OM (1887) Reduviidae novae et minus cognitae descriptae. Revue d'entomologie 6: 149–167.

Ronquist F, Huelsenbeck JP (2003) MrBayes: Bayesian Phylogenetic Inference under Mixed Models. Bioinformatics 19(12): 1572–1574. https://doi.org/10.1093/bioinformatics/btg180

Rosa JA, Mendonça VJ, Rocha CS, Gardim S, Cilense M (2005) Characterization of the external female genitalia of six species of Triatominae (Hemiptera: Reduviidade) by scanning electron microscopy. Memórias do Instituto Oswaldo Cruz, Rio de Janeiro 105(3): 286–292. https://doi.org/10.1590/S0074-02762010000300007

Satria R, Kurushima H, Herwina H, Yamane Sk, Eguchi K (2015) The trap-jaw ant genus *Odontomachus* Latreille form Sumatra, with a new species description. Zootaxa 4048(1): 1–36. https://doi.org/10.11646/zootaxa.4048.1.1

Schuh RT, Weirauch C (2020) True bugs of the world (Hemiptera: Heteroptera). Classification and natural history. 2nd edn. Siri Scientific Press, Manchester, 767 pp.[, 32 pls]

Shekhovtsov SV, Golovanova EV, Peltek SE (2013) Cryptic diversity within the Nordenskiold's earthworm, *Eisenia nordenskioldi* subsp. *nordenskioldi* (Lumbricidae, Annelida). European Journal of Soil Biology 58: 13–18. https://doi.org/10.1016/j.ejsobi.2013.05.004

Simon C, Frati F, Beckenbach A, Crespi B, Liu H, Flook P (1994) Evolution, weighting, and phylogenetic utility of mitochondrial gene sequences and a compilation of conserved polymerase chain reaction primers. Annals of the Entomological Society of America 87(6): 651–701. https://doi.org/10.1093/aesa/87.6.651

Stål C (1863) Formae speciesque novae Reduviidum. Annales de la Société Entomologique de France 3: 38. https://doi.org/10.1080/00379271.1863.11755426

Stål C (1867) Bidrag till Reduviidernas Uennedom. Öfversigt af Kongl. Vetenskaps-akademiens forhandlingar 23: 290.

Truong XL, Cai WZ, Tomokuni M, Ishikawa T (2015) The assassin bug subfamily Harpactorinae (Hemiptera: Reduviidae) from Vietnam: an annotated checklist of species. Zootaxa, ISSN: 1175-5326: 101–116. https://doi.org/10.11646/zootaxa.3931.1.7

Zhang G, Weirauch C (2013) Molecular phylogeny of Harpactorini (Insecta: Reduviidae): correlation of novel predation strategy with accelerated evolution of predatory leg morphology. Cladistics 30(4): 339–351. https://doi.org/10.1111/cla.12049

Zhang J, Kapli P, Pavlidis P, Stamatakis A (2013) A general species delimitation method with applications to phylogenetic placements. Bioinformatics 29(22): 2869–2876. https://doi.org/10.1093/bioinformatics/btt499

Supplementary material 1

R-script used for morphometric analyses

Author: Ngoc Linh Ha

Data type: statistical data

Link: https://doi.org/10.3897/zookeys.1118.83156.suppl1

Supplementary material 2

Female morphometric dataset
Author: Ngoc Linh Ha
Data type: species data

Link: https://doi.org/10.3897/zookeys.1118.83156.suppl2

Supplementary material 3

Male morphometric dataset
Author: Ngoc Linh Ha
Data type: species data

Link: https://doi.org/10.3897/zookeys.1118.83156.suppl3

ZooKeys 1118: 181–189 (2022)
doi: 10.3897/zookeys.1118.91192
https://zookeys.pensoft.net

BOOK REVIEW

A peer-reviewed open-access journal
ZooKeys
Launched to accelerate biodiversity research

Ecology and Conservation of the Dutch Ground Beetle Fauna – Lessons from 66 Years of Pitfall Trapping

By Hans Turin, D. Johan Kotze, Stefan Müller-Kroehling, Pavel Saska, John Spence and Theodoor Heijerman. Wageningen Academic Publishers, 2022, 452 pages. eISBN: 978-90-8686-921-3; ISBN: 978 90-8686-369-3 https://doi.org/10.3920/978-90-8686-921-3. Euro 99.

Dietrich Mossakowski[1]

1 *University of Bremen, Bremen, Germany*

Corresponding author: Dietrich Mossakowski (dmossa@uni-bremen.de)

Academic editor: Lyubomir Penev | Received 2 August 2022 | Accepted 3 August 2022 | Published 24 August 2022

https://zoobank.org/AC0FCCEF-4413-4AEF-B253-9D6E9DC9CAFC

Citation: Mossakowski D (2022) Ecology and Conservation of the Dutch Ground Beetle Fauna – Lessons from 66 Years of Pitfall Trapping. ZooKeys 1118: 181–189. https://doi.org/10.3897/zookeys.1118.91192

Carl H. Lindroth was the first to present a comprehensive survey with his fundamental work on the Fennoscandian carabid beetles, covering all ecological aspects. The knowledge of the Dutch carabid beetle fauna is also exceptionally good what is especially thanks to Piet den Boer's initiative and the work of his followers.

Apart from the comprehensive book by Hans Turin (2000) on The Netherlands carabid beetles, I only see major publications on parts of a country or certain aspects, respectively, such as Trautner et al. (2017) on carabids of a German Federal State, Baden-Württemberg or Paill (2009) on endemic species in Austria.

Turin et al. (1991) analysed the data bank on Dutch carabid beetles on the basis of 1.616 year samples from the period 1953–1983. The present book contains updated and extended analyses of the extraordinary huge data bank on Dutch carabid beetles of 4.363 pitfall trap year samples with more than 3 million specimens covering additionally the period 1984–2018.

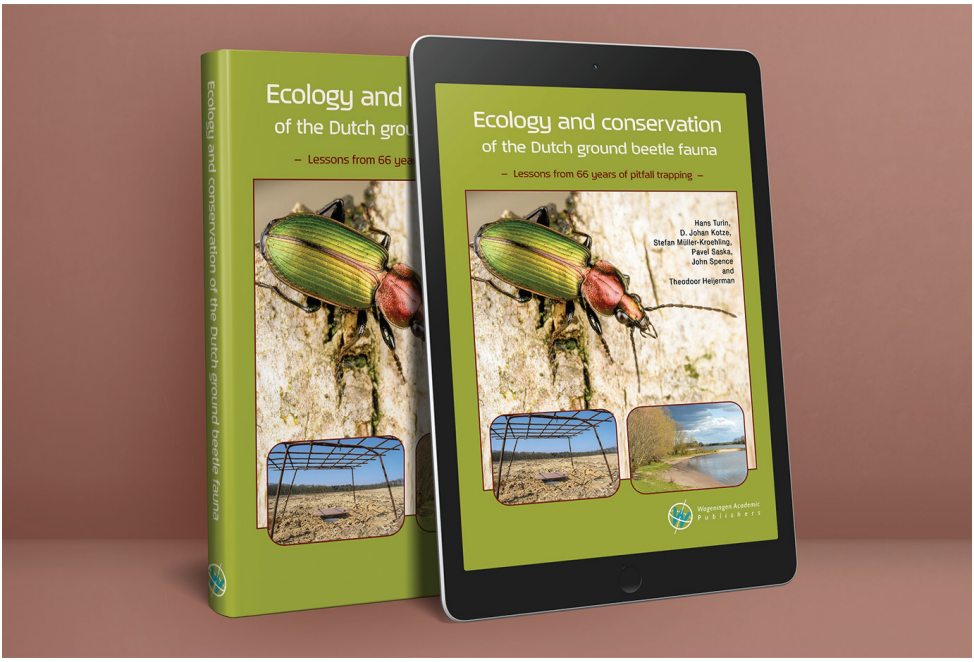

The authors

This book was produced through exemplary teamwork. This makes it difficult to briefly describe the individual contributions; in the book, this cooperation is described in detail on half a page. Hans Turin developed the concept of the book, created most of the text, the figures, the tables, and most of the habitat photos. He also organised the cooperation of the team. The other authors contributed parts of the methodology, parts of the text, habitat and species photos, and read critically and discussed the manuscript.

Chapter 1 Introduction to the chapters provides a very helpful, concise summary of the contents of the remaining chapters with references to the relevant paragraphs. It also contains two substantial maps of The Netherlands with the locations of the traps and the hand catches, respectively, which clearly show both the hot spots of the investigations and the geographical gaps.

In general, the text of the whole book is optimally supplemented by impressive figures and tables and is best illustrated by very good habitat photos and mostly perfect photos of the beetles. All are optimally placed in relation to each other.

Chapter 2 Carabidology provides a general introduction to the biology and ecology of carabids in particular the aspects relevant to the evaluation of pitfall trap sampling. This chapter represents a revision and update of what is contained in Turin's (2000) book.

The comparison of the numbers of beetles caught by hand versus those sampled with pitfall traps is very revealing (P. 38). Somewhat complicated to acquire at first glance, but is made easy by the original catch figures of the 12-year-samples shown in the tables nearby.

Heijerman et al. (1989) showed that the placement of pitfall traps is actually more important than the number of traps in order to obtain the most complete list of carabid species present (P. 55).

According to Hutchinson (1959), the ecological niche is the hyperdimensional space of a species' habitat. Following this concept, a niche cannot be occupied and speciation is niche development (P. 46).

The figures 2.24 and 2.25 (p. 48, 49) are incomprehensible to me. The x-axis has 120%, and some of the bars are placed on the x-axis above 100%. These graphs were taken in their original from Desender (1989).

Although in the references, the work of Lindroth (1946) on the heritability of wing dimorphism is not mentioned here (P. 48).

There seems to be a contradiction: *Carabus nemoralis* is represented in table 2.5.b as found only on the mainland, in the text (p. 74, last paragraph) this species is mentioned for the NO-Polder. In consequence, the discussion about the inheritance of the ability to fly might become obsolete.

An interesting aspect considering phenology/development may be added: in mark-recapture experiments, Althoff et al. (1992) found that *Carabus auronitens* can skip nearly an entire generation. As a result of too low temperatures in May, reproduction of most specimens failed and the beetles overwintered a second time. This effect could not have been detected with normal pitfall trapping.

Chapter 3 Database work and pitfall traps. This chapter describes the Dutch carabid database and the strengths and limitations of the pitfall trap method.

Two aspects can be highlighted: (i) The plea for a standard pitfall trap even though "…the problem of incomparability of pitfall results … can be solved by applying the correct statistics…" (P. 87). and (ii) the question of what pitfall trap catches reflect: "… most carabidologists have made peace with the fact that their catch is not equivalent to abundance." (P. 92).

Pitfall trapping in flooded habitats is possible after all (P. 88). Several trapping methods exist that are not susceptible to flooding but operate during low tides (Floating trap Kiel and Bremen, resp.; Air bell trap (see Dormann 2000)).

Chapter 4 Exploring the database, methods. Because evaluation methods are important for understanding, they will be briefly described here.

In a former paper, Turin et al. (1991) described the basis for the evaluation of the samples of the database containing the year samples of 1953–1983. They established 33 habitat types (H1–H33) in seven habitat groups and allocated the carabid species to these groups (HAB1).

In the present book, the scheme was rearranged and named HAB2. Habitats were ordered in three levels: (i) 33 habitat types (e.g., # X1–X5 for heathland) that were allocated to (ii) 17 habitat groups (e.g., peat, wet and dry heath), and in level (iii) the carabid species were allocated to habitats in six affinity groups (e.g., heathland species).

The basic structure, the habitat types H1–H33 in HAB1 and X1–X33 in HAB2, is identical. But the meta-structure of habitat groups differs significantly in a number of groups and assignments.

After testing other modern statistical methods, the basic structure of the original habitat types was maintained and the habitat types form the basis for all further comparisons. But the habitat groups were reorganised significantly, and their compliance with the European Habitat Directive was indicated.

The allocation of the carabid year samples to the habitat structure resulted in the habitat preference. The data were manipulated as already described in Turin et al. (1991): The data of a year-sample were standardised by calculating the number of specimens per decimetre pitfall edge and year (SDY), SDY was transformed to ln(SDY+1), and the resulting values adapted to relative abundances by setting the highest value of a species to 100%.

The investigation of a sample or groups of samples was done generally by comparing the data in focus with the reference matrix of the 33 habitat types of the HAB1 classification. The results were presented in three ways: (i) As habitat charts of the 33 Renkonen Indices per sample, (ii) As similarity matrix of the Renkonen Indices and (iii) As species ordination and centroids. Heijerman and Turin (1991) found the Renkonen Index as the most suitable of several measures for the relationship between the data of a pitfall sample and the basic HAB1 matrix of habitat preferences. The results are presented in three ways:

Habitat charts. The graphs show the bars of the 33 values (X01–X33, HAB2). The height of the bars indicates the agreement with the preferences of HAB1 and was considered a fingerprint of the sample. The first and second highest bars were used to allocate the sample to one of the 17 habitat groups (GR01–GR17). Studying the habitat charts, the reader of the book should have in mind that the order of habitat types in the habitat charts is X1–X33 sequentially throughout the text but in the habitat groups (HG) the arrangement differs: X29 is coupled with X12 as habitat group GR8 and X24 with X30 as GR14.

Similarity matrices. Similarity matrices are used to compare multiple samples, for example, to show changes over time in certain habitats.

Ordination and centroids. The species and their abundances were presented in a DCA ordination that resulted from the HAB1 classification. Habitat conditions were indicated within the graph, which was compiled from the literature, independent of the habitat classification of the book. The location of a sample or the occurrence of a species within this ordination plot can be shown in centroid plots. The reliability of the method is shown in detail in one example, it is well proven.

Characteristic and accompanying species. The affinity to one or more habitat groups was performed using the procedure described by Müller-Kroehling (2015): X^2 values were calculated in a test of a four-field contingency table containing the number of samples, in which the focus species and all other species are present or not. Species with a striking high value only in one of the 17 habitat groups were classified as primary characteristic species, those with a maximum in two or three habitat groups as secondary characteristics, and all other species as eurytopic. The characteristic species were listed in table 4.11.

The most abundant eurytopic species that occur in several habitat types were denominated as accompanying species if they co-occur with a characteristic species in at least 40% of year samples.

Table 4.11 (P. 132) provides a quick overview of the characteristic and accompanying species of the habitat groups. A full list according to habitat groups is given in Appendix A. The denomination of habitat groups is listed on p. 177.

Affinity groups. The 203 characteristic species established were grouped into the six affinity groups and described in short in chapter 4.6 (P. 135 ff): Heathland (H), Dunes (D), Grassland (G), Forest (F), and Ruderal and Pioneer (R) species.

The discussion of other classifications led to the insight that the larger the area that is covered the weaker the habitat information and the geographical distribution of species has an important effect.

Chapter 5 Ground beetle fauna of the Netherlands is the main part of the book. It contains the evaluation with regard to the six affinity groups, the species accounts and an update on the species accounts in Turin's (2000) book.

The **first** part deals with affinity groups and their relationships to traits, habitat groups, and their distribution across regions, assemblages, etc. The fact that the geographical occurrence of the species plays an important role is vividly demonstrated in the biography sub-chapter 5.9 with an illustration of the geographic occurrence of eight Dutch forest species.

The **second** part deals with the habitat group accounts.

The 33 habitat types are combined into the 17 habitat groups because the overlap of some types was so great that they did not need to be considered separately. Nevertheless, the habitat types were discussed within the groups. The habitats were classified according to their carabid fauna of a total of 4359 year-samples (table 4.10, p. 130). The presentation follows the same scheme for all 17 groups: an assignment to the EU habitat directive, a short description of the habitat types that belong to the respective group, characteristic and accompanying species, habitat reference, and a summary.

They include map(s) of the locations of the affinity group samples, a plot of the centroids of the group, and a table of the affinity values X^2 of the characteristic species for all 17 affinity groups by which the reader can very well understand the assignment of the species to the respective affinity group, a table with traits of the characteristic species, a table of accompanying species in relation to characteristic ones, habitat charts of selected samples, habitat photo(s), and photo(s) of selected species.

Chapter 5.10 covers pages 175–300.

The **third part** of chapter 5 is an update of Turin's (2000) species account.

I want to address the discussion of Section 4.7 here, the transferability of the Dutch habitat classification to other regions. It has been made clear that a comparison of the entire classification is only possible in individual cases. This is not only due to methodological reasons of comparable studies (e. g. quantitative data instead of quantitative

data, areas of different size), but also to the ecological and geographical conditions of the Dutch landscape. This may be illustrated by three habitat groups.

Salt marshes. The carabids of salt marsh habitats contain a group of species highly specific, in consequence, the characteristic species of this group are also found in salt marshes along the North Sea coast of the adjacent countries. However, the zonation within the salt marsh fauna could not be found because no traps could be set up in the flooded areas.

Forests. It was shown that the results considering forests are difficult to transfer to other countries. This is mainly due to two facts. (i) The distribution of some forest species only partially extends into The Netherlands, which is clearly demonstrated by the distribution maps of eight forest species (P. 164–65, fig. 5.22). (ii) "…it seems most likely that the weak similarities between the Bavarian and the Dutch forest faunas result mainly from the anthropogenic distortion of forest habitats in the Netherlands." With the exception of the forest fauna of southern Limburg (P. 141).

Peat bogs, Habitat GR01: "…little is left in a near-pristine condition." (P. 178), "… the ground beetle fauna on peaty soils includes a small number of typical inhabitants, such as *Agonum ericeti*, *A. munsteri*, …" (P. 181). But *A. ericeti* was found as characteristic species of GR03 (Dry heath). Additionally, it was found in all habitat groups (Tab. 5.14 shows values >0 for GR01–Gr17), thus indicating that this species was found in low numbers as well in dunes as in forests, etc.

These findings are quite different from the situation in Northern Germany. I see four reasons that may interpret these differences. (i) Remainders of raised bogs in a near-pristine status do they really further exist nowadays in the Netherlands? It is unlikely that the situation is better than in northern Germany; (ii) Some GR01 habitats were described as very wet renatured locations (P. 179), but these habitats are not comparable with raised bogs, they harbour only a restricted bog fauna, and do not have hummocks, which are a must for overwintering of *A. ericeti* (Främbs 1994); they do not have bog pools where *A. munsteri* lives in the siltation zone; (iii) Both species are known to be able to survive habitat changes for a long time in low numbers, in consequence, the species may be characterised at such locations as a succession relict; (iv) The realised ecological niche may be different at the border of the distribution area of the species considered (Kühnelt's principle of regional stenoecia).

The number of km-squares (73) differs in the caption of figure 5.34.A (GR01) from that present within the figure (114). The number of samples in figure 5.34.B shows minor deviations from those of the text and in table 4.10, like in six other habitat groups.

Chapter 6 Trend analysis begins with an introduction to the trend analyses already available, in general, for The Netherlands and the Carabids in particular. The data were standardised in terms of effort and analysed using the Generalised Additive Mixed Modelling. The evaluation was done for the whole material and separately with selected habitats: Dunes, Heathlands, grasslands, forest and ruderal habitats. To test the validity of the results, calculations were additionally carried out with reduced material.

The global analyses resulted in a weak but significant decline of the mean catch, which added up to 47% in 2018 to that observed in 1970. The global analysis of species richness did not indicate a change.

The results of the six affinity groups differ from group to group as well considering catch numbers and species richness. Trends were found for heathlands, grasslands, and forests. Several characteristic heathlands species showed a slow but continuous decline in catch numbers that were interpreted as caused by nitrogen deposition from farmland. A low but significant decline was found in catch numbers of forests, while their species richness remained stable. They found a significant decline for non-characteristic grasslands species but not for characteristic species, a fact that is discussed in the light of fertilisers input, vegetation changes and management measures.

Chapter 7 Conservation. The importance of carabids for nature conservation and their various threats are described. The chapter emphasises that the focus of conservation should not be on the individual species, but on the communities. "The work of this book is clearly focussed on the relationship between species and habitat and specially between typical communities (habitat groups) and habitats." In consequence, the usefulness of red lists for conservation management is regarded as limited. The habitat reference method as used in the book was applied to demonstrate by three examples its usefulness for conservation purposes.

An agricultural index was calculated to determine the agricultural influence on the carabid fauna. It is the sum of the X^2 values of the habitat types X12 (farmland intensive, sandy soils) plus X26 (farmland intensive, clay soils) and demonstrated in charts with 14 classes strongly demonstrating the agricultural influence.

The habitats most threatened in The Netherlands are the heathlands and the forest of the hills of southern Limburg.

Chapter 8 General summary and conclusions. A summary of the book's content on one page.

References. A compendium of 35 pages of (mainly) carabid literature.

Appendices. Species list. It contains the species number in Turin (2000), scientific name, its abbreviation, wing development, reproductive period, geographical position, ecology according to Lindroth (1949), affinity group, numbers of pitfall samples with the species, the same number incl. other sample methods and the number of specimens.

Data contributions list the samples with number, year, province, kind of object (Habitat chart, figure, photo, plot of centroids, table), source, chapter and figure or table number, resp.

Terms list. In this list, 70 terms frequently used in the book were explained.

Index. Five pages covering keywords and their most important section of occurrence.

I only found 18 typing errors in the whole book, but they do not affect the understanding.

Conclusion

The book presents the successful approach to evaluating the enormous amount of data on the Dutch carabid beetles. The methods used are not only described but their applicability is tested and their selection justified in detail. The naming and labelling are clear and well- arranged and consistent throughout the book. The presentations and results are supported in detail by tables and illustrations and illustrated by impressive habitat pictures and photos of the species, especially the excellent live photographs by Heijerman.

Whereas in Turin (2000) the species is the focus of the presentation, here it is the habitat, the habitat group, the characteristic species and the communities that are the focus of interest.

Besides pitfall catches, the data set takes also into account hand samples. This could only be managed by considering year traps (catches at a minimum of eight weeks in spring plus eight weeks in summer/autumn), which have the advantage to correspond most closely to the actual abundances.

Tables and figures are very well arranged in relation to the text. It is very helpful that not only the page numbers are available in the header, but also the detailed naming of the chapters with numbers and text, so that you always know exactly where to find what.

Among many other interesting studies, the Dutch carabidologists were very good at using the polders of the IJsselmeer and Lauwersmeer, which had been created by diking, for their research. Chapeau!

I strongly recommend putting this volume next to Turin (2000).

References

Althoff G-H, Ewig M, Hemmer J, Hockmann P, Klenner J, Niehues F-J, Schulte R, Weber F (1992) Ergebnisse eines Zehn-Jahres-Zensus an einer *Carabus auronitens*-Subpopultion im Münsterland (Westf.). Abhandlungen aus dem Westfälschen Museum für Naturkunde, Münster 54(4): 3–64.

Desender K (1989) Dispersievermogen en ecologie van loopkevers Coleoptera, Carabidae) in België: en evolutionaire benadering. Studiedocumenten van het Koninklijk Belgisch Instituut voor Natuurwetenschappen 54: 136 pp.

Dormann W (2000) A new pitfall trap for use in periodically inundated habitats. In: Brandmayr P, Lövei G, Zetto-Brandmayr T, Casale A, Vigna Taglianti A (Eds) Natural History and applied Ecology of Carabid Beetles. Proc. IXth European Carabaridologist's Meeting. Cosenza 1998. Pensoft Publishers, Sofia-Moscow, 247–250.

Främbs H (1994) The Importance of Habitat Structure and Food Supply for Carabid Beetles (Coleoptera, Carabidae) in Peat Bogs. Memoirs of the Entomological Society of Canada 169: 145–159. https://doi.org/10.4039/entm126169145-1

Heijerman Th, Booij CJH, Laders K (1989) De onderbemonstering van de Nederlandse loopkeverfauna (Coleoptera, Carabidae). Entomologische Berichten, Amsterdam 49: 161–167.

Heijerman Th, Turin H (1994) Towards a method for the biological assessment of habitat quality using carabid samples. In: Desender K et al. (Eds) carabid beetles. Ecology and evolution. Series Entomologica 51. Springer, Dordrecht, 305–312. https://doi.org/10.1007/978-94-017-0968-2_46

Hutchinson GE (1959) Homage to Santa Rosalia, or why are there so many kinds of animals? American Naturalist 93: 145–159. https://doi.org/10.1086/282070

Müller-Kroehling S (2015) Laufkäferarten als charakteristische Arten in Bayerns Wäldern. – Eine methodenkritische Auseinandersetzung mit Definition und Verfahren zur Herleitung charakteristischer Arten und zur Frage der Artengemeinschaften. BfN-Skripten 424(1): 312 pp (Teil 1 Hauptteil); 424(2): 365 pp (Teil 2 Anlagen).

Paill W (2009) Coleoptera. In: Rabitsch W, Essl F (Hrsg.) Endemiten. Kostbarkeiten in Österreichs Pflanzen- und Tierwelt. Naturwissenschaftlicher Verein für Kärnten und Umweltbundesamt GmbH, Klagenfurt, 627–783.

Trautner J, Bräunecke M Forth J, Fritze MA, Geigenmüller Hannig K, Harry I, Herrmann G, Rietze J, Schmidt J (2017) Die Laufkäfer Baden-Württembergs. Band 1–2. Ulmer, Stuttgart, 848 pp.

Turin H (2000) De Nederlandse Loopkevers. Verspreiding en ecologie (Coleoptera, Carabidae). Nederlandse fauna 3. Nationaal Natuurhistorisch Museum Naturalis. KNNV-Uitgeverij & EIS-Nederland, Leiden, 666 pp.

Turin H, Alders K, Den Boer PJ, Heijerman Th, Laane W, Penterman E, Van Essen S (1991) Ecological characterization of carabid species in the Netherlands from thirty years of pitfall sampling. Tijdsschrift voor Entomologie 138: 279–304.